ДОКЛАДЫ
АКАДЕМИИ НАУК СССР

Volume 140, Numbers 1-6
September-October, 1961

PROCEEDINGS OF THE ACADEMY OF SCIENCES

OF THE USSR

(DOKLADY AKADEMII NAUK SSSR)
Physical Chemistry Section

M. I. T. Lincoln Laboratory
Received-Library
MAY 1

IN ENGLISH TRANSLATION

c/b

CONSULTANTS BUREAU

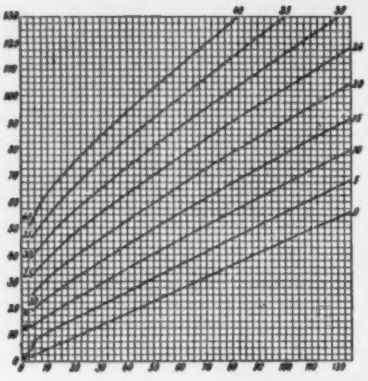

TABLES AND NOMOGRAMS OF HYDROCHEMICAL ANALYSIS

by I. Yu. Sokolov

Translated from Russian

Upon completion of analytical experiments, every research chemist, whether he uses a "test tube" or a "пробирка," must calculate his findings in the international language of figures in two forms (weights and equivalents), and often three (weights, equivalents and percent-equivalents), and then compare experimental data with theoretical values.

Technicians and statisticians working with the results of hydrochemical analyses performed at different times by different laboratories inevitably face the problem of converting their figures to one system.

All such calculations are considerably simplified by the use of the tables and nomograms in this book, originally published by the State Scientific and Technical Press for Literature on Geology and the Conservation of Mineral Resources, Moscow.

All the tables and nomograms are based on analytical results expressed in the form widely used in hydrogeological practice—milligrams per liter (weight form) and milligram-equivalents per liter (equivalent form). For calculation of percent-equivalents, the sum of cation equivalents and the sum of anion equivalents are taken as 100% each. Several new tables are presented for the first time, and the many tables for converting water-analysis results from one form to another make it possible to find the milligram-equivalents for any practically possible content of a component in water, accurate to the second decimal place, and the weight content of substances to tenths of a milligram.

CONTENTS

Introduction

Tables for converting water-analysis results from one form to another

I. Table for converting hardness, expressed in German degrees, into milligram-equivalents

II. Table for converting milligram-equivalents of Ca^{2+}, Mg^{2+} and HCO_3^- into German degrees of hardness

III. Tables for converting milligrams into milligram-equivalents

IV. Tables for converting milligram-equivalents into milligrams

V. Tables for converting oxides to ions

VI. Tables for converting nitrogen into nitrogen-containing ions

VII. Table for converting milligrams of NH_3 into milligrams of NH_4^+

VIII. Table for converting oxidizability with milligrams of $KMnO_4$ into milligrams of O

Factors for converting the results of water analysis from one form into another

Average value of activity coefficient f_{av}

Nomogram for calculating percent-equivalents

Nomogram for calculating pH from given values of free CO_2 and HCO_3^-

Calculation of aggressive carbon dioxide

Relation between different forms of weak acids in natural waters at different pH values and ionic strengths μ

Factors for converting different forms of expressing aqueous solution concentrations into milligrams and milligram-equivalents

International atomic weights (Appendix)

83 pages **$4.35**

CONSULTANTS BUREAU
227 W. 17 ST., NEW YORK 11, N. Y.

Volume 140, Numbers 1-6

September-October, 1961

PROCEEDINGS OF THE ACADEMY OF SCIENCES

OF THE USSR

(DOKLADY AKADEMII NAUK SSSR)

Physical Chemistry Section

A publication of the Academy of Sciences of the USSR

IN ENGLISH TRANSLATION

Year and issue of first translation:
Vol. 112, Nos. 1-6 Jan.-Feb. 1957

Annual subscription	*$160.00*
Single issue	*35.00*

Copyright © 1962
CONSULTANTS BUREAU ENTERPRISES, INC.
227 West 17th Street, New York, N. Y.

A complete copy of any paper in this issue may be purchased from the publisher for $5.00

Note: The sale of photostatic copies of any portion of this copyright translation is expressly prohibited by the copyright owners.

Printed in the United States of America

PROCEEDINGS OF THE ACADEMY OF SCIENCES OF THE USSR

Physical Chemistry Section

Volume 140, Numbers 1-6 September-October, 1961

CONTENTS

	PAGE	RUSS. ISSUE	RUSS. PAGE
Kinetic Conditions for the Burning of Condensed Mixtures. N. N. Bakhman	655	1	141
Active Intermediate States During the Mechanical Disintegration of Polymers. P. Yu. Butyagin	658	1	145
Electrochemical Determination of the Heat of Adsorption of Hydrogen on Finely Divided Palladium. Zh. L. Vert, I. A. Mosevich, and I. P. Tverdovskii	662	1	149
Critical Phenomena in the Oxidation of Hydrocarbons in the Presence of Inhibitors in Open Systems. A. B. Gagarina, Z.K. Maizus, and N. M. Émanuél	665	1	153
Electron Paramagnetic Resonance in some Aqueous Complexes of Ti^{3+} Salts. N. S. Garif'yanov and E. I. Semenova	668	1	157
The Vapor Pressure of Thallium Determined by the Use of Radioactive Tracers. L. Kh. Genov, An. N. Nesmeyanov, and Yu. A. Priselkov	670	1	159
The Nature of the Fluorescence Quenching of Chlorophyll by Nitrocompounds. I. I. Dilung and I. N. Cheruyuk	673	1	162
The Pressure Limit for Spontaneous Propagation of the Reaction Zone in Acetylene. S. M. Kogarko and B. A. Ivanov	676	1	165
The Specific Adsorption of Iodide Ions on Silver. Ya. M. Kolotyrkin and L. A. Medvedeva	678	1	168
The Kinetics of Cathodic Processes on Semiconducting Electrodes, Involving Participation of the Electrons of the Valence Zone. R. M. Lazorenko-Manevich and S. O. Izidinov	681	1	172
Synthetic Additives of the Dispersing Agent Type. P. I. Sanin, L. F. Chernyavskaya, V. V. Sher, and N. V. Melent'eva	684	1	176
The Thermodynamic Properties of Cobalt Antimonides Determined from EMF Measurements. V. A. Geiderikh and Ya. I. Gerasimov	687	2	391
The Capacitance of the Electrical Double Layer in N-Methyl Formamide Solutions. B. B. Damaskin and Yu. M. Povarov	690	2	394
The Effect of Lyophilic Colloids on the Solubilization of Hydrocarbons in Detergent Solutions. P. A. Demchenko and A. V. Dumanskii	694	2	398
The Nature of the Surface of Catalytically Active Aluminum Oxide. M. M. Egorov	697	2	401
The Mechanism of Chain Branching in the Liquid-Phase Oxidation of Methylethylketone. G. I. Zaikov, Z. K. Maizus, and N. M. Émanuél	701	2	405
A Unidimensional Model of Unstable Burning. S. S. Novikov and Yu. S. Ryazantsev	704	2	409
Dynamics of Nonstationary Physicochemical Processes Following a Bimolecular Rate Law. G. M. Panchenkov	706	2	412

CONTENTS (continued)

	PAGE	RUSS. ISSUE	RUSS. PAGE
A Polarographic Investigation of the Method of Electrolytic Reduction of Simple and Complex Nickel Ions. Ya. I. Tur'yan	710	2	416
EPR Spectra of Acetylene and Its Derivatives when Irradiated by γ-Rays. D. N. Shigorin, V. I. Smirnova, G. S. Zhuravleva, E. P. Gracheva, and M. F. Shotakovskii	713	2	419
Differential Capacity Curves in $K_4Fe(CN)_6$ Solutions. B. B. Damaskin, E. Shvarts, and A. N. Frumkin	717	3	630
Specific Activity of Nickel Catalysts and Adsorption of Thiophene. G. D. Lyubarskii, N. V. Kul'kova, R. Kh. Burshtein, G. G. Isaeva, L. N. Ivanovskaya, and N. A. Shurmovskaya	721	3	634
The Quasi-Stationary Theory of Thermal Explosion. A. G. Merzhanov	723	3	637
Characteristic Features of the Electrode Behavior of Glasses Containing Two Acidic (Glass-Forming) Oxides. B. P. Nikol'skii, M. M. Shul'ts, N. V. Peshekhanova, and A. A. Belyustin	727	3	641
Some Regular Features of Chemical Interaction, Given by the Law of Mass Action. I. E. Starik and Yu. A. Barbanel'	730	3	644
The Reciprocal Effect of Reacting Molecules Adsorbed on the Surfaces of Dehydration Catalysts. V. É. Vasserberg, A. A. Balandin, and T. V. Georgievskaya	733	4	859
The Dehydrogenation of Cyclohexane over some Carbide, Boride, and Silicide Catalysts. G. A. Gaziev, O. V. Krylov, S. Z. Roginskii, E. A. Fokina, and M. Y. Yanovskii	737	4	863
The Burning Stability of Porous High Explosives. A. D. Margolin	741	4	867
Polarization Curve for Anodically Dissolving Germanium when the Semiconductor is of Finite Length. V. A. Myamlin	743	4	870
Deemulsifying Effect of Surface-Active Substances and the Structural Mechanical Properties of their Adsorption Layers. M. A. Filatova, S. A. Nikitina, A. B. Taubman, and P. A. Rebinder	747	4	874
The Detection of HO_2 Radicals by the Use of EPR Spectroscopy. L. I. Avramenko and R. V. Kolesnikova	750	5	1100
The Mechanism of Rectification on an Oxidized Zirconium Electrode. N. G. Bardina and P. D. Lukovtsev	751	5	1102
The Biradical Paradox. A. I. Burshtein and Yu. I. Naberukhin	754	5	1106
Slowing Down of Surface Reactions on Catalysts and the Mobility of Adsorbed Molecules. V. É. Vasserberg, A. A. Balandin, and T. V. Georgievskaya	757	5	1110
Theory of the Autooscillations of the Electrochemical Systems Free of Passivation and with a Falling Characteristic. A. Ya. Gokhshtein	761	5	1114
Effect of the Physicochemical Nature of a Lubricant on its Effectiveness in the Pressure Treatment of Metals. V. M. Korbut, S. Ya. Veiler, and N. V. Petrova	765	5	1118
The Kinetics of the Growth of a Carbon Surface during the Thermal Decomposition of Methane over the Range of Temperature 1400-1700°C. I. L. Mar'yasin and P. A. Tesner	767	5	1121
Chemical Reactions under Chromatographic Conditions. S. Z. Roginskii, M. I. Yanovskii, and G. A. Gaziev	771	5	1125
Degree of Dispersion and Stability of Emulsions Stabilized by Solid Emulsifiers. A. B.			

CONTENTS (continued)

	PAGE	RUSS. ISSUE	RUSS. PAGE
Taubman and A. F. Koretskii	774	5	1128
Thermomechanical Curves Study of the Thermal Transformations of Some Rubbers. B. Ya. Teitel'baum, T. A. Yagfarova, M. P. Dianov, and É. F. Gubanov	778	5	1132
The Effect of Paramagnetic Contaminates on the Nuclear Magnetic Resonance Spectra of Some Organic Substances. Yu. Ya. Shamonin and K. A. Gol'dgammer	782	5	1136
The Explosion Pressure Limit for Gaseous Hydrazoic Acid as a Function of the Spark Pulse Power. T. A. Aizatullin, V. G. Voronkov, and V. P. Zubov	784	6	1356
Explosion Method and Heat of Formation of CF_4, CF_3Cl, $CFCl_3$, and CCl_4. V. F. Baibuz	786	6	1358
Equilibrium Distribution of Tritium in Hydrogen Isotope Exchange. Ya. M. Varshavskii and S. É. Vaisberg	789	6	1361
Photoionization of Esters and Metal Carbonyls in the Gaseous Phase. F. I. Vilesov and B. L. Kurbatov	792	6	1364
Formation of Amalgams of Metals of the Iron Group on a Mercury Drop Electrode. V. F. Ivanov and Z. A. Iofa	796	6	1368
Some General Inequalities of Chemical Thermodynamics. A. S. Pleshanov	800	6	1372
Formation of Acetylene on Adiabatic Compression of Methane. D. S. Tsiklis and M. D. Borodina	804	6	1376
Radiation-Chemical Transformations of Iron Ions in $HClO_4$ Solutions Saturated with Hydrogen and Oxygen under Pressure. V. N. Shubin and P. I. Dolin	808	6	1380

KINETIC CONDITIONS FOR THE BURNING OF CONDENSED MIXTURES

N. N. Bakhman

Institute of Chemical Physics, Academy of Sciences of the USSR
Presented by Academician V. N. Kondrat'ev, April 13, 1961
Translated from Doklady Akademii Nauk SSSR, Vol. 140, No. 1,
pp. 141-144, September, 1961
Original article submitted April 8, 1961

In the general case, the burning velocity of condensed mixtures is determined by the velocity of three processes: the mixing of the components, the chemical reaction between them, and heat transfer from the reaction zone to the fresh mixture.• However, in certain cases, the mixing process has no effect on the burning velocity and the latter proceeds under kinetic conditions.

One such case has been briefly considered in an earlier paper [1]. The main point in this case is the fact that the mixing processes will have no influence on the burning velocity if they can be definitely completed within the limits of the intermediate zone between the fresh material and the reaction zone (the effect of mixing on the thermal constant will be ignored). It is obvious in this case that, in general, the burning velocity does not depend on the diameter of the particles of the components (while they are not too large), and is equal to the burning velocity of a homogeneous system of the same chemical composition.

1. Let us examine this case in more detail. To realize the given conditions, it is necessary to achieve two conditions, the first of which should be that the mutual solubility of the components at the existing temperatures in the preparatory zone must be sufficiently great.

We shall consider a mixture of two solid components for which the degree of heterogeneity•• is proportional to the particle diameter $\underline{d}$ of one component. In the preparatory zone each of the components may either remain in the solid phase or be liquefied or gasified. Hence, these variants are possible:

1) solid + solid; 2) solid + liquid; 3) solid + gas;

4) liquid + liquid; 5) liquid + gas; 6) gas + gas.

Complete mixing of the components within the limits of the preparatory zone is known to be possible in case 6, and is practically excluded in cases 3 and 5, because the amount of gas in grams which may be dissolved or sorbed by a gram of the condensed component, as a rule, is much less than the usual weight relation of the components in condensed mixtures. The gaseous component may be consumed only in the reaction zone. In cases 1, 3, and 4 the possibility that the components will be mixed completely may be assumed only for each definite mixture.

2. The conditions in question may only be observed with sufficiently small values of $\underline{d}$ (with $d \leq d_{min}$). The value d_{min} increases with increase in the diffusion velocity and has a lower limit because, in every case, it must exceed the effective diameter of the molecules

•With the thermal mechanism of burning.

••The degree of heterogeneity may be defined as the value proportional to $\frac{1}{N}\sum_{i=1}^{N} x_i$, where $\sum_{i=1}^{N} x_i$ is the path which the molecules of the given mixture of the components must pass through (the original components or those formed as a result of decomposition, if this precedes the mixing), in order to obtain a completely homogeneous mixture (on the molecular scale). In certain important special cases (cf. the earlier paper by Belyaev and the author [2]), the degree of heterogeneity is proportional to the particle diameter of one of the components.

$$d_{min} \gtrsim 10^{-8} \div 10^{-7} \text{ cm}. \tag{1}$$

As a consequence, in the conditions under examination, the second condition is that the mutual diffusion velocity of the components should not be too small [such that condition (1) is satisfied].

Starting from the considerations discussed in an earlier paper [1], we shall follow the mutual diffusion of the components in a certain section of the charge (x = 0). In the time dt, the boundary of the mixing zone shifts in a transverse direction by a value of the order:

$$d(y^2) \sim D\,dt, \tag{2}$$

where D cm²/sec is the diffusion coefficient. Assuming that the combustion front with respect to the given section moves with a constant velocity v, we may write x = x' − vt, where x' is measured from the combustion front. Using the known expression for the thermal wave profile in front of the combustion front

$$x' = \frac{a}{v} \ln \frac{T - T_0}{T_m - T_0}, \tag{3}$$

where a cm²/sec is the thermal diffusivity, and where the temperatures T_0 and T_m refer respectively to the cold mixture and the reaction zone. After substitution of dt = dx'/v in (2), and integration from the order of magnitude, we find that d_{min} is equal to:

$$d_{min} \sim \frac{1}{m} \sqrt{\frac{\bar{\lambda}}{\bar{c}}} \left[\int_{T_1}^{T_m} \frac{\rho D}{T - T_0} dT \right]^{1/2}, \tag{4}$$

where m g/cm² · sec is the mass burning velocity (with $d \leq d_{min}$), ρ g/cm³ is the density; we take average values along the preparatory zone for the value $\bar{\lambda}$ cal/cm · sec · deg and $\bar{c}$ cal/g · deg. If phase conversions take place in this zone, then it is divided into certain sectional subzones and integration of Eq. (4) is carried out in succession for each of them. For brevity we shall assume that the mixture mainly occurs in one subsectional zone lying in the range from T_1 to T_m (where $T_0 < T_1 < T_m$). For the mutual diffusion of gases, usually $D = D_0(T/T_0)^n$, where n = = 1.75-2. With n = 2, from (4) we obtain

$$d_{min} \sim \frac{1}{m} \sqrt{\frac{\bar{\lambda}}{\bar{c}} \rho_0 D} \sqrt{\frac{T_m - T_1}{T_0} + \ln \frac{T_m - T_0}{T_1 - T_0}}. \tag{5}$$

For diffusion in solid and liquid phases, $D = D_0 e^{-Q/RT}$, and then from (4) it follows that

$$d_{min} \sim \frac{1}{m} \sqrt{\frac{\bar{\lambda}\bar{\rho}}{\bar{c}}} \times \times \sqrt{D_0 \{ \mathrm{li}(e^{-Q/RT_1}) - \mathrm{li}(e^{-Q/RT_m}) + e^{-Q/RT_0} [\mathrm{li}(e^{Q/RT_0} e^{-Q/RT_m}) - \mathrm{li}(e^{Q/RT_0} e^{-Q/RT_1})] \}}. \tag{6}$$

The value li z is obtained from tables, but with Q >> RT (for example with $e^{-Q/RT} < 10^{-4}$ and $e^{Q/RT_0} e^{-Q/RT} > 10^4$) it is possible to assume that li z is approximately equal to z/ln z with an error of not more than 10-12%. If, in addition, $e^{-Q/RT_m} \gg e^{-Q/RT_1}$, then from (6) we obtain

$$d_{min} \sim \frac{1}{m} \sqrt{\frac{\bar{\lambda}\bar{\rho}}{\bar{c}}} \sqrt{D_0 \frac{RT_m}{Q} e^{-Q/RT_m}}. \tag{7}$$

In principle, formulas (5), (6), and (7) allow us to calculate d_{min} for each definite system.

3. It is of interest to calculate the range in which the value d_{min} applies for a given type of system. This is easily obtained for the variant gas + gas. The fact is, that the value of the complex $\vartheta = \sqrt{\frac{\bar{\lambda}}{\bar{c}} \rho_0 D_0}$ for all gases which may appear as gasification products of different condensed mixtures, and for which there are tables of data, vary within comparatively narrow limits: thus, for example, at temperatures from about 200-300°C, assuming T_0 = = 273°K, all di- and triatomic gases, different gaseous hydrocarbons including extremely heavy hydrocarbons, vapors of many organic liquids, etc., fall within the range $\vartheta = 10^{-4}$-10^{-3} g/cm · sec. Moreover, if the relation m(p,T), which is obtained from experiment, is not considered, then the right-hand part of Eq. (5) does not depend on pressure

and depends comparatively slightly on the choice, within a reasonable range of temperatures, of T_m, T_1, and T_0. Assuming, for example, that the temperatures T_m and T_1 may vary independently within the ranges 1500-3000°K and 600-1000°K, respectively, we obtain from (5) the following range of values of d_{min}:

$$d_{min} \sim \frac{1.5 - 35}{m} \mu. \quad (8)$$

In the work of Belyaev and the author [2], the experimental value of d_{min} for a stoichiometric mixture of $KClO_4$ and bitumen with $m \simeq 0.2$ g/cm² · sec was approximately 70μ, which lies within the calculated limits in formula (8).•

The conditions for the variants liquid + liquid, solid + liquid, and especially solid + solid are far worse because there are no data on diffusion in systems of metal + salt, tar + salt, etc. Indirect data (diffusion of metals in metals and slags, mutual diffusion of salts, etc.), show that for solid + solid systems the diffusion coefficient depends extremely slightly on the nature of the components, and this eliminates the possibility of any kind of estimation of d_{min} from indirect data. For diffusion in a liquid phase the dependence on the properties of the components is considerably less, but the range of values of d_{min}, which gives indirect data, being substituted in Eq. (6) (with reasonable assumptions with regard to the range of variation of T_1 and T_m) nevertheless is made up of about four series. Such a wide range in the determination is of no practical interest.

4. There is still one case, when the burning of condensed mixtures may occur under kinetic conditions. It will be observed if the reaction proceeds on the surface of the particle of one component where the supply rate of the second component does not limit the velocity of the whole process. It is necessary here that the degree of heterogeneity and the value of T_m should not be too great, and that D_1 should be $\gg D_2$, where D_1 and D_2 are, respectively, the diffusion coefficients of the first component (the reacting particle) and the second component in the reaction products. This case is most apparent for the variant solid + gas, where it is possible to derive data on the combustion of carbon in air or oxygen. The combustion of condensed mixtures where this variant is realized in the reaction zone has been considered in other investigations [3,4]. In addition, as distinct from the case considered above in paragraphs 1-3, in this case the burning velocity u depends on the diameter of the particles (Novozhilov [4] obtained u as approximately equal to $d^{-1/3}$) and, consequently, the heterogeneous system here is not equivalent to the homogeneous system. Apart from the variant solid + gas, this type of system, in principle, may be observed for the variants solid + liquid and (less probably) liquid + liquid.

5. In conclusion, we observe that the kinetic conditions of combustion, related to the mixture of components in the preparatory zone is of major importance in understanding the normal burning velocity u_n of condensed mixtures. The latter must satisfy stationary conditions and is reproduced in an identical manner. Meanwhile, with $d > d_{min}$, the burning velocity undergoes a variation with a period of approximately d/u, and may be considered constant only with sufficiently long charges. Moreover, it is practically impossible to prepare a mixture absolutely identical with the standard, since for this it is necessary to select particles not only with the same size distribution but with the same shape, etc. Of course, mistakes because of nonstationary combustion and dissimilarity of the mixtures may be made extremely small, but it is of fundamental importance to note that with $d \leq d_{min}$ they definitely disappear and the burning velocity acquires the meaning of a physicochemical constant ($u = u_n$).

I wish to express my thanks to A. G. Merzhanov, L. G. Bolknovitinov, and S. S. Novikov for a discussion of the results.

LITERATURE CITED

1. N. N. Bakhman, Dokl. Akad. Nauk SSSR 129, 5, 1079 (1959).
2. N. N. Bakhman and A. F. Belyaev, Dokl. Akad. Nauk SSSR 133, 4, 866 (1960).
3. O. I. Leipunskii, Zhur. Fiz. Khim. 34, 1, 177 (1960).
4. B. V. Novozhilov, Dokl. Akad. Nauk SSSR 131, 6, 1400 (1960).
5. N. N. Bakhman, Dokl. Akad. Nauk SSSR 137, 5, 1141 (1961).

• In the paper by Belyaev and the author [2], the expression for d_{min} was derived by considering both molecular and turbulent diffusion. However, from the discussion in a recent paper by the author [5], and from formula (8), it was shown that it is obviously necessary to consider molecular diffusion only at values close to d_{min}.

ACTIVE INTERMEDIATE STATES DURING THE MECHANICAL DISINTEGRATION OF POLYMERS*

P. Yu. Butyagin

(Presented by Academician V. N. Kondrat'ev, April 13, 1961)
Translated from Doklady Akademii Nauk SSSR, Vol. 140, No. 1,
pp. 145-148, September, 1961
Original article submitted April 6, 1961

Intensive mechanical action on polymeric materials is accompanied by disintegration of the structure of the material and by destruction of the macromolecules [1]. In our work, attention has been mainly directed to the intermediate states in this process; they were studied in solid polymers where secondary reactions are strongly hindered, especially at low temperatures.

The polymeric materials were mechanically treated in a laboratory vibromill [2] for which it was possible to change the medium, the temperature, and the intensity of the energy supplied. The degree of disintegration of the solid polymer was estimated from the changes in the specific surface area (S) measured by the BET method, and the destruction of the macomolecules from the fall in the molecular weight (viscometric method). The concentration, structure, and conversion of free radicals were studied by means of electron paramagnetic resonance (epr) in a radiospectrometer of the type described in [3]. The luminescence accompanying the destruction was registered by means of the FEU-19 electronic photomultiplier. The following polymers were investigated: polymethylmethacrylate (PMMA), polystyrene (PS), polyacrylonitrile (PAN), polyvinyl alcohol (PVA), polyacrylic ester (PAE), linear polyethylene (PE), a copolymer of polystyrene with divinylbenzene (CPS), poly α-methylstyrene (PMS), and carboxymethyl cellulose (CMC) (see Fig. 3).

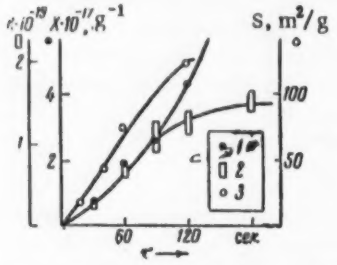

Fig. 1. Destruction of PMMA at 77°K: 1) number of broken bonds X; 2) concentration of radicals R; 3) specific surface area S.

During mechanical dispersion of polymers, as in other solids, an increase in the specific surface area was observed. As a rule, S increased with time in a linear fashion, up to a definite limit; the limit and the rate of increase strongly depended on the temperature under otherwise equivalent conditions.

For PMMA, PS, polypropylene – polymers of the vinyl series with a CH_3 group in the α-position – S reached 120-150 m^2/g (Fig. 1, curve 3) in 2-3 mins. Such high values were only obtained in those experiments for which the dispersion measurements and all intermediate operations were carried out at the temperature of liquid nitrogen, 77°K. During gradual warming of the samples (see Fig. 2) near 130°K, intensive sintering occurred with tenfold decrease of the surface area to 3-8 m^2/g. Under ordinary conditions, i.e., considerably above the temperature of sintering, the final S values were essentially at the dispersion limit for the polymers.

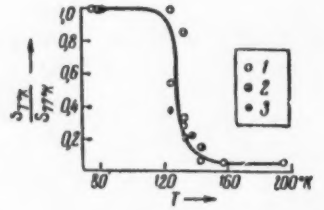

Fig. 2. Specific surface area: 1) PMMA, $S_{77°K}$ = 115 m^2/g; 2) PMS, $S_{77°K}$ = 150 m^2/g; 3) polypropylene $S_{77°K}$ = 27 m^2 per g.

The sintering indicates the occurrence of activeness in the stressed macromolecules at 120°K. This effect is possibly associated with a

*I. V. Kolbanev and A. R. Kuznetsov assisted in carrying out the experiments.

structural transition on warming up, dependent on the freedom of rotation of the α-methyl groups which was detected around this temperature by the method of nuclear magnetic resonance [4,5]. For polymers with H atoms in the α-position, the temperature of sintering must be considerably below 77°K and possibly for this reason in none of the experiments with PS, PAN, PVA, etc., was a surface area attained greater than 10-15 m^2/g.

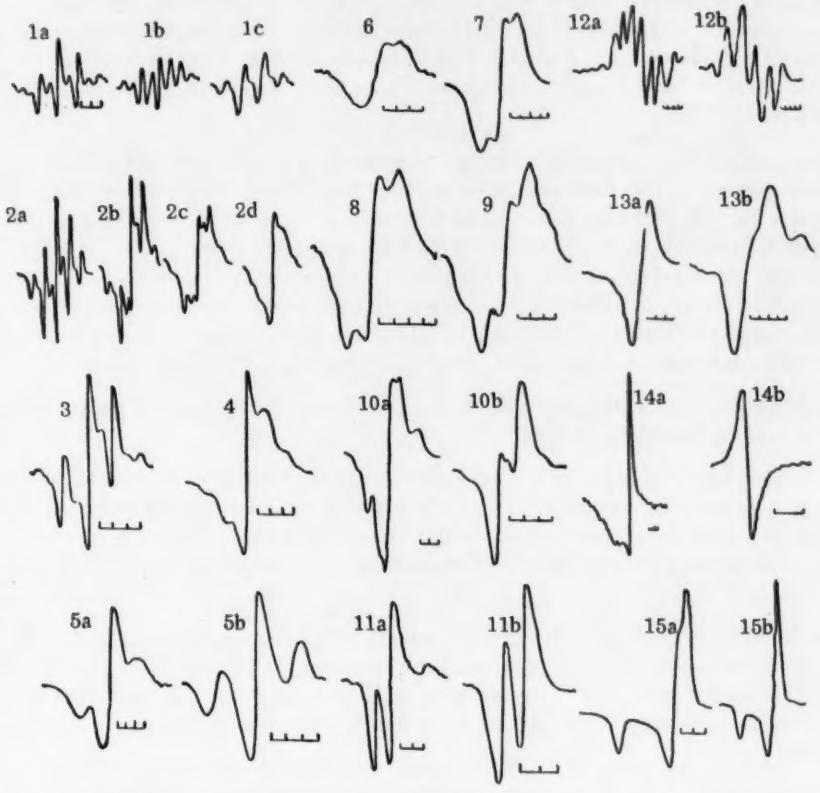

Fig. 3. Electron paramagnetic resonance spectra: 1) PMMA; 2) reaction of PMMA with acrylonitrile; 3) PAE; 4) PAN; 5) PVA; 6) PS; 7) and 8) CPS; 9) PMS; 10) gelatine; 11) CMC; 12) PE; 13) cellulose; 14) quartz; 15) spectra of the peroxide radicals in PMMA and PE. The spectra 5b, 8, and 13b, obtained after radiation destruction, the rest after mechanical destruction. Scale – one division equals 20 oersteds.

During observations of the light emission, a characteristic intensive luminescence was noted consisting of flashes following one after the other, corresponding to disintegration of individual granules of polymer; it was observed in quartz, PMMA, PS, PAE, etc., at room temperature. For natural rubber and PE a weaker luminescence was observed in the process of relaxation of the stresses, for a rapid break of the pressure applied to the sample. Continuous chemiluminescence of the type described in [6] arose through recombination of peroxide radicals. Measurement of the luminescence was a convenient method of stage-wise investigation and detection of destruction.

The molecular weight of the investigated linear polymers after mechanical treatment was reduced by 10 to 100 times, as a rule to $M \sim 10^4$. Under the experimental conditions the limit of destruction was reached in 10-20 mins. In three-dimensional systems there was a considerable increase in solubility of the polymer; an analogous effect for quartz was known previously [7].

In experiments where the molecular weight is measured over a wide enough range (PMMA, PS, PAN), the rate of destruction follows very satisfactorily an exponential [8] law (Fig. 1, curve 1):

$$M = M_0 \exp(-k\tau), \text{ или } X \approx A \exp(k\tau),$$

where $X = 6 \cdot 10^{23} \left(\frac{1}{M} - \frac{1}{M_0}\right)$ is the number of broken bonds in 1 g, k is the total destruction rate constant, and τ is the time.

E.p.r. spectra of radicals, arising during the mechanical destruction, are shown in Fig. 3. Radicals with a free valency at a carbon atom are characterized by e.p.r. spectra with hyperfine structure. The spectrum of PMMA (1a) corresponds to two stereoisomeric radicals [9]; on mild heating the spectrum of the less stable radical gradually disappears (1b), and finally a single quadruplet remains (1c). The spectra of PS, CPS, and PMS are coincident with one another; probably the spectrum may be considered not as a triplet but as a superimposition of single lines of different width, but with the same g-factor.

Radicals of this type are stable in an inert atmosphere up to temperatures close to the temperature of the glass formation. The activation energy (E) of the destruction reaction for PMMA is 37 ± 4 kcals/mole. The radicals are active and free to enter into different reactions: one with another, with monomers, with oxygen, etc. Changes of the epr spectra through reaction of the PMMA radicals with acrylonitrile are shown in Fig. 3, spectra 2a,b,c,d. Through reaction with oxygen peroxide radicals are formed (15a,b) with a characteristic anisotropic e.p.r. spectrum [10]. This reaction proceeds at 120°K and above with E = 3.8 kcals/mole. Destruction of the peroxide radicals at room temperature is completed in minutes (for PMMA, E = 16 kcal/mole), during which the rate of destruction in the stressed polymer is many times greater than in the previously unstressed material.

In quartz the primary radicals (14b) react with oxygen only during the mechanical action; otherwise this reaction does not occur even on heating up to 200°C.

For gelatine the specific e.p.r. spectrum can be observed only after destruction at 77°K (10a); on heating, this complex spectrum, corresponding to at least two different radicals, changes into double and single lines superimposed on one another (10b). A similar but simpler picture is also observed for CMC (11a,b). The spectra, stable at 77°K, correspond probably to the primary radicals and the doublet appears after migration of the free valency to an atom of oxygen [11].

The e.p.r. spectra of radicals obtained by the mechanical method in many cases coincide with the spectra of the radicals formed by the action of ionizing radiation on the polymers. For PMMA, PS, PAE, CPS, PVA, CMC, gelatine, both types of spectra are identical (see, for example, spectra 5a, 5b, 7, and 8). The difference lies only in the stability of the radicals: after irradiation they are more stable. For cellulose and quartz both types of spectra differ from each other.

The concentration of radicals in the products of the destruction were measured by the e.p.r. method and from the consumption of oxygen in their oxidation. The experimental results for PMMA are shown in Fig. 1. The curve showing the accumulation of radicals has an S-form character, and in 2-3 mins the concentration of radicals reaches the limiting value, although destruction is continued. The occurrence of limiting concentrations was found for the majority of the investigated polymers: the limiting concentrations varied from 10^{18} g^{-1} (PE, PS, PAN, PVA) to 10^{20} g^{-1} (PAE, CPS).

In Fig. 1 the scales for curves 1 and 2 differ by 40 times, i.e., the concentration of radicals which is recorded by the e.p.r. method is many times greater than the number of broken bonds, calculated from the changes in the molecular weight.

In solutions of polymers frozen at 77°K, where the macromolecules are dispersed in the crystalline lattice of the solvent, the destruction is more intensive, and the maximum concentrations of radicals are increased 10-100 times, up to $5 \cdot 10^{20}$ g^{-1} for PMMA and $3 \cdot 10^{20}$ g^{-1} for PS, dissolved in toluene, butyl acetate, acetone, etc. These, in fact, are probably also the limiting concentrations since now in one macromolecule there are 20-100 paramagnetic centers. The nature of the solvent greatly influences the course of the destruction and may indicate an unusual protective effect of benzene, dioxan, and a few other substances with respect to mechanical action in solvents at low temperatures. The e.p.r. spectra of polymers in frozen solutions remained unchanged, with the exception of special cases when solutions of polymers in monomers were investigated.

The processes of development of a new surface, diminution of molecular weight, and formation of radicals in solid polymers proved to be dissimilar from one another; the number of radicals exceeds many times the number of

breaks in the main chain, the laws of dispersion and destruction are different, etc. These discrepancies cause doubt of the fact that the main process during mechanical destruction is a break of the main chain of the macromolecule. It can be assumed that the primary act during mechanical action is the genesis of intermediate nonequilibrium states of the macromolecules; the subsequent chain of secondary processes, including rupture of bonds (probably also side chains), formation of radicals, and their transformations is already considerably determined not by the primary action but by the structure of the polymer or, more precisely, by the structure of the polymer in the stressed state. From this point of view, the anomalously high concentrations of radicals and the similarity between radiation and mechanical destruction of the polymers becomes explicable.

LITERATURE CITED

1. A. A. Berlin, Usp. Khim. 27, 94 (1958).
2. M. I. Aronov, Pribory i Tekhn. Eksp. No. 1, 153 (1959).
3. A. G. Semenov and N. N. Bubnov, Pribory i Tekhn. Eksp. No. 1, 92 (1959).
4. K. M. Sinnot, J. Polymer Sci. 42, No. 139, 3 (1960).
5. J. G. Powles and H. S. Gutowsky, J. Chem. Phys. 21, 1695 (1953).
6. R. F. Vasil'ev, O. N. Karpukhin, and V. Ya. Shlyapintokh, Doklady Akad. Nauk SSSR 125, 106 (1959).
7. G. S. Khodakov and E. P. Plutsis, Doklady Akad. Nauk SSSR 123, 725 (1958).
8. B. V. Pavlov, Bysokomolek soed. 1, 1227 (1959).
9. R. J. Abraham, H. W. Melville, D. V. Ovenall, and D. H. Wiffen, Trans. Faraday Soc. 54, 1133 (1958).
10. Yu. N. Molin, Yu. D. Tsvetkov, and V. V. Voevodskii, Zhur. Tekh. Fiz. 33, 1231 (1959).
11. L. A. Blyumenfel'd and A. E. Kalmanson, Biofizika 2, 552 (1957).

All abbreviations of periodicals in the above bibliography are letter-by-letter transliterations of the abbreviations as given in the original Russian journal. *Some or all of this periodical literature may well be available in English translation.* A complete list of the cover-to-cover English translations appears at the back of this issue.

ELECTROCHEMICAL DETERMINATION OF THE HEAT OF ADSORPTION OF HYDROGEN ON FINELY DIVIDED PALLADIUM

Zh. L. Vert, I. A. Mosevich, and I. P. Tverdovskii

Leningrad State Institute of Applied Chemistry
(Presented by Academician A. N. Frumkin, April 19, 1961)
Translated from Doklady Akademii Nauk SSSR, Vol. 140, No. 1,
pp. 149-152, September, 1961
Original article submitted February 18, 1961

When the absorption of hydrogen by palladium is investigated in the gas phase, one cannot separate the adsorption and solution stages. This can only be accomplished in the presence of an electrolyte by studying appropriate charge curves [1].

Hydrogen is adsorbed on palladium over a wide range of pressures from 10^{-10}-10^{-2} atm, while the specific adsorption of anions from solution shows up in the shape of corresponding isotherms. In acidic solutions the effect of anions on the hydrogen–metal bond decreases in the order $Br^- > Cl^- > SO_4^{2-}$. Experiments done on platinum electrodes [2] have shown that the specific adsorption of SO_4^{2-} ions is quite insignificant, and hence one would expect the heat of adsorption of hydrogen on palladium determined in sulfuric acid to be in best agreement with data obtained for adsorption from the gas phase.

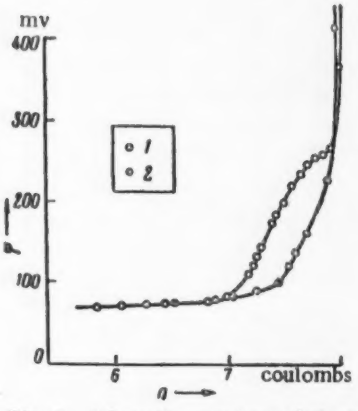

Fig. 1. Adsorption sections of charge curves recorded on Pd electrode in: 1) 1N H_2SO_4; 2) 1N HCl; t = 18°.

The manner in which the experiment is set up, and the description of apparatus used for recording the charge curves are given elsewhere [1]. The method itself was slightly altered: the hydrogen dissolved in palladium was ionized with a 0.6 mamp current, but when the adsorption section of the charge curve was studied the current was reduced to 0.1 mamp. Palladium black (0.006-0.012 g) was deposited on a platinum electrode from a hydrochloric acid solution of $PdCl_2$ at a current density of 70 mamp/cm^2. To avoid errors arising from the shrinkage of surface area caused by heating, the first experiment was always done at the highest temperature which, in our case, was 43°C. Charge curves obtained in different electrolytes enabled us to separate the absorption region from the adsorption region since the ionization of dissolved hydrogen is independent of the nature of the electrolyte.

In general, the adsorption sections of charge curves obtained on palladium in hydrochloric and sulfuric acids all look like those shown in Fig. 1. Since there is considerable adsorption of Cl^- ion, the bonding between the adsorbed hydrogen atom and the metal is weakened, so that the ionization requires less energy and the charge curve in HCl falls at lower anodic potentials than the corresponding curve in H_2SO_4.

The characteristic leveling at φ = 250 mv* found on all the palladium charge curves obtained in sulfuric acid has previously been reported for several Pd – Ag alloys [3]. This section appears on both anodic and cathodic charge curves and changes very little in shape when the temperature is changed. In HCl the leveling occurs at lower φ and is not so pronounced. The point at which the charge curves of any one electrode determined in different solvents separately gives the potential and consequently the pressure at which the hydrogen begins to dissolve. Without introducing any significant errors, one can assume that the adsorption of hydrogen is completed at that potential and the entire Pd surface is covered with hydrogen.

*All the potentials are with reference to a hydrogen electrode in the same solution.

At 43° our palladium black adsorbs 0.09 mole H/mole Pd. Slightly less material is adsorbed at lower temperatures.

Experiments were carried out at 43, 23, 18, and 0° using the same electrode and without taking the apparatus apart; the temperatures were simply varied by changing the settings on the thermal regulator. Since the entire cycle lasted from 2 to 4 days, the surface area of the palladium black would change a little, and hence adsorption sections of charge curves obtained at 43°C at the beginning and the end of the cycle differed slightly in length.

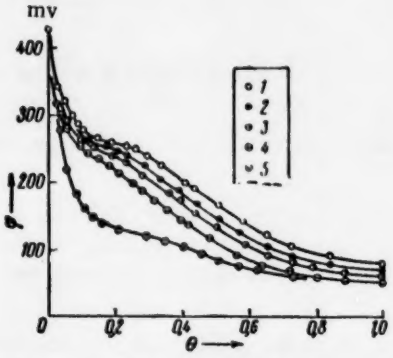

Fig. 2. The Pd electrode potential as a function of the fraction of surface covered by hydrogen. H_2SO_4: 1) 0°; 2) 18°; 3) 23°; 4) 43°; HCl: 5) 43°.

In working with individual curves we determined the beginning of adsorption ($\theta = 0$) from the point at which the slightly inclined portion of the charge curve changed into the sharply rising linear section, which represents the charging of the double layer (φ = 400 to 700 mv); the beginning of solution ($\theta = 1$), as we have already pointed out, was determined from the point at which the charge curves for any one electrode determined in two different electrolytes (HCl and H_2SO_4) part. The major error in the determination of the point at which adsorption begins occurs in the potential, while errors along the time axis (amount of current) are small.

A series of individual experiments at 43, 23, 18, and 0°C showed that hydrogen begins dissolving at 54, 65, 70, and 82 mv, respectively. In determining the length of our charge curves we made a correction for the quantity of current needed to charge the double layer at potentials in the range from beginning of solution to the start of adsorption, just as was done by A. N. Frumkin and A. N. Shlygin [4] in their study of the platinum electrode.

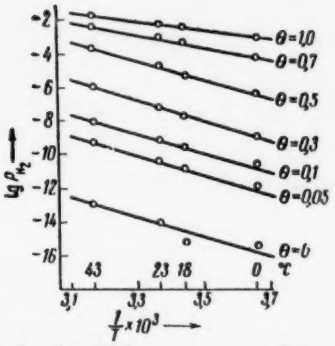

Fig. 3. $(\log P_{H_2})\theta$ = const. as a function of temperature for Pd in H_2SO_4.

Adsorption sections of charge curves (plotted as surface coverage versus voltage) determined at any one temperature coincided to within 2-3 mv, whether determined on the same electrode or on different amounts of palladium black. Experimental results from measurements done at four different temperatures in H_2SO_4 are shown in Fig. 2. Since the Nernst equation relates the electrode potential to pressure, our curves represent adsorption isotherms plotted in $\log P_{H_2}$ and θ coordinates. Right after the leveling at φ = 240-260 mv is the linear portion of the charge curve, which corresponds to the semi-log adsorption isotherm [5]. Subsequent inclined section represents large surface coverages. Similar experiments were done in HCl solutions. In Fig. 2 we have also included the adsorption section of the corresponding charge curve determined at 43°. In this case though the leveling before the linear portion is less pronounced than in the case of H_2SO_4 solutions; it extends to larger values of θ.

Using the Clausius-Clapeyron equation we can calculate from our experimental data the heat of adsorption of hydrogen on palladium for a given θ.

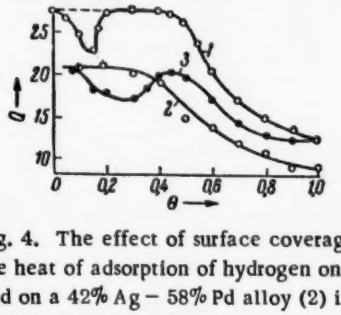

Fig. 4. The effect of surface coverage on the heat of adsorption of hydrogen on Pd(1) and on a 42% Ag − 58% Pd alloy (2) in H_2SO_4; on Pd in HCl (3).

The data plotted in Fig. 3 for several surface coverages show that $(\log P)_{\theta = \text{const.}}$ is inversely proportional to temperature.

The slight scattering of points at small θ and 0°C results from the fact that at lower temperatures the first leveling on the charge curve (Fig. 2) extends over a wider range of surface coverages. The calculated heats of adsorption Q are shown in Fig. 4. We find that, in the presence of SO_4^{2-} ions the heats of adsorption remain constant in the range $0 < \theta < 0.5$; the same has previously been reported by

Maxted and Hassid [6] and Quan [7] for the adsorption of hydrogen on platinum. The heat of adsorption remains independent of coverage over almost the entire semilog region of the isotherm. At these θ values the heat of adsorption of hydrogen on palladium is 27.5 kcal/mole, which is very close to the value reported by Beek [8] for adsorption from the gas phase; as the metal surface becomes more extensively covered, Q declines. In its general appearance the curve of heat of adsorption versus surface coverage resembles the plot of $Q = f(\theta)$ for the sliding layers formed during the dissociation of diatomic molecules into atoms [9].

The very small values of Q at θ = 0.05-0.15 may result from the fact that we are dealing with different forms of hydrogen-to-metal bonds.

As one would expect, in HCl solutions the heat of adsorption of hydrogen on palladium is much lower (Fig. 4). The region of constant Q is in this case almost completely distorted.

The way in which the heat of adsorption of hydrogen on palladium varies with surface coverage resembles the corresponding heat of solution curve [10].

We also determined the heats of adsorption on several Pd – Ag alloys in 1 N H_2SO_4. An alloy containing 8 mole% silver yielded the same $Q = f(\theta)$ curve as pure Pd. Charge curves determined on alloys containing more than 32% Ag exhibited no leveling at φ = 240-260 mv; similarly, the curve shown in Fig. 4 for an alloy containing 42% Ag shows no distortions at low θ values.

Our results for Pd are similar to those reported by Bold and Breiter [11] for Rh though they used a slightly different electrochemical technique for determining the heat of adsorption of hydrogen as a function of θ. They also reported that only in the range $0.5 \leq \theta \leq 0.75$ does the heat of adsorption on Pt change a little. The linear relationship between Q and θ in the semilog portion of the isotherm was not observed in all their cases.

The authors wish to thank Academician A. N. Frumkin for his valuable comments and appraisal of our results.

LITERATURE CITED

1. A. I. Stetsenko and I. P. Tverdovskii, Zhur. Fiz. Khim. 26, 647 (1952).
2. A. M. Shlygin, A. N. Frumkin, and V. I. Medvedovskii, Acta physicochimica URSS 4, 922 (1936).
3. Zh. L. Vert and I. P. Tverdovsky, Zhur. Fiz. Khim. 28, 317 (1954).
4. A. N. Frumkin and A. M. Shlygin, Izv. AN SSSR, ser. khim. 5, 773 (1936).
5. A. M. Shlygin and A. N. Frumkin, Acta physicochimica 3, 791 (1935).
6. E. Maxted and N. Hassid, J. Chem. Soc. 30, 3313 (1931).
7. T. Quan, Catalysis, A Study of Heterogeneous Reactions [Russian translation] (IL, 1956) p. 314.
8. O. Beeck, Disc. Faraday Soc. 8, 118 (1950).
9. B. Trepnel, Chemisorption [Russian translation] (IL, 1958) p. 202.
10. R. A. Karpova and P. A. Tverdovskii, Zhur. Fiz. Khim. 33, 1393 (1959).
11. W. Bold and M. Breiter, Z. Electrochem. 64, 897 (1960).

All abbreviations of periodicals in the above bibliography are letter-by-letter transliterations of the abbreviations as given in the original Russian journal. *Some or all of this periodical literature may well be available in English translation.* A complete list of the cover-to-cover English translations appears at the back of this issue.

CRITICAL PHENOMENA IN THE OXIDATION OF HYDROCARBONS IN THE PRESENCE OF INHIBITORS IN OPEN SYSTEMS

A. B. Gagarina, Z. K. Maizus, and Corresponding Member of the Academy of Sciences of the USSR, N. M. Émanuél

Institute of Chemical Physics, Academy of Sciences of the USSR
Translated from Doklady Akademii Nauk SSSR, Vol. 140, No. 1, pp. 153-156, September, 1961
Original article submitted May 20, 1961

According to current ideas on the oxidation of hydrocarbons, a chain production-branching reaction occurs in the liquid phase. The chemical mechanism of the reaction may be represented by the following sequence of elementary stages:

0) $RH + O_2 \xrightarrow{\omega_0} R^\cdot$	Production of chains
1) $R^\cdot + O_2 \xrightarrow{k_1} RO_2^\cdot$	Continuation of chains
2) $RO_2^\cdot + RH \xrightarrow{k_2} ROOH + R$	
3) $ROOH \xrightarrow{k_3} RO^\cdot + OH^\cdot$	Degenerate branching
4) $RO_2^\cdot + RO_2^\cdot \xrightarrow{k_4}$	Breaking of chain
i) $RO_2^\cdot + In\,H \xrightarrow{k_i} ROOH + In^\cdot$	

N. N. Semenov [1] has shown that if the oxidation is carried out in the presence of inhibitors some critical inhibitor concentration should exist, below which an autoaccelerated reaction is observed, and above which a very slow stationary process is observed.

The experimental proof of the existence of a critical inhibitor concentration was given in [2]. Studying the kinetics of the buildup of hydroperoxides during the oxidation of n-decane in the presence of α-naphthol, we have shown that at an α-naphthol concentration above critical, the decane is practically not oxidized; what is observed is simply decomposition of the hydroperoxides built up in the system before the inhibitor is added. A slight reduction in the α-naphthol concentration is sufficient to change the nature of the reaction completely. The reaction becomes autoaccelerated as in the absence of inhibitor.

Some papers have been published recently which established the critical nature of the relation between the induction period for the oxidation of polypropylene and the concentration of inhibitors, which were phenol and amines [3, 4].

The critical inhibitor concentration phenomenon and the oxidation of n-decane has so far been studied by us in a closed system. However, these phenomena should be observed in open systems too, i.e., in systems which exchange not only energy but also matter with the external medium. The exchange rate is determined by the parameter $v = W/V$, where W is the volume of material entering the vessel per unit time, and V is the volume of the reacting mixture.

The change in concentration of the components of a reaction in an open system is the result not only of chemical transformations but of material exchange. A characteristic property of an open system is the establishment of a stationary state after a certain period of time, which depends on the rate of the chemical reactions and the rate of exchange.

A mathematical analysis of the kinetic scheme describing the oxidation of hydrocarbons in the presence of inhibitors in an open system has been given by V. M. Andreev. It was shown that if the inhibitor is added continuously

to the reaction vessel along with the initial hydrocarbon and the reaction products are removed continuously at the same rate, two types of kinetic curves can occur for the buildup of primary reaction product (peroxide), corresponding either with the stationary or with an autoaccelerated development of the reaction. At some critical inhibitor concentration a sharp change should be observed in the stationary peroxide concentration, which corresponds with the transition from one form of the process to the other.

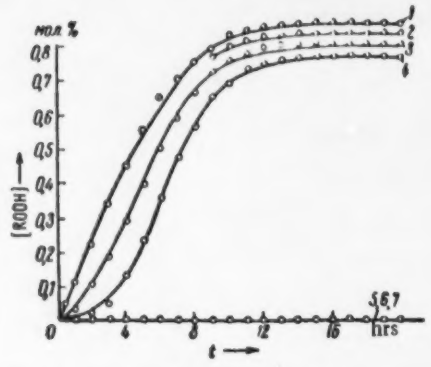

Fig. 1. Kinetic curves of the buildup of hydroperoxides in the oxidation of n-decane in an open system at 135°, with the following concentrations of α-naphthol (in mol/ml): 1) pure decane without inhibitor; 2) $3.0 \cdot 10^{-9}$; 3) $7.50 \cdot 10^{-9}$; 4) $9.0 \cdot 10^{-9}$; 5) $9.05 \cdot 10^{-9}$; 6) $9.2 \cdot 10^{-9}$; 7) $1 \cdot 10^{-8}$.

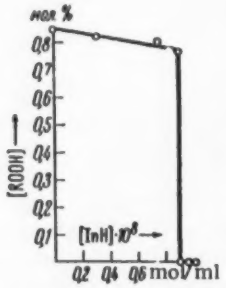

Fig. 2. Stationary concentration of hydroperoxides in a function of inhibitor concentration in the oxidation of n-decane in an open system at 135°.

The present paper gives the results of an experimental investigation of the critical inhibitor concentration phenomenon in the oxidation of n-decane in an open system.

The experiments were made according to the technique described in [5]. Five ml of decane containing inhibitor was admitted to the vessel, and from the very beginning of oxidation the same solution of inhibitor in decane was automatically added continuously to the vessel at a rate of 2.6 ml/hr. Here, $v = 0.53$ hour^{-1}. Oxygen was bubbled through the reacting mixture at a rate of 1.6 liter/hr, which, at the same time, provided the necessary mixing of the mixture. The reaction was monitored from the buildup of peroxides, which were analyzed iodometrically.

Figure 1 shows a series of kinetic curves where the peroxide buildup at 135° for different inhibitor concentrations. For the slight change in inhibitor concentration from $9 \cdot 10^{-9}$ to $9.05 \cdot 10^{-9}$ mol per ml, the value of the stationary concentration of hydroperoxides dropped sharply (practically to zero).

The critical nature of the stationary peroxide concentration has a function of the concentration of inhibitor in a decane added to the reaction and is likewise truly visible in Fig. 2.

Thus, for α-naphthol concentrations less than $9 \cdot 10^{-9}$ mol/ml the oxidation of n-decane develops as a chain formation-branching reaction, in which the stationary concentration for peroxides drops off proportionally to the increase in the initial concentration of inhibitor. Increasing the inhibitor concentration above the critical value, equal to $9 \cdot 10^{-9}$ mol/ml, the system goes over into another stationary state, where the scale of the chemical reaction in the system is determined solely by the formation of primary active centers.

The kinetics of hydrocarbon oxidation in the presence of an inhibitor in an open system in accordance with the mechanism described above is given by the following differential equations:

$$\frac{d[RO_2^{\cdot}]}{dt} = \omega_0 + k_3[ROOH] - k_4[RO_2^{\cdot}]^2 - k_i[RO_2^{\cdot}][InH] - v[RO_2^{\cdot}]; \quad (1)$$

$$\frac{d[ROOH]}{dt} = k_2[RO_2^{\cdot}][RH] - k_3[ROOH] - v[ROOH]; \quad (2)$$

$$\frac{d[InH]}{dt} = -k_i[RO_2^{\cdot}][InH] + v[InH]_0 - v[InH], \quad (3)$$

where $v[RO_2^{\cdot}]$, $-v[ROOH]$, $-v[InH]$, and $v[InH]_0$ are terms giving the change in concentration of the components in question as a result of replacement and continuous addition of inhibitor to the reaction vessel.

The stationary state of the open system is described by the algebraic equations obtained from Eqs. (1), (2), and (3) by setting the derivatives equal to zero.

The solution of the system of algebraic equations leads to an expression for the stationary concentration of the radicals $[\overline{RO_2^{\cdot}}]$ as a function of the initial concentration of inhibitor $[InH]_0$:

$$[\mathrm{In}\,H_0] = \left(\frac{[\overline{RO_2^{\cdot}}]}{v} + \frac{1}{k_i}\right)\left(\frac{2a_2k_3}{k_3+v} - v + k_4[\overline{RO_2^{\cdot}}] + \frac{\omega_0}{[\overline{RO_2^{\cdot}}]}\right), \quad (4)$$

where $[\overline{RO_2^{\cdot}}]$ is the stationary concentration of radicals and ω_0 is the rate of formation of the chains

Since Eq. (2) gives a linear relationship between $[\overline{RO_2^{\cdot}}]$ and $[\overline{ROOH}]$, $[\overline{ROOH}] = \frac{a_2}{k_3 + v}[\overline{RO_2^{\cdot}}]$, the curve of slant $[\overline{ROOH}]$ against $[InH]_0$ remains the same.

This relationship is shown graphically in Fig. 3. Mathematical analysis of Eq. (4) showed that in the oxidation of hydrocarbons in the presence of an inhibitor there are two stable stationary states: ab and cd. The state bc is unstable and does not exist in reality. Thus, for example, if the inhibitor concentration is equal to [InH], and the initial peroxide concentration at the moment the reaction enters the continuous cycles lies within the region l – m, the open system goes into state m. If, on the other hand, the initial concentration of peroxides lies in the range l – n, the open system goes into state n. It also follows from Fig. 3 that the critical inhibitor concentration depends on the initial concentration of peroxides. In the oxidation of pure decane, the change in the open system as a function of inhibitor concentration should follow the path afcd. This is the part which we used in our experiments (Fig. 2).

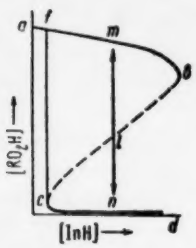

Fig. 3. Theoretical curve of the stationary concentration of radicals as a function of inhibitor concentration in continuous oxidation of a hydrocarbon.

V. M. Andreev has found the following expression for the critical inhibitor concentration $[InH]_{cr}$ in the oxidation of pure decane:

$$[InH]_{cr} = 2\sqrt{\frac{2a_2k_3\omega_0}{k_i v(k_3+v)}} + \frac{2a_2k_3}{k_i(k_3+v)} + \frac{\omega_0}{v},$$

from which it follows that the ratio k_1/k_2 is equal to

$$\frac{k_i}{k_2} = \frac{2[RH]k_3}{k_3+v}\cdot\frac{1}{(\sqrt{[InH]_{cr}} - \sqrt{\omega_0/v})^2}.$$

We have determined the ratio k_1/k_2 for α-naphthol using the value which we found of $[InH]_{cr} = 9 \cdot 10^{-9}$ mol per ml, and the following constants and parameters: k_3 is the rate constant of the degenerate branching of the chains [6], $v \doteq 0.5$ hrs^{-1}, $[RH] = 5.2 \cdot 10^{-3}$ mol/ml, $\omega_0 = 1.8 \cdot 10^{-9}$ mol/ml, is the rate of change formation fixed by the rate of consumption of α-naphthol in the induction period in the closed system. For these parameters we obtain

$$k_i/k_2 = e^{(E_2 - E_i)/RT} = 1{,}33 \cdot 10^5.$$

The activation energy of the reaction of the $RO_2^{\cdot}$ radical with the n-decane molecule is equal to 15.1 kcal per mol (from the data of [7]), including the recently obtained value of the rate constant for chain branching [6]. Thus, the activation energy for the reaction of $RO_2^{\cdot}$ with the α-naphthol molecule is equal to 5.4 kcal per mol.

LITERATURE CITED

1. N. N. Semenov, Some Problems of Chemical Kinetics and Reactivity [in Russian] (AN SSSR Press, 1958) p. 632.
2. A. B. Gagarina, Z. K. Maizus, and N. M. Émanuél, Dokl. Akad. Nauk SSSR 135, 354 (1960).
3. M. B. Neiman, V. B. Miller, Yu. A. Shlyapintokh, and E. S. Torsueva, Dokl. Akad. Nauk SSSR 136, 647 (1961).
4. D. Ryshava, High Molecular Compounds [in Russian] A-3, (1961) p. 464.
5. E. T. Denisov, Z. K. Maizus, I. P. Skibia, and N. M. Émanuél', Dokl. Akad. Nauk SSSR 128, 755 (1959).
6. D. G. Knorre, Z. K. Maizus, and N. M. Émanuél', Dokl. Akad. Nauk SSSR 123, 123 (1958).
7. D. G. Knorre, Z. K. Maizus, and N. M. Émanuél', Dokl. Akad. Nauk SSSR 112, No. 3 (1956).

ELECTRON PARAMAGNETIC RESONANCE IN SOME AQUEOUS COMPLEXES OF Ti^{3+}

N. S. Garif'yanov and E. I. Semenova

Physicotechnical Institute of the Kazan Branch of the
Academy of Sciences of the USSR

(Presented by Academician A. E. Arbuzov, April 17, 1961)
Translated from Doklady Akademii Nauk, SSSR, Vol. 140, No. 1,
pp. 157-158, September, 1961
Original article submitted April 13, 1961

EPR studies have been carried out in our laboratory [1] in aqueous, alcoholic, and glycerin solutions of the violet modification of the salts $TiCl_3 \cdot 6H_2O$ and $Ti_2(SO_4)_3 \cdot 4H_2O$. The EPR lines in alcoholic and glycerin solutions were observed both in the liquid and in the supercooled state. The intensity of the lines in the liquid state was very small. Resonance absorption and aqueous solutions of these salts could not be observed.

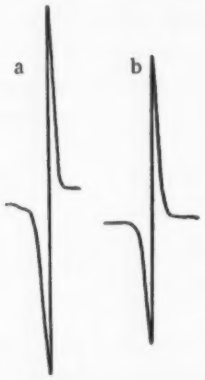

Fig. 1. EPR curves in aqueous complexes of Ti^{3+} salts: 0.1 mole/liter, $\nu = 9430$ mc at 295°K, a) for $[TiF_n(H_2O)_{6-n}]^{3-n}$, and b) $[TiI_n(H_2O)_{6-n}]^{3-n}$.

This note gives the results of studies on the EPR lines in aqueous complexes of the salts TiF_3, TiI_3, and $TiBr_3$. The green hydrated complexes* $[TiF_n](H_2O)_{6-n}]^{3-n}$ and $[TiI_n(H_2O)_{6-n}]^{3-n}$ were prepared by dissolving the salts TiF_3 and TiI_3, respectively, in hydrofluoric and hydriodic acids. The solutions were diluted with water. Dissolving the salt $TiBr_3$ in water gave the violet aqueous complex $[Ti(H_2O_6)]^{3+}$.

Solutions with two concentrations 0.01 and 0.001 M were prepared for measurement. The measurements were made in thin glass capillaries at a frequency of 9430 mc at 295°K on a standard radiospectroscope. The line width δH is given by the distance between the maximum and the minimum of the first derivative of the absorption curve. Intense EPR lines were observed in the green aqueous complexes with a spectroscopic splitting factor $G = 1.946 \pm 0.001$, and a width $\delta H = 20$ oersted, for $[TiF_n(H_2O)_{6-n}]^{3-n}$ and $g = 1.948 \pm 0.001$ and $\delta H = 16$ oersted, for $[TiF_n(H_2O)_{6-n}]^{3-n}$. It turned out that in these complexes δH and the value of the g factor remain practically unchanged when the concentration of the solutions is changed from 0.01 to 0.001 M. Obviously, the fact that δH is independent of the concentration of the solution shows that there is no effect of magnetic dipole–dipole interaction on the width. In addition to the relaxation width, which will be spoken about later, a rather large contribution to δH is also made by the magnetic moments of the protons in the F^{19} and I^{127} nuclei. As may be seen from Fig. 1, the EPR curves are somewhat asymmetric. This line asymmetry is explained by radio frequency power losses from conductivity [2], since the complexes studied are stable only in acid medium and the solutions have a large conductivity. This argument is supported by the fact that if the diameter of the glass capillary is increased the asymmetry of the curve increases.

No resonance absorption could be observed in the violet solutions of $TiBr_3$. The absence of EPR in these solutions is explained by the fact that in the octahedral $[Ti(H_2O)_6]^{3+}$ complexes by analogy with the model given in [3] for the violet aqueous $[Cr(H_2O)_6]^{3+}$ complexes, the electric field on the magnetic ion has essentially cubic symmetry with a small admixture of fields of lower symmetry, due to particles of the second coordination sphere. Since the low symmetry electric field component is small, the resulting splitting Δ of the low arbitral triplet will also be small. In view of this fact, the spin-lattice relaxation time ρ_1, at room temperature, seems to be too short.

*A detailed description of the preparation of these complexes will be given by E. I. Semenova in one of the chemical journals.

In the asymmetric complexes $[TiFn(H_2O)_{6-n}]^{3-n}$ and $[TiIn(H_2O)_{6-n}]^{3-n}$, if $n \neq 0$ and $n \neq 6$, there is a rather large axle field component, and the splitting Δ is so large that the relaxation time at room temperature will be large, since $\rho_1 \sim \Delta^6$.

Another explanation for the long spin-lattice relaxation time in aqueous complexes is to be found in a possible tetrahedral environment of the magnetic ion. In this case, the levels for Ti^{3+} will be similar to the levels of Cu^{2+}, i.e., an orbital singlet will show up underneath.

In conclusion, the authors with to express their thanks to B. M. Kozyrev for discussion of the results.

LITERATURE CITED

1. V. I. Avvakumov, N. S. Garif'yanov, and E. I. Semenova, JETP 39, 11 (1960).
2. N. I. Bloembergen, J. Appl. Phys. 23, 1379 (1952).
3. V. I. Avvakumov, N. S. Garif'yanov, B. M. Kozyrev, and P. G. Tishkov, JETP 37, 1564 (1959).

THE VAPOR PRESSURE OF THALLIUM DETERMINED BY THE USE OF RADIOACTIVE TRACERS

L. Kh. Genov, An. N. Nesmeyanov, and Yu. A. Priselkov

M. V. Lomonosov Moscow State University and the
Institute of Chemical Technology, Sofia, Bulgaria
(Presented by Academician V. I. Spitsyn, April 6, 1961)
Translated from Doklady Akademii Nauk SSSR, Vol. 140, No. 1,
pp. 159-161, September, 1961
Original article submitted March 29, 1961

Since contradictory vapor pressures have been reported by different workers for thallium [1-6], it became desirable to reexamine the problem in order to obtain more reliable data. The vapor pressure of solid thallium has not yet been reported by anyone.

We determined the vapor pressure of liquid and solid thallium, and the corresponding heats of vaporization and sublimation over a wide range of temperatures using a modification of Knudsen's effusion method and Langmuir's method (which involved evaporation from an open surface) and thallium radioisotope Tl^{204} as tracer. For our work we built an instrument similar to that described in [7]. The new apparatus differed from the old in that evaporation was achieved by heating the effusion chamber and the beaker with an electrical resistance furnace located inside the vacuum chamber.

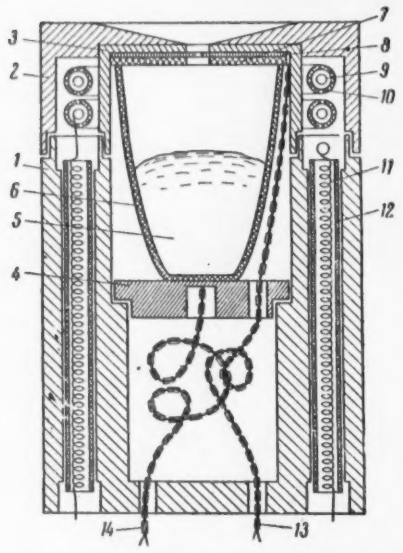

Fig. 1. Design of the effusion chamber: 1) outer shell; 2) cover; 3) molybdenum beaker; 4) crucible support; 5) thallium; 6) beryllium oxide crucible; 7) ceramic cover; 8) diaphragm with effusion hole; 9) heater for cover; 10) quartz coil; 11) heater for chamber shell; 12) ceramic tubes (12 segments); 13) and 14) chromel–alumel thermocouples.

The design of the chamber is shown in Fig. 1. The outer shell 1 and cover 2 were made of "Armco" steel while inside parts were made of molybdenum (3 and 4). Thallium metal was placed in crucible 6 (which was made of crystallized beryllium oxide), which was covered with a ceramic cover 7 and a molybdenum foil 8. The crucible was made gas-tight in the same way as before [7]. The cover and the shell were heated independently by means of two separate coils, so that a vertical temperature gradient could be set up to prevent any condensation of the metal vapor on the diaphragm. The temperatures of the diaphragm and at the bottom of the crucible were recorded by means of two chromel–alumel thermocouples connected to model PMS-48 potentiometers. Errors in the recorded temperature caused by heat losses in the thermocouples were negligible and, consequently, disregarded in our calculations. The temperatures could be determined with an accuracy of ± 0.5°.

We used very pure thallium which contained radioactive Tl^{204} and less than $1 \cdot 10^{-4}$% of each of Fe, In, Cd, Cu, Sn, and Pb metals. The specific activity of our radioactive sample was 2 mC/g. We also showed radiometrically that our Tl^{204} was not contaminated with any other radioactive materials.

The evaporation rate was determined from the radiation level of the condensed vapor. Thallium vapor condensed in the receiver was washed out with nitric acid (1:3) containing nonradioactive thallium as a carrier. Subsequently the acidic solution was neutralized with excess ammonia (2:1), heated at 60-70°C, and treated with potassium dichromate to precipitate thallium chromate quantitatively.

The precipitate was filtered on a Buchner funnel, washed with 1% potassium dichromate, and dried. The radioactivity of the precipitate was measured with a Geiger counter and compared with the activity of a reference sample.

The vapor pressure of thallium was calculated from the formula

$$\lg P = 17{,}14\, G \sqrt{\frac{T}{M}}, \qquad (1)$$

where P is the vapor pressure in mm Hg, M is the molecular weight of the vapor, T is the absolute temperature in °K, and G is the effusion velocity calculated from

$$G = \frac{g}{\tau K \sigma},$$

where g is the weight of evaporated material, τ is the exposure time, σ is the area of the effusion pinhole, and K is Klausing's coefficient.

The experimental results are shown in Table 1. To make sure that the radioactivity itself does not affect the rate of evaporation we also did a parallel set of experiments using ordinary thallium (experiments 1-4). The amount of material evaporated was, in these cases, determined polarographically [9]. It turned out that an activity of 2 mC per g has practically no effect on the experimental results.

Results obtained by the effusion method at various pinhole sizes (expts. 1-19) and by evaporation from an open surface (expts. 20-29) can all be well represented, within the range of experimental errors, by the same straight line:

TABLE 1. Thallium Vapor Pressure

Expt. Nos.	T, °K	τ, sec.	g, r	G, g/cm² · sec.	P, mm Hg	ΔH_0^0 kcal/mole
			$S = 3{,}835 \cdot 10^{-4}$ см²			
1	719	10800	$6{,}85 \cdot 10^{-6}$	$1{,}656 \cdot 10^{-6}$	$5{,}324 \cdot 10^{-5}$	43,07
2	816	3600	$53{,}5 \cdot 10^{-6}$	$3{,}875 \cdot 10^{-5}$	$1{,}327 \cdot 10^{-3}$	43,62
3	882	3600	$358 \cdot 10^{-6}$	$2{,}593 \cdot 10^{-4}$	$9{,}233 \cdot 10^{-3}$	43,63
4	912	3600	$846 \cdot 10^{-6}$	$6{,}128 \cdot 10^{-4}$	$2{,}219 \cdot 10^{-2}$	43,42
5	656	14400	$0{,}60 \cdot 10^{-6}$	$1{,}091 \cdot 10^{-7}$	$3{,}350 \cdot 10^{-6}$	43,09
6	689	10800	$2{,}30 \cdot 10^{-6}$	$5{,}553 \cdot 10^{-7}$	$1{,}750 \cdot 10^{-5}$	42,74
7	749	7200	$12{,}23 \cdot 10^{-6}$	$4{,}430 \cdot 10^{-6}$	$1{,}453 \cdot 10^{-4}$	43,30
8	790	7200	$72{,}1 \cdot 10^{-6}$	$2{,}610 \cdot 10^{-5}$	$8{,}796 \cdot 10^{-4}$	42,71
9	819	3600	$78{,}8 \cdot 10^{-6}$	$5{,}704 \cdot 10^{-5}$	$1{,}957 \cdot 10^{-3}$	42,89
10	872	3600	$299{,}5 \cdot 10^{-6}$	$2{,}169 \cdot 10^{-4}$	$7{,}654 \cdot 10^{-3}$	43,15
11	924	3600	$1225 \cdot 10^{-6}$	$8{,}821 \cdot 10^{-4}$	$3{,}215 \cdot 10^{-2}$	42,68
			$S = 2{,}691 \cdot 10^{-3}$ cm²			
12	663	7200	$2{,}73 \cdot 10^{-6}$	$1{,}409 \cdot 10^{-7}$	$4{,}350 \cdot 10^{-6}$	43,18
13	737	5200	$66{,}4 \cdot 10^{-6}$	$3{,}429 \cdot 10^{-6}$	$1{,}116 \cdot 10^{-4}$	42,90
14	802	3600	$337{,}5 \cdot 10^{-6}$	$3{,}483 \cdot 10^{-5}$	$1{,}183 \cdot 10^{-3}$	42,86
15	840	3600	$910{,}4 \cdot 10^{-6}$	$9{,}397 \cdot 10^{-5}$	$2{,}898 \cdot 10^{-3}$	43,28
16	835	1800	$549 \cdot 10^{-6}$	$1{,}133 \cdot 10^{-4}$	$3{,}969 \cdot 10^{-3}$	43,23
17	902	900	$1066 \cdot 10^{-6}$	$4{,}402 \cdot 10^{-4}$	$1{,}585 \cdot 10^{-2}$	43,24
			$S = 9{,}079 \cdot 10^{-2}$ cm²			
18	646	7200	$53{,}6 \cdot 10^{-6}$	$8{,}209 \cdot 10^{-8}$	$2{,}499 \cdot 10^{-6}$	42,84
19	760	1860	$1105 \cdot 10^{-6}$	$6{,}762 \cdot 10^{-6}$	$2{,}235 \cdot 10^{-4}$	43,25
			$S = 1{,}413$ cm²			
20	519	10800	$0{,}56 \cdot 10^{-6}$	$3{,}644 \cdot 10^{-11}$	$9{,}951 \cdot 10^{-10}$	42,73
21	544	7200	$1{,}93 \cdot 10^{-6}$	$1{,}897 \cdot 10^{-10}$	$5{,}306 \cdot 10^{-9}$	42,94
22	562	3600	$3{,}2 \cdot 10^{-6}$	$6{,}253 \cdot 10^{-10}$	$1{,}777 \cdot 10^{-8}$	42,88
23	572	3600	$5{,}60 \cdot 10^{-6}$	$1{,}107 \cdot 10^{-9}$	$3{,}174 \cdot 10^{-8}$	43,06
24	579	1800	$4{,}7 \cdot 10^{-6}$	$1{,}829 \cdot 10^{-9}$	$5{,}275 \cdot 10^{-8}$	43,24
25	610	1200	$17{,}1 \cdot 10^{-6}$	$1{,}007 \cdot 10^{-8}$	$2{,}981 \cdot 10^{-7}$	43,13
26	640	1200	$62{,}2 \cdot 10^{-6}$	$4{,}082 \cdot 10^{-8}$	$1{,}238 \cdot 10^{-6}$	43,41
27	665	900	$200 \cdot 10^{-6}$	$1{,}607 \cdot 10^{-7}$	$4{,}962 \cdot 10^{-6}$	43,13
28	708	900	$1{,}262 \cdot 10^{-6}$	$9{,}924 \cdot 10^{-7}$	$3{,}166 \cdot 10^{-5}$	43,18
29	757	600	$5233 \cdot 10^{-6}$	$6{,}162 \cdot 10^{-6}$	$1{,}618 \cdot 10^{-4}$	43,66
						Av. = 43,12±0,27

$\log P = 8.0871 - 8899.4/T$, which was derived by the method of least squares. This would suggest that the condensation coefficient of both liquid and solid thallium is close to one.

The condensation coefficient depends mainly on three factors: composition of the vapor phase, energy states at the surface, and the presence of oxide or other films on the surface [11]. The fact that the condensation coefficient is close to one would indirectly indicate that thallium vapor is monoatomic.

At any one temperature Tl_2O has a much higher vapor pressure than does thallium metal [10]. Before determining the vapor pressure of any sample, we heated the thallium for a long period of time in vacuo to free the surface of any oxide film, so that the third factor can be eliminated from consideration.

The average heat of vaporization of thallium in the 519-924°K temperature range is $\Delta H_T = 40.72$ kcal/mol.

Using our experimental vapor pressures and the Φ^* potentials of gaseous, solid, and liquid thallium given in [12], we calculated the ΔH_0^0 in each experiments (see Table 1) with the help of the equation

$$R \ln P = \Phi_r^* - \Phi_c^* - \frac{\Delta H_0^0}{T}, \qquad (2)$$

The values were all internally consistent and showed no systematic trends when the temperature was changed, thus providing additional evidence for the accuracy of our data. The average $\Delta H_0^0 = 43.12 \pm 0.27$ kcal/mol. Moreover, the 0°K heat of sublimation calculated for the average temperature of our experimental range (700°K) by using the equation

$$\Delta H_0^0 = \Delta H_T - \Delta (H_T - H_0^0)$$

comes out to be 42.79 kcal/mol, which is in good agreement with the ΔH_0^0 calculated from Eq. (2).

LITERATURE CITED

1. W. Leitgebel, Z. anorg. Chem. 202, 305 (1931).
2. G. E. Gibson,
3. H. Wartemberg, Z. Electrochem. 19, 482 (1913).
4. F. F. Colleman and A. Egerton, Phil. Trans. A234, 177 (1934).
5. J. Fischer, Chem. Z. 1, 4208 (1937).
6. F. Muller, Helv. phys. Acta 8, 152 (1935).
7. Yu. A. Priselkov, A. V. Tseplyaeva, and K. I. Smirnov, Apparatus for the Determination of Saturated Vapor Pressure by the Effusion Method [in Russian] (Izd. Fil. VINITI, 1958) Topic 39, No. P-58-95/6.
8. Ya. A. Priselkov, Yu. A. Sapozhnikov, and A. V. Tseplyaeva, Izv. AN SSSR, OTN No. 1, 106 (1959).
9. T. A. Kryukova, S. I. Sinyakova, and T. V. Aref'eva, Polarographic Analysis [in Russian] (1959) p. 269.
10. M. G. Shakhtakhtinskii and A. A. Kuliev, Dokl. Akad. Nauk SSSR 123, No. 6 (1958).
11. O. Knacke and I. N. Stranski, Coll. Progr. Metal Physics [Russian translation] (Moscow, 1960) Vol. 3, p. 222.
12. L. V. Gurvich, Zhur. Fiz. Khim. 34, 217 (1960).

All abbreviations of periodicals in the above bibliography are letter-by-letter transliterations of the abbreviations as given in the original Russian journal. *Some or all of this periodical literature may well be available in English translation.* A complete list of the cover-to-cover English translations appears at the back of this issue.

THE NATURE OF THE FLUORESCENCE QUENCHING OF CHLOROPHYLL BY NITROCOMPOUNDS

I. I. Dilung and I. N. Cheruyuk

L. V. Pisarzhevskii Institute of Physical Chemistry,
Academy of Sciences of the USSR
(Presented by Academician A. N. Terenin, April 10 , 1961)
Translated from Doklady Akademii Nauk SSSR Vol. 140, No. 1,
pp. 162-164, September, 1961
Original article submitted April 7, 1961

Although at the present time a considerable amount of information has accumulated on the fluorescence quenching of chlorophyll, which permits, for example, the principal quantitative regularities of this phenomenon to be deduced [1], there is only very meager knowledge concerning the primary act. Starting from the fact that, as a rule, quenchers of the fluorescence of chlorophyll are compounds which possess more or less clearly defined oxidation or reduction properties, E. Rabinowitch [2] expressed the view that quenching in the present case depends mainly on chemical interaction. The "chemical" hypothesis of quenching was, as is known, formulated in a more general form even earlier by Weiss [3]. According to this hypothesis the elementary act in quenching the fluorescence of a number of organic and inorganic compounds is associated with the transfer of an electron between the fluorescing molecule and the quencher molecule. As far as chlorophyll is concerned, apart from considerations of a general character, the results offer no basis on which conclusions can be reached regarding the quenching mechanism.

V. B. Evstigneev and V. A. Gavpilova [4], by studying the kinetics of photochemical oxidation and reduction of pigments of the chlorophyll series, showed that the relative ease of oxidation increased in the series pheophytin a< < chlorophyll b < chlorophyll a. A reversal of the series was noted for reduction processes. We suppose therefore that by a parallel study of the fluorescence quenching of all these pigments under comparable conditions it would be possible to establish a connection between their oxidation–reduction properties and the degree of quenching. On the other hand, the specific dependence of the effect on the potential of the quencher could be obtained by using an oxidizing agent of the same series.

For this purpose in the present work, aromatic nitro compounds were used, in which, as is known, an increase in the number of nitro groups through the series, leads to a simultaneous increase of the oxidation potential [5]. Nitrobenzene, 1,3-dinitrobenzene, 1,4-dinitrobenzene, m-nitrophenol, 2,4-dinitrophenol, and 2,4,6-trinitrophenol were employed as quenchers. Commercial preparations of these compounds (chem. pure grade) were subjected to additional double recrystallization. Chlorophyll and pheophytin were extracted from the dried leaves of nettles. Separation of the pigments into the a and b components was accomplished by the method described in [6]. Benzene purified from quenching agents and dried was used as solvent.

For investigation of the fluorescence a FEU-22 photomultiplier was used. The value of the photocurrent was determined in relative units from the readings of a microvoltmeter with a 28 IM lamp amplifier. The fluorescence of solutions was excited by a blue light from a PRK-4 mercury-quartz lamp filtered by means of a SZS-10 light filter. Assessment of the quenching action of specific additions was made on the basis of the changes in the fluorescence intensity at $\lambda = 670$ mμ on introduction of definite amounts of nitrocompounds into the solutions of the pigments. This wavelength corresponds to the maximum emission of chlorophyll a and is located close to the corresponding maxima of chlorophyll b and pheophytin a. It was resolved by means of a UM-2 universal monochromator.

In Fig. 1 are presented the results of the fluorescence quenching of chlorophyll a, chlorophyll b, and pheophytin a with nitrobenzene. From the given results it is clearly seen that nitrobenzene quenches the fluorescence of chlorophyll a the most strongly, its effect being somewhat weaker in the case of chlorophyll b. The intensity of the luminescence of pheophytin a under these conditions is only negligibly changed.* A completely analogous regularity is observed for all the other nitrocompounds.

*The same is true for pheophytin b.

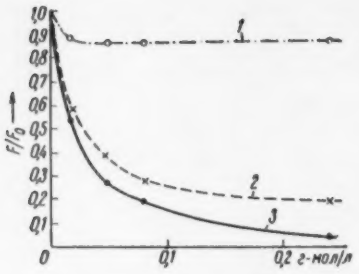

Fig. 1. Quenching by nitrobenzene of the fluorescence of pheophytin a: 1) $0.86 \cdot 10^{-5}$ mole/liter; chlorophyll b, 2) $0.7 \cdot 10^{-5}$ mole/liter; chlorophyll a, 3) $0.8 \cdot 10^{-5}$ mole/liter.

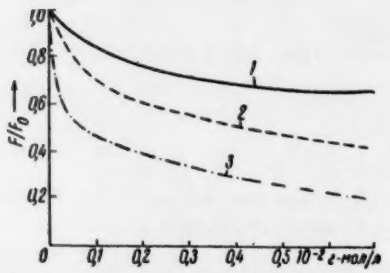

Fig. 2. Quenching of the fluorescence of chlorophyll a by m-nitrophenol (1), 2,4-dinitrophenol (2), and 2,4,6-trinitrophenol (3).

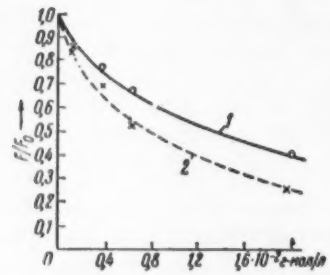

Fig. 3. Quenching of the fluorescence of chlorophyll a with m-nitrobenzene (1), and p-nitrobenzene (2).

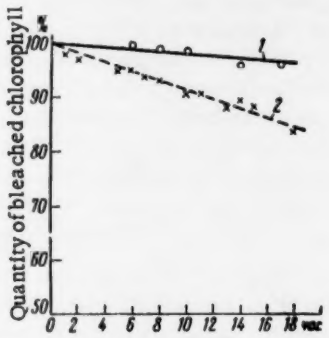

Fig. 4. Photochemical bleaching of benzene solutions of chlorophyll a in the presence of nitrobenzene (1) and m-dinitrobenzene (2).

Thus the effect of fluorescence quenching of a pigment is greater the more strongly expressed is its electron-donor activity.

In Fig. 2 the results are given for the fluorescence quenching of a chlorophyll a solution with m-nitrophenol, 2,4-dinitrophenol, and 2,4,6-trinitrophenol. From these results it is seen that the degree of quenching increases with increase of the nitro groups on the aromatic nucleus. An analogous picture is also observed for additions of nitro- and dinitrobenzene to chlorophyll a solution. Dinitrobenzene quenches the fluorescence several times more strongly than nitrobenzene. As might be expected, the effect of m-dinitrobenzene was found to be somewhat less than that of the p-derivative in which the mutual action of the substituents transmitted by the conjugated chain must effect the oxidation potential to a greater extent. The corresponding results are given in Fig. 3. Thus, the results obtained show that the effect of quenching the fluorescence of the same pigment with different quenchers from a series of nitro compounds is stronger, the greater the number of nitro groups in the molecule and, consequently, the more strongly expressed is its electron acceptor activity.

The relationships which we noted are explicable if it is assumed that the quenching process in the case we are considering is dependent on the transfer of an electron from the pigment to the nitro compound, which, in a general form, can be written as follows:

$$Chl^{*} + RNO_2 \rightleftarrows Chl^{+} + RNO_2^{-}.$$

It is necessary to assume that the transfer of an electron, corresponding to the act of quenching, is reversible. The ion radicals formed in this way remain for a known interval of time in close proximity to one another in a single "cell" of the solution. In this way, favorable conditions are established for their easy recombination and almost complete reversal of the process. In fact, during measurements of the fluorescence, the concentration of pigment does not change. Nevertheless, during a very lengthy exposure of carefully degassed solutions of chlorophyll a containing nitro compounds, a slow photoreaction is detected which leads to the destructive breakdown of the pigment. As might be expected, the rate of bleaching of the chlorophyll during this process is also greater in the presence of dinitrobenzene than nitrobenzene (see Fig. 4). It is possible that a transfer of an electron in this photochemical reaction may also occur between a singlet excited molecule of pigment present in the same "cell" of solution with a molecule of the nitro compound.

The authors express their thanks to Professor B. Ya. Dain, under whose direction the present work was carried out.

LITERATURE CITED

1. R. Livingston and Chun-Lin Ke, J. Am. Chem. Soc. 72, 909 (1950).
2. E. Rabinowitch, Photosynthesis [Russian translation] (IL, 1953) p. 188.
3. J. Weiss, Trans. Faraday Soc. 34, 451 (1938); 35, 48 (1939).
4. V. B. Evstigneev and V. A. Gavrilova, Dokl. Akad. Nauk SSSR 74, 781 (1950); 100, 131 (1955).
5. J. B. Connant and R. Lutz, J. Am. Chem. Soc. 45, 1047 (1923).
6. F. Zschcile and C. Comar, Bot. Gaz. 102, 463 (1941); H. Fischer and A. Stern, Die Chemie des Pyrrols (Leipzig, 1940) Vol. 2, p. 329.

All abbreviations of periodicals in the above bibliography are letter-by-letter transliterations of the abbreviations as given in the original Russian journal. *Some or all of this periodical literature may well be available in English translation.* A complete list of the cover-to-cover English translations appears at the back of this issue.

THE PRESSURE LIMIT FOR SPONTANEOUS PROPAGATION OF THE REACTION ZONE IN ACETYLENE

S. M. Kogarko and B. A. Ivanov

Institute of Chemical Physics, Academy of Sciences of the USSR
(Presented by Academician V. N. Kondrat'ev, April 5, 1961)
Translated from Doklady Akademii Nauk SSSR, Vol. 140, No. 1,
pp. 165-167, September, 1961
Original article submitted March 31, 1961

Nowadays, on account of numerous data in the literature, it is universally taken that the pressure limit at which spontaneous propagation of the reaction zone from the point of ignition is still possible in pure acetylene amounts to 1.35-1.40 atm. An analysis of the data in the literature shows that the energy required for igniting acetylene in the bulk considerably exceeds the amount of energy appropriate to inflammate even critical fuel-air mixtures. Moreover, the amount of energy required for initiating the decomposition of acetylene depends strongly on pressure; it becomes greater when the pressure is decreased. It is also universally known that an electric spark, as is usually employed for igniting fuel-air mixtures, does not suffice to create in acetylene the reaction zone as would be required for a spontaneous propagation through the entire volume, and this is not the case even at initial pressures of 4-5 atm.

Fig. 1. Flame propagation in acetylene. Initial pressure 640 mm Hg. Tube diameter 160 mm, length 1500 mm. Ignition by a heated Nichrome spiral.

It should be mentioned that the limiting tube diameters at which spontaneous propagation of the reaction zone in acetylene becomes possible are very great when compared with the limiting tube diameters for fuel-air mixtures. So, at a pressure of 1.4 atm, the limiting tube diameter is 60 mm; at 12 atm pressure it is 8 mm, whereas for fuel-air mixtures the limiting tube diameter does not exceed one millimeter.

All these data indicate that the width of the chemical reaction zone propagating spontaneously through acetylene is much greater than those values which we know for fuel-air mixtures.

Since, in the technical use of acetylene, in particular in its transportation under raised pressure through pipelines, ignition sources of the most variegated shape and power (sparks, static electricity, burner torch, etc.) may be encountered, an experimental determination of the minimum pressure at which a spontaneous propagation of the reaction zone over the entire volume filled with acetylene is still possible seems to be of great importance.

The decomposition of acetylene was studied at various initial pressures in a steel tube with a diameter of 160 mm and a length of 1500 mm, i.e., its volume amounted to 30 liter. In order to observe the propagation of the reaction zone through the acetylene, the tube was provided with four windows each 250 mm long and covered by plexiglass sheets. The propagation of the reaction zone from the point of ignition along the entire length of the tube was recorded on a photosensitive film mounted on the rotating drum of a photorecorder. For a check experiment we used a steel tube with a diameter of 400 mm and a length of 20 m, i.e., its volume amounted to 2500 liter. The decomposition of acetylene was initiated at one end of the tube either by a red-hot heated helix of Nichrome wire, or

by discharging a capacitor over the gap between two electrodes placed in the acetylene to be tested, or by igniting in the acetylene a certain amount of an explosive mixture coated by a thin rubber film. The experimentally determined value of the lower pressure limit did not depend on the kind of ignition source used in the test.

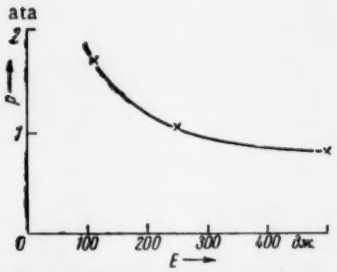

Fig. 2. The limit value of the initial pressure plotted versus the energy of the initiating spark. Tube diameter 160 mm, length 1500 mm.

As an illustration, in Fig. 1 a typical photorecord of the propagation of the reaction zone in acetylene is given.

The distance along the length of the tube is plotted along the ordinate axis and time along the abscissa axis. As is evident from the photorecord shown, a time of about 1.1 sec has elapsed between the instant at which glow of the Nichrome wire appears and the start of the visible flame propagation.

In Fig. 2 the experimentally determined values of the minimum pressure at which formation and spontaneous propagation of a reaction zone is possible are plotted as a function of the spark energy used for initiating the decomposition of acetylene. An analysis of the relation shown in Fig. 2 indicates that spontaneous propagation of the reaction zone in acetylene is possible up to a pressure of 580 mm Hg, that is, down to 0.76 atm pressure, and not to 1.35-1.40 atm as is usually mentioned in the literature. The width of the reaction zone may be estimated from our experimental data. At 580 mm pressure it was found to be about 16 mm, that is, considerably longer than it is in the usual fuel-air mixtures. The difference between the value of the low-pressure limit which we have found for acetylene and that used in the literature has to be explained by the fact that in the published studies inefficient sources were used for initiating the decomposition of acetylene, and that they were only able to heat up a gas layer of such a width as was equivalent to the actual reaction zone in acetylene at an initial pressure of 1.35-1.40 atm.

If upon initiating the decomposition of acetylene by an electric spark one is able to create at once in the gas a heated zone corresponding to the actual reaction zone at its spontaneous propagation, then in the initiating by the heated Nichrome spiral at first a certain volume of acetylene is ignited and then a heated layer corresponding to the reaction zone is formed.

At 1.0 atm initial pressure an experiment on the decomposition of acetylene was done in the tube with diameter 400 mm and length 20 m. The decomposition of acetylene was initiated at one end of the tube by discharging a capacitor over a spark gap. The reaction zone propagated along the entire length of the tube at a mean velocity of 30 m/sec.

The experimental data obtained in this study confirmed our suppositions that a spontaneous propagating reaction zone in acetylene has a great width and requires much more powerful initiating sources than are applied for the usual fuel-air mixtures. If one wants to create safe conditions for handling acetylene, one must take into account the lower value found in this study for the pressure limit at which a decomposition zone generated in a certain point may still spread over the entire volume.

THE SPECIFIC ADSORPTION OF IODIDE IONS ON SILVER

Ya. M. Kolotyrkin and L. A. Medvedeva

L. Ya. Karpov Physicochemical Institute
(Presented by Academician V. A. Kargin, February 2, 1961)
Translated from Doklady Akademii Nauk SSSR, Vol. 140, No. 1,
pp. 168-171, September, 1961
Original article submitted February 1, 1961

In order to verify the mechanism proposed some time ago [1,2] to explain the effect of adsorbed anions on the rates of electrode reactions, we investigated the specific adsorption of iodide ions on silver and the effect of adsorption on hydrogen overvoltage on this metal in 0.1N H_2SO_4. The adsorption was investigated radiochemically using I^{131} as a tracer. The amounts adsorbed were determined by measuring the residual activity of solutions. The method and experimental procedure followed in these radiochemical and polarization measurements, both done in the same apparatus, have already been described in another paper [1].

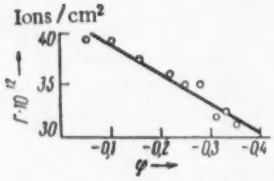

Fig. 1. The adsorption of I^- ion as a function of the electrode voltage in 1.0N H_2SO_4 solutions containing 10^{-7} equiv/liter KI.

The great affinity exhibited by silver toward iodide ions enabled us to use smooth electrodes with a visible surface of 10 cm^2. The I^- ion concentration in solution was varied from 10^{-9} to 10^{-5} equiv/liter. In working with low concentrations (less than 10^{-7} equiv/liter) only the radioisotope I^{131} was introduced into solution. The volume of solutions used in our adsorption studies ranged from 25 to 50 cm^3.

Prior to each experiment the electrode surface was cleaned with very fine glass powder and thoroughly washed with twice-distilled water. The specific surface of our electrodes was calculated from the double-layer capacitance, which, in turn, was measured by a method described before [3]. The measurements yielded a roughness factor of about 3 for our electrodes. All the measurements were carried out at room temperature under hydrogen from which all traces of oxygen were carefully removed.

The experiments were carried out in such a way that the electrodes would be maintained long enough at any given voltage to ensure the attainment of adsorption equilibrium in the system. This enabled us to determine the equilibrium surface coverage at any given voltage and its dependence on the initial KI concentration in solution (at the same voltage). Combining these results with results obtained from polarization measurements, we were able to establish the relationship between the fraction of electrode surface covered by the adsorbed I^- ions and the changes in hydrogen overvoltage brought about by this adsorption.

The state of the silver surface in the presence of adsorbed I^- ions was examined by measuring the differential capacitance of the electrical double layer next to the metal surface over a wide range of voltages, and also by measuring the rate of desorption as a function of the adsorption and desorption voltages.

Figure 1 shows that within the relatively narrow range of investigated voltages adsorption increases linearly with increasing (in the positive direction) voltages. A similar linear relationship was observed at practically all the investigated initial KI concentrations.

At any fixed voltage an increase in the KI concentration results in increased adsorption, and over a large range of concentrations, from 10^{-9} to 10^{-6} equiv/liter, the relationship between the two is linear.

As in the case of lead [1], iodide ion adsorption on silver is completely reversible in the sense that, regardless of whether the adsorption is measured by increasing or decreasing the polarization, the amount adsorbed has a fixed value for a given voltage. Accordingly, a shift toward more negative voltages results in a partial desorption of I^- ions, while a similar shift in the positive direction leads to additional adsorption.

The adsorption of I^- on silver, as in the previously reported case of iron [4], decreases the differential capacitance of the double layer by a factor of 2-3, which definitely indicates a specific interaction between these ions and and the surface atoms of the metal electrode.

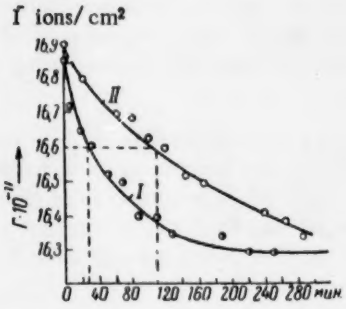

Fig. 2. Desorption rate of iodide ions at $\varphi = -0.335$ v for various adsorption voltages: I) for $\varphi = -0.174$ v; II) for $\varphi = -0.124$ v.

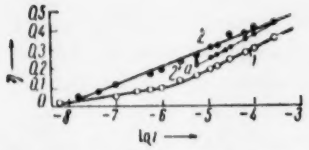

Fig. 3. Hydrogen overvoltage as a function of the logarithm of current density: 1) in 1.0N H_2SO_4; 2) in the same acid in presence of $2.6 \cdot 10^{-9}$ equiv/liter of KI.

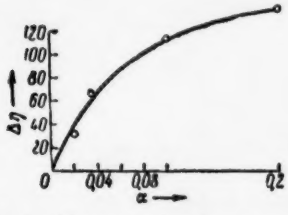

Fig. 4. Change in hydrogen overvoltage as a function of the fraction of silver surface covered by the adsorbed iodide ions.

The desorption measurements would indicate that the adsorption-bond energy does not remain constant but increases appreciably at more positive voltages. The data shown in Fig. 2 favor this interpretation. These data were obtained in experiments where the electrode was first polarized at a voltage at which all the iodide ions in solution would be adsorbed. As a result, even at different adsorption voltages (in our case at -0.174 and -0.124 v, respectively) the surface coverage remained the same, about $16.9 \cdot 10^{11}$ ions/cm^2 in our experiments. And yet the more positive the original adsorption voltage, the slower would the subsequent desorption be at any fixed voltage (-0.335 v in our case). Thus, for example, for samples adsorbed at the above-mentioned voltages the desorption of the same amount of I^-, $3 \cdot 10^{10}$ ions/cm^2, took 27 and 110 min, respectively.

That the desorption rate depends on the preliminary polarization voltage can also be seen in Table 1. The tabulated data were obtained in experiments where the desorption voltage was maintained at -0.335 v, while adsorption was carried out at -0.145-0.050, and $+0.100$ v, respectively; the initial KI concentration was $1.2 \cdot 10^{-9}$ equiv/liter.

Other conditions being the same, the desorption rate also depends greatly on the desorption voltage. We have established that, for any given adsorption voltage (and equal surface coverage), the desorption rate increases as the voltage is made more negative.

Polarization measurements have shown that, over a wide range of KI concentrations, from 10^{-9} to 10^{-3} equiv/liter, the adsorption of iodide ions on silver, unlike the case of lead, is accompanied by increased hydrogen overvoltage only.

In Fig. 3 we have plotted the rate of hydrogen evolution as a function of voltage in 1.0N H_2SO_4 before (curve 1) and after (curve 2) $2.6 \cdot 10^{-9}$ equiv/liter of KI were introduced into the solution.

Since it takes a long time to establish an adsorption equilibrium in these systems, the exact shape of polarization curves obtained in solutions containing KI will depend to a large extent on how rapidly the measurements are conducted. This is well illustrated in Fig. 3 where the data along curve 2' were recorded more rapidly than those represented by curve 2. When the electrode was maintained for an extended period of time at the current density represented by point a, the potential gradually shifted toward more negative voltages, to the corresponding equilibrium value along the slowly recorded curve. Simultaneous adsorption measurements revealed that this shift is accompanied by an increase in the number of I^- ions adsorbed on the silver surface. We have thus been able to prove that the experimentally observed decrease in the slope of the hydrogen overvoltage curve results from an increased surface coverage (by the adsorbed ions) and the accompanying shift in the electrode potential toward more positive values. By combining the results from polarization and adsorption measurements obtained under similar conditions, we constructed a curve showing how the observed increase in overvoltage depends on the fraction of surface covered by the adsorbed iodide ions (Fig. 4). The assumption was made that the adsorption of one iodide ion per silver atom on the surface represents complete surface coverage.

The results presented above show that the adsorption of ions in amounts barely sufficient to form a hundredth part of a monolayer slows the evolution of hydrogen appreciably, and the retardation steadily increases as the fraction

of surface covered by the adsorbed ions is increased. Similarly, at a given imposed current density, the overvoltage will also sharply increase when the KI concentration in solution is raised. For example, when we raised the KI concentration from $0.9 \cdot 10^{-9}$ N to $8 \cdot 10^{-7}$ N, the overvoltage (at $\log i = 1 \cdot 10^{-5}$ amp/cm^2) increased by almost 110 mv. It should be noted, however, that the overvoltage will only keep rising in this way until a certain KI concentration is attained, and after that it becomes independent of the salt concentration.

TABLE 1.

Amount of I^- ($g \cdot 10^{-10}$) desorbed from 1 cm^2	Time in minutes at various desorption voltages		
	−0.145 v	−0.050 v	−0.100 v
1.6	2.5	15.0	20
2.1	7.5	27.5	45
2.45	12.5	37.5	110

Of some value to a better understanding of the mechanism by which adsorbed I^- ions interfere with the evolution of H_2 on a silver electrode are the results obtained in this work which show that the introduction of even minute amounts of KI ($8 \cdot 10^{-7}$ equiv/liter) into the acid solution greatly reduces hydrogen retention time on the charge curve or, in other words, it reduces the amount of hydrogen adsorbed on the electrode surface.

This provides direct evidence in support of a previously proposed mechanism [1,2], according to which the specific adsorption of a halide ion on the surface of a metal electrode is not only accompanied by structural changes in the electrical double layer at the metal – solution interface, but also by changes in the catalytic properties of the surface, as reflected in the reduced hydrogen adsorption energy, which would naturally lead to an increased activation energy for the discharge of hydrogen ions and consequently increased overvoltage.

The observed differences between the effects of I^- ion adsorption on the rate of hydrogen evolution on silver and lead electrodes are undoubtedly connected with the fact that the adsorbancy of hydrogen on silver is much greater so that effects connected with the poisoning of the electrode surface by the adsorbed anions are therefore more pronounced and exceed in magnitude other effects connected with structural changes in the double layer.

LITERATURE CITED

1. L. A. Medvedeva and Ya. M. Kolotyrkin, Zhur. Fiz. Khim. 31, 2668 (1957).
2. Ja. M. Kolotyrkin, Trans. Faraday Soc. 55, 455 (1959).
3. T. I. Borisova, B. V. Ershler, and A. I. Frumkin, Zhur. Fiz. Khim. 22, 925 (1948).
4. V. V. Losev, Dokl. Akad. Nauk SSSR 88, 3, 499 (1953).

All abbreviations of periodicals in the above bibliography are letter-by-letter transliterations of the abbreviations as given in the original Russian journal. *Some or all of this periodical literature may well be available in English translation.* A complete list of the cover-to-cover English translations appears at the back of this issue.

THE KINETICS OF CATHODIC PROCESSES ON SEMICONDUCTING ELECTRODES, INVOLVING PARTICIPATION OF THE ELECTRONS OF THE VALENCE ZONE

R. M. Lazorenko-Manevich and S. O. Izidinov

L. Ya. Karpov Physicochemical Institute
(Presented by Academician A. N. Frumkin, April 10, 1961)
Translated from Doklady Akademii Nauk SSSR, Vol. 140, No. 1,
pp. 172-175, September, 1961
Original article submitted April 4, 1961

The theory of cathodic processes on semiconductors has been developed for the case where conductivity electrons take part in the process [1]. There exists, however, a group of cathodic processes which involve participation of electrons of the valence zone [2-5]. Without dealing here with the conditions under which valence electrons may take part in a cathodic process [3], let us examine how their participation influences the form of the kinetic equations. For this we shall start from the results obtained in [1].

Let us first consider the case where the proportion in which the valence electrons take part in the reaction is equal to unity. This case has already been discussed in [6]. Here we shall examine it from another viewpoint and, on the basis of this examination, we shall discuss the case where electrons of the two zones take simultaneous part in the reaction [4]. For simplicity let us assume that surface states are absent [1]. In addition, let us assume that the Ψ_1-potential is equal to zero. Let η_H be the displacement of the potential in the Helmholtz part of the double layer when a current of density $\underline{i}$ is passed; $\Delta\varphi_{bc}$ the displacement of the potential in the layer of bulk charge in the semiconductor; and Δq the change in the charge on the ionic layer when current is passing.

If η is the measured overvoltage, then

$$\eta = \eta_H + \Delta\varphi_{bc}. \tag{1}$$

As a first approximation is is assumed, as in [1], that the surface state of the electrode remains unchanged on polarization.

It is known that

$$i = i_e\,(C/C_0)\,e^{-\alpha\eta_H F/RT}. \tag{2}$$

Here i_e is the exchange current density; C is the concentration of electrons on the surface of the semiconductor with polarization; C_0 is the same for i = 0; while the other symbols have their usual significance. Equation (2) describes a process whose rate is determined by the rate of one of the stages of the electrochemical reaction. This means that the passage of current does not break down the electronic equilibrium in the semiconductor. This simplified representation is sufficient for examination of the fundamental aspect of the problem.

In [1], C and C_0 are considered as the concentrations of only the conductivity electrons. Formula (2) has a more general significance, however, and is also applicable when valence electrons take part in the process. Assuming C and C_0 to be the total concentrations of electrons on the surface, we obtain $C \cong C_0$, since, under the conditions generally employed for electrochemical reactions, the total concentration of electrons on the electrode surface remains practically unchanged.

From (2) we have

$$\eta_H = \frac{RT}{\alpha F} \ln \frac{i_e}{i}. \tag{3}$$

From this and (1) we obtain

$$\eta - \Delta\varphi_{bc} = \frac{RT}{\alpha F} \ln \frac{i_o}{i}, \tag{4}$$

whereas, if we assume that C and C_0 are the concentrations of the conductivity electrons, we obtain from (2) the equation

$$\eta + \frac{1-\alpha}{\alpha} \Delta\varphi_{bc} = \frac{RT}{\alpha F} \ln \frac{i_o}{i}. \tag{5}$$

i_e in formulas (4) and (5) are not equal, since when $\eta = 0$ the concentrations of the electrons taking part in the reaction are not equal.

When $i \to 0$, as shown in [1],

$$\eta = -\frac{RT}{nFi_o} i. \tag{6}$$

When valence electrons take part in the reaction, however, this equation relates not η and $\underline{i}$, but η_H and $\underline{i}$, as follows from (3). Thus,

$$\eta - \Delta\varphi_{bc} = -\frac{RT}{nFi_o} i. \tag{7}$$

Comparison of (4), and (5), and (6) and (7), shows that it is easier to displace the equilibrium of the reaction involving valence electrons (i.e., to obtain a potential differing from the equilibrium potential) than to displace the equilibrium of the reaction in which conductivity electrons take part. The reason for this is that when valence electrons take part in the reaction, its rate can increase only as a result of a decrease in the activation energy with a change in the potential jump in the Helmholtz layer. In this case, therefore, η_H should be greater than when conductivity electrons take part in the reaction (for the same i/i_e), where an acceleration is produced not only by a decrease in the activation energy, but also by an increase in the concentration of the reagent – the conductivity electrons. Since a larger $\Delta\varphi_{bc}$ also corresponds to a larger η_H, η will be greater in the case where valence electrons are used. It is also significant that the relationship between $\Delta\varphi_{bc}$ and η_H also depends on whether or not the semiconductor surface is degenerate. For a nondegenerate surface, $\Delta\varphi_{bc}$ is much greater than η_H and makes up the greater part of the total overvoltage. It therefore follows from (1), (4), or (7), and the relationship between η_H and $\Delta\varphi_{bc}$ [1], that the polarizability under these conditions is very high. For a degenerate surface, $\Delta\varphi_{bc}$ is comparable with η_H, so that from the same equations (1) and (4) or (7), and the corresponding relationship between η_H and $\Delta\varphi_{bc}$ for a degenerate surface [1], it follows that the polarizability will be much lower than in the former case, leading to a sharp decrease in the slope of the overvoltage curve. Thus, for example, for a hole semiconductor on whose surface there is an enriched layer in the absence of external current, the cathodic overvoltage curve for the case where valence electrons are used has a step with a height approximately equal to the width of the forbidden zone (the section with the low slope in the region of the enriched layer is replaced by a section with a high slope with movement into the nondegenerate range; displacement of the Fermi level from below upwards through the whole of the forbidden zone leads again to degeneration which, in turn, leads to a decrease in the slope). This qualitative conclusion (a quantitative result can also be obtained by using the appropriate relationships between η_H and $\Delta\varphi_{bc}$, given in [1]) agrees with the conclusions reached in [6] by a different method.

Let us now examine the case where both valence electrons and conductivity electrons take part in the reaction. Let us assume that the surface of the semiconductor is nondegenerate. In this case, Eq. (2) remains applicable, but it is difficult to determine the concentrations of electrons taking part in the reaction from the two zones. It is therefore better to obtain a kinetic equation containing a quantity which can be determined experimentally – the fraction of valence electrons in the total current [4].

Let us denote the current for the valence electrons by i_v and the current for the conductivity electrons by i_c. It is obvious that

$$i_v + i_c = i. \tag{8}$$

Let

$$i_v/i = x. \tag{9}$$

Let us consider first the case of low currents ($i \ll i_e$).

If it is assumed that the currents i_c and i_v are independent of one another, i.e., that the reaction in which conductivity electrons are used takes place independently of the reaction in which valence electrons are used, then, in accordance with (6) and (7),

$$-\frac{RT}{nF}\frac{i_v}{i_{ev}} = \eta_r; \quad -\frac{RT}{nF}\frac{i_c}{i_{bc}} = \eta. \tag{10}$$

Here i_{ev} is the exchange current for the reaction involving valence electrons, and i_{ec} is the exchange current for the reaction involving conductivity electrons. It is obvious that

$$i_{ev} + i_{ec} = i_e. \tag{11}$$

Equations (8), (10), and (11) form a system whose solution, together with (9), gives the required expression:

$$-\frac{RT}{nF}\frac{i}{i_e} = \frac{\eta(\eta - \Delta\varphi_{bc})}{\eta - \Delta\varphi_{bc}(1-x)}. \tag{12}$$

If we assume in analogous fashion that the reaction involving valence electrons and the reaction involving conductivity electrons take place independently in the range where $i \gg i_e$, we obtain from (4) and (5) the expressions:

$$i_v = i_{ev}e^{-\alpha F\eta H RT}; \quad i_c = i_{ec}e^{-F\Delta\varphi_{bc}/RT}\, e^{-\alpha F\eta H RT}. \tag{13}$$

Solution of (13) and (8) and (11) gives

$$i = i_e\frac{e^{-F\Delta\varphi_{bc}/RT}\, e^{-\alpha F\eta H/RT}}{1 - x\left(1 - e^{-F\Delta\varphi_{bc}/RT}\right)}. \tag{14}$$

It should be emphasized that these results are applicable only when there is no diffusion delay for the conductivity electrons taking part in the reaction.

These features are most clearly revealed for the polarization of Si in alkaline solutions [7]. The current of spontaneous dissolution of Si in 10 N KOH, measured from the rate of evolution of hydrogen, is equal to $\sim 10^{-3}$ amp per cm^2; the steady-state potential is equal to ~ -300 mv versus a hydrogen electrode in the same solution. A cathodic current of $\sim 10^{-4}$ A/cm^2 displaces the potential of p-Si by 100 mv, compared with the fraction of a millivolt expected for the case where conductivity electrons are used [1]. On n-Si a current of $(2\text{-}3) \cdot 10^{-4}$ amp/cm^2 displaces the potential by about 200 mv instead of several millivolts. These high overvoltages are difficult to explain as voltage drops in an oxide film, since in this range of potential Si dissolves actively, indicating that there can be no high-resistance oxide film on its surface. These facts correspond qualitatively to the picture of a reduction process involving valence electrons, as described above. The possible participation of valence electrons in the reduction of water on Si is responsible for the marked difference between the normal potentials for the processes of Si dissolution ($E_0 = -1.7$ v) and water reduction.

According to [3] there is a direct correspondence between this difference and the probability that valence electrons take part in the reaction. It should be noted that the above data for an Si cathode can also be explained by assuming that the Si reacts chemically with the solution, and this leads to a noncorrespondence between the observed overvoltages and the current of spontaneous dissolution. The available experimental data do not appear to refute either hypothesis.

The authors with to thank Professor V. I. Veselovskii, L. A. Aladzhalova, T. I. Borisova, and V. M. Novakovskii for discussion of this work.

LITERATURE CITED

1. M. Green, Modern Aspects of Electrochemistry (London, 1959) Vol. 2, p. 6.
2. H. Gerischer and F. Beck, Z. Phys. Chem., N. F. 133, 89 (1957).
3. F. Beck and H. Gerischer, Z. Elektrochem. 63, 943 (1959).
4. Yu. V. Pleskov, Doklady Akad. Nauk SSSR 126, No. 1, 111 (1959); 130, No. 2, 362 (1960).
5. E. N. Paleolog, A. V. Fedotova, and N. D. Tomashov, Doklady Akad. Nauk SSSR 129, No. 3 (1959).
6. Yu. A. Vdovin, B. M. Grafov, and V. A. Myamlin, Doklady Akad. Nauk SSSR 129, 827 (1959).
7. S. O. Izidinov, T.I. Borisova, and V. I. Veselovskii, Doklady Akad. Nauk SSSR 133, No. 2, 392 (1960).

SYNTHETIC ADDITIVES OF THE DISPERSING AGENT TYPE

P. I. Sanin, L. F. Chernyavskaya, V. V. Sher,

and N. V. Melent'eva

Petrochemical Synthesis Institute, Academy of Sciences of the USSR
(Presented by Academician A. V. Topchiev, April 8, 1961)
Translated from Doklady Akademii Nauk SSSR, Vol. 140, No. 1,
pp. 176-178, September, 1961
Original article submitted April 4, 1961

At the present time extensive use is made of synthetic additives to lubricating oils which, in addition to other properties, exhibit a "wetting" action. In some additives this property is so marked that they are usually described as "wetting" additives. In the presence of these additives there is a considerable decrease in the amount of carbonaceous deposits formed in an engine from the products of oxidation and incomplete combustion of the hydrocarbons in the oil and fuel. The term "wetting" additives has been extensively used chiefly because the action of these additives is in some respects similar to the action of familiar wetting agents used in aqueous solution (salts of organic acids, sulfonates, etc.). In one of our papers [1] it was pointed out that this term is not apt when applied to this type of additive. A rational name for a type of additive should have a scientific basis and should reflect primarily the actual mechanism of its action. The mechanism of action of additives has been discussed to some extent in a number of papers [1-7].

In the present work it has been shown that the "wetting" action of additives is due to their adsorption on the insoluble particles of oil suspensions, which leads to an increase in the degree of dispersion of the suspension and to stabilization of the suspension.

The greater part of the studies was carried out with polyfunctional additives of the nickel dialkyldithiophosphate type. As shown in our previous work [8], nickel di-n-octadecyldithiophosphate $[(C_{18}H_{37}O)_2PSS]_2Ni$ exhibits a powerful "wetting" action.

A suspension of carbon black in toluene was used as a model suspension. The suspension was prepared from carbon black and a known quantity of a solution of the dialkyldithiophosphate in toluene. When adsorption equilibrium had been established and the carbon black had been separated, the quantity of dialkyldithiophosphate remaining in the solution was determined; from the difference between this quantity and the quantity of dialkyldithiophosphate taken, it was possible to determine the quantity of dialkyldithiophosphate adsorbed on the quantity of carbon black taken. In this type of measurement considerable difficulty is usually encountered in the determination of the extremely small quantities of additive present in the dilute hydrocarbon solutions. We carried out this determination as follows. After removal of the toluene, the nickel dialkyldithiophosphate was decomposed with a mixture of concentrated nitric and sulfuric acids, the resultant nickel salt was converted to the intensely colored complex compound of nickel with dimethylglyoxime, and the nickel content was determined colorimetrically.

Figure 1 gives the results of experiments on the adsorption of different nickel dialkyldithiophosphates on carbon black. The equilibrium concentration of the dialkyldithiophosphates in the individual experiments varied from 37 to 700 mg, or from 0.03 to 0.5 mM per liter of solvent toluene.

Figure 1 shows that the observed relationships between the quantity of adsorbed dialkyldithiophosphate and its equilibrium concentration are typical adsorption isotherms. It has thus been shown that additives of the nickel dialkyldithiophosphate type are in fact adsorbed from a hydrocarbon solution on carbon black particles.

The values of the maximum limiting adsorption corresponding to complete saturation of the adsorption layer at the toluene – carbon black boundary (A_∞), determined from the adsorption isotherms, amounted to 5.70, 4.08, and 3.17 mM per 1 g of carbon black (channel black) for nickel n-butyl-, n-decyl-, and n-octadecyldithiophosphates, respectively. In other words, 1 g of the carbon black adsorbed 3.1 g of the di-n-butyldithiophosphate, 3.6 g of the di-n-decyldithiophosphate, and 4.2 g of the di-n-octadecyldithiophosphate.

It is interesting to note that for the adsorption of nickel dialkyldithiophosphates on carbon black (from toluene) we obtained a relationship which, as far as the influence of the length of the hydrocarbon radicals is concerned, is contradictory to that obtained for the adsorption of the same additives at a hydrocarbon–water interface. The hydrocarbon radicals of the nickel dialkyldithiophosphate molecules adsorbed on the carbon black apparently have a spatial arrangement which is different from that for the case of adsorption on a hydrocarbon–water interface; the molecules with the longer radicals have a less compact structure and occupy a greater area on the carbon black surface.

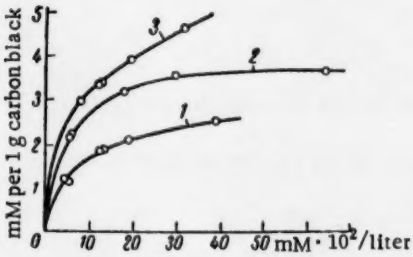

Fig. 1. Isotherms for the adsorption of nickel dialkyldithiophosphates on carbon black. Carbon black – toluene suspension. Carbon black concentration 0.00061%. 1) Nickel di-n-octadecyldithiophosphate $[(C_{18}H_{37}O)_2PSS]_2Ni$; 2) nickel di-n-decyldithophosphate $[(C_{10}H_2O)_2PSS]_2Ni$; 3) nickel di-n-butyldithiophosphate $[(C_4H_9O)_2PSS]_2Ni$.

We recorded electron-microscope photographs of specimens of carbon black obtained from suspensions of carbon black in toluene, with and without added nickel dialkyldithiophosphate. These photographs were used to determine the average size of the carbon black particles [9] and, from the qualitative results of the adsorption experiments, the average number of additive molecules adsorbed on one carbon black particle. One (averaged) carbon black particle adsorbs approximately $6 \cdot 10^4$ molecules of nickel di-n-octadecyldithiophosphate.

As a result of the adsorption, the particles of the carbon black are covered with a layer of nickel dialkyldithiophosphate molecules with their hydrocarbon groups directed toward the hydrocarbon medium. In accordance with this, the oleophilic nature of the particles increases sharply and the suspension as a whole becomes more stable.

It should be noted that the surface of the particles of different types of carbon black are not uniform and are oxidized to different degrees. This is particularly true of channel carbon black, whose suspensions in a hydrocarbon medium can also be regarded as models of real oil suspensions. The nature of the surface of the carbon black particles is also responsible for the adsorption of the dialkyldithiophosphate molecules by means of their polar groups, while the nonpolar part of the molecules (the hydrocarbon groups) are directed toward the hydrocarbon medium.

The stabilization of a carbon black suspension was studied by two methods. In the first case we determined the time required for complete precipitation of the carbon black from the suspension in special cylinders or by centrifuging in a centrifuge fitted with an assembly for controlling the temperature. In the second case we determined the relative change in the concentration of carbon black in the suspension with time by measuring the optical density of the suspension. In the case of additives of different structure, it was shown that the stabilizing action of the additives corresponds exactly to their activity as "wetting" additives.

In the dialkyldithiophosphate series, the stabilizing effect increases with increase in the length of the hydrocarbon radical present in the molecule. This relationship would appear to contradict the results of the study of the adsorption of these compounds.

Thus, for example, the number of nickel di-n-butyldithiophosphate molecules adsorbed on one particle of channel carbon black was approximately double the number of molecules of the di-n-octadecyldithiophosphate. The hydrocarbon radicals of the di-n-octadecyldithiophosphate are, however, almost 5 times longer than the hydrocarbon radicals of the di-n-butyldithiophosphate, and this is the decisive factor. It is apparently only sufficiently long hydrocarbon radicals which are able to make the carbon black particle, covered with the adsorption layer, sufficiently oleophilic for stabilization.

Thus, additives of this type which, in addition to the dialkyldithiophosphates, include the salts of organic acids (alkylphenolates and sulfonates), are surface-active substances which are adsorbed from a hydrocarbon medium (oil) on to the surface of insoluble particles, preventing their adhesion (agglomerization) and formation of larger particles, with deposition from the oil suspension. The large agglomerates already formed, in which the fine particles are bound by relatively weak molecular adhesive forces, can be broken down and dispersed in the presence of the additives.

The over-all action of the additives thus involves an increase in the degree of dispersion of the oil suspension formed during running of the engine, and stabilization of this suspension. In other words, a process of adsorptive

dispersion of the insoluble products in the oil takes place. Since the agglomerization of particles (flocculation) in the oil yields relatively loose aggregates, their dispersion is essentially a peptization process [10].

The "wetting" action of additives can be regarded as a dispersing (or peptizing) action, so that "wetting" additives should be referred to as dispersing (or peptizing) agents.

LITERATURE CITED

1. P. I. Sanin and N. S. Nametkin, Collection: Additives in Lubricating Oils [in Russian] (Moscow-Leningrad, 1946) p. 97.
2. N. I. Chernozhukov, S. E. Krein, and B. V. Losikov, The Chemistry of Mineral Oils [in Russian] (Moscow-Leningrad, 1951) pp. 232, 284.
3. E. A. Myshkin, Khim. i Tekh. Topliv i Masel No. 12, 50 (1959).
4. A. R. Badeley, A. H. Nisson, and F. H. Garner, J. Inst. Petrol 35, No. 303, 141 (1949).
5. F. H. Garner, C. W. Nutta, and M. F. Mohtadi, J. Inst. Petrol. 36, No. 317, 292 (1950); 37, No. 332, 426 (1951); 38, No. 348, 974 (1952); 38, No. 348, 986 (1952); 39, No. 358, 677 (1953).
6. R. Courtel, B. Bernelin, and J. Larbre, Revue de l'Inst. Francais du Pétrole 10, No. 5, 477 (1955).
7. J. Larbre, Revue de l'Inst. Francais du Pétrole 11, No. 10, 1298 (1956).
8. P. I. Sanin and V. V. Sher, Khim. i Tekh. Topliv i Masel No. 3, 38 (1957).
9. E. Ya. Rabinovich, T. D. Snegireva, and P. A. Tesner, Collection: The Treatment and Transport of Natural Gases [in Russian] (Moscow-Leningrad, 1953) p. 55.
10. A. Schwartz and J. Perry, Surface Active Agents [Russian translation, edited by A. B. Taubman] (IL, 1953) p. 325.

All abbreviations of periodicals in the above bibliography are letter-by-letter transliterations of the abbreviations as given in the original Russian journal. *Some or all of this periodical literature may well be available in English translation.* A complete list of the cover-to-cover English translations appears at the back of this issue.

THE THERMODYNAMIC PROPERTIES OF COBALT ANTIMONIDES DETERMINED FROM EMF MEASUREMENTS

V. A. Geiderikh and Corr. Member Acad. Sci. USSR

Ya. I. Gerasimov

M. V. Lomonosov Moscow State University

Translated from Doklady Akademii Nauk SSSR, Vol. 140, No. 2,
pp. 391-393, September, 1961
Original article submitted June 10, 1961

Three cobalt antimonides are known: $CoSb_3$ with scutterudite structure [1,2], $CoSb_2$ with a marcasite structure [1,3], and CoSb with a nickel arsenide structure [3,4].

The phase diagram of the Co–Sb system has been reported [5]. The compound CoSb does not deviate to any appreciable extent from the stoichiometric composition. According to Rosenqvist [1], the compound $CoSb_2$ contains a slight excess of cobalt (some sulfur atoms are replaced in the crystal lattice by cobalt atoms). In another paper [6], Rosenqvist assigned the formula $CoSb_{1.9}$ to the compound. In the phase diagram of the Co–Sb system [5], the region corresponding to homogeneous $CoSb_2$ is represented by a broken curve in the range from 64 to 66.7 mole% of Sb. Other workers (among them [2]) fail to mention the nonstoichiometric composition of $CoSb_2$. According to Ageev and Makarov [7], the CoSb phase exists in the region from 43.4 to 49.2 mole% of Sb, while the excess cobalt atoms occupy doubled tetrahedral vacancies in the antimony sublattice.

We have calculated the integral thermodynamic functions for the compositions of $CoSb_3$, $CoSb_2$, and CoSb even though $CoSb_2$ deviates from the stoichiometric ratio, while the upper limit for a homogeneous CoSb phase richest in antimony is observed at 49.2 mole% of Sb (the experimental data were obtained using a compound of this composition). The errors introduced by rounding off the figures in our calculations are smaller than the experimental errors.

The thermodynamic properties of cobalt–antimony alloys were determined by measuring the emf's of appropriate cells. The technique has been described in detail elsewhere [8,9]. The equation representing emf as a function of absolute temperature (a linear relationship) was obtained from the experimental data by the method of least squares; data obtained from all the experiments and all alloys for any given heterogeneous region of the phase diagram were combined. The method of least squares [10] was also used for calculating the errors in the emf and the coefficients in the equation $E = f(T)$.

The alloys were made up by mixing antimony purified by zone melting (99.999% Sb) with cobalt prepared from analytical reagent grade nickel-free $Co(NO_3)_2$.

The reaction

$$Co + 3Sb = CoSb_3 \tag{1}$$

is responsible for the potential difference in the electrochemical cell

$$(-)\ Co \mid \underset{\text{Melt}}{CoCl_2 + KCl + LiCl} \mid \underset{\text{Solid heterogeneous alloy}}{CoSb_3 + Sb}\ (+). \tag{I}$$

The free energy change accompanying reaction (1) can be expressed in terms of the emf of cell (I),

$$\Delta F_1 = -zFE_1, \tag{A}$$

where z = 2 is the ionic charge of cobalt, F is Faraday's number, and E_I is the emf of cell (I).

In investigating the 790-890°K temperature range, we represented our experimental data by the equation

$$E_I = (302{,}2 + 1{,}45 \cdot 10^{-3}T)\text{mv} \pm 9{,}6\text{mv}.$$

From which we get

$$\Delta F_1 = (-13{,}94 - 0{,}067 \cdot 10^{-3} T) \text{ kcal/mole } CoSb_3.$$

The reaction

$$Co + 2CoSb_3 = 3CoSb_2 \tag{2}$$

is responsible for the potential difference in the cell

$$(-)\ Co \mid \underset{\text{melt}}{CoCl_2 + KCl + LiCl} \mid \underset{\text{solid heterogeneous alloy}}{CoSb_3 + CoSb_3}\ (+). \tag{II}$$

For the 800-990°K temperature range,

$$E_{II} = (136{,}3 + 30{,}4 \cdot 10^{-3} T) \text{ mv} \pm 15{,}0 \text{ mv}.$$

And using Eq. (A) we get

$$\Delta F_2 = (-6{,}29 - 1{,}40 \cdot 10^{-3} T) \text{ kcal/mole Co}.$$

The formation of $CoSb_2$ from its elements,

$$Co + 2Sb = CoSb_2 \tag{3}$$

can be expressed as a combination of reactions (1) and (2), so that

$$\Delta F_3 = \frac{2\Delta F_1 + \Delta F_2}{3} = (-11{,}39 - 0{,}51 \cdot 10^{-3} T) \text{ kcal/mole } CoSb_2.$$

The reaction

$$Co + CoSb_2 = 2CoSb \tag{4}$$

is responsible for the potential difference in the cell

$$(-)\ Co \mid \underset{\text{melt}}{CoCl_2 + KCl + LiCl} \mid \underset{\text{solid heterogeneous alloy}}{CoSb + CoSb_2}\ (+). \tag{III}$$

For the 770-980°K temperature range

$$E_{III} = (98{,}8 + 35{,}5 \cdot 10^{-3} T) \text{ mv.} \pm 4{,}2 \text{ mv.}$$

$$\Delta F_4 = (-4{,}56 - 1{,}55 \cdot 10^{-3} T) \text{ kcal/mole Co}.$$

The formation of CoSb from its elements,

$$Co + Sb = CoSb \tag{5}$$

can be expressed as a combination of reactions (3) and (4), so that

$$\Delta F_5 = \frac{\Delta F_3 + \Delta F_4}{2} = (-7{,}98 - 1{,}03 \cdot 10^{-3} T) \text{ kcal/mole CoSb}$$

The heats and entropies of formation of the cobalt antimonides were obtained from ΔF_1, ΔF_2, and ΔF_3 by using the equations

$$\Delta S = -\left(\frac{\partial \Delta F}{\partial T}\right)_p \text{ and } \Delta H = \Delta F + T\Delta S.$$

The changes in the free energy, heat, and entropy of formation of solid cobalt antimonides from its elements have been evaluated per mole of cobalt antimonide and are compiled in Table 1:

TABLE 1.

	$\Delta F = f(T)$, kcal	$\Delta F_{850°K}$, kcal	ΔH, kcal	ΔS, e.u.
$CoSb_3$	$-3{,}48 - 0{,}02 \cdot 10^{-3} T$	$-3{,}50 \pm 0{,}11$	$-3{,}5 \pm 0{,}6$	$0{,}0 \pm 0{,}7$
$CoSb_2$	$-3{,}80 - 0{,}17 \cdot 10^{-3} T$	$-3{,}94 \pm 0{,}17$	$-3{,}8 \pm 0{,}7$	$+0{,}2 \pm 0{,}8$
CoSb	$-3{,}99 - 0{,}52 \cdot 10^{-3} T$	$-4{,}43 \pm 0{,}18$	$-4{,}0 \pm 0{,}6$	$+0{,}5 \pm 0{,}7$

LITERATURE CITED

1. T. Rosenqvist, Acta Metallurgica 1, 761 (1953).
2. L. D. Dudkin and N. Kh. Abrikosov, Problems in Metallurgy and Semiconductor Physics [in Russian] (Moscow, 1957) p. 97.
3. U. Fürst and F. Halla, Z. Phys. Chem. B40, 285 (1938).
4. I. Oftedal, Z. Phys. Chem. 128, 135 (1927).
5. M. Hansen and K. Anderko, Constitution of Binary Alloys (1958).
6. T. Rosenqvist, Magnetic and Crystallographic Studies on the Higher Antimonides of Iron, Cobalt, and Nickel (Trondheim, 1953).
7. N. V. Ageev and E. S. Makarov, Izv. AN SSSR, OKhN, 1943, 87.
8. A. V. Nikol'skaya, V. A. Geiderikh, and Ya. I. Gerasimov, Doklady Akad. Nauk SSSR 130, 1074 (1960).
9. V. A. Geiderikh, A. A. Vecher, and Ya. I. Gerasimov, Zhur. Fiz. Khim. 34, 2789 (1960).
10. V. V. Nalimov, Analytical Applications of Mathematical Statistics [in Russian] (1960).

All abbreviations of periodicals in the above bibliography are letter-by-letter transliterations of the abbreviations as given in the original Russian journal. *Some or all of this periodical literature may well be available in English translation.* A complete list of the cover-to-cover English translations appears at the back of this issue.

THE CAPACITANCE OF THE ELECTRICAL DOUBLE LAYER IN N - METHYL FORMAMIDE SOLUTIONS

B. B. Damaskin and Yu. M. Povarov

M. V. Lomonosov Moscow State University
(Presented by Academician A. N. Frumkin, June 27, 1961)
Translated from Doklady Akademii Nauk SSSR, Vol. 140, No. 2,
pp. 394-397, September, 1961
Original article submitted June 27, 1961

The capacitance of an electrical double layer in nonaqueous solutions has been investigated by several workers [1-6]. The workers referred to used aliphatic alcohols as solvents. Since the dielectric constant of aliphatic alcohols is much lower than that of water, it is not surprising that the capacitance of the double layer decreases when water is replaced by alcohols [1,3,4]. Another peculiarity is that when the differential capacitance (C) in aliphatic alcohols is plotted as a function of the electrode potential (φ) the characteristic hump which in aqueous solutions occurs near the null point (n.p.) is completely absent. According to [7], the hump on the C vs. φ plot appears when the effective dielectric constant of the adsorbed dipole layer is at a maximum and hence its absence in CH_3OH and C_2H_5OH solutions may either be connected with a more compact arrangement of alcohol molecules at the mercury surface, which is very little affected by the field of the dipole layer, or with the lower freezing point of alcohols; therefore, capacitance data obtained in CH_3OH and C_2H_5OH at 25° should be compared with the $C - \varphi$ plots for water at higher temperatures [1,8].

In our current work we have used an impedance bridge [9] for measuring C as a function of φ on a mercury drop electrode in N-methylformamide solutions of various salts; the dielectric constant of N-methylformamide is much higher than that of water (D = 182.4 [10]). The potentials were measured with reference to a normal calomel electrode, which was connected to the cell through a bridge filled with a saturated aqueous solution of KCl. The commercial $HCONHCH_3$ was distilled twice in vacuo (at ~1 mm of Hg), shaken with CaO, and vacuum-distilled again. The last operation was repeated twice. After that the $HCONHCH_3$ was fractionally distilled under reduced pressure in a nitrogen atmosphere. The resulting N-methylformamide had a specific conductance of $(2\text{-}4) \cdot 10^{-7}$ $ohm^{-1} \cdot cm^{-1}$ at 20°, a freezing point of −3.4°, and a refractive index $n_D^{20} = 1.4300$. Before measuring the capacitance we subjected the experimental solutions to cathodic polarization over mercury in a hydrogen atmosphere by passing a current of $(1\text{-}6) \cdot 10^{-5}$ amp/cm^2 for 20 hrs.

The results are presented in Figs. 1-4.* The figures show that the double layer capacitance in N-methylformamide is generally smaller than in water. Thus, C = 8.8 $\mu F/cm^2$ in 0.1N KCl and φ = −1.8 v and 13.9 $\mu F/cm^2$ at φ = −0.6 v. Since the n.p. in this solution is at −0.41 v,** the indicated potentials represent a negatively charged mercury surface. One possible reason for the decreased capacitance (relative to water) may be the increased radius of the solvated cation in $HCONHCH_3$. On the other hand, the small values of the double layer capacitance in N-methylformamide indicate that the effective dielectric constant is much smaller in the vicinity of the surface than it is in the bulk of the solution [11].

In the case of positive surface charge, the capacitance rises sharply due to the specific adsorption of Cl^- ions. As in the case of aqueous solutions [12], the adsorbance of anions increases in the order $Cl^- < Br^- < I^-$, and the ascending portion of the $C - \mu$ curve shifts toward more negative potentials in the same order (Fig. 1). When Cs^+ is

*The double layer capacitance remained independent of the alternating current frequency, which we varied from 400 to 10,000 cps, over the entire range of investigated potentials. The data given here were obtained at 400 cps.
**The n.p. was determined from the maximum on the electrocapillary curve for a 0.1N KCl solution in N-methylformamide.

present in solution a similar rise is also observed at very negative polarizations, which indicates that at negative potentials in $HCONHCH_3$ solutions much more cesium is adsorbed in excess of the equivalent amount than is the case in aqueous solutions [13]. In N-methylformamide the adsorbance of Rb^+ ions on mercury is intermediate between that of K^+ and Cs^+ ions resembling more the former. In the series $K^+ - Na^+ - Li^+$, the capacitance rises slightly at potentials below −1.2 v and slightly declines in the region of the maximum (Fig. 1). This effect, which is not observed in aqueous [13,14] and alcoholic [4,5] solutions, requires further investigations.

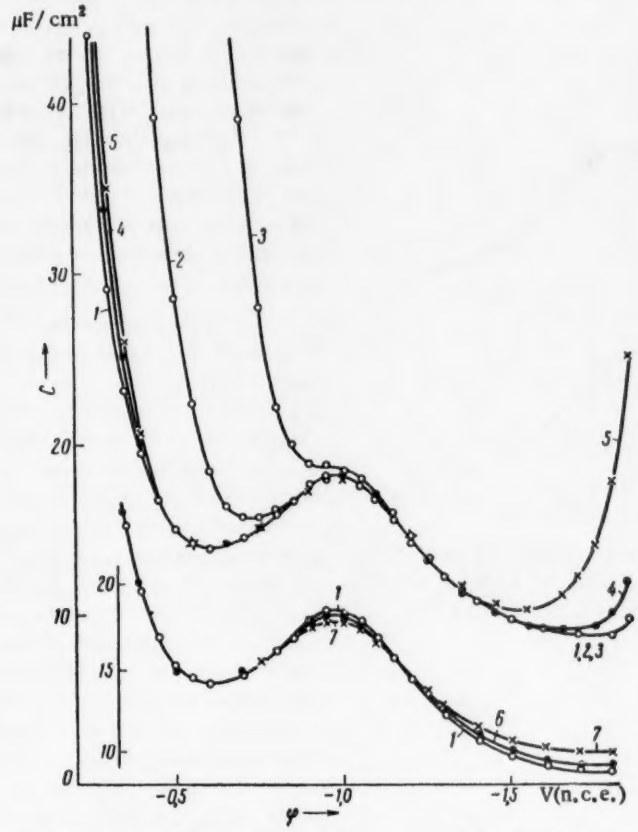

Fig. 1. The differential capacitance curves of 0.1N solutions of: 1) KCl; 2) KBr; 3) KI; 4) RbCl; 5) CsCl; 6) NaCl; 7) LiCl in N-methylformamide at 25°C.

When the solutions are diluted, the double layer becomes more diffuse and the capacitance near the n.p. decreases (Fig. 2a). Yet in N-methylformamide the decline in capacitance is much smaller than it is in water at comparable electrolyte concentrations. This is due to the fact that the capacitance of the dense layer (C_{ds}) in N-methylformamide is smaller than in water, while the capacitance of the diffusion layer (C_{dl}) is greater (because of higher dielectric constant). Hence, when C_{ds} and C_{dl} are connected in series, the capacitance of the diffusion layer (which is a function of concentration) has much less effect on the total differential capacitance in N-methylformamide than it does in water.

A distinct feature of the $C-\varphi$ curves in N-methylformamide is the maximum (hump) at potentials between −0.95 and −1.05 v. The effect of temperature on the capacitance at the maximum of the $C-\varphi$ curve (see Fig. 3*) led us to the conclusion that the hump on the capacitance curves obtained in $HCONHCH_3$ is of the same nature as

*We were unable to determine the capacitance at higher temperatures since at $t > 50°$, $HCONHCH_3$ begins to decompose appreciably.

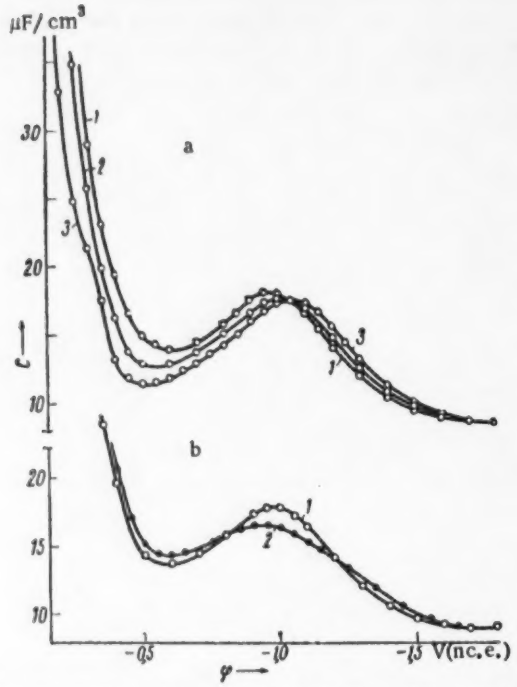

Fig. 2. Differential capacitance in N-methylformamide solutions at 25°C: a) KCl solutions: 1) 0.1N; 2) 0.03N; 3) 0.01N; b) NaCl solutions: 1) 0.1N; 2) 0.1N NaCl + + 10^{-3}N $(C_4H_9)_4NBr$.

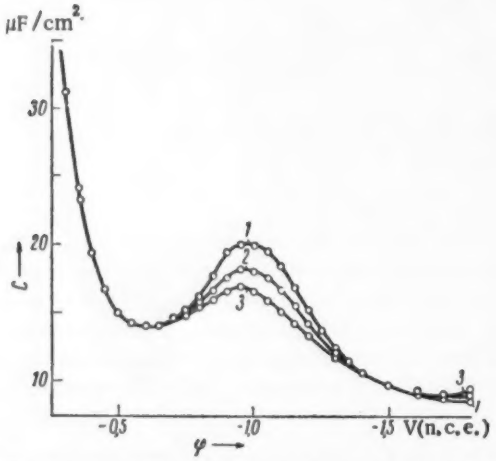

Fig. 3. The differential capacitance curves of 0.1N KCl in N-methylformamide at: 1) 0°; 2) 25°; 3) 50°.

the corresponding hump in aqueous solutions, i.e., it is connected with a change in the orientation of solvent dipoles [15]. The fact that the capacitance has a much smaller temperature coefficient in N-methylformamide than it does in aqueous solutions [8, 15] may be attributed to a stronger adsorption of $HCONHCH_3$ dipoles on the surface of mercury. In support of this conclusion we can cite the low surface tension in N-methylformamide solutions (in 0.1N KCl, σ_{max} = 382.0 dynes/cm), and the capacitance data obtained for solutions of 0.1N NaCl + + 10^{-3} N $[(C_4H_9)_4N]Br$ (Fig. 2b). In the latter case, as one can see in Fig. 2, the strongly adsorbed $HCONHCH_3$ molecules interfere with the adsorption of $(C_4H_9)_4N^+$ ions on mercury; as is well known [6,16], introduction of the tetrabutylammonium ion usually lowers the capacitance of a double layer to 4-5 μF/cm².

Since the lump on the $C - \varphi$ curves for N-methylformamide solutions occurs in the region of negative surface charge, and also since the $HCONHCH_3$ molecules are strongly adsorbed to the mercury surface, we can neglect the effect of specific adsorption on the orientation of solvent dipoles [15] at potentials in the vicinity of the hump. Therefore, on the basis of the most recent ideas [7], we can assume that the hump on the $C - \varphi$ curves in N-methylformamide solutions arises when the effective dielectric constant of the adsorbed layer of $HCONHCH_3$ molecules attains a maximum. Though the minimum dielectric constant does not in this case coincide with the n.p., we can explain this fact by assuming that most of the $HCONHCH_3$ molecules are lined up with the negative end of the dipole toward the mercury surface. If the explanation is right, the hump on the $C - \varphi$ curve should be practically independent of the nature of the electrolyte, which is consistent with the experimental data shown in Fig. 1.

Small amounts of water have very little effect on the shape of the $C - \varphi$ curve in N-methylformamide. As the water concentration is increased, the adsorbed layer of $HCONHCH_3$ molecules is disturbed and the hump on the $C - \varphi$ curves declines (as when the temperature is raised); at the same time, the capacitance at more negative potentials increases due to the adsorption of hydrated cations and the accompanying decrease in the width of the double layer [4] (Fig. 4). On the other hand, N-methylformamide is so strongly adsorbed on mercury that even minute amounts of it in water will disrupt the adsorbed water dipoles, with the result that the hump on the $C - \varphi$ curves disappears entirely, as in the case of elevated temperatures [8, 15].

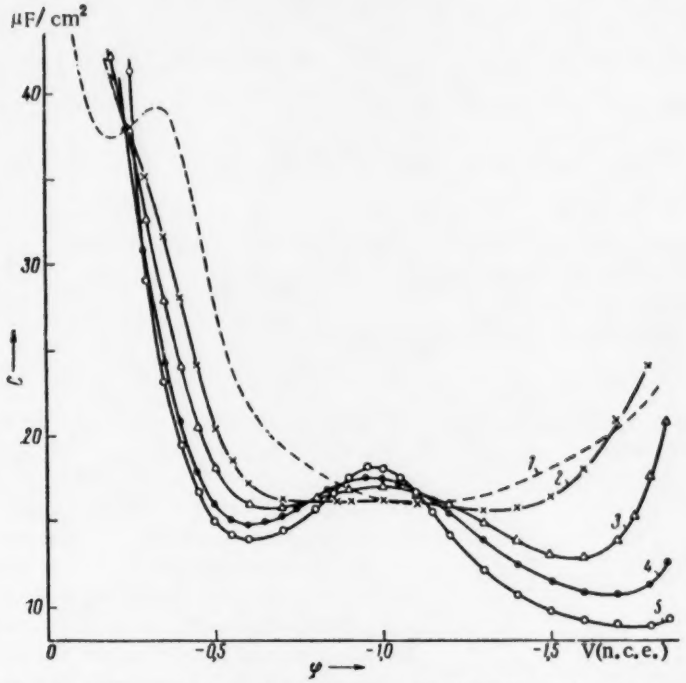

Fig. 4. Differential capacitance curves of 0.1N KCl solutions in aqueous N-methylformamide at 25°. The N-methylformamide concentration (in mole%): 1) 0; 2) 3.3; 3) 11.6; 4) 31.4; 5) 100.

We wish to express our deep gratitude to Academician A. N. Frumkin for his undivided attention to our work and discussion of experimental results.

LITERATURE CITED

1. D. C. Grahame, Z. Elektrochem. 59, 740 (1955).
2. V. L. Kheifets, B. S. Krasikov, V. V. Sysoeva, and I. V. Guseva, Vestnik LGU, ser. fiz. i khim. No. 22, 128 (1956); No. 22, 148 (1957).
3. A. A. Moussa, H. M. Sammour, and H. A. Chaley, J. Chem. Soc. 1958, 1269; Egypt. J. Chem. 1,165 (1958).
4. S. Minc and J. Jastrzebska, Roczn. chem. 31, 735 (1957); Dokl. Akad. Nauk SSSR 120, 114 (1958); J. Electrochem. Soc. 107, 135 (1960).
5. S. Minc and M. Brzostowska, Roczn. chem. 34, 1109 (1960).
6. P. A. Kirkov, Zhur. Fiz. Khim. 34, 2375 (1960); Dokl. Akad. Nauk SSSR 135, 651 (1960).
7. R. J. Watts-Tobin, Philos. Mag. 6, No. 61, 133 (1961).
8. D. C. Grahame, J. Am. Chem. Soc. 79, 2093 (1957).
9. D. C. Grahame, J. Phys. Chem. 61, 701 (1957).
10. G. R. Leader and J. F. Gormley, J. Am. Chem. Soc. 73, 5731 (1951).
11. A. N. Frumkin, Z. phys. Chem. 103, 43 (1923).
12. M. A. Vorsina and A. N. Frumkin, Zhur. Fiz. Khim. 19, 171 (1945).
13. A. N. Frumkin, B. B. Damaskin, and N. V. Nikolaeva-Fedorovich, Dokl. Akad. Nauk SSSR 115, 751 (1957); 121, 129 (1958).
14. D. C. Grahame, J. Electrochem. Soc. 98, 343 (1951).
15. B. B. Damaskin, E. Shwarts, and A. N. Frumkin, Dokl. Akad. Nauk SSSR (in press); Zhur. Fiz. Khim. (in press).
16. B. B. Damaskin and N. V. Nikolaeva-Fedorovich, Zhur. Fiz. Khim. 35, No. 6 (1961).

THE EFFECT OF LYOPHILIC COLLOIDS ON THE SOLUBILIZATION OF HYDROCARBONS IN DETERGENT SOLUTIONS

P. A. Demchenko, and Corr. Member of the Acad. of Sciences of the USSR A. V. Dumanskii

Institute of General and Inorganic Chemistry, Academy of Sciences of the USSR
Translated from Doklady Akademii Nauk SSSR, Vol. 140, No. 2, pp. 398-400, September, 1961
Original article submitted May 22, 1961

Solutions of lyophilic colloids do not have a detergent action or marked surface activity, but they have found wide application as active additives, which increase the effectiveness of detergents, drilling fluids, emulsifiers, and flotation agents [1-6]. The mechanism of the action of lyophilic colloids on the micellar structures of surface active materials is still insufficiently understood. It is believed that lyophilic colloids on adsorption from solution onto a surface impart to it a negative charge and prevent the settling of impurities from the bulk of the detergent solution onto the washed surface [7]. According to other ideas, carboxymethylcellulose and its solutions in water are not adsorbed onto the washed surface but onto the impurity particles [4]. By this, protective layers of lyophilic colloid molecules are formed on their surface. Because of this, the impurity particles cannot adhere to each other and settle on the washed surface. Up till now the ideas indicated have not been experimentally confirmed.

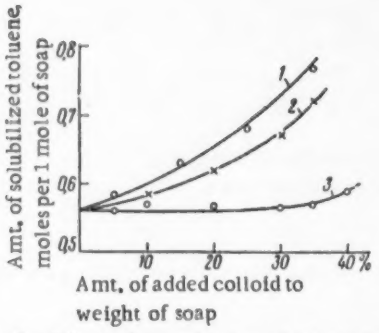

Fig. 1. Effect of the addition of (1) gelatine, (2) casein, (3) starch, on the solubilization of toluene in 0.3M potassium laurate solutions.

We have shown that the critical concentration for micell formation and the solubilizing capacity are specific properties of detergents [8,9], and the relative effectiveness of different surface active agents can be objectively evaluated according to these values. Any addition which changes the critical concentration for micell formation and the solubilizing capacity also changes the practically important properties of the detergent solution. The positive effect of addition of lyophilic colloids on the detergent action and other properties of detergents consists apparently in the fact that they displace the degree of their colloidal character to an optimal region.

In the present work the results of investigations of the effect of carboxymethylcellulose, gelatine, casein, saponin, starch, lecithin, and sodium humate on the solubilizing capacity of a 0.3M solution of potassium laurate and of sodium naphthenates are presented. Determination of the change in solubilization of hydrocarbons in soap solutions on addition of increasing amounts of lyophilic colloids was carried out by the volume method described earlier [10]. The results of the investigations are given in Figs. 1, 2, 3, and 4. From the experimental results it is seen that additions of gelatine, casein, or starch have different effects on the solubilizing capacity of the soap solutions. Additions of amounts of soluble starch up to 35% of the weight of potassium laurate showed no significant effect on the solubilization of toluene. An increase in solubilization of toluene in a 0.3M solution of potassium laurate was observed for casein and gelatine, gelatine addition being the more effective (Fig. 1). Increasing additions of saponin, carboxymethylcellulose (sodium salt), sodium humate, and lecithin showed a still greater effect on the solubilizing capacity of potassium laurate solutions (Fig. 2). Lecithin and sodium humate enhanced the solubilizing capacity of the soap solutions more sharply in comparison with carboxymethylcellulose. Saponin, gelatin, and casein were less effective than carboxymethylcellulose (Figs. 1 and 2). The lyophilic colloids investigated with respect to their effect on the solubilizing capacity of 0.3M potassium laurate solutions can be arranged in the decreasing series: lecithin > sodium humate > carboxymethylcellulose > saponin ≥ gelatine > casein > starch.

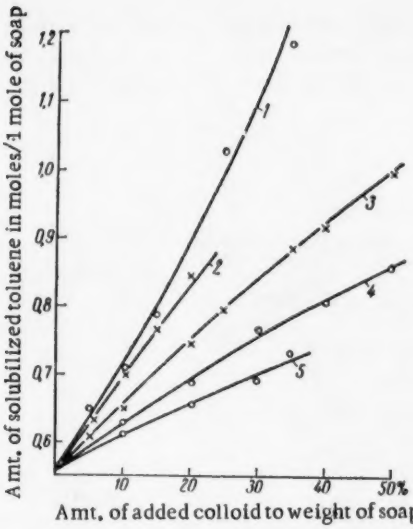

Fig. 2. Effect of the additions of 1) lecithin; 2) sodium humate (chlorinated); 3) sodium humate; 4) carboxymethylcellulose (sodium salt); and 5) saponin, on the solubilization of toluene in 0.3M potassium laurate solutions.

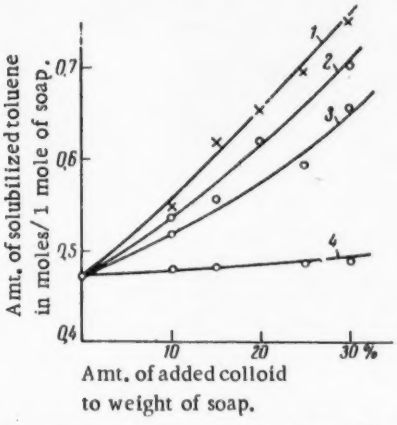

Fig. 4. Effect of the addition of: 1) sodium humate; 2) carboxymethylcellulose (sodium salt); 3) gelatine; 4) starch, on the solubilization of toluene in 0.3M solutions of sodium naphthenate (mol. wt. 242).

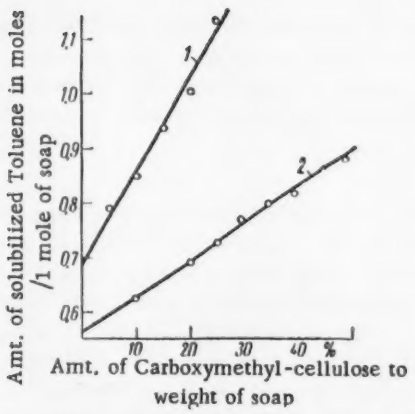

Fig. 3. Effect of the addition of carboxymethylcellulose on the solubilization of toluene in 0.3M solutions of 1) sodium naphthenate (mol. wt. 270); 2) sodium naphthenate (mol.wt.242).

Carboxymethylcellulose had the effect of increasing the solubilization of toluene in 0.3M sodium naphthenate solutions. The solubilizing capacity of a solution of sodium naphthenate of higher molecular weight was more sharply increased for the same additions of carboxymethylcellulose than a lower molecular weight homolog (Fig. 3). Thus, for example, by additions of carboxymethylcellulose 25% by weight of the sodium naphthenates with molecular weight of 242 or 270, solubilization of toluene was increased 1.3 and 1.7 times, respectively. Comparative results for the increase in the solubilizing capacity of sodium naphthenate solutions (mol. wt. 242) through addition of certain lyophilic colloids are given in Fig. 4.

Additions of soluble starch had practically no effect on the solubilization of toluene in sodium naphthenate solutions or in the case of potassium laurate (Figs. 1, 4). Gelatine was less effective than carboxymethylcellulose. Sodium humate prepared from lignite of the Alexandrian layer by the method described previously [11] was found to be a more effective intensifier of hydrocarbon solubilization than carboxymethylcellulose. The lyophilic colloids studied can be arranged as a series according to their effect in increasing the solubilization of toluene in 0.3M sodium naphthenate solutions: sodium humate > carboxymethylcellulose > gelatine > > starch. The lyophilic colloids at the experimental temperature (around 60°) had practically no solubilizing capacity.

On the basis of the experimental data obtained, and of earlier studies [8,9], it can be concluded that lyophilic colloids are adsorbed on the soap micellar structures and by joint association with the detergent forms compound micelles. The solubilizing capacity of the compound micellar structures is higher than that of micelles. In addition, lyophilic colloids and detergents, in peptizing hydrocarbons to a colloidal degree of dispersion, form on their surface protective layers of negatively charged, hydrophilic groups which face into the aqueous phase. Such particles with a protective layer acquire lyophilic properties, similar to detergent micelles, containing solubilized hydrocarbon and they can be designated pseudomicelles. The impurities are held in the volume of the detergent solutions because of the colloidal structure, which is one of the factors increasing their effectiveness.

Such compound micelles possess more oleophilic properties which approximate to the micellar structures formed by soap homologs with more developed hydrocarbon radicals. In the present work it was shown that by means of carboxymethylcellulose and other lyophilic colloids it is possible to regulate the degree of colloidal character of detergent solutions and their practically important properties.

LITERATURE CITED

1. A. V. Dumanskii, Lyophilicity of Dispersed Systems [in Russian] (Kiev, 1960).
2. A. Schwartz, J. Perry, and J. Birch, Surface-Active Agents and Detefgents [Russian translation] (IL, 1960).
3. F. V. Nerolin, Khim nauki i prom. 4, 586 (1959).
4. G. Shtyupel', Synthetic Washing and Purifying Agents [in Russian] (Moscow, 1960).
5. W. Fong and H. Lundgren, Text. Res. J. 23, 769 (1953).
6. H. Freedman, J. Mason, and A. J. Medolia, J. Organ. Chem. 23, 76 (1958).
7. E. Bartholome, and K. F. Buschmann, Melliand Textilber. 30, 249 (1949).
8. P. A. Demchenko, Masloboino-shirovaya promyshlennost' No. 7, 36 (1959).
9. P. A. Demchenko and A. V. Dumanskii, Koll. zhurn. 22, 272 (1960).
10. P. A. Demchenko, Koll. zhurn. 23, 31 (1961).
11. P. A. Demchenko and L. G. Demchenko, Water Filtration Control in Loess Soils: Collected Studies [in Russian] (Kiev, 1954) p. 93.

All abbreviations of periodicals in the above bibliography are letter-by-letter transliterations of the abbreviations as given in the original Russian journal. *Some or all of this periodical literature may well be available in English translation.* A complete list of the cover-to-cover English translations appears at the back of this issue.

THE NATURE OF THE SURFACE OF CATALYTICALLY ACTIVE ALUMINUM OXIDE

M. M. Egorov

M. V. Lomonosov Moscow State University
(Presented by Academician M. M. Dubinin, April 5, 1961)
Translated from Doklady Akademii Nauk SSSR, Vol. 140, No. 2,
pp. 401-404, September, 1961
Original article submitted March 28, 1961

The surface of aluminum oxide and, in particular, of the catalytically active γ-form is hydrated. The degree of hydration of the surface determines to a considerable extent its adsorptive and, apparently, its catalytic properties. In an earlier paper [1] the content of structural water in aluminum oxide samples, subjected to thermal treatment over a wide temperature range was determined, and the heats of wetting these samples with water were also determined. The results obtained permitted division of the total quantity of structural water into water belonging to the volume and to the surface hydrates of the alumina. It is of interest to calculate the degree of surface hydration for the different modifications of Al_2O_3 based on the crystallography of the volume phases, and to compare the calculated results with experiment.

Although crystallographic calculations for the surface of silica have been made by many authors [2-5], they have not been carried out for aluminum oxide. In the present communication we will consider the surface of hydrargillite ($Al_2O_3 \cdot 3H_2O$), corundum (α-Al_2O_3), and γ-Al_2O_3. The structures of the volume phases of these modifications are described in [6-8].

The simplest calculation of the hydroxyl concentration on the surface of hydrargillite is for the ideal cleavage plane (001), where each hydroxyl ion is bound to two Al ions, and each Al ion is bound to three hydroxyls lying above and to three lying below.

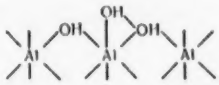

(1)

On the unit cell area, $a_0 + b_0$ are 6 hydroxyls which amounts to 11.4 μmoles/m^2 of H_2O. Formation of the (100) plane is accompanied by breaking of the coordination bonds* of Al–OH and disturbance of the normal octahedral coordination of Al:

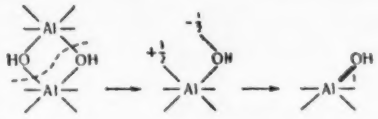

(2)

By contact of such a surface with water (hydration) normal coordination is restored

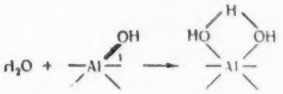

During this conditions are established in which a proton is associated with two anions. The degree of hydration of such a surface is approximately 10.2 μmoles/m^2 of H_2O.

The hydrated surface of corundum is analogous in structure to a layer of hydrargillite (scheme 1). On the

*Each coordination bond in the aluminum oxide structures (except the γ-form) has a valency of $\frac{1}{2}$. We have used the idea of a fractional valency as a convenient working terminology. It is analogous to the "strength" of a coordination bond introduced by Pauling.

hexagonal unit cell area (a_0 = 4.76) are three anions, which corresponds to a degree of hydration of the surface (0001) equal to 12.7 μmoles/m^2 of H_2O. The processes of thermal dehydration and rehydration can be represented by the scheme:

(3)

The dehydrated condition of the surface is stabilized analogously to scheme (2) by a decrease in the coordination number of part of the Al atoms to 4 and part to 5.

On passing to the cubic modification of aluminum oxide (γ-Al_2O_3) it must be noted that its structure is a defect spinel. The defectiveness of the structure is inferred from the fact that in a number of known tetrahedral interstitial close packings of oxygen ions there are located trivalent aluminum ions instead of divalent cations, as in the case of ordinary spinel. In a number of others the interstitial cations are absent, i.e., there is a local excess or a shortage of cations in the crystal structure. The surface of a break in the structure (according to the plane of the octahedron) will contain the following centers:

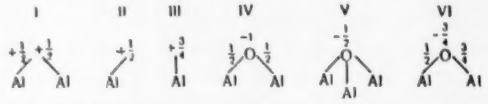

Mutual linking of the broken bonds disturbs the coordination of the aluminum atoms, but does not lead to complete saturation of the valencies. On the surface, as in the volume, local defects are partly preserved. In the process of hydration of the surface, formation of the following groups can be expected:

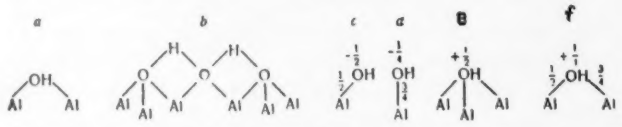

Mutual compensation of defects of opposite sign (c,d,e,f) in neighboring groups is only partially possible. It may also be assumed that hydration of the surface is accompanied by the introduction of hydrogen (H_2) into the tetrad interstices under the surface layer of anions,* where by virtue of the defect spinel structure of γ-Al_2O_3 there is a local deficiency of cations. In this way a considerable part of the surface defects is removed, but the stoichiometry is upset.

Assuming that these two variants of the hydration could combine, we obtain the following results for the composition of the surface:

1. "Buried" hydrogen (H_2)	1.0 μmoles/m^2
2. Isolated hydroxyls (a)	7.7 μmoles/m^2
3. Protons bound equally with two anions [in (b) groups]	3.1 μmoles/m^2
4. Protons bound $^3/_4$ with one anion and $^1/_4$ with another or still more complexly. Protons in groups with incomplete saturation of the valencies. Hydroxyls bound not only with Al atoms, but also with "buried" hydrogen	11.7 μmoles/m^2

By complete dehydration, 11.7 μmoles/m^2 of water and 0.5 μmoles/m^2 of hydrogen (H_2) can be removed from unit surface area. If on the surface (001) of the corundum each hydroxyl is bound with two underlying aluminum atoms, then on the hydrated surface of γ-Al_2O_3 an appreciable part of the anions is bound with the volume by one bond (scheme). Such anions will be broken off from the surface in the first instance. The dehydration–rehydration process can proceed, for example, according to the following scheme:**

*This hydrogen can be termed "buried."

**Reaction of the dehydrated surface with alcohol molecules can apparently be represented by an analogous scheme with formation not only of OH^- groups but also OR groups, where R is the corresponding radical.

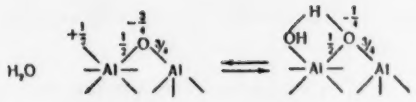

(4)

The defect surface structures and the variation of its composition in the dehydrated and hydrated states, as well as the possible presence of superstoichiometric hydrogen could probably be connected with the known catalytic properties of γ-Al_2O_3 (for example in hydrogenation [9]). The defects, apparently can move ("creep") to the surface within the limits of small regions, i.e., they can be localized on different atoms of the surface. On adsorbing a molecule, the surface of the γ-Al_2O_3 can, as it were, "adjust" to its size by changing the distance between two of its own defects of opposite sign. Development of similar ideas is of interest from the point of view of the multiplet theory of catalysis.

TABLE 1. Phase Composition, Degree of Hydration of Surface, Heats of Wetting, and Irreversible Adsorption for Aluminum Oxide Samples•

Number	Temperature of calcination, °C	Phase composition of surface layer	Heat of wetting erg/cm²		Degree of hydration of surface of samples, μmoles H_2O/1 m²		Calculated values of degree of hydration	Irreversible adsorption of ethanol
			water	ethanol	calcined	rehydrated		
1	200••		342		9.4		11.7	
2	300	Distorted γ-form	384	330	7.75			3.0
3	400	The same	420		6.32			
4	500	The same	495	407	4.8	9.35		3.1
5	600	The same	520		4.43	9.7		
6	700•••	Intermediate phases and corundum	590	500	4.3			
7	900	Corundum	670	555	1.4	11.1	12.7	3.6

•Data for degree of hydration heat of wetting with water and phase composition of the samples taken from [1].
••Beginning at 200° the samples did not contain a hydrate.
•••Beginning at around 700° a recrystallization occurs in the surface layer, with formation of corundum [1].

On passing to a comparison with experiment, it is necessary to stress that the crystallographic calculations made have a valuable character. The real surface of the solid can be distinguished from the ideal profile [10]. In Table 1 are given the experimental data for the degree of hydration of the surface of the aluminum oxide samples and heats of wetting with water [1], as well as the irreversible adsorption and heats of wetting with ethanol.

The maximum values for the degree of hydration of the surface of corundum and of the γ-form found from experiment agree satisfactorily with the theoretical estimates. This shows that, in the previous paper [1], the division of water entering into the composition of the volume hydrates and surface water was rightly made. The results from rehydration of the calcined samples confirm that the processes described in schemes (3) and (4) are completely reversible.

The heat of wetting of aluminum oxide with water increases according to the dehydration of the surface. Consequently, the energy of rehydration prevails over the energy of reaction of a water molecule with the hydrated surface. The heat of wetting of corundum by water is greater than that for the γ-form at approximately equal values for the degree of hydration. This agrees with our assumption that the surface hydroxyls on corundum are bound with the volume more firmly than on the surface of the γ-Al_2O_3. In [11] such an increase in the heat of wetting with water with rise in temperature of treatment and with decrease in the water content in the aluminum oxide samples is found.

The irreversible adsorption of ethanol vapor increases according to the dehydration of the Al_2O_3 surface. Probably the alcohol molecules react not only with the surface hydroxyls [12] but also with the dehydrated regions by schemes analogous to (3) and (4). The energy of reaction of alcohol with the dehydrated regions is greater than for

the hydrated regions since the heat of wetting of aluminum oxide with alcohol, as in the case of water, increases with decrease in the degree of hydration of the surface.

The author thanks Academician N. V. Belov for his interest in the work, and also V. F. Kiselev and K. G. Krasil'nikov for help and discussion of the results.

LITERATURE CITED

1. M. M. Egorov, B. F. Kiselev, K. G. Krasil'nikov, and Yu. P. Simanov, Izv. Vyssh. uch. zav. Khimiya i Khim. Tekhnol. 2, 360 (1959).
2. R. K. Aller, Colloid Chemistry of Silica and Silicates [in Russian] (Moscow, 1959).
3. W. Stöber, Koll. Zs. 145, 17 (1956).
4. S. P. Zhdanov and A. V. Kiselev. Zhur. Fiz. Khim. 31, 2213 (1957).
5. J. H. De Boer and J. M. Vleeskens, Proc. Kon. Ned. Akad. v. Wetensch. B61, 2 (1958).
6. A. G. Betekhtin, Mineralogy [in Russian] (Moscow, 1950).
7. B. F. Ormont, The Structures of Inorganic Materials [in Russian] (1950).
8. N. V. Belov, The Structure of Ionic Crystals and Metallic Phases [in Russian] (1947).
9. G. A. Mills, S. Weller, S. Hindin, and T. H. Milliken, Zs. Elektrochem. 60, 823 (1956).
10. W. A. Weyl and E. C. Marboe, Formation of Amorphous Solids and Characterization of their Structure by Energy Profiles (Munich, 1959).
11. W. H. Wade and N. Hackerman, J. Phys. Chem. 64, 1196 (1960).
12. K. V. Topchieva, K. Yun-Pin, and I. V. Smirnova, Collection: Surface Chemical Compounds and their Role in Adsorption Phenomena [in Russian] (Moscow, 1957).

All abbreviations of periodicals in the above bibliography are letter-by-letter transliterations of the abbreviations as given in the original Russian journal. *Some or all of this periodical literature may well be available in English translation.* A complete list of the cover-to-cover English translations appears at the back of this issue.

THE MECHANISM OF CHAIN BRANCHING IN THE LIQUID PHASE OXIDATION OF METHYLETHYLKETONE

G. I. Zaikov, Z. K. Maizus, and Corr. Member Acad. Sci. USSR N. M. Émanuél

Institute of Chemical Physics, Academy of Sciences of the USSR

Translated from Doklady Akademii Nauk SSSR, Vol. 140, No. 2, pp. 405-408, September, 1961
Original article submitted May 20, 1961

The degenerate branching reactions observed in the liquid-phase oxidation of hydrocarbons are currently attributed to the accumulation of peroxides, which readily break up into radicals. Recently it has been experimentally demonstrated that hydroperoxides are indeed the products primarily responsible for chain branching [1]. By the use of inhibitors, the branching rate at various stages of n-decane oxidation was determined, and a linear relationship was established between the branching rate and hydroperoxide concentration. Yet hydroperoxides are not always the sole branching agents in the liquid-phase oxidation of hydrocarbons. For example, it has been shown that when cyclohexane is oxidized in steel vessels in addition to the radicals formed by the decomposition of cyclohexyl hydroperoxides, cyclohexanone is also involved in promoting chain branching [2].

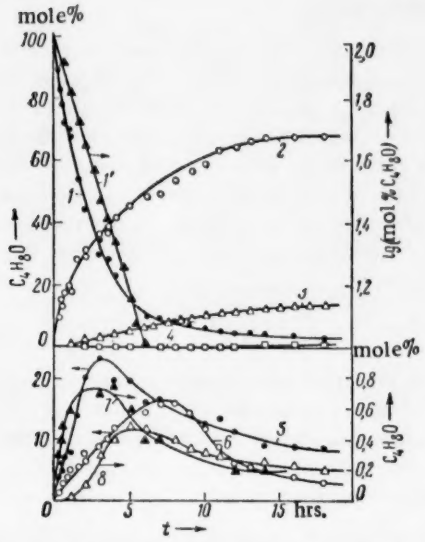

Fig. 1. Rate curves for decomposition of methyl ethylketone and accumulation of reaction products at t = 145°, 50 atm pressure, and a 20 liters per hr rate of air flow: 1) decomposition of methylethylketone; 1') semilog plot of curve 1; 2) accumulation of acetic acid; 3) CO_2; 4) CO; 5) ethylacetate; 6) diacetyl; 7) ketohydroperoxide (right-hand scale); 8) ethanol (right-hand scale).

In the present work, by studying the liquid-phase oxidation of methylethylketone we proved that degenerate chain branching proceeds through the decomposition into radicals of two active intermediates: ketohydroperoxide and diacetyl. This result is also of great importance in connection with the liquid-phase oxidation of low-molecular-weight hydrocarbons, since methylethylketone is an intermediate product in the combustion of n-butane [3].

The literature dealing with liquid-phase oxidation contains practically no data on the oxidation of methylethylketone by molecular oxygen. Work has been done on its oxidation by trifluoroacetic acid [4], oxides of manganese [5], chromic acid [6], etc. We investigated the oxidation of methylethylketone in the liquid phase by using air oxygen at a pressure of 50 atm at temperatures between 100 and 145° in an autoclave-like apparatus [7]. The oxidation products (acetic acid, ethylacetate, diacetyl, ethanol, peroxides, CO, and CO_2) were analyzed by ordinary chemical methods as well as by means of a specially developed technique involving paper chromatography [8-10].

The general shape of the rate curve for the decomposition of methylethylketone (Fig. 1), and the fact that a semilog plot transforms it into a straight line, indicate that the oxidation of methylethylketone follows first-order kinetics. Of course, we are dealing with a complex process which only imitates a kinetically simple reaction; this type of behavior has frequently been observed in branching chain reactions at high initial concentrations of active centers. That this is indeed the case can be deduced from the fact that (as we have shown in this work), the oxidation of methylethylketone is a chain reaction, and that the frequency factor in the rate expression is abnormally small, $k = 5.2 \cdot 10 \exp(-11{,}200/RT)\,sec^{-1}$.

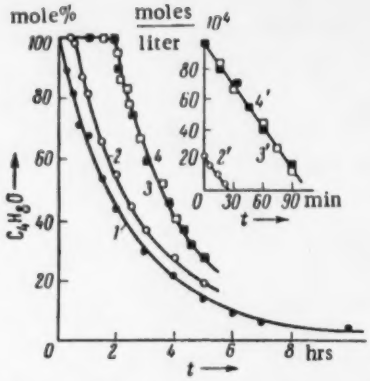

Fig. 2. Rate curves for oxidation of methylethylketone at t = 145° and 50 atm pressure: 1) in absence of inhibitor; 2) when $1.59 \cdot 10^{-3}$ moles per liter α-naphthol are added to initial methylethylketone; 3) and 4) when $9.54 \cdot 10^{-3}$ moles/liter of α-naphthol are added; 2'), 3'), and 4') corresponding curves for rate of inhibitor consumption during induction period in oxidation of methylethylketone.

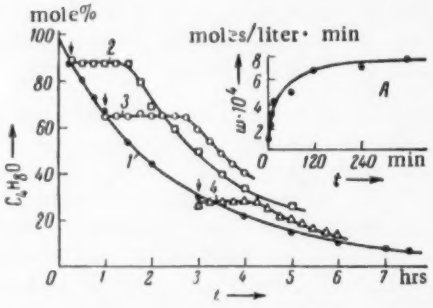

Fig. 3. Rate curves for oxidation of methylethylketone in presence of α-naphthol at t = 145° and p = 50 atm. The times at which the inhibitor was introduced are marked by arrows: 1) in absence of α-naphthol; 2) $3.1 \cdot 10^{-2}$ moles/liter of α-naphthol; 4) $5.2 \cdot 10^{-2}$ moles/liter of α-naphthol. A—The rate curve for chain initiation during reaction.

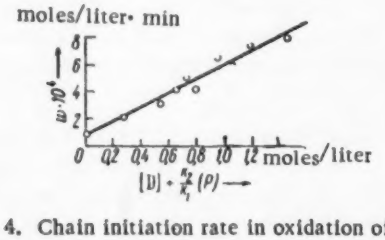

Fig. 4. Chain initiation rate in oxidation of methylethylketone as a function of combined concentration of ketohydroperoxide and diacetyl at t = 145°, p = 50 atm.

To prove that we are dealing with a chain reaction, we added to the methylethylketone some α-naphthol, which is known to be a strong oxidation inhibitor. In the presence of α-naphthol one observes a long induction period, the length of which increases with increasing inhibitor concentration (Fig. 2).

From the rate at which the inhibitor is used up during the induction period, one can determine the rate of chain initiation during the oxidation of methylethylketone, $w_0 = 1.5 \cdot 10^{-6}$ moles/liter · sec at 145°. This figure exceeds considerably the corresponding w_0 in similar oxidation reactions in acetone and cyclohexanol [11,12]. Once the oxidation is in full swing, the chain initiation rate increases over the initial w_0 due to degenerate branching. The initiation rate in the course of the reaction was determined by measuring the rate at which the inhibitor, when added to the reaction mixture at various time intervals, after the oxidation has begun, is used up.

Figure 3 shows that the oxidation of methylethylketone proceeds solely by a chain route, since, as soon as the inhibitor is added, the decomposition of the compound comes to a complete stop.

The relative increase in the initiation rate once the reaction is in progress is small. Thus, over a segment of the rate curve from 0.5 to 5 hrs, the initiation rate increased by only a factor of two. This apparently explains why the chain reaction obeys simple kinetics. As a matter of fact, from an equation representing hydrocarbon oxidation rate as a function of the initiation rate [13], one can derive an expression for the oxidation of methylethylketone in the form shown below:

$$w = \frac{k_2}{\sqrt{k_5}} [RCOR_1] w_i^{1/2},$$

While the initiation rate is double in the course of the reaction, $w_i^{\frac{1}{2}}$ increases only by a factor of 1.3, which makes the reaction rate almost linearly dependent on the methylethylketone concentration or, in other words, we get an apparent first-order reaction.

Only at the beginning of the reaction proper does the chain branching rate increase in direct proportion to the concentration of the accumulated ketohydroperoxide. After that the over-all rate of radical formation (determined from the rate at which the inhibitor is consumed) exceeds by a large margin the value expected for a simple decomposition of ketohydroperoxide into free radicals. This would indicate that in addition to ketohydroperoxides other intermediates also participate in the chain branching in the oxidation of methylethylketone.

The other participating product could reasonably be diacetyl, since it is present in large concentrations among the reaction products and can readily break up into two free radicals [14]. In fact, whenever small amounts of diacetyl are added to methylethylketone in the course of its

oxidation the rate of chain branching increases right away. In order to get a quantitative picture of the chain branching processes we determined the rate of branching as a function of the combined concentration of both branching products, ketohydroperoxide and diacetyl.

The rate of chain initiation at any instant during the reaction can be expressed by the equation

$$w_1 = k_1 [D]_1 + k_2 [P]_1 = k_1 \left\{ [D_1] + \frac{k_2}{k_1} [P]_1 \right\}, \quad (1)$$

where [D] and [P] are the concentrations of diacetyl and ketohydroperoxide, respectively, k_1 and k_2 are the respective specific decomposition rates of the two compounds. Should we introduce into the reaction mixture at that instant an additional amount of diacetyl, we will have to modify Eq. (1) as shown below:

$$w_2 = k_1 [D]_2 + k_2 [P]_1 = k_1 \left\{ [D]_2 + \frac{k_2}{k_1} [P]_1 \right\}. \quad (2)$$

Dividing Eq. (1) by Eq. (2), we get

$$\frac{w_1}{w_2} = \frac{[D]_1 + \frac{k_2}{k_1} [P]_1}{[D]_2 + \frac{k_2}{k_1} [P]_1}.$$

We can readily evaluate k_2/k_1 since all the other parameters can be determined experimentally. Substituting the value of k_2/k_1 into Eq. (1) we get an expression in which the rate of chain branching is given as a function of the over-all concentration of the two branching products (Fig. 4). The fact that this function is linear clearly indicates that no products other than ketohydroperoxide and diacetyl participate in chain branching. The slope of the line in Fig. 4 yields $k_1 = 1.0 \cdot 10^{-5}$ sec^{-1} for the specific rate of decomposition of diacetyl into radicals at 145°C.

Experiments in which the decomposition of pure diacetyl, which we synthesized for that specific purpose, was examined yielded a similar value for k_1 and the expression $k_1 = 2.9 \cdot 10^{13} \exp(-35{,}400/RT)\,\text{sec}^{-1}$ for the temperature dependence of the specific rate. The fact that the frequency factor has a value one would expect for a true monomolecular reaction supports the postulated reaction mechanism in which chain branching is promoted by the break of diacetyl molecules into two radicals.

From k_1 and k_2/k_1 we can also determine the specific decomposition rate of the hydroperoxide of methylethylketone into radicals, $k_2 = 1.4 \cdot 10^{-4}$ sec^{-1}. Since k_2 exceeds k_1 by one order of magnitude, under the same experimental conditions, one would expect the ketohydroperoxide to play a predominant role in promoting chain branching. However, it turns out that the difference in rate constants is compensated by the relatively greater amount of diacetyl formed in the reaction.

The ratio w/w_{branch}, which yields the chain length, rapidly decreases during the oxidation of methyethylketone from 360 at the beginning to 12 toward the end of the reaction.

LITERATURE CITED

1. D. C. Knorre, Z. K. Maizus, and N. M. Émanuél', Dokl. Akad. Nauk SSSR 123, 123 (1958).
2. I. V. Berezin, N. F. Kazanskaya, and V. F. Privalov, Dokl. Akad. Nauk SSSR 126, 809 (1959).
3. N. M. Émanuél', Dokl. Akad. Nauk SSSR 110, 245 (1956).
4. W. D. Emmons and G. B. Lucas, J. Am. Chem. Soc. 77, 2287 (1955).
5. J. S. F. Pode and W. A. Waters, J. Chem. Soc. 1956, 717.
6. W. A. Waters, J. Chem. Soc. 1946, 1151.
7. É. A. Blyumberg, Z. K. Maizus, and N. M. Émanuél', Collection: Liquid Phase Oxidation of Hydrocarbons [in Russian] (Izd. AN SSSR, 1959) p. 125.
8. G. E. Zaikov, Zhurn. analit. khim. 15, 104 (1960).
9. G. E. Zaikov, Zhurn. analit. khim. 15, 639 (1960).
10. G. E. Zaikov, Zhurn. analit. khim. 16, No. 6 (1961).
11. E. T. Denisov, Collection: Kinetics and Catalysis [in Russian] (Izd. AN SSSR, 1960) p. 92.
12. E. T. Denisov, Dokl. Akad. Nauk SSSR 130, 1065 (1960).
13. D. G. Knorre, Z. K. Maizus, L. K. Obukhova, and N. M. Émanuél', Usp. khim. 26, 416 (1957).
14. R. P. Taylor and F. E. Blacet, Ind. Eng. Chem. 48, 1505 (1956).

A UNIDIMENSIONAL MODEL OF UNSTABLE BURNING

S. S. Novikov and Yu. S. Ryazantsev

Institute of Chemical Physics, Academy of Sciences of the USSR
Presented by Academician V. N. Kondrat'ev, April 13, 1961
Translated from Doklady Akademii Nauk SSSR, Vol. 140, No. 2,
pp. 409-411, September, 1961
Original article submitted April 10, 1961

The value of the acoustic impedance of a burning surface serves as an extreme case in the problem of the stability of natural oscillation in theories of resonance combustion [1-3] and, to a considerable extent, determines the possibility of stable burning conditions. But the experimental difficulties do not permit this value to be measured by standard acoustic methods. At the same time, expressions for impedance obtained from theories of combustion [4,5] are rather arbitrary due to the different methods used for the combustion process. Comparison of theory with experimental results obtained by other investigators [1-3] is difficult, since, in their work, combustion was considered as taking place in a space having a complex geometry and the conditions at its outlet, to a significant degree, were arbitrary. This prevents the same expression from being derived for the acoustic impedance of a burning surface.

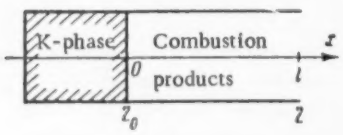

Fig. 1.

These difficulties may be avoided if a unidimensional model is examined in which the instability can arise only in longitudinal acoustic directions (Fig. 1). The stability of combustion was considered from the point of view of maintaining the gas balance, by Andreev and Belyaev [6,7]. This kind of acoustic instability observed in the burning of condensed systems in a tube, for example, is known as pyrotechnic whistles [13]. This phenomenon occurs when certain compositions are burned in a tube; for example, a mixture of 30% potassium benzoate and 70% potassium perchlorate generate a sound with a frequency approximately equal to the fundamental tone of the tube. Raushenbakh investigated the stability of a system analogous to that in question, in the case of the burning of gases [8]. His work also showed that by studying this type of system the way was opened to investigate nonstationary parameters of combustion. In the case of the burning of condensed systems, complicating circumstances such as the curving of the combustion front are removed. Instability in a similar type of system leads to the autooscillation process, the frequency of which is the natural frequency of the system [9,10].

As a linear approximation the question of burning stability of a condensed system in a tube may be formulated as the acoustic problem of natural oscillations in a tube closed by the impedances Z_0 and Z_l. In addition, it is assumed that the burning velocity is small, so that the variation of the tube length due to the change of position of combustion in the time during which the oscillations are set up may be neglected. The natural frequencies of these types of systems are determined from the following equation [11]:

$$\frac{Z_0+1}{Z_0-1}=\frac{Z_l-1}{Z_l+1}e^{-2ikl}, \tag{1}$$

where $k = \omega/c$ is the wave vector; Z_0 is the impedance of the burning surface; Z_l is the impedance of the open end of the tube.

The roots of Eq. (1) are generally complex, $\omega = \alpha + i\beta$. If $\beta < 0$, then the amplitude of the natural frequency will increase with time. The value $\beta = 0$ corresponds to neutral oscillations and determines the range of stability of the system. The condition of autoexcitation of the system, from Eq. (1), may be written in the form

$$r_0 r_l > 1, \tag{2}$$

where $r_0 = |R_0|$, $R_0 = r_0 e^{2i\delta_0}$ is the coefficient of reflection of the burning surface; $r_l = |R_l|$, $R_l = r_l e^{2i\delta_l}$ is the coefficient of reflection of the open end of the tube. Condition (2) has a simple physical measuring: a decrease in the amplitude of the wave at the open end of the tube due to radiation in the presence of instability must be

superimposed by an increase in the amplitude of the wave with reflection from the burning surface. At the limit of stability the equality $r_l = 1$ applies. If the impedances Z_0 and Z_l are known then, by using equations (1) it is possible to find the values ω_{cr} and l_{cr} corresponding to the limit of stability. On the other hand, if the system has a region of instability then, by using the experimental values of the frequency of oscillation ω_{cr} and the tube length l_{cr} corresponding to it, it is possible, with the help of Eq. (1), to determine the impedance of the burning surface $z_0(\omega_{cr}) = X_0(\omega_{cr}) + iY_0(\omega_{cr})$; for this purpose it is also necessary to know the value Z_l. The impedance of the open end of a cylindrical tube Z_l has been found by Gutin [12]. With $ka \ll 1$ it equals $Z_l = k^2a^2/4 + i \cdot 2ka/\pi$.

It is necessary to note that the possibility of using this expression for the acoustic impedance of an open end of the tube [12] is restricted by a number of factors, such as the presence of the flow of gas in the tube; the existence of a contact explosion separating the jet of gases flowing from the tube from the surrounding gas, the nonisentropicity of the flow. Usually the effect of these factors is small and, to a first approximation, may be neglected.

By varying the radius of the tube so that the criterion which ensures that only longitudinal acoustic modes are present in the system, and by fixing the values ω_{cr} and l_{cr} for each value of the radius, it is possible to determine the relation between the frequency and the impedance of the burning surface $Z_0(\omega)$. It is usually considered that the frequency of autooscillation in similar systems is the natural frequency of the system [9,10]. This indicates that even at a great distance from the stability limit the relation $2\delta_0 + 2\delta_l - 2kl = 2\pi n$, remains applicable. If it is assumed that δ_l does not depend on β, this relation will determine the frequency relation $\delta_0(\alpha)$.

If the acoustic impedance of the burning surface does not depend on frequency, and $r_0 > 1$, then the qualitativ representation for the development of combustion is as follows: while the length of the tube is less than l_{cr}, burning is stable; as the condensed phase burns, the natural frequency of the system falls and finally reaches the value

$$\omega_{kp} = \frac{c_1}{a}\sqrt{1 - \frac{1}{r_0^2}},$$

Commencing from this instant of time, the process is unstable and the system will produce sonic oscillations. The case is somewhat different if the frequency relation $Z_0(\omega)$ has the form predicted by theory developed by Hart and McClure [4]. In this case, both upper and lower limits of unstable frequencies must exist so that the region of instability occupies a certain band of frequencies. In addition, it is possible to have the case when the region of instability is completely absent, despite the fact that for sufficiently large values of ω the coefficient of reflection $r_0(\omega) > 1$.

LITERATURE CITED

1. H. Grad, Comm. on Pure and Appl. Math. 2, 79 (1949).
2. S. I. Cheng, Problems of Rocket Engineering [in Russian] (1954) p. 6.
3. F. T. McClure, R. W. Hart, and J. F. Bird, J. Appl. Phys. 31, 884 (1960).
4. R. W. Hart and F. T. McClure, Problems of Rocket Engineering [in Russian] (1960) p. 2.
5. J. F. Bird, L. Haar, R. W. Hart, and F. T. McClure, J. Chem. Phys. 32, 1423 (1960).
6. K. K. Andreev, Thermal Decomposition and the Burning of High Explosives [in Russian] (1957).
7. A. F. Belyaev, Doctoral Thesis [in Russian] (Inst. Khim. Fiz. AN SSSR).
8. B. V. Raushenbakh, Zhur. Tekh. Fiz. 23, 2, 358 (1953).
9. L. Crocco and J. Grey, Combustion Instability in Liquid Propellant Rocket Motors, Proc. Gas Dynamics Symposium Aerothermochemistry (Evanston, 1955) pp. 55-70; S. I. Cheng and A. A. Kovitz, Ignition in the Laminar Wake of a Flat Plate, Sixth Symposium on Combustion (1956) pp. 418-427.
10. D. I. Blokhintsev, Acoustics of a Heterogeneous Moving Medium [in Russian] (Moscow, 1946).
11. S. N. Rzhevkin, Course of Lectures on the Theory of Sound [in Russian] (Moscow State University, 1960).
12. L. Ya. Gutin, Zhur. Tekh. Fiz. 1, 10, 1097 (1937).
13. W. Maxwell, Fourth Symposium on Combustion (1953).

DYNAMICS OF NONSTATIONARY PHYSICOCHEMICAL PROCESSES FOLLOWING A BIMOLECULAR RATE LAW

G. M. Panchenkov

I. M. Gubkin Moscow Institute of Petroleum Chemistry and Gas Industry
Presented by Academician A. V. Topchiev, March 29, 1961
Translated from Doklady Akademii Nauk SSSR, Vol. 140, No. 2,
pp. 412-415, September, 1961
Original article submitted March 28, 1961

Questions in the dynamics of nonstationary chemical and physicochemical processes (for example sorption and ion exchange) are assuming more and more practical importance. However, because of the mathematical difficulties involved, they have not been satisfactorily treated. The present paper will consider a method of solving the problem of the dynamics of a nonstationary physicochemical process in which the reaction rate is subject to a bimolecular law.

Let a sorbable substance be flowing through a tube (the axis of which we shall take as the axis of coordinates designated by the letter l) filled with a sorbent at constant temperature. Let $C(l,t)$ be the concentration of the substance in question occurring in the pores of the sorbent at a distance l from the first sorbent layer. The function $y(l,t)$ gives the quantity of substance being sorbed by unit volume of sorbent at the instant of time t. It is assumed that the sorbent fills the entire volume of the tube. Let the substance move in the sorbent with a constant linear velocity u large enough that longitudinal diffusion may be neglected.

If the concentration is calculated as the quantity of substance per unit sorbent-free volume, the material balance equation must employ two cross sections: ρ, the total cross section of the tube, and $\rho' = \kappa\rho$, the sorbent-free cross section. We shall consider the sorbent volume between the distances l_1 and l_2 over the time interval from t_1 to t_2. The material balance equation may be written in the following form:

$$[(uC)_{l_1} - (uC)_{l_2}]\,\varkappa\rho\Delta t = [(y + \varkappa C)_{t_1} - (y + \varkappa C)_{t_2}]\,\rho\Delta l. \tag{1}$$

After division by $\Delta l\ \Delta t$ and passing to the remnant at $\Delta l \to 0$, the equation takes the form

$$-u\varkappa\partial C/\partial l = \partial y/\partial t + \varkappa\partial C/\partial t. \tag{2}$$

The quantity $u\kappa$ is equal to the linear rate of flow of the substance in the sorbent. We are considering processes, the kinetics of which are subject to the equation

$$dy/dt = kCz, \text{ where } z = y_0 - y; \tag{3}$$

and y_0 is the equilibrium quantity of substance sorbed per unit volume of sorbent. From the expression $z = y_0 - y$ it follows that

$$dy/dt = -dz/dt. \tag{4}$$

In many cases the sorption of gases and vapors by porous sorbents [1] follows Eq. (3), as well as ion exchange at low electrolyte concentrations [2].

Substituting Eq. (4) in Eq. (3), we find that

$$dz/dt = -kcz. \tag{5}$$

The initial and boundary conditions are found in the following way. It follows from experiment that

$$C(0, t) = C_0; \tag{6}$$

$$C(l, 0) = 0 \quad \text{at} \quad l > 0; \qquad C(l, 0) = C_0 \quad \text{at} \quad l \leqslant 0; \tag{7}$$

$$z(l, 0) = z_0 = y_0 \quad \text{at} \quad l \geqslant 0, \tag{8}$$

where C_0 is the concentration of substance being sorbed at the input to the tube. Expression (7), which gives one of the initial conditions, is a discontinuous function for $l \geq 0$. To simplify the integration of the system of Eqs. (2) and (5), this initial condition may be replaced by a continuous function of the form

$$C(l, 0) = C_0 e^{-al} \quad \text{at} \quad l \geqslant 0, \tag{9}$$

which, for a sufficiently large value of the arbitrary constant, will give a result which is close to experiment.*

It follows from Eq. (5), after substituting Eq. (6), that

$$dz(0,t)/dt = -kC_0 z(0, t), \tag{10}$$

from which, after integration in using Eq. (8),

$$z(0, t) = z_0 e^{-kC_0 t}. \tag{11}$$

Equations (6), (11), (9), and (8) are the system of initial and boundary conditions needed to solve Eqs. (2) and (5), i.e., to find the concentration of substance in the volume and on the surface of the sorbent as a function of the coordinate l and the time t.

It follows from Eq. (5) that

$$C = -\frac{1}{kz}\frac{\partial z}{\partial t}. \tag{12}$$

Substituting Eqs. (12) and (4) and Eq. (2) we obtain

$$\frac{u\varkappa}{k}\frac{\partial}{\partial l}\left(\frac{1}{z}\frac{\partial z}{\partial t}\right) = -\frac{\partial z}{\partial t} - \frac{\varkappa}{k}\frac{\partial}{\partial t}\left(\frac{1}{z}\frac{\partial z}{\partial t}\right). \tag{13}$$

Differentiating, dividing by κ, regrouping, and setting $u\partial z/\partial l + \partial z/\partial t = w$, we obtain

$$z\frac{\partial w}{\partial t} = -\frac{k}{\varkappa}z^2\frac{\partial z}{\partial t} + \frac{\partial z}{\partial t}w \tag{14}$$

or

$$\frac{\partial}{\partial t}\left(\frac{w}{z}\right) = -\frac{k}{\varkappa}\frac{\partial z}{\partial t}. \tag{15}$$

Integrating Eq. (15), keeping l fixed, and substituting w, we obtain

$$u\frac{\partial z}{\partial l} + \frac{\partial z}{\partial t} = -\frac{k}{\varkappa}z^2 + z\Phi(l), \tag{16}$$

where $\Phi(l)$ is some function of l.

It follows from Eq. (16) that the differential equations of the process are

$$dl/u = dt/1 = dz\Big/\left[-\frac{k}{\varkappa}z^2 + z\Phi(l)\right], \tag{17}$$

from which

$$l = ut + c_1. \tag{18}$$

$$z = \frac{b}{1 - c_2 b e^{-\frac{kb}{\varkappa}t}}, \tag{19}$$

where $b = \frac{\kappa}{k}\Phi(l)$, and c_1 and c_2 are integration constants.

The value of $\Phi(l)$ may be found by substituting the value of z(0,t) in Eq. (16), i.e.,

*This function could be found from Eq. (2), since, according to Eqs. (4), (5), and (8), $-u\varkappa\, dC(l, 0)/dl = kC(l, 0)z_0 + \varkappa\,\partial C(l, 0)/\partial t$, but, according to Eq. (7), beyond the region of discontinuity of the function $C(l, 0)$, $\partial C(l, 0)/\partial t = 0$. After substituting this value into the preceding expression and integrating, we obtained $C(l, 0) = C(l, 0) = C_0 e^{\frac{-kz_0 l}{\kappa u}}$. Consequently, in this case, $a = kz_0/\kappa u$. This approach is not as good as the one that we have taken, since here the discontinuous function is neglected.

$$u\frac{\partial z(l,0)}{\partial l}+\frac{\partial z(l,0)}{\partial t}=-\frac{k}{\varkappa}[z(l,0)]^2+z(l,0)\,\Phi(l). \tag{20}$$

Equation (8) gives

$$\partial z(l,0)/\partial l=0. \tag{21}$$

It follows from Eq. (5) that

$$\partial z(l,0)/\partial t=-kC(l,0)\,z(l,0). \tag{22}$$

Substituting Eqs. (9) and (8) in Eq. (22), we obtain

$$\partial z(l,0)/\partial t=-kC_0z_0e^{-al}. \tag{23}$$

Substituting Eqs. (23) and (21) in Eqs. (8) and (20) we find that

$$\Phi(l)=\frac{k}{\varkappa}z_0-kuC_0e^{-al}. \tag{24}$$

Therefore,

$$b=\frac{\varkappa}{k}\Phi(l)=\frac{\varkappa}{k}\left[\frac{k}{\varkappa}z_0-kuC_0e^{-al}\right]. \tag{25}$$

Substituting Eqs. (25) and (18) in Eq. (19), we obtain

$$z=\frac{z_0-\varkappa uC_0e^{-a(ut+c_1)}}{1-c_2{}^{z_0-\varkappa uC_0e^{-a(ut+c_1)}}e^{-[(k/\varkappa)z_0-kuC_0e^{-a(ut+C_1)}]t}}. \tag{26}$$

We shall consider the solution for the region where $l-ut\leq 0$. Set $t=t_0$ at $l=0$. Then it follows from Eq. (11) that

$$z(0,t_0)=z_0e^{-kC_0t_0}. \tag{27}$$

It follows from Eq. (18) that here

$$t_0=-c_1/u. \tag{28}$$

Substituting Eq. (28) in Eq. (27) we obtain

$$z(0,t_0)=z_0e^{kC_0\frac{c_1}{u}}. \tag{29}$$

Taking $l=0$ and $t=t_0$, and substituting Eq. (29) in Eq. (26), we find

$$z_0e^{kC_0\frac{c_1}{u}}=\frac{z_0-\varkappa uC_0e^{-a(ut_0+c_1)}}{1-c_2{}^{z_0-\varkappa uC_0e^{-a(ut_0+c_1)}}e^{-[\frac{k}{\varkappa}z_0-kuC_0e^{-a(ut_0+c_1)}]t}}. \tag{30}$$

Substituting the value of t_0 from Eq. (28) in Eq. (30) we find the value of the constant

$$c_2=\left[\frac{\varkappa uC_0+z_0\{e^{kC_0\frac{c_1}{u}}-1\}}{z_0e^{[kC_0+(k/\varkappa)z_0-kuC_0]c_1/u}}\right]^{\frac{1}{z_0-\varkappa uC_0}} \tag{31}$$

Substituting Eq. (31) and $c_1=l-ut$ in Eq. (26) we obtain

$$z=\{z_0-\varkappa uC_0e^{-al}\}\left\{1-\left[\frac{\varkappa uC_0+z_0[e^{kC_0(l/u-t)}-1]}{z_0e^{[kC_0+(k/\varkappa)z_0-kuC_0][l/u-t]}}\right]^{\frac{z_0-\varkappa uC_0e^{-al}}{z_0-\varkappa uC_0}}\times e^{-[(k/\varkappa)z_0-kuC_0e^{-al}]t}\right\}^{-1}. \tag{32}$$

which is the solution we are interested in, which holds for the region $l-ut\leq 0$.

The solution for the region $l-ut\geq 0$ is found in the following way. Taking $t=0$ and substituting Eq. (8) in Eq. (26) we obtain

$$c_2=\left[\frac{\varkappa uC_0e^{-ac_1}}{z_0}\right]^{\frac{1}{z_0-\varkappa uC_0e^{-ac_1}}}. \tag{33}$$

Substituting Eq. (33) and the value of the constant c_1 from Eq. (18) in Eq. (26) we find the solution for the region $l - ut \geq 0$:

$$z = \{z_0 - \varkappa u C_0 e^{-al}\}\left\{1 - \left[\frac{\varkappa u C_0 e^{-a(l-ut)}}{z_0}\right]^{\frac{z_0 - \varkappa u C_0 e^{-al}}{z_0 - \varkappa u C_0 e^{-a(l-ut)}}} \times e^{-[(k/\varkappa)z_0 - k u C_0 e^{-al}]t}\right\}^{-1}. \tag{34}$$

Going to the limit as $a \to \infty$ leads, as may be seen from Eqs. (32) and (34) to the desired function in the form

$$z(l, t) = z_0\left\{1 - \left[\frac{z_0\{e^{kC_0(l/u-t)} - 1\} + \varkappa u C_0}{z_0 e^{[kC_0 + (k/\varkappa)z_0 - k u C_0](l/u-t)}}\right]^{\frac{z_0}{z_0 - \varkappa u C_0}} e^{-\frac{k}{\varkappa} z_0 t}\right\}^{-1}$$

$$\text{for} \quad l - ut \leqslant 0; \tag{35}$$

$$z(l, t) = z_0 \quad \text{for} \quad l - ut \geqslant 0. \tag{36}$$

The solution for $l - ut \leq 0$ must be used if the tube is sufficiently long. The solution given by Eqs. (32) and (34) satisfies both the initial and boundary conditions and the original differential equations. For practical calculations we are interested in Eq. (35) for the region $l - ut \leq 0$. For the region $l - ut \geq 0$, the solution is trivial, as may be seen from Eq. (36).

To find the distribution of concentration $c(l, t)$ of the substance being absorbed in the volume for any given values of t and l, we must use Eq. (12), in which we must substitute the value of z and its derivative from Eqs. (32) and (34). For practical calculations we are interested only in the region $l - ut \leq 0$, for which we find

$$C(l,t) = \left\{\frac{z_0 - \varkappa u C_0 e^{-al}}{z_0 - \varkappa u C_0} \frac{\left(kC_0 + \frac{k}{\varkappa} z_0 - k u C_0\right)[\varkappa u C_0 + z_0(e^{kC_0(l/u-t)} - 1)] - kC_0 z_0 e^{kC_0(l/u-t)}}{\varkappa u C_0 + z_0[e^{kC_0(l/u-t)} - 1]} - \right.$$

$$\left. - \frac{k}{\varkappa} z_0 - k u C_0 e^{-al}\right\}\left\{k - k\left[\frac{z_0 e^{(kC_0 + (k/\varkappa)z_0 - k u C_0)(l/u-t)}}{\varkappa u C_0 + z_0[e^{kC_0(l/u-t)} - 1]}\right]^{\frac{z_0 - \varkappa u C_0 e^{-al}}{z_0 - \varkappa u C_0}} \times e^{\left(\frac{k}{\varkappa} z_0 - k u C_0 e^{-al}\right)t}\right\}^{-1}. \tag{37}$$

Since, in accordance with condition (9), a must be very large, passing to the limit gives the final formula for the distribution of the concentration of the substance being sorbed along the tube under the condition that $l - ut \leq 1$:

$$C(l, t) = \left\{\frac{z_0}{z_0 - \varkappa u C_0} \frac{\left(kC_0 + \frac{k}{\varkappa} z_0 - k u C_0\right)[k u C_0 + z_0(e^{kC_0(l/u-t)} - 1) - kC_0 z_0 e^{kC_0(l/u-t)}}{\varkappa u C_0 + z_0[e^{kC_0(l/u-t)} - 1]} - \right.$$

$$\left. - \frac{k}{\varkappa} z_0\right\}\left\{k - k\left[\frac{z_0 e^{(kC_0 + (k/\varkappa)z_0 - k u C_0)(l/u-t)}}{\varkappa u C_0 + z_0[e^{kC_0(l/u-t)} - 1]}\right]^{\frac{z_0}{z_0 - \varkappa u C_0}} e^{\frac{k}{\varkappa} z_0}\right\}^{-1}. \tag{38}$$

The solutions hold not only for sorption processes and ion exchange, but may be applied to chemical reactions between a solution or gas and a solvent under the condition that the reaction kinetics are subject to Eq. (3).

LITERATURE CITED

1. G. M. Panchenkov, and V. A. Skoblo, Izv. Vyssh. uchebn. zaved, Neft' i gas No. 12, 69 (1959).
2. V. I. Gorshkov, Study of Ion Exchange of Alkali Metals on Sulfo-Resins in Different Solvents, Dissertation [in Russian] (MGU, 1958).

A POLAROGRAPHIC INVESTIGATION OF THE METHOD OF ELECTROLYTIC REDUCTION OF SIMPLE AND COMPLEX NICKEL IONS

Ya. I. Tur'yan

Lisichanskii Branch of the State Scientific-Investigation and Development Institute of the Nitrogen Industry and Products of Organic Synthesis

(Presented by Academician A. N. Frumkin, May 17, 1961)
Translated from Doklady Akademii Nauk SSSR, Vol. 140, No. 2, pp. 416-418, September, 1961
Original article submitted May 17, 1961

We have shown [2], on the basis of the theory of A. N. Frumkin [1], that the overpotential η of the process

$$\underset{\text{I}}{\text{Ni}\,(H_2O)_q^{2+} + 2e \rightarrow \text{Ni}\,(\text{Hg})^*} \rightarrow \underset{\text{II}}{\text{Ni}\,(\text{Hg})} \qquad (1)$$

depends on the retardation of the electrochemical stage I.

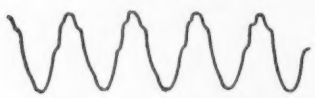

Fig. 1. Oscillogram of 1M potassium nitrate + 0.1M pyridine + $2 \cdot 10^{-3}$M nickel sulfate.

Fig. 2. Oscillogram of 1M potassium thiocyanate + $2 \cdot 10^{-3}$M nickel sulfate.

In the case of complexes formed by the ion $Ni(H_2O)_q^{2+}$ with pyridine [3], rhodanides [4,5], and other addenda (X), it is the complex ion which undergoes electrolytic reduction:

$$\underset{\text{III}}{\text{Ni}\,(H_2O)_q + pX^{-b} \rightarrow \text{Ni}\,(H_2O)_{q-p} \cdot X_p^{(2-pb)+}} + \underset{\text{IV}}{2e \rightarrow \text{Ni}\,(\text{Hg})^*} \rightarrow \underset{\text{II}}{\text{Ni}\,(\text{Hg})}. \qquad (2)$$

From a previous work [6] it follows that the value of η is smaller, the greater the value of p:

$$\text{Ni}\,(H_2O)_{q-2} \cdot (CNS)_2 < \text{Ni}\,(H_2O)_{q-1}\,CNS^+ < \text{Ni}\,(H_2O)_q^{2+}.$$

We have also shown [3,4,6] that for low concentrations of X (pyridine, CNS^-), the rate of stage III is comparable with the rate of diffusion (the kinetic current). From the value for the rate constant of stage III found in [6], it follows that further combination of X occurs the more rapidly the more the water is displaced from the hydration sheath.

With increase in the concentration of X, the rate of process III becomes appreciably greater than the rate of diffusion and, owing to the appearance of an appreciable concentration of a larger complex which is reduced with an inconsiderable value of η, stage IV becomes reversible also [3,4,7,8].

At the same time, the following two facts indicate the presence of the reversible process II (more rapid than stage I), the disactivation of the amalgam in a similar way to the behavior of manganese [9].

In the first place, the values of the half-wave potential of the hydrated nickel ion $Ni(H_2O)_q^{2+}$, by extrapolation to zero X concentration, has different values in potassium thiocyanate, and in potassium nitrate + pyridine. In the second place, an oscillographic study* has shown the absence of an anode step (Figs. 1 and 2). The two upper steps in Fig. 1 arise through the capacity effect of the pyridine [10].

*Carried out with the participation of V. G. Ravdin.

TABLE 1.

Pyridine + 1M KNO_3*				0.15 M KNO_3 + Imidazole + + 0.05% Gelatin [8]				KCNS			
C_{Py}, mmole per liter	$-(\varphi\frac{1}{2})_c$, mv	$b \cdot 10^3$*	$-(\varphi\frac{1}{2})_s$ calc, mv	C_{Im}, mmole per liter	$-(\varphi\frac{1}{2})_c$, mv	$b \cdot 10^3$	$-(\varphi\frac{1}{2})_s$ calc, mv	C_{CNS^-}, mmole per liter	$-(\varphi\frac{1}{2})_c$, mv	$b \cdot 10^3$	$-(\varphi\frac{1}{2})_s$ calc, mv
12.7	780	28	771	0.962	1069		736	1.02	711	38	647
27.3	784	30	767	1.032	1073	37	736	1.30	716	–	643
53.1	791	29	765	1.038	1074	38	737	1.56	721	–	642
99.1	804	–	767	1.129	1082	37	737	1.81	726	–	641
124.0	808	27	763	1.236	1089	38	737	2.22	736	39	643
363.0	845	27	776				av. 737	3.11	746	36	639
604.0	862	30	776					3.48	751	–	640
			av. 769					3.86	756	–	640
								4.20	761	39	641
								4.60	766	–	642
											av. 642

*b is the slope of the straight line of φ against $\log i/(i_d - i)$.

Evaluation of stage II gives:

$$i = k_a\,[\mathrm{Ni\,(Hg)^*}] + k_r\,[\mathrm{Ni\,(Hg)^*}]. \tag{3}$$

On the basis of Eq. (3) for reversibility of stages III and IV and the stepwise complex formation [11], we obtain:

$$\varphi_c = (\varphi_0^*)_{Hg} - \frac{RT}{2F}\ln\frac{k_C}{k_a + k_r} - \frac{RT}{2F}\times\ln\left(1 + \frac{C_X}{K_1} + \frac{C_X^2}{K_2} + \ldots + \frac{C_X^p}{K_p}\right) - \frac{RT}{2F}\ln\frac{i}{i_d - i}; \tag{4}$$

$$(\varphi_{1/2})_c = (\varphi_0^*)_{Hg} - \frac{RT}{2F}\ln\frac{k_c}{k_a + k_r} - \frac{RT}{2F}\ln\left(1 + \frac{C_X}{K_1} + \frac{C_X^2}{K_2} + \ldots + \frac{C_X^p}{K_p}\right); \tag{5}$$

$$(\varphi_{1/2})_s = (\varphi_0^*)_{Hg} - \frac{RT}{2F}\ln\frac{k_s}{k_a + k_r}; \tag{6}$$

where k_r is a quantity proportional to the rate constant of stage II; k_s is the constant for the diffusion current of simple nickel ions; k_a is the same for nickel atoms in the amalgam; k_c is the same for complex nickel ions; C_X is the concentration of the addend; K_1 and K_2 are the instability constants (dissociation constants) of the complexes.

Although stage II also takes place, we may obtain the Deford and Hume equation [11] from Eqs. (5) and (6):

$$(\varphi_{1/2})_c = (\varphi_{1/2})_s + \frac{RT}{2F}\ln\frac{k_s}{k_c} - \frac{RT}{2F}\ln\left(1 + \frac{C_X}{K_1} + \frac{C_X^2}{K_2} + \ldots + \frac{C_X^p}{K_p}\right). \tag{7}$$

According to Eq. (4), the relationship between the half-wave potential φ_c and $\log\frac{i}{i_d - i}$ is a straight line with slope $\frac{RT}{2F}2.3$, which is also observed experimentally (cf. Table 1, in which the potential is given relative to the saturated calomel electrode).

From the relationship between half-wave potential $(\varphi\frac{1}{2})_c$ and $\log C_{Py}$ up to a value of C_{Py} = 0.6 M [13], as well as from spectrophotometric data up to C_{Py} = 0.5 M [14], the formation of complexes with p = 1, 2, and 3 takes place. The curve for $(\varphi\frac{1}{2})_c$ against $\log C_{CNS^-}$ shows (Fig. 3) that complexes with p = 1, 2, 3, and 4 occur, while spectrophotometric measurements up to C_{CNS^-} = 0.5 M [15] reveals values of p = 1, 2, and 3 and for large values of C_{CNS^-}, p = 4 also. When the concentration of imidazole is greater than 1 M, polarographic potentiometric data (pH) [8] give a value of p = 6.

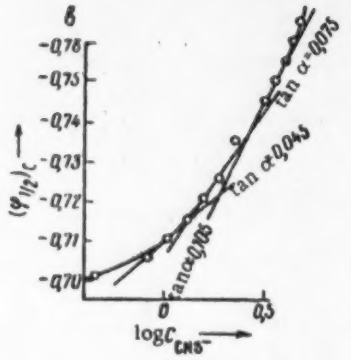

Fig. 3. Relationship between $(\varphi_{\frac{1}{2}})_C$ and $\log C_{CNS^-}$.

TABLE 2.

Solutions	$(\varphi_{\frac{1}{2}})_s$ calc, mv	$(\varphi_{\frac{1}{2}})_s$ exp, mv
Ni^{2+} + Py	769 ± 4.0	776
Ni^{2+} + Im	737 ± 0.4	–
Ni^{2+} + CNS^-	642 ± 2.0	693

Thus, a comparison of the results as to the composition of the complexes confirms the applicability of Eqs. (4) to (7) (cf. [11,13,17]).

Equation (7) also serves to confirm the constance of the calculated value of the half-wave potential for various values of C_X (Table 1). In these calculations, $k_C \cong k_s$ and K_1, K_2, etc., are taken from the spectrophotometric [14,15] and potentiometric (pH) [8] measurements, while $K_4(CNS^-) = 5.34 \cdot 10^{-2}$, obtained from Fig. 3 and K_3 [15].

It can be seen from Table 2 that there is good agreement between the values of $(\varphi_{\frac{1}{2}})_C$ for potassium nitrate + pyridine and the found extrapolations [3]. The difference between these quantities for potassium thiocyanate is to be explained by the less accurate values of the half-wave potential $(\varphi_{\frac{1}{2}})_s$ obtained by extrapolation, since the irreversibility of the process becomes more important the lower the thiocyanate ion concentration [4].

The deactivation of the amalgam may also be used to explain the difference between the calculated values of $(\varphi_{\frac{1}{2}})_s$ in potassium nitrate and pyridine, potassium nitrate and imidazole in the presence of gelatin, and potassium thiocyanate, since the nature and concentration of the addend undergoing adsorption on mercury would be expected to exert an influence on the value of k_r [Eq. (6)]. The calculated value of $(\varphi_{\frac{1}{2}})_s$ is displaced in a negative direction in the order thiocyanate – imidazole (gelatin) – pyridine; that is, in the same direction as increase in the retardation of the deactivation process.

By analogy with [18], taking into account Eqs. (6) and (7), we may obtain

$$(\varphi_{\frac{1}{2}})_s = \varphi^0 + E_s + \frac{RT}{2F}\ln C_{\text{satur.}} - \frac{RT}{2F}\ln\frac{k_s}{k_a + k_r} - \frac{RT}{2F}\ln(1 + K_{Hg}), \qquad (8)$$

where K_{Hg} is the equilibrium constant of the process $Ni(Hg)^* \rightleftharpoons Ni(Hg)$. It is hardly possible to calculate the normal potential φ^0 of nickel from $(\varphi_{\frac{1}{2}})_s$, since the values of k_r and K_{Hg} are unknown. Our calculations of φ^0 [3,4] included in these two final components, so that values were obtained which were different for different solutions.

In conclusion we would like to express our deep thanks to Academician A. N. Frumkin for his valuable advice.

LITERATURE CITED

1. A. N. Frumkin, V. S. Bagonskii, Z. A. Iofa, and B. N. Kabanov, The Kinetics of Electrode Processes [in Russian] (Moscow, 1952).
2. Ya. I. Tur'yan, Doklady Akad. Nauk SSSR 113, 3, 631 (1957).
3. Ya. I. Tur'yan and G. F. Serova, Zhurn. Fiz. Khim. 31, 1976 (1957).
4. Ya. I. Tur'yan, Zhurn. Fiz. Khim. 31, 2423 (1957).
5. N. V. Nikolaeva-Fedorovich and Yu. M. Povarov, Zhurn. Analyt. Khim. 14, 663 (1959).
6. Ya. I. Tur'yan and G. F. Serova, Doklady Akad. Nauk SSSR 125, 3, 595 (1959).
7. E. Roselli, An. Direcc. nac. quim. 9, 43 (1956);
8. C. Li, T. L. Chu, Ch. T. Fujii, and J. M. White, J. Am. Chem. Soc. 77, 859 (1955).
9. J. Biernat and J. Koryta, Coll. Czech. Chem. Comm. 25, 38 (1960).
10. J. Heyrovsky, F. Sorm, and J. Forejt, Coll. Czech. Chem. Comm. 12, 11 (1947).
11. D. D. Deford and D. N. Hume, J. Am. Chem. Soc. 73, 5321 (1951).
12. Ya. I. Tur'yan and G. F. Serova, Zhurn. Fiz. Khim. 31, 2200 (1957).
13. K. B. Yatsimirskii, Collection of Articles on General Chemistry [in Russian] (1953) Vol. 1, p. 193.
14. A. V. Ablov and L. V. Nazarova, Zhurn. Prikl. Khim. 2, 53 (1957).
15. S. Fronaeus, Acta Chem. Skand. 7, 21 (1953).
16. A. Kiss and P. Ksokan, Z. anorg. Chem. 245, 355 (1941).
17. Ya. I. Tur'yan, Zhurn. Obshch. Khim. 26, 2084 (1956).
18. J. J. Lingane, J. Am. Chem. Soc. 61, 2099 (1939).

EPR SPECTRA OF ACETYLENE AND ITS DERIVATIVES WHEN IRRADIATED BY γ-RAYS

D. N. Shigorin, V. I. Smirnova, G. S. Zhuravleva,

E. P. Gracheva, and Corr. Member AN SSSR M. F. Shostakovskii

L. Ya. Karpov Physicochemical Institute

Translated from Doklady Akademii Nauk SSSR, Vol. 140, No. 2,
pp. 419-422, September, 1961
Original article submitted May 25, 1961

In the present study, in order to establish the relation between the structure of the original molecule and that of the radical formed from it by γ-rays, we have investigated the EPR spectra of irradiated acetylene, methylacetylene, methyldeuteroacetylene, ethyl- and butylacetylene, and even phenyl- and methylphenylacetylene at 77°K. The yield of radicals was determined as a function of irradiation dose.

The compounds studied were irradiated in ampoules made from a special glass which does not given an EPR spectrum at the applied doses of γ-radiation. Before the experiment the ampoules were evacuated to 10^{-3} mm Hg. We used the radiation of a Co^{60} source. The EPR spectra were recorded by means of a radiospectroscope of the superheterodynic type. The magnetic field was calibrated by means of the EPR spectrum of the pyroxylamindisulfone ion $[NO(SO_3)_2^{2-}]$ ion in chloroform. We used a single crystal of cupric chloride ($CuCl_2 \cdot 2H_2O$) in order to determine the concentration of the radicals obtained. The relative error in the determination of the yield of radicals was about 20%; the g factor was found by using DPPH as a standard. The acetylenes studied were prepared and purified by known methods and had constants agreeing with data in the literature.

The results of the experimental investigations are given in Tables 1 and 2 and in Fig. 1.

TABLE 1. Integral Dose of γ-radiation ~10^7 rad

Prep. No.	Original compound (b.p., °C)	Proposed radical	Number of lines	Total width, oe
1	$H_3C-C\equiv C-H$ (−23,3)	$\cdot H_2C-C\equiv C-H$	4	50,2±1,4
2	$H_3C-C\equiv C-D$	$\cdot H_2C-C\equiv C-D$	[2]	97,5±1,4
3	$C_2H_5-C\equiv C-H$ (8,5)	1. $\cdot H_2C-CH=C=C-H$ 2. $\cdot H_2C-C\equiv C-H$	6 (8)	54,8±1,6
4	$C_4H_9-C\equiv C-H$ (70,0)	1. $\cdot CH_2-CH_2-CH_2-CH=C=CH$ 2. $\cdot H_2C-C\equiv C-H$ 3. $\dot{C}_2H_5$	11	104,4±2,4
5	$C_6H_5-C\equiv C-H$ [3]	—	—	—
6	$C_6H_5-C\equiv C-CH_3$ (71–72)	$C_6H_5-C\equiv C-\dot{C}H_2$	3	34±1,1
7	$HC\equiv CH$ (−83,6)[4]	1. $-C=\dot{C}H-CH=CH-CH=CH-$ 2. $\dot{C}\equiv C-H$ $H-C\equiv C-H$ $H-C\equiv C-H$	10 (12)	112±4

[1] The indicated line widths refer to the first derivatives of the absorption curve.
[2] It was difficult to determine the number of lines, obviously, because the spectrum of further deuterated methylacetylenes was superposed.
[3] We were unable to obtain a spectrum of phenylacetylene even at doses (1-40) · 10^6 rad.
[4] EPR spectrum obtained at a dose 1.5 · 10^7 rad.

Just as should be expected, the most simple EPR spectrum was obtained for irradiated methylacetylene. The spectrum comprises a symmetrical quadruplet of equidistant lines with intensity ratios 1:2, 1:2, 2:1, and resulting, obviously, from the interaction between an unpaired electron and three protons.

The EPR spectrum of methyldeuteroacetylene (which was prepared by decomposing lithium methylacetylenide by means of heavy water) points to an interaction of an unpaired electron in the radical with the protons of the CH_2 group and the deuteron of CD.

TABLE 2. Yield of Radicals as a Function of the γ-Irradiation Dose

Prep. No.	Original compound	$1 \cdot 10^6$ rad.		$10 \cdot 10^6$ rad.		$12 \cdot 10^6$ rad.		$20 \cdot 10^6$ rad.		$40 \cdot 10^6$ rad.	
		mole 10^{21}	mole%	mole 10^{21}	mole%	mole 10^{21}	mole%	mole 10^{21}	mole%	mole 10^{21}	mole%
1	$H_3C-C\equiv C-H$	0,15	0,02	1,1	0,18	2,1	0,34	4,4	0,73	1,8	0,30
2	$H_3C-C\equiv C-D$			2,4	0,42			0,23	0,04		
3	$C_2H_5-C\equiv C-H$	0,5	0,08	1,6	0,26	2,2	0,35	2,9	0,48	2,5	0,41
4	$C_4H_9-C\equiv C-H$			2,2	0,37	0,7	0,12				
5	$C_2H_5-C\equiv C-CH_3$	1,37	0,23			0,47	0,09			0,16	0,03
6	$HC\equiv CH$					0,38[2]	0,06			0,13	0,02

[1]The yield of radicals was determined at the dose $15 \cdot 10^6$ rad.
[2]The yield of radicals was determined at the dose $2 \cdot 10^6$ rad.

On account of these data, the EPR spectrum of methylacetylene irradiated by γ-rays may be ascribed to the (propynyl) radical having the structure (I):

$$[H_3C^1-C^2\equiv C^3H]^{\bullet} \qquad (I)$$

When carrying out a theoretical analysis of the EPR spectrum of the propynyl radical, one gets a better fit to the experimental spectral curve, if it is taken into account that the hydrogen atoms at the carbon atoms C^1 and C^3 have a somewhat different influence. The "free" electron density near the hydrogen nuclei of the methylene group should be taken somewhat higher (by about 20%) than that of the methyl group.

Data obtained by investigating the EPR spectrum of the radical formed by the action of ultraviolet light on methylacetylene at the temperature 77°K [1] are in agreement with the results of our study. From an energetical point of view, the formation of the propynyl radical (I) from methylacetylene appears to be completely justified. In the radical (I) the unpaired electron has a high delocalization energy and for breaking the C–H bond in the molecule at the instant of radical formation a small amount of energy is required.

When irradiated by γ-rays, ethyl- and butylacetylene, which have longer hydrocarbon chains than does methylacetylene, give more complex EPR spectra: the latter are unsymmetric, the number of lines and the total spectral width are greater (Table 1). Obviously, by irradiating acetylene derivatives of the type $R-CH_2C\equiv CH$, where R = $= C_2H_5$, C_3H_7, etc., there are formed several radicals of the type $R-\dot{C}H-C\equiv CH$, R and $CH_2-C\equiv CH$. Dependent on the irradiation dose, there are also found variations in the shape of the spectrum (the spectral width and the number of components varies). This may indicate that at 77°K secondary reactions take place. From Table 2 it follows that the yield of radicals at a given irradiation dose for methyl-, ethyl-, and butylacetylene is greater for a longer hydrocarbon chain. When the irradiation dose is raised from $1 \cdot 10^6$ to $40 \cdot 10^6$ rad, the yield of radicals also increases and attains a maximum at a dose of about $20 \cdot 10^6$ rad, and then begins to fall.

Above it has been shown that in a propynyl radical the unpaired electron is delocalized owing to the triple bond. Therefore, it was of interest to investigate γ-irradiated methylphenylacetylene. In this case somewhat unexpected results were obtained. The EPR spectrum of γ-irradiated methylphenylacetylene consists of a symmetrical triplet. The spectrum observed may be explained in two ways. The hyperfine structure of the EPR spectrum consisting of three lines originates from an interaction between the unpaired electron and the protons of the methylene group in a radical with the structure $C\equiv C-\dot{C}H_2$ or, alternatively, the methyl group of the original compound, which group primarily absorbs the energy of γ-quanta, is preserved and the EPR spectrum belongs to the substituted phenyl radical $Ar-C\equiv C-H$.

It is known that the hyperfine structure of the EPR spectrum for a benzene ring is characterized by three components [2]. However, for irradiated benzene the total line width and that of the separate components in the EPR spectrum are considerably greater than those in the spectrum of γ-irradiated (simultaneously with benzene) methylphenylacetylene. Moreover, the intensity of the EPR spectrum for γ-irradiated benzene is much lower, and under the conditions where the spectrum of methylphenylacetylene is recorded, that of benzene does not come through. Therefore, we suppose that the hyperfine structure in the EPR spectrum of γ-irradiated methylphenylacetylene results from the interaction of the unpaired electron with the protons of the methylene group and the phenyl ring via the triple C ≡ C bond weakly participates in the delocalization of the unpaired electron. This is also confirmed by the EPR spectrum of γ-irradiated ethylacetylene, which contains five hyperfine structure components.

Fig. 1. EPR spectra of γ-irradiated acetylenes at T = 77°K: a) methylacetylene; b) methyldeuteroacetylene; c) ethylacetylene; d) butylacetylene; e) methylphenylacetylene; f) acetylene (a-d: integral dose $1 \cdot 10^7$ rad; e: $3 \cdot 10^6$ rad; f: $2 \cdot 10^7$ rad).

The EPR spectrum of γ-irradiated acetylene (Fig. 1) is of particular interest. An intensive EPR spectrum is observed only at high irradiation doses (about $1.3 \cdot 10^7$ rad), which points to a considerable redistribution of the energy in the system. To a still greater extent this is apparent for phenylacetylene, which does not give an EPR spectrum even at high irradiation doses. The effective redistribution of the absorbed energy in such systems, obviously, is connected with the presence of complexes formed from the molecules. The EPR spectrum of γ-irradiated acetylene is complicated (it contains approximately 12 lines) and upon raising the irradiation dose to $4 \cdot 10^7$ rad, the shape of the spectrum changes somewhat. The great number of hyperfine structure lines in the EPR spectrum of γ-irradiated acetylene originates from the interaction of the unpaired electron with the various protons of the system. The observed EPR spectrum of γ-irradiated acetylene may be explained in two ways: by the formation of polymer radicals (polyacetylene) $-C=CH-CH=CH-CH=CH-$ or, alternatively, by the existence of radical complexes of the type

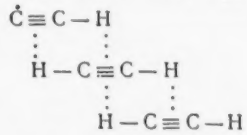

In fact, in several experiments we have detected polymer films on the walls of the ampoules. The occurrence of complexes formed from acetylene molecules in the liquid phase is pointed out in [3,4]. For acetylene the yield of radicals falls and the yield of polymer film rises, when the irradiation dose is raised. The g factor for the centers of the hyperfine structure lines in the EPR spectra of all compounds studied corresponds to the g factor of crystalline DPPH.

The analysis of the EPR spectra recorded for the γ-irradiated compounds indicates that there is a certain relation between the structure of the original molecule and that of the radical originating from its dissociation by the action of irradiation. It has been found that, when frozen acetylene (T = 77°K) is treated with high doses of γ-irradiation, a polymer is formed. Obviously, the polymerization proceeds via radicals and is accompanied by the

formation of complicated radicals or radical complexes. It is important to note that in the cases discussed the formation of a radical is connected with the rupture of a C–H bond in the methyl group of the original compound, which gives a more stable radical.

LITERATURE CITED

1. C. P. Poole and S. Anderson, J. Chem. Phys. 31, No. 2, 346 (1959).
2. I. I. Chkheidze, Yu. N. Molin, N. Ya. Buben, and V. V. Voevodskii, Doklady AN SSSR 130, 1291 (1960).
3. D. N. Shigorin, M. I. Shemyakin, and M. N. Kolosov, Izv. AN SSSR, ser. khim. No. 9, 1133 (1958).
4. R. West and Ch. Kreinzel, J. Am. Chem. Soc. 84, No. 4, 765 (1961).

All abbreviations of periodicals in the above bibliography are letter-by-letter transliterations of the abbreviations as given in the original Russian journal. *Some or all of this periodical literature may well be available in English translation.* A complete list of the cover-to-cover English translations appears at the back of this issue.

DIFFERENTIAL CAPACITY CURVES IN $K_4Fe(CN)_6$ SOLUTIONS

B. B. Damaskin, E. Shvarts, and Academician A. N. Frumkin

M. V. Lomonosov Moscow State University

Translated from Doklady Akademii Nauk SSSR, Vol. 140, No. 3,
pp. 630-633, September, 1961
Original article submitted June 27, 1961

Curves showing the relationship between the differential capacity C and electrode potential φ in the presence of different singly and doubly charged anions have been studied in [1-4], and it has been shown that the peak on the $C - \varphi$ curves at potentials more anodic than the electrocapillary zero (e.c.z.) depends to a considerable extent on the nature of the anion. It was considered of interest to study the influence of the adsorption of the polyvalent anion $Fe(CN)_6^{4-}$ on the shape of the $C - \varphi$ curve.

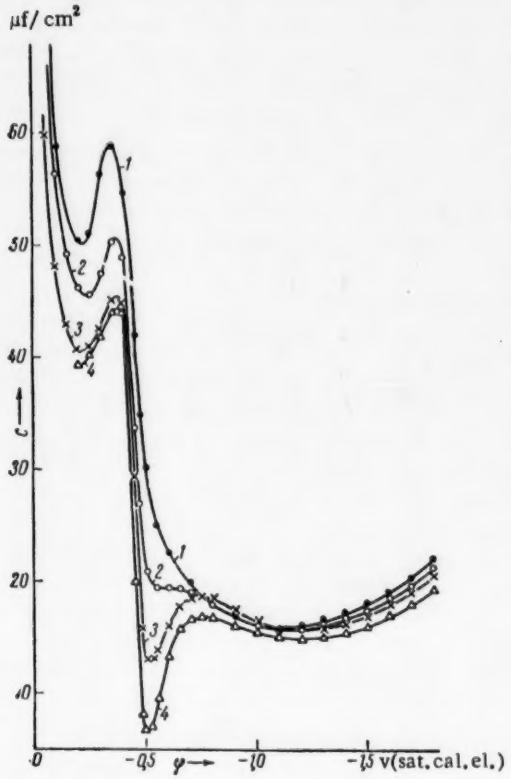

Fig. 1. Differential capacity curves in $K_4Fe(CN)_6$ solutions: 1) 1N; 2) 0.1N; 3) 0.01N; 4) 0.001N; 400 cps, 25°.

For this purpose we used an impedance method, which has been described in [5], to measure the $C - \varphi$ curves at a dropping mercury electrode in 1, 0.1, 0.01, and 0.001N solutions of $K_4Fe(CN)_6$ at 25°. The data obtained are given in Fig. 1. The figure shows that for negative charges on the surface the shape of the $C - \varphi$ curves resembles that of the analogous curves obtained in NaF solutions [6]: in dilute solutions close to the e.c.z., the $C - \varphi$ curve shows a clearly defined minimum, which is related to the diffusion structure of the double layer, and with subsequent increase in the negative polarization the capacity passes through a sloping maximum at $\varphi \cong -0.75$ v (sat.cal.el.). With change in the potential toward positive charges on the surface; however, the $C - \varphi$ curves close to the e.c.z. show a sharp, almost vertical increase in capacity, followed by a characteristic maximum (peak) which is much higher and narrower than the analogous maxima in solutions containing other anions. This shape for the $C - \varphi$ curve was not observed in the presence of the other anions previously studied [1-4], and requires more detailed examination.

By means of Grahame's method [6] and the data for the differential capacity in 1N $K_4Fe(CN)_6$, we calculated the $C - \varphi$ curves in 0.1, 0.01, and 0.001N solutions of $K_4Fe(CN)_6$, on the assumption that the $Fe(CN)_6^{4-}$ anion is not specifically adsorbed on mercury, and that the e.c.z. in all the solutions is equal to −0.473 v (sat.cal.el.), i.e., is equal to the e.c.z. in NaF solutions [6].* The calculated and experimental curves

*It should be noted that the e.c.z. in 1N $K_4Fe(CN)_6$ solution cannot be determined by the method of reverse integration [7], since the negative branch of the $C - \varphi$ curve in 1N $K_4Fe(CN)_6$ lies slightly lower than that for 1N KCl. This result is apparently related to the decrease in the activity of the K^+ cations due to the reaction $K^+ + Fe(CN)_6^{4-} = KFe(CN)_6^{3-}$ at high $K_4Fe(CN)_6$ concentrations, and not to breakdown of the complex $H_2O + K_4Fe(CN)_6 = K_3Fe(CN)_5(H_2O) + KCN$ [8], since the appearance of CN^- would lead us to expect the increase in the $C - \varphi$ curve at much more negative potentials [4].

for 0.01N $K_4Fe(CN)_6$ solution are given in Fig. 2. The figure shows that the displacement of the minimum on the $C - \varphi$ curve from the e.c.z. is the same for the experimental and calculated curves and is thus due to the fact that $K_4Fe(CN)_6$ is of unsymmetrical valence type and not to specific adsorption of the $Fe(CN)_6^{4-}$ anion at the e.c.z. Moreover, at values of φ more negative than −0.65 v (sat.cal.el.), the experimental and calculated curves practically coincide. On the other hand, for positive charges on the surface, the calculation based on the assumption that there is no specific adsorption differs considerably from the experimental values of the capacity. We thus reach the conclusion that for positive charges on the surface the $Fe(CN)_6^{4-}$ anion exhibits appreciable specific adsorption on the mercury surface, whereas on going to the case of negative charges on the surface, desorption of this anion takes place, accompanied by a sharp decrease in the capacity. The agreement for the descending branches of the calculated and experimental $C - \varphi$ curves indicates that the sharp desorption of the $Fe(CN)_6^{4-}$ anion is due chiefly to the electrostatic interaction of the polyvalent anion with the mercury surface.

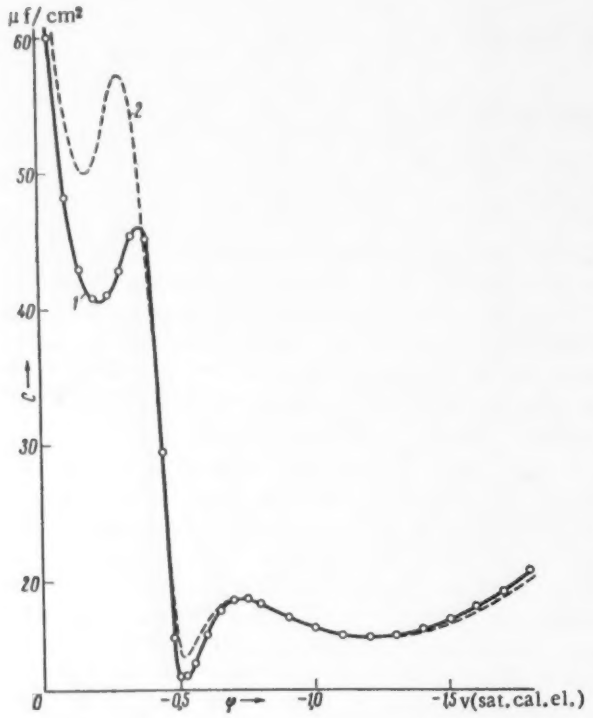

Fig. 2. Differential capacity curves in 0.01N $K_4Fe(CN)_6$ solution: 1) experimental; 2) calculated.

A characteristic feature of the data which we have obtained in 1N $K_4Fe(CN)_6$ solution is the relatively high value of the capacity at the maximum on the $C - \varphi$ curve (C_M = 59.0 μf/cm², whereas, in 1N KCl, C_M = 43.2 μf/cm²), and also the existence, at the potentials of the maximum, of a polarization resistance equal to 0.31 ohm/cm². According to Watts-Tobin's theory [9], the peak on the $C - \varphi$ curves is related to a maximum value of the effective dielectric constant for the layer of adsorbed water dipoles. This theory does not consider the influence of the specific adsorption of anions on the change in the orientation of the water dipoles, and the absence of a peak on the $C - \varphi$ curves in KOH and K_2CO_3 solutions [2] is attributed, by analogy with KI solutions, to a sharp increase in the capacity, which masks the peak and is due to the strong specific adsorption of the OH^- and CO_3^{2-} anions, which is comparable with the adsorption of the I^- anion. It is difficult to accept this explanation, since the adsorption of OH^- and CO_3^{2-} ions, unlike the adsorption of I^-, does not lead to displacement of the e.c.z. toward negative values [2]. Moreover, according to [9], we should expect the absence of a peak in $K_4Fe(CN)_6$ solutions also, since the adsorption of the $Fe(CN)_6^{4-}$ anion leads to a sharp increase in capacity, but this is not observed experimentally (Fig. 1). Finally, this theory [9] cannot, without further assumptions, explain the production of the polarization resistance at the potentials of the peak on the $C - \varphi$ curves.

In the general case the presence of a peak on the $C - \varphi$ curves is determined by the negative value of $\partial C/\partial \varphi$. If ϵ is the charge on the electrode, φ_a the potential read from the e.c.z. in the given solution, ξ the potential of the electrocapillary zero corresponding to the orientation of water dipoles at the given potential $\varphi_a[\xi = f(\varphi_a)]$, and K_0 is the true integral capacity, defined by the relationship $\epsilon = K_0(\varphi_a - \xi)$, then the differential capacity C and the formal integral capacity K can be expressed by the following equations:

$$C = \frac{\partial \varepsilon}{\partial \varphi} = \frac{\partial K_0}{\partial \varphi}(\varphi_a - \xi) + K_0\left(1 - \frac{\partial \xi}{\partial \varphi}\right), \quad (1)$$

$$K = \frac{\varepsilon}{\varphi_a} = K_0\left(1 - \frac{\xi}{\varphi_a}\right), \quad (2)$$

from which

$$\frac{\partial C}{\partial \varphi} = 2\frac{\partial K_0}{\partial \varphi}\left(1 - \frac{\partial \xi}{\partial \varphi}\right) + \frac{\partial^2 K_0}{\partial \varphi^2}(\varphi_a - \xi) - K_0\frac{\partial^2 \xi}{\partial \varphi^2}, \quad (3)$$

$$\frac{\partial K}{\partial \varphi} = \frac{\partial K_0}{\partial \varphi}\left(1 - \frac{\xi}{\varphi_a}\right) + \frac{K_0}{\varphi_a^2}\xi - \frac{K_0}{\varphi_a}\frac{\partial \xi}{\partial \varphi}. \quad (4)$$

It is natural to assume that $\partial K_0/\partial\varphi \geq 0$, and also that $|\xi/\varphi_a| < 1$ and $|\partial\xi/\partial\varphi| < 1$. Under these conditions, as can be seen from Eq. (3), the production of a region in which $\partial C/\partial\varphi < 0$ can be explained either by a negative value for $\partial^2 K_0/\partial\varphi^2$ or by a positive value for $\partial^2\xi/\partial\varphi^2$.

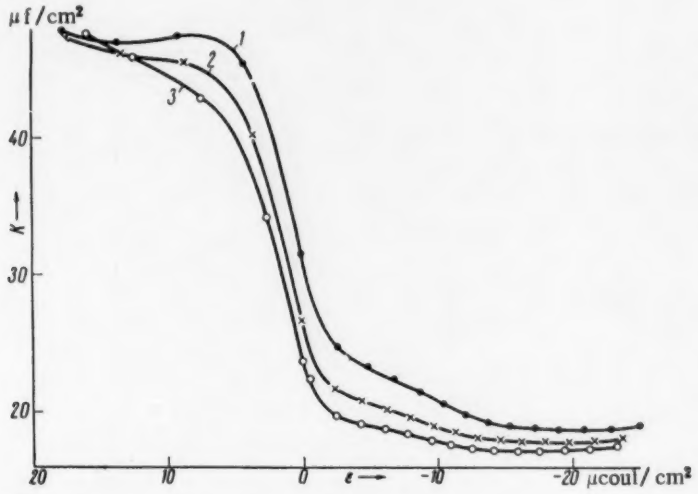

Fig. 3. Curves for the integral capacity in 0.1N $K_4Fe(CN)_6$ solution at temperatures of: 1) 0°; 2) 25°; 3) 50°; 400 cps.

As can be seen from Fig. 3 for 0.1N $K_4Fe(CN)_6$ solution at 0°, a maximum is also observed on the $K-\epsilon$ curve, i.e., in this case there exists a region where $\partial K/\partial\varphi < 0$. According to Eq. (4), this result indicates that either $\xi < 0$ for $\varphi_a > 0$, or $\partial\xi/\partial\varphi > 0$. The first variation was considered by Watts-Tobin [9], according to whom a fundamental part in the production of a negative value for $\partial C/\partial\varphi$ is played by the term with $\partial^2 K_0/\partial\varphi^2 < 0$ and, apparently, a positive value of $\partial^2\xi/\partial\varphi^2$ with $\xi < 0$, corresponding to completion of the reorientation of the water molecules. Another possible interpretation of the peaks on the $C-\varphi$ and $K-\epsilon$ curves is based on the assumption that the water dipoles are orientated with their negative end toward the mercury surface at the e.c.z., and that this orientation changes when anions with a sufficient polarizing power are introduced into the compact double layer. In this case, for $\varphi_a > 0$, the values of ξ_a, $\partial\xi/\partial\varphi$ and $\partial^2\xi/\partial\varphi^2$ are positive, while the last quantity plays a fundamental part in the production of a region with a negative value for $\partial C/\partial\varphi$ [see Eq. (3)]. The height and shape of the peak on the $C-\varphi$ curves under these conditions will depend on the adsorbability of the anion and its polarizing power (tendency to undergo hydration).

The $Fe(CN)_6^{4-}$ is strongly hydrated, and its adsorbability, as we have shown, increases sharply on going to the case of positive charges on the surface. We should therefore expect a sharp change in the orientation of the adsorbed water dipoles when $Fe(CN)_6^{4-}$ anions are introduced into the double layer. Thus, the experimental data which we have obtained in 1N $K_4Fe(CN)_6$ agree better with the second interpretation of the peak on the $C-\varphi$ curves. The sharp change in the orientation of the adsorbed water dipoles is responsible for the high and relatively narrow maximum on the $C-\varphi$ curve, and the polarization resistance observed at these potentials corresponds to the process of reconstruction of the double layer when $Fe(CN)_6^{4-}$ anions are introduced into it. The second interpretation of the peak on the $C-\varphi$ curves in the presence of different anions will be considered in more detail later [10].

LITERATURE CITED

1. M. A. Vorsina and A. N. Frumkin, Zhur. Fiz. Khim. 19, 171 (1945).
2. D. C. Grahame, M. A. Poth, and J. I. Cummings, J. Am. Chem. Soc. 74, 4422 (1952).

3. A. Watanabe, F. Tsuji, and S. Ueda, Bull. Inst. Chem. Res. Kyoto Univ. 34, 1, 65 (1956).
4. G. C. Barker and R. L. Faircloth, Advances in Polarography (Oxford, 1960) Vol. 1, p. 313.
5. B. B. Damaskin, Zhur. Fiz. Khim. 32, 2199 (1958).
6. D. C. Grahame, J. Am. Chem. Soc. 76, 4819 (1954).
7. D. C. Grahame, E. M Coffin, J. I. Cummings, and M. A. Poth, J. Am. Chem. Soc. 74, 1207 (1952).
8. W. L. Reynolds and R. H. Lumry, J. Chem. Phys. 23, 2460 (1955).
9. R. J. Watts-Tobin, Philos. Mag. 6, No. 61, 133 (1961).
10. E. Shvarts, B. B. Damaskin, and A. N. Frumkin, Zhur. Fiz. Khim. (In press).

All abbreviations of periodicals in the above bibliography are letter-by-letter transliterations of the abbreviations as given in the original Russian journal. *Some or all of this periodical literature may well be available in English translation.* A complete list of the cover-to-cover English translations appears at the back of this issue.

SPECIFIC ACTIVITY OF NICKEL CATALYSTS AND ADSORPTION OF THIOPHENE

G. D. Lyubarskii, N. V. Kul'kova, R. Kh. Burshtein,

G. G. Isaeva, L. N. Ivanovskaya, and N. A. Shurmovskaya

L. Ya. Karpov Institute of Physical Chemistry
(Presented by Academician S. S. Medvedev, April 26, 1961)
Translated from Doklady Akademii Nauk SSSR, Vol. 140, No. 3,
pp. 634-636, September, 1961
Original article submitted April 12, 1961

To investigate a series of complex catalysts it is necessary to be able to compare the catalytic activity of unit surface area of the active component of the catalyst. By the BET method it is only possible to determine the total surface area of the complex catalyst, for example, the total surface area of the metal plus carrier.

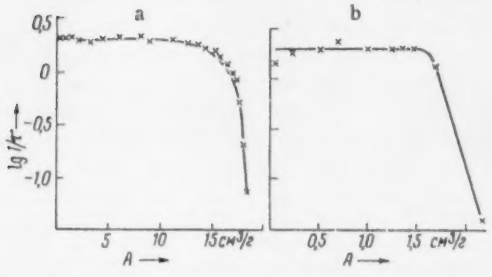

Fig. 1. Adsorption of oxygen A on the catalysts: Ni on Cr_2O_3 (a) and Ni prepared from the formate (b).

The method suggested by Burshtein [1] of chemisorption of oxygen at ambient temperatures and low pressures, proved to be a convenient method for the determination of the surface area of active metals. Characteristic curves, expressing the rate of adsorption of oxygen on nickel determined by this method, are presented in Fig. 1. A sharp fall in the adsorption rate was observed after a definite quantity of oxygen was absorbed. In the case of iron the quantity of adsorbed oxygen was $2 \cdot 10^{15}$ mole/cm^2, and in the case of nickel the rapid adsorption of oxygen was $1.3 \cdot 10^{15}$ mole/cm^2 of surface. These results are based on a comparison of the results of the adsorption of oxygen with the data obtained by the BET method for pure metals [2].

TABLE 1. Surface Area, Activity, and Adsorption of Thiophene on Various Nickel Catalysts

Series	Nickel catalyst	Nickel content, wt.%	Surface area			Activity at 100° mmoles/hr on 1 g Ni	Adsorption of thiophene at 120° mmole/g Ni	Specific values on 1 m² of nickel	
			m²/g of catalyst	nickel•• m²/g of catalyst	nickel, m²/g			activity mmole/hr	adsorption of thiophene mmole · 10³
I	From the formate	100.0	4	3.8	3.8	1.74	0.028	0.46	7.4
	From the oxalate	100.0	7	6.5	6.5	2.85	0.050	0.44	7.7
	On Cr_2O_3	50.0	130	30.0	60.0	35.0	0.47	0.58	7.8
	On MgO	65.0	200	42.0	65.0	44.0	0.50	0.68	7.7
	On carbon	9.1	660	15.0	170.0	120.0	1.23	0.70	7.3
II	Alloy Ni	75.0	90	87.0	87.0	286.0	0.65	3.30	7.5
	Ni on Al_2O_3	45.5	245	41.0	90.0	256.0	0.99	2.84	11.0

• From BET adsorption of nitrogen.
•• From adsorption of oxygen.

We used this method for the comparison of the specific activity (referred to 1 m^2 surface area of the nickel) of a series of supported nickel catalysts. First of all a determination was made of the surface area of the nickel catalysts without supports, prepared by decomposition in hydrogen of nickel formate or oxalate; the surface area of these samples was determined by the usual BET method (low-temperature adsorption of nitrogen or krypton) parallel with the determination of oxygen adsorption by the method described in [1].

The catalytic activity of the investigated catalysts was determined by hydrogenation of benzene in the vapor phase under steady conditions in the flow-circulation apparatus described in [3]. At the same time the specific adsorption of thiophene from its mixture with benzene vapor and hydrogen in the same flow-circulation apparatus, and on the same catalysts, was determined; analysis of the residual thiophene was carried out photocolorimetrically, with subsequent analysis of the catalyst for adsorbed sulfur. The results obtained are presented in Table 1.

The given data show that the surface area of nickel prepared from the formate or oxalate (without carriers) can be accurately determined both by the BET method and by the adsorption-of-oxygen method, since the same results are obtained.

Knowing the value of the surface area of nickel in complex catalysts, and their total activity in the hydrogenation of benzene, the specific activity, referred to 1 m^2 of Ni, is easily calculated. As seen from the data of Table 1, the specific catalytic activity for the series of investigated catalysts is found to be approximately constant and a several-fold increase of the surface area of the carrier does not have any appreciable effect on the value of the specific catalytic activity of nickel.

An analogous conclusion can also be reached on the basis of the results obtained for the sulfur capacity of these catalysts, i.e., the limiting adsorption of thiophenic sulfur at 120° in a current of hydrogen; the amount of thiophenic sulfur absorbed by unit surface area of nickel remained approximately constant. The size of the area of nickel atoms situated on different cross-sectional planes of the crystal amounts to: for the 111 plane – 5.3 A^2; for the 100 plane – 6.15 A^2; and for the 110 plane – 8.70 A^2; if it is assumed that the different planes are equally probable on the surface of the crystals of nickel, then the average area of the nickel atom is 6.75 A^2, i.e., 1 cm^2 of the surface area comprises $1.5 \cdot 10^{15}$ atoms of Ni. Since the rapid adsorption of oxygen on the Ni amounts to approximately $1.3 \cdot 10^{15}$ molecules of oxygen on 1 cm^2 surface then, apparently during adsorption, 1 nickel atom is bound to 1 molecule of oxygen.

The chemisorption of thiophene at 120° in a stream of hydrogen on average amounted to around $7.5 \cdot 10^{-3}$ mmoles/1 m^2 of nickel. Under these conditions hydrogenation of part of the thiophene occurred and the absorption of thiophene increased; at room temperature, however, in the absence of hydrogenation, the amount of thiophene absorbed from the vapor or from the liquid phase was found to be less and amounted to around $5 \cdot 10^{-3}$ mmoles on 1 m^2 of Ni. Using these results, we can evaluate the effective size of the thiophene molecule as approximately 33 A^2. With the size of the nickel atom as 6.75 A^2 we arrive at the conclusion that a thiophene molecule is disposed on 5 atoms of Ni, i.e., is adsorbed on the surface in a flat position. Thus, measurement of the limiting adsorption of thiophene is a method of determining the surface area of nickel in different catalysts.

From examination of the data given in Table 1, the fact stands out that nickel catalysts containing aluminum and alkali, prepared for example from nickel–aluminum alloy, with subsequent dissolving out of the greater part of the aluminum (Raney nickel) or by precipitation of the nickel with sodium aluminate, prove to be for the given reaction (hydrogenation of benzene) considerably more active per unit surface area of nickel than the nickel catalysts referred to above. At the same time through study of other reactions (for example, isotopic $H_2 - D_2$ exchange, hydrogenation of ethylene, etc.), such a difference in specific activity of these catalysts is not observed [4].

An oxygen-adsorption method was used for the determination of the differential surface area of nickel in supported nickel catalysts. The specific catalytic activity of unit surface area of nickel in a series of catalysts for the hydrogenation of benzene was found to be approximately the same. The specific activity of nickel in an alloy catalyst and Ni on aluminum oxide proved to be higher for this reaction than that of the other nickel catalysts.

LITERATURE CITED

1. R. Burshtein, N. Shumilova, and K. Gol'best, Zhur. Fiz. Khim. 20, 789 (1946).
2. I. A. Shurmovskaya and R. Kh. Burshtein, Zhur. Fiz. Khim. 31, 1150 (1957).
3. G. D. Lyubarskii, L. I. Ivanovskaya, and G. G. Isaeva, Kinetika i kataliz. 1, No. 2, 260 (1960).
4. P. Mars, J. Sholten, and P. Zwietering, Paper No. 60 of the Second Congress on Catalysis (Paris, 1960).

THE QUASI-STATIONARY THEORY OF THERMAL EXPLOSION

A. G. Merzhanov

Institute of Chemical Physics, Academy of Sciences of the USSR
(Presented by Academician V. N. Kondrat'ev, March 16, 1961)
Translated from Doklady Akademii Nauk SSSR, Vol. 140, No. 3,
pp. 637-640, September, 1961
Original article submitted March 10, 1961

In agreement with the quasi-stationary theory of thermal explosion developed for autoaccelerating reactions [1-3], an explosion* occurs as a result of a shift in the equilibrium position between the heat received and the heat escaping, which takes place due to an isothermal increase in the reaction rate. The quasi-stationary development of the preexplosion process in the conditions under examination is predetermined by the properties of the explosive reactions and by the presence of isothermal autoacceleration. However, quasi-stationary conditions of another kind are possible which are not dependent on the autoacceleration of the reaction. These are forced, nonautocontrolling conditions determined by the shift in the equilibrium conditions between the heat received and heat lost, due to a slow variation in time of some parameter of the system. This variation follows a definite law, unrelated to the development of the reaction.

In the present paper, within the framework of the quasi-stationary theory, the author examines the properties of thermal explosion under dynamic conditions for a linear increase of the temperature of the surrounding medium (heated at a constant rate).

The initial system of equations has the form

$$c\rho\frac{dT}{dt} = Qk_0e^{-E/RT}\varphi(\eta) - \alpha\frac{S}{V}(T - T_0), \quad \frac{d\eta}{dt} = k_0e^{-E/RT}\varphi(\eta), \quad T_0 = wt. \tag{1}$$

The initial conditions are t = 0, T = T_0, η = 0. Here T is the temperature in the reaction zone (°K); T_0 is the temperature of the surrounding medium (°K); η is the conversion depth; t is the time (sec); α is the heat-transfer coefficient (cal/cm^2 · sec · deg); V is the reaction space (cm^3); S is the surface which is losing heat (cm^2); Q is the heat of the reaction (cal per cm^3); E is the activation energy (cal/mole); k_0 is the preexponential factor; c is the specific heat (cal/g · deg); ρ is the density (g/cm^3); w is the rate of change of T_0 (deg/sec); $\varphi(\eta)$ are functions, expressing the law for the development of the reaction under isothermal conditions.

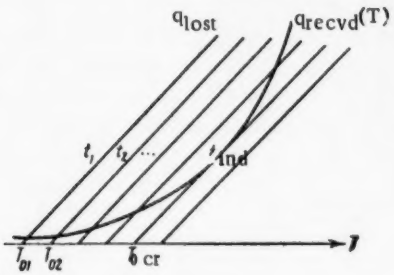

Fig. 1. Semenov diagram.

In the case when there is no distribution of temperatures in the reaction zone, α represents the heat-transfer coefficient from the surface of the charge (or, in the case of liquids, from the internal surface of the reaction vessel). In the presence of a distribution of temperatures, T and η have the meaning of averaged values over the volume, and α represents the effective heat-transfer coefficient [2].

The specific feature of forced conditions is the possibility of a quasi-stationary development of the preexplosion process for all types of reactions, independent of their kinetic laws.

Forced quasi-stationary conditions are easily reproduced on the Semenov diagram (Fig. 1), by using a model of a zero-order reaction. Under dynamic conditions (T_0 is a variable), the heat received is expressed by a set of

*In this work, as is usual in the theory of thermal explosion, we do not distinguish an explosion from ignition, and by the term explosion we understand a rapid, essentially nonstationary, development of the reaction.

lines corresponding to different values of T_0 (or t). In the reaction process a shift in the equilibrium position (the points of intersection of the heat received and the heat lost) occurs along the curve of the heat received. It is possible to consider the heat received and heat lost as related to different systems of coordinates, joined along the abscissae and moving relatively to each other with a velocity w. The explosion occurs at the moment of contact. With a linear increase of T_0, a reaction of zero order always ends with an explosion, with all values of w. If the heating rate w is less than the rate of establishment of thermal equilibrium, then the preexplosion process develops in a quasi-stationary manner. In the opposite case thermal equilibrium cannot be established, and the reaction which occurs is nonstationary.

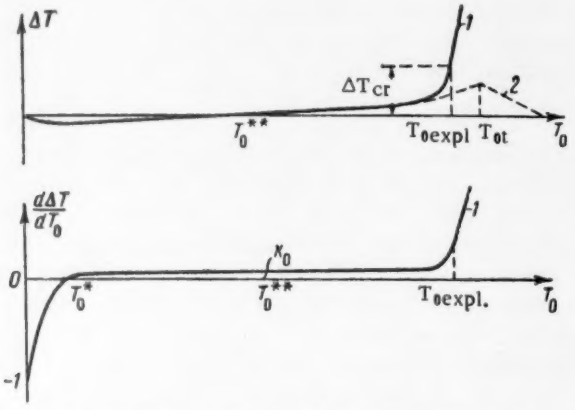

Fig. 2. Temperature conditions for the development of the reaction under dynamic conditions: 1) $w > w_{cr}$; 2) $w < w_{cr}$. $T_0^* < T_0 < T_{0\,expl}$ are the quasi-stationary conditions; $T_0^* < T_0$ is the establishment of quasi-stationary conditions; $T_0 > T_{0\,exp}$ is the disruption of quasi-stationary conditions.

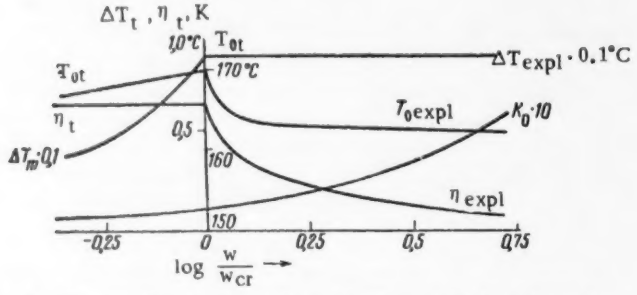

Fig. 3. The relation between the main characteristic values of thermal explosion and the rate of heating $w_{cr} \quad 2 \cdot 10^3$ deg/sec.

For real systems, due to burning out (to a decrease in the reaction rate due to the consumption of the original substance), a critical value of the heating rate w_{cr} exists. With slow heating ($w < w_{cr}$) the substance is able to react without explosion; with rapid heating ($w > w_{cr}$) a quiescent reaction ends with an explosion.

The mathematical meaning of forced quasi-stationary conditions is found in the small natural rate of heat accumulation in comparison with forced:

$$d(T - T_0)/dt \ll dT_0/dt \quad \text{or} \quad d(T - T_0)/dT_0 \leqslant 1 \text{ or } dT/dT_0 \simeq 1, \qquad (2)$$

i.e., in forced quasi-stationary conditions the rate of change of temperature in the reaction zone is close to the heating rate. The quasi-stationary character of the development of the reaction is illustrated in Fig. 2.

Before proceeding to a solution of the equations, it is of advantage to expand the exponent by the method of Frank-Kamenetskii [2]. In view of the very sharp temperature relation of the Arrhenius term, the expansion is always carried out close to the temperature at which the most intense reaction occurs. In the given problem this temperature is T_{0t}*(Fig. 2). The Arrhenius term $e^{-\frac{E}{RT}} \simeq e^{-\frac{E}{RT_{0t}^2}} e^{\frac{E}{RT_{0t}^2}(T-T_{0t})}$ This expansion is applicable at temperatures close to T_{0t}. At temperatures far from T_{0t}, the expansion is not applicable, but here the whole exponential term becomes unimportant. Due to this circumstance, the use of Frank-Kamenetskii's conversion gives only a small error and is extensively used in the thermal theory of the processes of combustion and explosion.

By stipulating quasi-stationary conditions [2], and introducing dimensionless values

$$\theta = \frac{E}{R\,T_{0m}^2}(T - T_{0m}),\quad \varkappa = \frac{Q}{\alpha S/V}\frac{E}{RT_{0t}^2}k_0 e^{-E/RT_{0t}},\quad \theta_0 = \frac{E}{RT_{0t}^2}(T_0 - T_{0t}),$$

$$\gamma = \frac{cp}{Q}\frac{RT_{0m}^2}{E},\quad \omega = \frac{w}{k_0 e^{-E/RT_{0m}}}\frac{E}{RT_{0m}^2},\quad \beta = \frac{E}{RT_{0m}},$$

we derive (1) in the form $(\theta_0 = -\beta;\quad \theta = -\beta;\quad \eta = 0)$

$$e^{\theta}\varphi(\eta) - \frac{1}{\varkappa}(\theta - \theta_0) - \omega\gamma = 0, \tag{3}$$

$$\omega\frac{d\eta}{d\theta} = e^{\theta}\varphi(\eta). \tag{4}$$

The dimensionless system of equations (3) and (4) describe the quasi-stationary development of the reaction under conditions of a linear increase in temperature. The method for its solution is obvious. Integrating (4) we obtain the relation $\eta(\theta)$ which we substitute in (3). The analysis of the relation $f(\theta,\theta_0) = 0$ allows us to calculate all the main parameters of thermal explosion.

We shall carry out a specific calculation of the parameters by taking the example of a unimolecular reaction. The determination of the critical rate of heating w_{cr}, the temperature $T_{0\,expl}$ at which explosion occurs, the depth of the preexplosion reaction η_{expl} and other parameters are the calculated values required. For a unimolecular reaction $\varphi(\eta) = 1 - \eta;\ \eta = 1 - e^{-\frac{1}{\omega}(e^{\theta}-e^{-\beta})}$. The term $e^{-\beta}$ exists only at large negative values of θ, i.e., when the reaction does not occur in practice. Therefore, the limiting case will be considered when $\beta \to \infty$.

Then

$$\eta = 1 - e^{-\frac{1}{\omega}e^{\theta}}, \tag{5}$$

$$\varphi[\eta(\theta)] = e^{-\frac{1}{\omega}e^{\theta}}. \tag{6}$$

Substituting (6) in (3) we obtain

$$e^{\theta - \frac{1}{\omega}e^{\theta}} - \frac{1}{\varkappa}(\theta - \theta_0) - \gamma\omega = 0. \tag{7}$$

The expressions (7) and (5) lead to the relations $\theta = \theta(\theta_0, \omega, \kappa, \gamma)$ and $\eta = \eta(\theta_0, \omega, \kappa, \gamma)$, representing the solution of the quasi-stationary system (3), (4). Because the maximum rise in temperature is found below the ignition limit, at $\theta_0 = 0$, then:

$$d(\theta - \theta_0)/d\theta_0|_{\theta_0=0} = 0. \tag{8}$$

Differentiating (7) with respect to θ_0 and taking Eq. (8) into account, we obtain

$$\theta_t = \ln\omega; \tag{9}$$

θ_t is the maximum rise in temperature of the system with the reaction taking place below the ignition limit. Substituting (9) in (5) we find the depth of the conversion, which corresponds to the maximum rise in temperature: $\eta_t = 1 - 1/e \approx 0.632$, and substituting (9) in (7), and assuming that $\theta_{0t} = 0$, we obtain the relation between the values ω, κ, and γ below the ignition limit.

*Above the ignition temperature, $T_{0\,expl}$ is substituted for T_{0t}.

$$\omega/e - \ln\omega/\varkappa - \gamma\omega = 0. \tag{10}$$

Analyzing this relation we arrive at the conclusion that at the ignition limit

$$\varkappa_{cr}(1/e - \gamma) = 1/e, \quad \omega_{cr} = e, \tag{11}$$

and also

$$\theta_{cr} = 1; \tag{12}$$

$$\eta_{cr} = 1 - 1/e. \tag{13}$$

Above the ignition limit (10) is not applicable. The relation between the parameters ω, κ, and γ is found from Eq. (7) by substituting $\theta_0 = 0$ and $\theta = \theta_{cr} = 1$.*

$$e^{(1-e'/\omega)} - (1/\varkappa + \omega\gamma) = 0. \tag{14}$$

The depth of the preexplosive reaction in agreement with (6) is equal to

$$\eta_{expl} = 1 - e^{-e/\omega}. \tag{15}$$

By the substitution of the expressions for the dimensionless values in (3) in Eqs. (10)-(15), all the basic parameters of thermal explosion are calculated. In particular, T_{0t} is found from (11), $T_{0\,expl}$ from (14), and w_{cr} from (12).

Figure 3 reproduces the results of the numerical calculations carried out with the following values of the parameters: $k_0 = 10^{18}\,sec^{-1}$, E = 45,000 cal/mole, Q = 1000 cal/cm^3, $\alpha = 10^{-3}$ cal/cm^2 · sec · deg, S/V = 4/d, d = 0.44 cm, c = 0.3 cal/g · deg, ρ = 1.5 g/cm^3.

Without going into a detailed analysis of the relations found, let us note the following:

1. The critical heating rate w_{cr} depends on the diameter of the heating vessel (or the charge); the less this diameter, the greater w_{cr}.

2. The preexplosive rise in temperature according to (13) and (3) is equal to $\Delta T_{cr} = RT^2_{0\,cr}/E$, i.e., related to the critical temperature in the same way as under static conditions (with T_0 = const).

3. The depth of the preexplosion reaction under kinetic conditions is considerable (η_{cr} is approximately 63%). The high value of η_{cr} is a specific feature of the quasi-stationary development of the reaction (under static conditions the explosion develops essentially in a nonstationary manner and η_{cr} is equal to a fraction of the value). With an increase of w/w_{cr} the depth of the preexplosion reaction decreases.

4. The dynamic temperature $(T_{0\,cr})_d$ exceeds the static temperature $(T_{0\,cr})_{st}$ by the value of the preexplosion increase in temperature ΔT_{cr}. With an increase of the ratio w/w_{cr}, the temperature at which the explosion occurs ($T_{0\,expl}$) falls, tending to the value $(T_{0\,cr})_{st}$.

5. The quasi-stationary criterion in the dimensionless values is equal to $K_0 \approx \omega\kappa\gamma$. Since the value of γ for reactions capable of thermal explosion are always small (10^{-2}-10^{-3}), then at the ignition limit $K_0 = e\gamma \ll 1$, i.e., close to the critical conditions, a quasi-stationary regime always takes place. The range of rates at which a quasi-stationary development of explosion occurs depends on the value of γ and may be considerable. In real cases, $1 < w/w_{cr} < (2\text{-}20)$.

In this paper the parameters of thermal explosion for a unimolecular reaction have been calculated. From the method considered here it is easily possible to carry out the required calculations for bimolecular, autocatalytic, and other reactions.

LITERATURE CITED

1. A. G. Merzhanov and F. I. Dubovitskii, Dokl. Akad. Nauk SSSR 120, 1068 (1958); 124, 364 (1959).
2. A. G. Merzhanov and F. I. Dubovitskii, Zhur. Fiz. Khim. 34, 2235 (1960).
3. D. A. Frank-Kamenetskii, Diffusion and Heat Transfer in Chemical Kinetics [in Russian] (AN SSSR Press, 1947).

*In the theory of thermal explosion the preexplosion process is assumed to differ from the explosion process by the value of the rise in temperature. The value $\theta - \theta_0 > \theta_{cr}$ corresponds to the development of explosion.

CHARACTERISTIC FEATURES OF THE ELECTRODE BEHAVIOR OF GLASSES CONTAINING TWO ACIDIC (GLASS-FORMING) OXIDES

Corr. Member AN SSSR B. P. Nikol'skii, M. M. Shul'ts, N. V. Peshekhonova, and A. A. Belyustin

A. A. Zhdanov Leningrad State University

Translated from Doklady Akademii Nauk SSSR, Vol. 140, No. 3, pp. 641-643, September, 1961
Original article submitted May 22, 1961

In [1] it was shown that the electrode behavior of glasses containing two acidic oxides (for example silica and boric oxide) depends on the distribution of the basic oxides between the acidic oxides in the glass.

Glass electrodes of binary alkali–silicate glasses, i.e., those containing only one acidic oxide – SiO_2, and electrodes of alkali glasses containing oxides of basic character (modifiers) such as the oxides of cesium, calcium, barium, lanthanum, etc., exhibit a hydrogen function over a wide pH range [2,3].

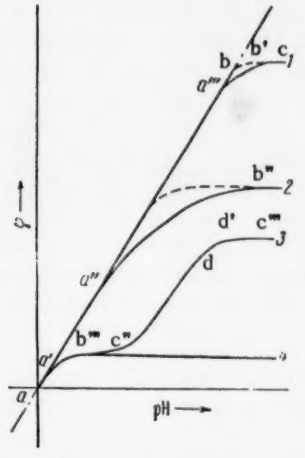

Fig. 1. Diagrammatic representation of the electrode behavior of glasses of different types: 1) binary alkali–silicate glasses and glasses containing modifier ions; 2) complex glasses containing glass-formers and modifiers; 3) simple glasses with small quantities of a second glass-former; 4) glasses containing relatively large quantities of a second glass-former. The broken section of Curves 1 and 2 corresponds to Eq. (3).

$$\varphi = \varphi^\circ + \vartheta \log a_{H+} \quad \left(\vartheta = \frac{RT}{F} \cdot 2{,}303\right), \qquad (1)$$

corresponding to the linear section aa of Curve 1 in Fig. 1. As a result of the process of ion exchange between the glass and the solution, which takes place according to the equation

$$H^+ \text{ (glass)} + M^+ \text{ (раствор)} \rightleftarrows H^+ \text{ (solution)} + M^+ \text{ (glass)} \qquad (2)$$

a transition takes place at definite pH values from a hydrogen function to a metallic function for the glass electrode [4-7] (section a'''b'c of Curve 1 in Fig. 1). According to the ion-exchange theory of the glass electrode [4], Curve 1 is described by the equation

$$\varphi = \varphi^0 + \vartheta \log(a_{H+} + K a_{M+}), \qquad (3)$$

where K is the equilibrium constant for process (2).

In the transitional section a'''b', however, certain deviations from Eq. (3) are observed experimentally, and these increase when a second acidic oxide such as B_2O_3 is introduced into the glass (Curve 2 in Fig. 1). This can be attributed to the presence, in the glass, of hydrogen ions whose bonds with the glass are of different strengths [5-7]. If a sufficiently large quantity of boron or aluminum oxides is introduced into the glass, it is possible to obtain a glass electrode with a metallic function over a wide pH range [9-11] (Curve 4 in Fig. 1).

It may be assumed that glasses containing no boron or aluminum behave as weak acids ($K \sim 10^{-12}$, Curve 1), while the introduction of boron and aluminum leads to the formation, in the glass, of the stronger boro- or alumino-silicic acids ($K \sim 10^{-12}$; $K \rightarrow 1$ for Curve 4), where the hydrogen ion is less firmly held [12]. Curves of types 2 and 4 are characteristic for complex glasses, such as those belonging to the $Na_2O - CaO - SiO_2$ system with added Al_2O_3, B_2O_3, ZrO_2, and other glass-forming oxides [13,14].

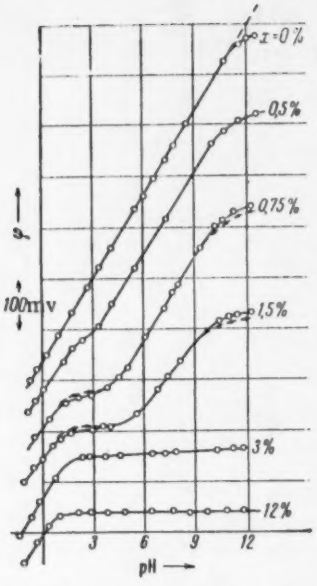

Fig. 2. Relationship between the potential of a glass electrode and pH (C_{Li^+} + 3N) for glasses of composition 27% Li_2O, X% Al_2O_3, (73 − X)% SiO_2 (mole%).

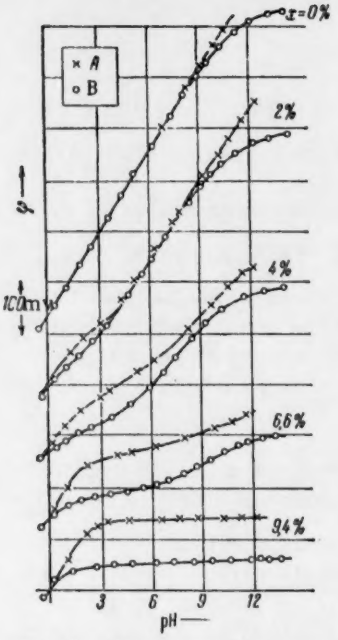

Fig. 3. Relationship between the potential of a glass electrode and pH for glasses of composition 22% Na_2O, X% B_2O_3, (78 − X)% SiO_2 (mole%). A) C_{Na^+} = 0.1N; B) C_{Na^+} = 3.0N.

The generalized theory of the glass electrode [8] also predicted the possibility of the existence of curves of type 3 (Fig. 1), where the section aa' corresponds to the hydrogen function for the glass, produced by hydrogen ions joined to the anions of both strong and weak acids in the glass phase; the section a'b‴c" corresponds to the transition range between the hydrogen and metallic functions, corresponding to the replacement by alkali metal ions of the hydrogen ions which are weakly bound to the anions of the glass. The section c"d shows (partly) the hydrogen function produced by the firmly held hydrogen ions, which are displaced by alkali metal ions at higher pH values (transition to the range d'c‴ corresponding to complete metallic function).

It has been possible for the first time to detect experimentally this differentiation in the electrode properties of a glass into properties depending on strongly acidic groups and properties depending on weakly acidic groups, in glasses of the ternary $Li_2O - Al_2O_3 - SiO_2$ system in the range of low aluminum oxide concentrations (0-3 mole%).

Figure 2 shows the relationship between the emf of the glass−calomel cell and the pH of a buffer solution of constant lithium concentration (3N). The value of the pH was measured by means of a hydrogen−calomel cell. The measurements were made at room temperature.* In the experiments, the pH was generally changed from low to high values. When the pH was changed in the opposite direction, the shape of the curve was reproduced fairly satisfactorily, a slight hysteresis being observed only in the transitional region (broken line with arrows).

Figure 3 shows the electrode behavior of glasses of the $Na_2O - B_2O_3 - SiO_2$ system. Curves are given for two concentrations of sodium ions in the solution: 0.1N and 3N. Figure 3 shows that boric oxide produces a differentiating effect, analogous in character to that produced by aluminum oxide. The relative position of the curves for different concentrations of sodium in the solution confirms the above interpretation of the individual sections of the curves of type 3 in Fig. 1. It can be seen from Fig. 3 that the distance along the vertical between the sections for the sodium functions of the curves for glasses with 6.6 and 9.4 mole% B_2O_3 is close to the theoretical value $\Delta E = \vartheta \log \frac{a''_{NaCl}}{a'_{NaCl}} = 83$ mv. We obtained similar curves for other glasses of these systems, with lower or higher lithium

*The curves in Figs. 2 and 3 have been displaced along the y axis.

oxide contents (from 24 to 33 mole%) or sodium oxide contents (from 16 to 25 mole%), and also for glasses of other systems containing two acidic (glass-forming) oxides:

$$Li_2O - R_nO_m - SiO_2 \quad (R_nO_m = B_2O_3,\ Ga_2O_3,\ ZnO_2) \tag{I}$$

$$Na_2O - R_nO_m - SiO_2 \quad (R_nO_m = Al_2O_3,\ Ga_2O_3,\ Fe_2O_3,\ GeO_2,\ SnO_2,\ TiO_2,\ ZrO_2,\ P_2O_5,\ Sb_2O_3,\ Bi_2O_3). \tag{II}$$

The extent of the differentiating influence for different oxides, shown at low concentrations of the oxides, depends on the oxide. A characteristic feature of most of these oxides is that the addition of relatively large quantities (3 to 9% for Al_2O_3, Fe_2O_3, B_2O_3, and ZrO_2) leads to disappearance of the second hydrogen region in the pH range 0-14, due to the presence of the weaker acid in the glass, as a result of which curves of type 4 in Fig. 1 are obtained. These phenomena appear to be directly related to the theory that the alkali metals in complex silicate systems combine first of all with oxides such as Al_2O_3, B_2O_3, etc. [15-17].

Thus the experimentally observed "differentiating effect" of a second acidic oxide at low concentrations in glasses of simple composition applies also for all glass-forming oxides. This effect confirms clearly the basic hypotheses of the generalized theory of the glass electrode, and agrees with modern views on the binding and coordination of atoms of glass-forming elements in glass [18,19].

LITERATURE CITED

1. B. P. Nikol'skii, N. P. Isakova, and M. M. Shul'ts, Dokl. Akad. Nauk SSSR (1961) (in press).
2. D. A. MacInnes and D. Belcher, J. Am. Chem. Soc. 53, 3315 (1931).
3. G. A. Perley, Anal. Chem. 21, 341, 394, 559 (1949).
4. B. P. Nikol'skii, Zhur. Fiz. Khim. 10, 495 (1937).
5. B. P. Nikol'skii and T. A. Tolmacheva, Zhur. Fiz. Khim. 10, 513 (1937).
6. M. M. Shul'ts, Uch. Zap. LGU, ser. khim. No. 13, 169 (1953).
7. B. P. Nikol'skii, M. M Shul'ts, and N. V. Peshekhonova, Zhur. Fiz. Khim. 32, 20 (1958).
8. B. P. Nikol'skii, Zhur. Fiz. Khim. 27, 724 (1953).
9. B. Lenguel and E. Blum, Trans. Faraday Soc. 30, 461 (1934).
10. M. M. Shul'ts and L. G. Aio, Vestn. LGU No. 8, 153 (1955).
11. G. Eisenmann, D. O. Rudin, and J. U. Casby, Science 126, 831 (1957).
12. L. Pauling, The Nature of the Chemical Bond [Russian translation] (Moscow, 1947) p. 382.
13. B. P. Nikol'skii and T. A. Tolmacheva, Zhur. Fiz. Khim. 10, 504 (1937).
14. B. Csakvári and B. Lengyel Acta Chim. Acad. Sci. Hung. 25, 369 (1960).
15. R. L. Myuller, Zhur. Tekh. Fiz. 25, 236 (1955).
16. A. A. Appen, Zhur. Fiz. Khim. 26, 569 (1953); 27, 121 (1954).
17. B. P. Nikol'skii and M. M. Shul'ts, The Vitreous State [in Russian] (AN SSSR Press, 1960) p. 292.
18. M. M. Shul'ts, Vestn. LGU No. 22, 40 (1960).
19. The Vitreous State [in Russian] (AN SSSR Press, 1960).

All abbreviations of periodicals in the above bibliography are letter-by-letter transliterations of the abbreviations as given in the original Russian journal. *Some or all of this periodical literature may well be available in English translation.* A complete list of the cover-to-cover English translations appears at the back of this issue.

SOME REGULAR FEATURES OF CHEMICAL INTERACTION, GIVEN BY THE LAW OF MASS ACTION

Corr. Member AN SSSR I. E. Starik and Yu. A. Barbanel'

V. G. Khlopin Radium Institute, Academy of Sciences of the USSR
Translated from Doklady Akademii Nauk SSSR, Vol. 140, No. 3,
pp. 644-647, September, 1961
Original article submitted February 3, 1961

The relationship between the yield of a reversible chemical reaction of the type $mA + nB \rightleftharpoons AmBn$, and the composition of the solution is given by the law of mass action in the form of the equation

$$\frac{y}{(C_A - my)^m (C_B - ny)^n} = K, \quad (1)$$

where y is the equilibrium concentration of the compound (yield of the reaction); C_A and C_B are the total concentrations of the components, and K is the concentration constant.

Formula (1) corresponds to those systems which, in addition to the reacting components A and B, contain a large excess of solvent which does not enter into the reaction; the absence of perceptible quantities of intermediate products of dissociation of the compound is also implied. When the ionic strength of the solution is kept constant, the above formula is applicable over a wide range of concentrations.

The isomolar diagram for the yield of compound of the type AmBn in the case of purely binary systems was studied by N. I. Stepanov [1], who paid particular attention to the study of the singular points lying on the diagram outside the region having physical significance. N. I. Stepanov's methods of measurement, which have made up a significant fraction of the theory of physicochemical analysis, have not, however, in recent years received the development they deserve. Moreover, in the practical application of the physicochemical analysis of complex compounds in solution, theories dealing with the relationship between the composition and the yield of compound, and based on considerations of qualitative order have become widespread. These theories are reflected in the well-known monograph by A. K. Babko [2], and can be summarized roughly as follows: With decrease in the concentration of one of the components compared with the stoichiometric value, the degree of dissociation of the compound decreases monotonously, and tends to 0 when the concentration of a given component tends to 0, i.e., when there is an infinitely large relative excess of the other component; in accordance with this, both in the case of isomolar series and in the case of series with varying concentration of one component, the relationship between the yield of the reaction and the composition of the solution is given by a curve which at all points is convex toward positive ordinates and has at the initial point a maximum slope, close to that observed for $K = \infty$.

These considerations are applicable for compounds of the type AB [2] for high values of the formation constants; the extension of these considerations to compounds of the type AB_n (A_mB) and A_mB_n, however, even at high values of K, requires certain restrictions, particularly if we are considering the range of fairly low concentrations. Mathematical analysis of Eq. (1) for the conditions: $C_A = \text{const}$, $C_B = x$, $C_B = \text{const}$, $C_A = x$, and $C_A + C_B = C = \text{const}$, $C_B/(C_A + C_B) = x$, where x is the composition variable, shows that in each of these cases the derivative y'_x at zero concentration of one of the components is equal to 0; thus, the curve at the initial point has not a maximum slope, but zero slope, and hence, over a certain initial section it is concave toward the positive ordinates; on this basis it may be concluded that with decrease in the concentration of one of the components compared with the stoichiometric values, the change in the degree of dissociation of the compound is complex in character, and when the concentration of a given component tends to 0 the degree of dissociation tends not to 0 but to 1. These conclusions, as can be shown by study of the derivative y'_x for the condition $m = 1$ or $n = 1$, do not extend to the case where the component whose concentration tends to 0 has index equal to 1 in the formula A_mB_n.

Thus, the nature of the change in the degree of dissociation of the compound when the concentration of one of the components tends to zero depends on whether the compound contains one or more particles of the given component;

if it contains more than one, then the degree of dissociation of the compound tends to 1, that is, the compound decomposes completely; if it contains only one, then the degree of dissociation decreases, and tends not to 0, but to a limit whose value depends on K.

Thus, for example, the curve showing the relationship between the yield of a compound of type AB_n and the composition in series with varying concentration of the component B has at the initial point (x = 0) a slope equal to zero, since the tangent of the angle of slope of the curve at this point, defined by the value of the derivative y'_x, is equal to 0 (and not 1/n, as follows from the theories given above); in series with varying concentration of component A, however, the tangent of the initial angle of slope is equal to $\frac{C_B^n}{C_B^n + 1/K}$ (and not 1); in isomolar series the slope is 0 (and not C/n) at the point corresponding to component A and $\frac{C^{n+1}}{C^n + 1/K}$ (and not C) at the point corresponding to component B. The corresponding values of the degree of dissociation can easily be shown to be equal to: $1, \frac{1}{1 + KC_B^n}$, $1, \frac{1}{1 + KC^n}$.

Analogous considerations apply to compounds of other types (A_mB_n, A_mB, and AB).

Since the slope of the composition-yield of compound curve is zero at the initial point, as already mentioned, the curve is concave over a certain initial section. In accordance with this, concavity in composition-property curves over the initial section is also a quite regular feature when one compound is formed in a system; this is illustrated by a large number of experimental curves given in the literature. The view that concavity in an experimental composition-property curve indicates the formation of more than one compound is not always correct.

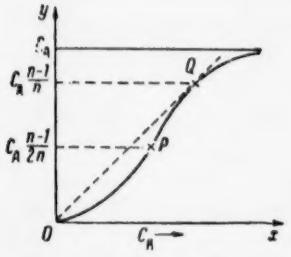

Fig. 1. Relationship between the yield of a compound of the type AB and the concentration of component B, C_A = const.

It should also be noted that when the initial section of the curve is concave, the curve should exhibit two unique points. We have made a study of these points, both for series with varying concentration of one of the components and for isomolar series, for compounds of the type AB_n (A_mB), and compounds of the type A_mB_n.

Figure 1* gives a curve showing the relationship between the yield of a compound of the type AB_n and the concentration of the component B. The curve has two unique points, one of which is a point of inflection (P), while the other (Q) may be determined by drawing a tangent from the origin. At the point P the first derivative y'_x passes through a maximum ($y''_x = 0$); at the point Q the ratio y/x reaches a maximum, i.e., $(y/x)'_x = 0$.

The derivative y'_x characterizes the intensity of the chemical reaction, i.e., the quantity of compound formed per unit of the added component B for a given composition of the solution; the ratio y/x, however, characterizes the relative yield of the reaction as a whole for attainment of a given composition. Thus, the unique points correspond to maximum intensity of the chemical reaction (P) and to the maximum relative yield of the reaction (Q).

The significance of these points may be revealed in more detail by determining their coordinates. Mathematical analysis shows that

$$y^{(P)} = C_A \frac{n-1}{2n}, \quad x^{(P)} = \frac{C_A}{2}(n-1) + \sqrt[n]{\frac{n-1}{K(n+1)}}; \tag{2}$$

$$y^{(Q)} = C_A \frac{n-1}{n}, \quad x^{(Q)} = C_A(n-1) + \sqrt[n]{\frac{n-1}{K}}. \tag{3}$$

From examination of these expressions it follows that the ordinates of the unique points are independent of the equilibrium constant and are determined entirely by the given chemical form; their abscissas, however, depend also

*The concentration of component B(x) is shown in Fig. 1 on a smaller scale than that for the concentration of the compound (y).

on the constant. The lower the stability of the compound, the further are these points displaced along the composition axis, while still remaining at the same distance from it. Thus, the points P and Q correspond to definite discrete concentrations of the compound. These concentrations are in a certain sense critical, since they separate qualitatively different regions of accumulation of reaction product. As the component B is added to component A, the accumulation of the compound AB_n at first takes place with an increase in the intensity of the chemical interaction; when $\frac{n-1}{2n}$ of the maximum possible quantity of compound ($y = C_A$) is reached, however, the intensity of the interaction passes through a maximum and then begins to decrease, although the relative yield of the reaction increases as before; when, however, the concentration of the compound increases by a further factor of 2 and reaches $(n-1)/n$ of the maximum value, subsequent accumulation of the reaction product takes place with a decrease in its relative yield. These discrete fractions are equal to $1/4$ and $1/2$ for compounds of the type AB_2, $1/3$ and $2/3$ for compounds of the type AB_3, etc.

In the case where a compound of the type A_mB_n is formed in the system, the ordinates of the points P and Q in a series with varying concentration of component B are given by

$$y^{(P)} = \frac{C_A}{m} \frac{\sqrt{mn} - \sqrt{m+n-1}}{(m-1)\sqrt{m+n-1}}; \tag{4}$$

$$y^{(Q)} = \frac{C_A}{m} \frac{n-1}{m+n-1}. \tag{5}$$

With isomolar change in the composition of the solution, the ordinates of the unique points depend on the equilibrium constant K; the relationship between the ordinates and the abscissas, however, is given by simple relationships in which the quantity K does not appear. Thus, for example, for a compound of the type AB_n, formed in an isomolar series, we have

$$ny^{(P)} + Cx^{(P)} = C\frac{n-1}{n+1}; \tag{6}$$

$$y^{(Q)} + Cx^{(Q)} = C\frac{n-1}{n}. \tag{7}$$

In conclusion, it should be noted that these regular features may find practical application in the physicochemical analysis of compounds in solutions; the most promising such application is the determination of the composition of compounds from the ordinate of the point Q in series with varying concentration of one of the components.

LITERATURE CITED

1. N. I. Stepanov, Izv. AN SSSR, OMEN, Ser. Khim. No. 2, 219 (1936).
2. A. K. Babko, The Physicochemical Analysis of Complex Compounds in Solutions [in Russian] (Kiev, 1955).

All abbreviations of periodicals in the above bibliography are letter-by-letter transliterations of the abbreviations as given in the original Russian journal. *Some or all of this periodical literature may well be available in English translation.* A complete list of the cover-to-cover English translations appears at the back of this issue.

THE RECIPROCAL EFFECT OF REACTING MOLECULES ADSORBED ON THE SURFACES OF DEHYDRATION CATALYSTS

V. É. Vasserberg, Academician A. A. Balandin, and T. V. Georgievskaya

N. D. Zelinskii Organic Chemistry Institute, Academy of Sciences of the USSR
Translated from Doklady Akademii Nauk SSSR Vol. 140, No. 4,
pp. 859-862, October, 1961
Original article submitted May 19, 1961

From a study of the mechanism of dehydration of lower aliphatic alcohols in an adsorbed layer on Al_2O_3 catalysts of different origins [1] we showed the presence of reciprocally related surface reactions during the dehydration of isopropyl and ethyl alcohols under certain conditions. Thus, at 120-150°, C_2H_5OH in amounts of 1-5 cm^3 (n.t.p.)/ g (i.e., at most up to 40-70% of the monolayer), is practically completely adsorbed without noticeable pressure in the gas phase. Under these conditions, the dehydration reaction either does not proceed at all, or proceeds very slowly. If then a relatively small amount [0.3 cm^3 (n.t.p.)/ g, i.e., 2-4% of the monolayer) of iso-C_3H_7OH is adsorbed, it is also completely adsorbed by the catalyst, and the gas-phase pressure is observed to rise, indicating that a reaction occurs. Moreover, the rate of dehydration of a standard amount of iso-C_3H_7OH always proved to be considerably less than in the absence of previously adsorbed C_2H_5OH. The rate of dehydration of C_2H_5OH considerably increased in a number of cases, as could be ascertained both from a considerable increase in the total pressure of the reaction products, and from the ethylene content of the reaction products.

Characteristics of the Al_2O_3 Catalysts Used

No.	Method of preparation	Specific surface area (m^2/ g)	Catalytic activity during dehydration in an adsorbed layer			
			iso-C_3H_7OH		C_2H_5OH	
			E, kcal/ mole	t_{20}*, °C	E, kcal/ mole	t_{20}*, °C
1	Precipitation with NH_4OH from aluminum nitrate solution at constant pH 6.3 and temp. 20°	176	24.3	126	28.7	217
2	Hydrolysis of aluminum isopropylate at 20°	210	24.5	110	29.0	218
3	Precipitation with gaseous CO_2 from sodium aluminate solution at 0°	220	26.1	126	27.5	213
4	Precipitation with NH_4OH from aluminum nitrate solution at 90°.**	195	14.2	110	26.0	217
5	Precipitation with bromine water from sodium aluminate solution at 60°	290	26.7	117	–	–
6	Al_2O_3 + Fe_2O_3 (7%) precipitated with NH_4OH from nitrate solution	–	not determined		–	–
7	As for No. 3, another preparation	220	30.0	108	–	–

*t_{20} is the temperature at which the half-decomposition period $\tau_{0.5}$ = 20 min.

**This catalyst was obtained from A. A. Tolstopyatovaya, whom the authors thank.

We carried out further experiments which showed that the reciprocally related dehydration reactions described in [1] are particular cases of a more general relationship, namely the reciprocal effect of reacting molecules on the rate of their dehydration in an adsorbed layer.

The characteristics of the aluminum catalysts which we used are given in the table (see [1] for procedures).

The dehydration kinetics in an adsorbed layer on the cited catalysts were studied for the following binary systems and corresponding individual components (the numbers in parentheses designate the catalyst reference numbers): a) iso-C_3H_7OH – ethyl alcohol (1,2,3,4,5,6,7); b) iso-C_3H_7OH – ethyl ether (3,5,7); c) iso-C_3H_7OH – methyl alcohol (1,2,3,4,5,7); d) iso-C_3H_7OH – water (1,2,3,5,7); e) iso-C_3H_7OH – isopropyl ether (1); f) iso-C_3H_7OH – methyl ether (5,7); g) (iso-$C_3H_7)_2O$ – ethyl ether (1,2,4,7); h) (iso-$C_3H_7)_2O$ – methyl alcohol (4); i) C_2H_5OH – sec-butyl alcohol (1,2,3); and j) C_2H_5OH – trimethylcarbinol (1,2,3).

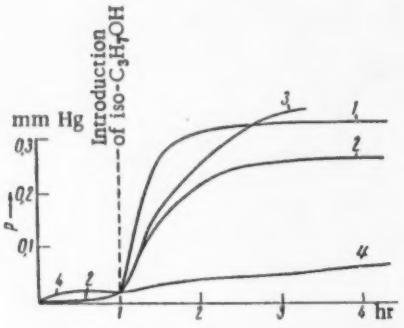

Fig. 1. Dehydration of iso-C_3H_7OH in an adsorbed layer on catalyst No. 7 at 110°: 1) pure iso-C_3H_7OH; 2) iso-C_3H_7OH + C_2H_5OH [0.3 cm^3 (n.t.p.)/ g]; 3) iso-C_3H_7OH + C_2H_5OH [5.3 cm^3 (n.t.p.)/ g]; 4) iso-C_3H_7OH + + $(C_2H_5)_2O$ [0.3 cm^3 (n.t.p.)/ g].

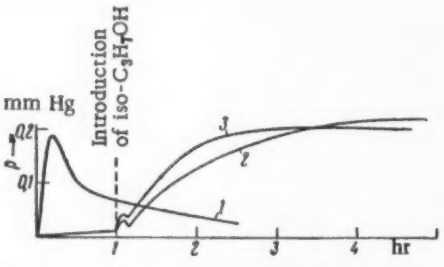

Fig. 2. Dehydration of iso-C_3H_7OH on catalyst No. 6 at 120°: 1) pure iso-C_3H_7OH; 2) iso-C_3H_7OH + C_2H_5OH [5.3 cm^3 (n.t.p.)/ g]; 3) iso-C_3H_7OH + C_2H_5OH [3 cm^3 (n.t.p.)/ g].

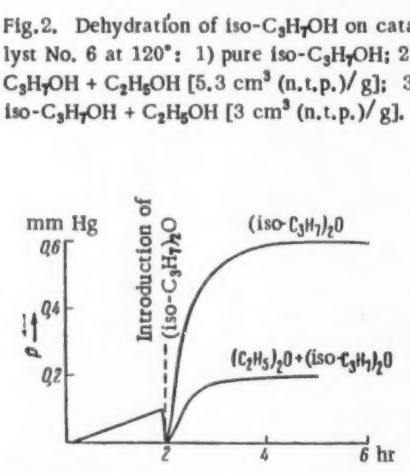

Fig. 3. Slowing down effect in the system ethyl ether – diisopropyl ether on catalyst No. 1 at 100°.

The concentration of the first component I was constant [0.3 cm^3 (n.t.p.)/ g] in all these binary systems, and the rate of dehydration of I in the mixture was compared with its rate of dehydration in the form at the same concentration. The concentration of the second component II varied from 0.3 to 5.3 cm^3 (n.t.p.) per g in different experiments.

In system a the rate of dehydration of I always decreased considerably in the mixture, whereas the rate of dehydration of II noticeably increased (four- to six-fold) in some cases, but sometimes did not change. In this case, the reaction was substantially influenced both by the nature of the catalyst and the reaction temperature, and also by the conditions under which the catalyst was regenerated between experiments; sometimes the initial rate of dehydration of II was anomalously high and did not increase after introduction of I. After careful regeneration – heating in a current of air at 400°, followed by subjection for many hours to a vacuum of the order of 10^{-5} mm Hg at 400° – the phenomenon of reciprocally related dehydration of II was detected anew. If C_2H_5OH was introduced not before, but after, the introduction of iso-C_3H_7OH, when the dehydration of I was complete, ethylene generally did not form, or formed at the same low rate as it did on a fresh catalyst specimen. A very substantial role was also played by the concentration of adsorbed ethyl alcohol. Thus, on catalysts Nos. 5 and 7 the phenomenon of reciprocally related dehydration was not observed in the presence of low concentrations of C_2H_5OH [0.3 and 1.2 cm^3 (n.t.p.)/ g, respectively], only a slowing down of the dehydration of the iso-C_3H_7OH being detected, whereas a clearly marked reciprocal effect occurred with a C_2H_5OH concentration of the order of 5.3 cm^3 (n.t.p.)/ g, the rate of formation of ethylene noticeably increasing (Fig. 1).

The phenomenon of reciprocally related dehydration was detected on catalysts Nos. 1, 2, 3, 4, 5, and 7 (in the latter case only at 120°, but not at 150°). In the case of dehydration of a mixture of I and II on catalyst No. 6 not only the rate, but also the whole character of the course of the reaction changed: the reaction product pressure curves for dehydration of I and I + II at 120° are shown in Fig. 1. The drop in pressure in the second portion of curve 1, evidently, is explained by polymerization of the initially formed propylene. Reciprocally related dehydration of C_2H_5OH to C_2H_4 did not occur in the I + II mixture, and the polymerization of C_3H_6 also ceased. At the same time, the dehydration of I slowed down considerably, and the half-decomposition period, $\tau_{0.5}$ = 40-60 min, depended on the concentration of II.

A very considerable reciprocal slowing down of the reaction was observed in system b; the addition of I, which dehydrates relatively faster than does II, not only did not increase the rate of dehydration of the I + II mixture, but sometimes even made its rate slower than for pure ethyl ether.

The presence of CH_3OH in system c decreased the rate of dehydration of I, $\tau_{0.5}$, at 120°, increasing from 13 to 14 min to 22-24 min on catalyst No. 4, or from 25 to 38 min on catalyst No. 5. It is interesting to note that on catalyst No. 4 methyl alcohol exhibited a smaller slowing down effect that did ethyl alcohol at the same concentrations, whereas the reverse relationship was observed on all other catalysts. Evidently, the intermediate methanol-isopropanol complexes which form [1] on this catalyst are less stable than those which form on the other catalysts.

Moderate concentrations [up to 1.5 cm^3 (n.t.p.)/g] of water (system d) to all intents and purposes did not slow down the rate of dehydration of iso-C_3H_7OH, but a higher concentration [5.3 cm^3 (n.t.p.)/g] caused a 1.3- to 1.5-fold increase in $\tau_{0.5}$. Evidently, water simply blocks the most active catalytic centers, driving the iso-C_3H_7OH onto the remaining unoccupied portions of the catalyst which have less adsorption and catalytic activity, but does not exhibit a slowing down effect.

The following values of the half-decomposition periods were found for system e at 120°: $\tau_{0.5}$ = 9 min for I; $\tau_{0.5}$ = 20 min for II; and $\tau_{0.5}$ = 12 min for I + II. The kinetic curve for the reaction product pressure in the I + II mixture is almost exactly additive from the curves obtained for I and II separately, and in this case, evidently, there is neither reciprocally related slowing down nor acceleration.

Methyl ether (system f) which, on its own, as would be expected, to all intents and purposes did not dehydrate under the reaction conditions in the adsorbed layer, exhibited a very strong slowing down effect on the rate of dehydration of iso-C_3H_7OH. Thus, for example, even at a concentration of the order of 1 cm^3 (n.t.p.)/g on catalyst No. 7 at 110°, $\tau_{0.5}$ increased to 60 min, from 14-18 min for pure I.

A wholly astonishing example of the strong reciprocal slowing down of two reactions, each of which takes place on its own at a relatively high rate, is the codehydration of $(C_2H_5)_2O$ and (iso-$C_3H_7)_2O$ (system g). Isopropyl ether dehydrated considerably faster than did ethyl ether on all the catalysts which were studied; therefore, when I and II were dehydrated separately, the total pressure of the olefin formed during a specific period was greater for (iso-$C_3H_7)_2O$, although the initial concentration of this ether on the catalyst was considerably less than that of the ethyl ether. In the case of the same I + II mixture with the same raw ether concentrations, the reaction slowed down so much that its rate did not exceed the rate for pure II. The pressure stopped increasing after about one and a half hours in the case of the I + II mixture on catalyst No. 1 (see Fig. 1), i.e., the two reactions reciprocally suppressed one another. With regard to this, it should be borne in mind that the (iso-$C_3H_7)_2O$, the amount of which did not exceed 2-3% of the monolayer on the catalyst surface, completely stopped the dehydration of a seven times greater amount of ethyl ether.

The presence of CH_3OH in the case of the dehydration of isopropyl ether (system h) did not lead to a noticeable decrease in reaction rate: at 110° the respective values of $\tau_{0.5}$ was 9 and 11 min. The different effect of CH_3OH in the mixtures with iso-C_3H_7OH and (iso-$C_3H_7)_2O$ (systems c and h) on the same catalyst confirms the opinion which we expressed earlier [2], that ethers do not appear as intermediate products during the dehydration of alcohols, and that the respective reactions proceed by different mechanisms and through different elementary stages.

Reciprocally related dehydrations, although more feebly marked than in system a, were observed in a number of cases with system i: $\tau_{0.5}$ for sec-C_4H_9OH increased from 2-4 to 10-16 min, and the rate of ethylene pressure rise increased from 0.02 to 0.03-0.04 mm Hg/hr.

Finally, the dehydration of trimethylcarbinol in the presence of C_2H_5OH (system j) was not accompanied by ethylene formation, but only by an increase in the maximum pressure of isobutylene formed from I. This phenomenon, which was particularly marked on catalysts Nos. 1 and 2, is similar to that described above for system a on catalyst No. 6. Evidently, on these catalysts a considerable portion (up to 50%) of the isobutylene, formed during the dehydration of pure trimethylcarbinol, does not desorb, but polymerizes on the catalyst surface. The presence of the second component, as also in the case of system a on catalyst No. 6, slowed down the parallel polymerization reaction.

Thus, the results of this work confirm the conclusion drawn earlier [1] that in dehydration reactions the reacting molecules cannot be considered as isolated structures, the character of the changes of which are independent of the nature and number of other molecules simultaneously present in the adsorbed layer. If there are other substances

present which can dehydrate (different alcohols and ethers), or even if they only form (under the given conditions) superficial intermediate structures similar to those forming during dehydration (methyl alcohol and methyl ether), the rates of decomposition of isopropyl, ethyl, and sec-butyl alcohols, and also ethyl and isopropyl ethers, change considerably. Moreover, the rate of dehydration of the component which dehydrates most rapidly always decreases, and that of the more stable component either increases (reciprocally related dehydrations) or decreases (reciprocal slowing down). This phenomenon, in contrast to certain catalytic reactions in the liquid phase which are slowed down by the reaction products or by foreign materials, does not depend on competition for a place on the catalyst surface (since in our experiments all the components were originally present in the adsorbed layer), but is probably explained by interaction of superficial complexes with the formation of compound complexes possessing, under the reaction conditions, greater or less stability in comparison with the original complexes.

LITERATURE CITED

1. V. É. Vasserberg, A. A. Balandin, and T. V. Georgievskaya, Doklady Akad. Nauk SSSR 134, 371 (1960).
2. V. É. Vasserberg and A. A. Balandin, Collection: Problems of Kinetics and Catalysis [in Russian] (AN SSSR Press, 1960) Vol. 9, p. 356.

All abbreviations of periodicals in the above bibliography are letter-by-letter transliterations of the abbreviations as given in the original Russian journal. *Some or all of this periodical literature may well be available in English translation.* A complete list of the cover-to-cover English translations appears at the back of this issue.

THE DEHYDROGENATION OF CYCLOHEXANE OVER SOME CARBIDE, BORIDE, AND SILICIDE CATALYSTS

G. A. Gaziev, O. V. Krylov, S. Z. Roginskii,

Corr. Member AN SSSR E. A. Fokina, and M. I. Yanovskii

Translated from Doklady Akademii Nauk SSSR, Vol. 140, No. 4,
pp. 863-866, October, 1961
Original article submitted June 3, 1961

It is well known that solids possessing electron conductivity are the typical catalysts for oxidation–reduction reactions [1]. It has recently become possible to extend this rule, which has been demonstrated for metals and for oxide and sulfide catalysts, to new types of semiconductors – the isoelectronic analogs of the elements of the fourth period [2].

At the present time compounds of the transitional metals with metalloids such as nitrogen, carbon, silicon, and boron are being studied and used widely as electrotechnical and abrasive materials [3]. An examination of the possibility that the rule mentioned above might extend to this class of materials appeared to be interesting. The corresponding carbides and borides are closest to the metals in their properties while some silicides (chromium, manganese, and rhenium) show semiconductor properties [4]; some nitride phases also fall into the semiconductor category [5], especially the nitrogen alloys of metals in the region where the corresponding nitride phases are homogeneous.

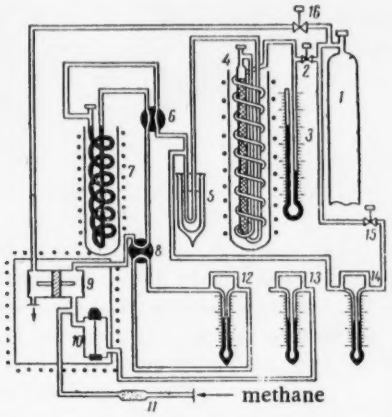

Fig. 1. Diagram of apparatus for impulse testing of catalysts: 1) carrier gas cylinder; 2), 15), 16) fine control valves; 3) mercury manometer; 4) catalyst column; 5) Dewar flask; 6), 8) 4-way cocks; 7) chromatographic column; 9) 147 ionization detector; 10) proportional counter for radioactivity measurement; 11) drying column ($CaCl_3$); 12), 13), 14) flow meters.

Until recently the carbides, silicides, borides, and nitrides of the transitional metals have hardly been studied in this connection. Studies concerned with the carbides and nitrides of iron and cobalt [6] associated with research on ammonia synthesis and Fischer–Tropsch hydrocarbon synthesis are an exception. Dowden suggests [7] that carbides, nitrides, and carbonitrides should be less active than the corresponding transitional metals since, according to his conception of the role of unfilled d shells in catalysis, the latter are filled in this case.

The dehydrogenation of cyclohexane, as it is typical of transitional metals, was chosen as the model reaction. It is also well known [8] that this reaction proceeds in the presence of some transitional metal oxides although at higher temperatures and with a higher activation energy. The chromatographic technique was chosen in order to expedite the experiments. The essential features of this technique are as follows. A flow tube packed with the catalyst was continuously purged with a carrier gas (Ar) and maintained at the reaction temperature. A sample of unsaturated cyclohexane vapor in argon was admitted into the upper portion of the catalyst tube by means of a jet. A chromatographic column 2.5 m long packed with refractory brick (particle size 1 mm), impregnated with dinonylphthalate (15% by weight), and a promethium 147 ionization detector were located immediately after the catalyst tube. Traces of the chromatographic analysis at the outlet were obtained on a EPPV-51 recording potentiometer having an input resistance of 1.5 ohms. A diagram of the apparatus is shown in Fig. 1. The impulse chromatographic technique for following catalytic reactions enabled a quantitative analysis of the dehydrogenation of cyclohexane to benzene to be carried out.

It has been shown [13,14] that the experimental data* offer confirmation, by virtue of the fact that there is a linear relationship between $\ln 1/(1-x)$ and P_i/W, that the reaction is first order (x is fractional conversion, W is the gas velocity, P_i is the pressure at the inlet of the catalyst column). The relationship between $\ln \ln 1/(1-x)$ and $1/T$ enables the energy of activation for the given conditions to be evaluated. The specific surface of the catalysts was determined by the chromatographic technique [9]. The surface area of ZrB_2 was checked by the volumetric method using krypton adsorption (2.4 m^2/g) and the surface area of CaO determined by heptane adsorption was equal to 48 m^2/g, which is in good agreement with the value obtained by the chromatographic method (2.4 m^2/g and 42 m^2/g, respectively).

Sample	Specific surface, m^2/g	Weight of sample in catalyst column, g	E, kcal/mol	X* at 500°	t, °C at start of reaction	Resistance ρ, microohms/cm
TiB_2	0.6	5.8	–	–	600	14.4
ZrB_2	2.4	13.4	–	–	650	16.6
CrB_2	2.9	1.4	–	–	600	56.0
W_2B_5	1.4	3.5	–	–	650	43.0
LaB_6	0.5	8.4	–	0.09	400	16.1
GdB_6	1.4	3.0	–	–	600	140.0
TiC	1.2	5.5	4.0	0.16	350	52.5
ZrC	1.1	7.5	8.9	0.17	450	50.0
Mo_2C	2.2	5.8	10.5	0.52	300	71.0
W_2C	1.1	9.7	–	–	650	–
WC	0.4	11.5	–	0.10	400	19.2
$MoSi_2$	1.7	8.6	18.7	0.65	300	21.6
V_3Si	0.2**	1.8	9.7	0.25	300	–
Mo_3Si	–	1.2	19.8	0.076	400	–
CaO	42.0	1.3	11.2	0.08	450	–
Alumosil catalysis	260.0***	1.5	21.6	0.12	400	–

*X corresponds to a constant argon flow rate equal to 20 cm^3/min.

**By krypton adsorption.

***By cyclohexane adsorption under static conditions.

The dehydrogenation of cyclohexane was also studied with some of the samples under static conditions under vacuum. The initial pressure was 1.5 mm Hg, the catalyst charge was 2 g, and the volume of the system 200 ml. In the dehydrogenation of C_6H_{12} a rise in pressure occurred during the course of the reaction. Gases (in the reaction products) which did not condense out in a liquid air trap were recorded and hydrogen was determined separately as gas which passed through a heated palladium capillary. The results of trials using the chromatographic technique on some borides, carbides, and molybdenum silicide are shown in the table. The electrical resistance of these samples are quoted from the data given in [1] in the same table.

The chromatograms for the dehydrogenation of cyclohexane over Mo_2C at 486° and 530° are shown in Figs. 2a and 2b. The fractional conversion was determined from the chromatogram by the ratio of the area under the benzene peak to the sum of the areas under the benzene and cyclohexane peaks.

It was shown by specially conducted experiments that cyclohexene was not present in the reaction products.**

Experiments on the dehydrogenation of cyclohexane under static vacuum conditions showed satisfactory agreement with the chromatographic runs. Kinetic curves for the dehydrogenation of C_6H_{12} over Mo_2C at an initial pressure of 1.4-1.8 mm Hg and temperatures of 300-500° are given in Fig. 3. The figure shows that these curves become reasonably linear when plotted on the coordinates $\ln[P_0 - (p/3)]$ against t, which indicates that the reaction kinetics

*Part of the measurements were carried out by I. G. Galkina and Liu Chzhun-khue, to whom the authors express their gratitude.

**Cyclohexene was kindly supplied by G. V. Isagulyants, for which we acknowledge our indebtedness to him.

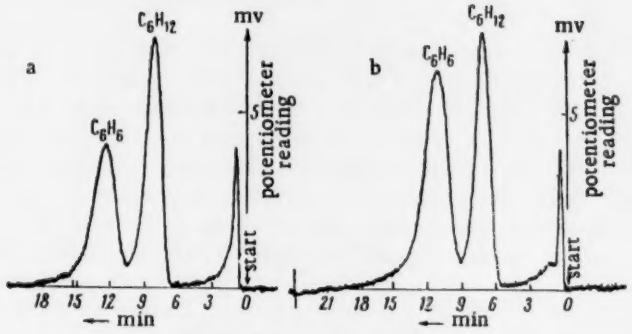

Fig. 2. Chromatograms of the products obtained by passing C_6H_{12} vapor in an argon stream over Mo_2C: a) 486°; b) 530°. Ar flow rate 20 cm^3/min.

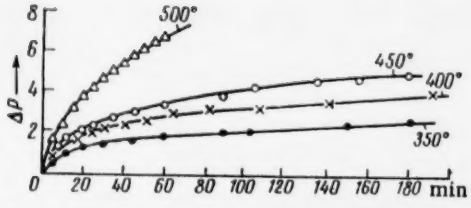

Fig. 3. Kinetic curves for the dehydrogenation of cyclohexane over Mo_2C at an initial pressure of 1.4-1.8 mm Hg.

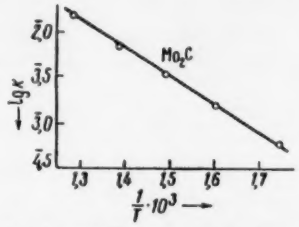

Fig. 4. Relationship between the logarithm of the first-order velocity constant and the reciprocal of temperature for the dehydrogenation of C_6H_{12} over Mo_2C.

conform to a first-order equation. An Arrhenius plot, the slope of which indicates that the activation energy is equal to 14.2 kcal/mol, is constructed from these data in Fig. 4. A similar calculation for ZrC yielded a figure of 11 kcal per mol. Comparison of these figures with the data of the table reveals that these figures are somewhat higher (by 2.5-3.0 kcal) than the corresponding values in the table, but the relative values are in approximately the same ratio. The first-order reaction rate constant at 500° is $1.6 \cdot 10^{-2}$ min^{-1} for Mo_2C, $2.3 \cdot 10^{-3}$ min^{-1} for ZrC, and $1 \cdot 10^{-4}$ min^{-1} for TiB_2. Thus, the order of magnitude of the activities in tests by either method is the same. The data show some divergence with respect to the composition of the reaction products. Thus, for example, after analysis of the reaction products from the low-pressure runs over Mo_2C the amount of gas which did not condense in the liquid air trap remaining after passage through the palladium capillary was 0.8% at 350°, 1.5% at 400°, 14.8% at 500°, and 16.1% at 550°, i.e., at low temperatures it is practically only the dehydrogenation of cyclohexane to benzene which occurs, but at a high temperature a portion of the cyclohexane cracks, possibly to CH_4 and C_2H_4. On the other hand, according to the chromatographic data the proportion of the C_1-C_2 fraction, which forms about 5% of the total yield at 460°, falls slightly with increase in temperature.

Partial sintering and a change in the structure of the surface layer as determined by electron diffraction was observed with TiB_2 after reaction, although the TiB_2 structure as determined by x-ray analysis was preserved.

The data obtained show that the series of catalysts tested possess high activity for the dehydrogenation of cyclohexane, comparable with the activity of the transitional metals. The reaction occurs in the same temperature range and at approximately the same rate. As in the case of the metal catalysts, dehydrogenation to benzene occurs, whereas, according to Balandin [10], cyclohexene may be formed with certain oxide catalysts. Their electrical conductivity and, in many cases their crystal lattices, are similar to those of the transitional metals. The activation energies for C_6H_{12} dehydrogenation are low (4.0-18.7 kcal/mol) which is also typical of metals. Considerably higher activation energies are observed in the case of oxides: 25-40 kcal/mol [8,10,11]. Runs carried out over 0.5% Pt supported

on Al_2O_3 with the chromatographic system showed a higher activity than Pt catalyst, and indicated that the reaction could be carried out at only 80°.

In comparing the activity data for the substances investigated the high activity of the carbides and of molybdenum silicide, and the low activity of the borides merit attention. The latter may be explained by the fact that the d electron levels of the transitional metals are statistically filled by electrons of the readily ionized boron atom [12]; in the case of carbides, the higher ionization potential of carbon leads to a reduction in the degree of filling of the d electron levels of the transitional metals, this reduction effect becoming increasingly apparent the fewer the number of unfilled orbits in the d level, which is characterized by the ratio $1/Nn$, where N is the principal quantum number for the d level, and n is the number of electrons at that level [12]. In this sense, the marked rise in cyclohexane conversion x in going from TiC and ZrC ($1/Nn = 0.167$-0.125) to Mo_2C ($1/Nn = 0.050$) is characteristic. The further rise in activity in the case of molybdenum disilicide may be due to the formation of a significant proportion of covalent Si—Si bonds and a corresponding reduction in the probability of filling the d electron levels of the molybdenum. In going from $MoSi_2$ to $MoSi_3$, cyclohexane conversion x falls sharply due to the reduction in the proportion of silicon, in the number of Si—Si bonds, and in the enhanced valence electron acceptor properties due to these bonds. In the case of V_3Si, the V atom possesses a high proportion of unfilled d shells and for this reason gives a relatively high conversion.

A possible reason for this connection between activity and the electronic properties of the solid state may be the transfer of 1s-electrons by hydrogen atoms to the vacant electron levels.

Experiments specially conducted by the authors have shown that Mo_2C, ZrC, WC, and $MoSi_2$ are also active catalysts for the dehydrogenation of alcohols.

LITERATURE CITED

1. S. Z. Roginskii, Problema kinetiki i kataliza 10, 5 (1960).
2. O. V. Krylov and E. A. Fokina, Zhur. Fiz. Khim. 35, No. 3 (1961).
3. G. V. Samsonov, and Ya. S. Umanskii, Solid Compounds of the High-Melting Metals [in Russian] (Moscow, 1957); G. V. Samsonov, Zhurn. Vses. khim. Obshch. im. D. I. Mendeleeva 5, 515 (1960); Fiz. tverd. tela 2, 2202 (1960).
4. V. S. Neshpor, and G. V. Samsonov, Doklady Akad. Nauk SSSR 133, 817 (1960).
5. G. V. Samsonov, Zhurn. strukt. khim. 1, 447 (1960).
6. R. Anderson, "Catalysts for organic reactions," Collection: Catalysis [Russian translation] (IL, 1955).
7. D. A. Dowden, J. Chem. Soc. 1960, 242.
8. A. A. Balandin and I. I. Brusov, Zhur. Fiz. Khim. 7, 18 (1937).
9. S. Z. Roginskii, M. I. Yanovskii, Lu Pei-Chzhan, G. A. Gaziev, G. M. Zhabrova, B. M. Kadenatsi, V. B. Brazhnikov, I. E. Neimark, and M. A. Piontkovskaya, Kinetika i Kataliz 1, 287 (1960).
10. A. A. Balandin, A. A. Tolstepyatova, and V. A. Ferapontov, Izvest. AN SSSR, OKhN No. 10, 761 (1960).
11. O. V. Krylov and E. A. Fokina, Zhur. Fiz. Khim. 33, 2555 (1950).
12. G. V. Samsonov, Zhur. Tekh. Fiz. 26, 716 (1956).
13. D. W. Bassett and H. W. Habgood, J. Phys. Chem. 64, 769 (1960).
14. S. Z. Roginskii, M. I. Yanovskii, and G. A. Gaziev, Doklady Akad. Nauk SSSR 140, No. 5 (1961).

All abbreviations of periodicals in the above bibliography are letter-by-letter transliterations of the abbreviations as given in the original Russian journal. *Some or all of this periodical literature may well be available in English translation.* A complete list of the cover-to-cover English translations appears at the back of this issue.

THE BURNING STABILITY OF POROUS HIGH EXPLOSIVES

A. D. Margolin

Institute of Chemical Physics, Academy of Sciences of the USSR
(Presented by Academician V. N. Kondrat'ev, May 25, 1961)
Translated from Doklady Akademii Nauk SSSR, Vol. 140, No. 4,
pp. 867-869, October, 1961
Original article submitted May 15, 1961

The burning velocity of a powdered and porous high explosive suddenly increases when the pressure increases above a certain critical pressure with the "disruption" of normal burning conditions [1,2]. This phenomenon is usually connected with the eruption of hot combustible products into the pores of the high explosive by the action of the so-called dynamic increase of pressure over the burning surface [1,2].

Normal flame propagation is possible if the characteristic dimensions of the surface roughness δ is substantially less than the effective width of the combustion zone l ($\delta \ll l$). If the diameter of the surface roughness exceeds the effective width of the chemical reaction zone ($\delta > l$), then the linear flame propagation velocity may significantly exceed the normal burning velocity, because burning occurs over a large area of roughness and pores. A qualitative examination of this problem was carried out in an earlier work [2]. The critical condition for the description of the regime of normal burning may be written in the following form:

$$\delta/l = b = \text{const}. \tag{1}$$

The constant b may depend on the shape and type of roughness and the properties of the high explosive. Substituting the expression for the width of the combustion zone given by Zeldovich [3] in the equation developed by Andreev [1], we shall obtain the condition for disruption of the regime of normal burning

$$\frac{\delta \rho u c_p}{\lambda} = \frac{\delta B P^{\nu} c_p}{\lambda} = b, \tag{2}$$

where ρu is the mass burning velocity, P is the pressure, B and ν are constants, c_p is the specific heat, and λ is the coefficient of thermal conductivity.

If the high explosive in question has continuous pores, then the value of the roughness may be determined knowing the porosity m and permeability k: $\delta = d\sqrt{k/m}$. The value of d slightly depends on the pore shape [4] (so-called ideal soil). Condition (1) now takes the form

$$\sqrt{\frac{k}{m}}\frac{\rho u c_p}{\lambda} = \sqrt{\frac{k}{m}}\frac{B P^{\nu} c_p}{\lambda} = \frac{b}{d}. \tag{3}$$

The burning velocity and pressure at which the description of normal burning conditions occur equal

$$(\rho u)_{\text{кр}} = \frac{\lambda b}{c_p d} = \frac{\lambda b}{c_p d}\sqrt{\frac{m}{k}}, \quad P_{\text{кр}} = \left(\frac{\lambda \delta b}{c_p B}\right)^{1/\nu} = \left(\frac{\lambda b}{c_p B d}\sqrt{\frac{m}{k}}\right)^{1/\nu}. \tag{4}$$

It is found that an increase in the burning velocity and dimensions of the pores facilitates the disruption of normal burning, which agrees qualitatively with experiment [1,2].

It is quite obvious physically that an intense oscillation of pressure favors the penetration of hot gases into the pores of the high-explosive charge burning with the velocity u. In order to investigate this phenomenon, unidimensional equations of motion and continuity of the gas in a porous medium are used:

$$\rho\left(\frac{\partial v}{\partial t} + v\frac{\partial v}{\partial x}\right) = -\frac{\partial p}{\partial x} - \frac{m\mu}{k}v,$$
$$\frac{\partial \rho}{\partial t} + \frac{\partial}{\partial x}(\rho v) = 0, \tag{5}$$

where $\underline{x}$ is a coordinate, $\underline{t}$ is the time, μ is the viscosity, $\underline{v}$ is the velocity of the gas. The boundary conditions are: $P = P_1 \cos \omega t + P_0$ with $x = ut$; $P = P_0$ with $x = -\infty$.

We shall solve the problem for small variations in pressure and gas density. For an exact solution of the problem it is necessary to describe the equation of state of the gas and the law of heat and mass transfer of the gas with the surrounding medium. For simplicity we shall confine ourselves to the case of polytropic and isothermal permeation. In general, with a varying pressure the burning velocity will vary, but up to the present no attention has been paid to this problem.

In the limiting case when the viscous forces significantly exceed the inertial, we shall obtain the following criterion for the permeation of gases in a burning compound:

$$\frac{P_1}{P_0}\sqrt{\frac{N}{2}} \geqslant 1 \qquad (6)$$

with $\sqrt{N} \gg 1$ and $M^4N^2 \ll 1$. Here $M = u/a$, where $\underline{a}$ is the velocity of sound in the permeating gas; $N = 2\omega a^2 \rho_0 k/u^2 m\mu$, where ω is the frequency of oscillation, ρ_0 is the average density of the gas. Under isothermal conditions $N = 2\ P_0 k\omega u^2 m\mu$. It is obvious that an increase in amplitude and in the frequency of oscillations favors an inrush of gas into the pores of the high explosive [under exactly the same conditions, Eq. (6) takes the form of $\frac{P_1}{P_0}\sqrt{\omega} \geq \text{const}$].

The permeation of the gases considerably affects the burning when they penetrate sufficiently deeply, at a depth S. This value S must be proportional to a definite width of the heated layer l. The coefficient of proportionality must depend on the conditions of heat transfer and the ignition of the high explosive. Evidently this coefficient of proportionality increases with an increase of the permeability and porosity of the charge.

The depth of the permeation S of the gases in the burning compound is of the order $S \simeq \frac{2\pi}{\omega}(v - u)$. We shall describe the conditions for the permeation of gas at the depth S as follows:

$$\frac{P_1}{P_0}\sqrt{\frac{N}{2}} \geqslant 1 + \frac{S\omega}{2\pi u}. \qquad (7)$$

The minimum amplitude of the oscillations $(P_1/P_0)_{min}$, required for the permeation of the gas at the depth S is obtained at the frequency ω_1:

$$\omega_1 = \frac{2\pi u}{S}, \quad \left(\frac{P_1}{P_0}\right)_{\min} = \frac{2\sqrt{2}}{\sqrt{N(\omega_1)}},$$

If $S = l$, then

$$\left(\frac{P_1}{P_0}\right)_{\min} = \sqrt{\frac{\varkappa m\mu}{2\pi P_0 k}}, \quad \omega_1 = \frac{2\pi u^2}{\varkappa},$$

where κ is the thermal diffusivity of the high explosive. The most hazardous period of oscillations for the gas to penetrate the depth of the heater layer is approximately equal to the relaxation time of the hot layer of burning high explosive.

At each value of the pressure P_0 there is an optimum frequency of oscillation ω_1 which is the most advantageous for disruption of normal burning. The physical measuring of this optimum frequency lies in the fact that an increase of frequency facilitates the penetration of gas into the burning explosive, but at too high a frequency the gas only permeates into the fine surface layer of the high explosive.

LITERATURE CITED

1. K. K. Andreev, Doklady Akad. Nauk SSSR 53, 237 (1946).
2. A. F. Belyaev, Combustion Mechanism of High Explosives (Dissertation) [in Russian] (Inst. Khim. Fiz. AN SSSR, 1946).
3. Ya. B. Zel'dovich, Zhur. Eksp. i Teor. Fiz. 12, 498 (1942).
4. L. S. Leibenzon, Motion of Natural Liquids and Gases in a Porous Medium [in Russian] (1947).

POLARIZATION CURVE FOR ANODICALLY DISSOLVING GERMANIUM WHEN THE SEMICONDUCTOR IS OF FINITE LENGTH

V. A. Myamlin

Institute of Electrochemistry, Academy of Sciences of the USSR
(Presented by Academician A. N. Frumkin, May 15, 1961)
Translated from Doklady Akademii Nauk SSSR, Vol. 140, No. 4,
pp. 870-873, October, 1961
Original article submitted May 6, 1961

In the paper [1] dissolution of germanium was discussed under the assumption that the semiconductor kept in the electrolyte has an infinite length. We will give a further extension by discussing dissolution of germanium in the case where the length of the semiconductor is comparable to, or shorter than the diffusional length. Such investigations have been carried out by several experimenters, for instance in the studies [2] and [3]. Therefore, it makes sense to carry out calculations for this case. One may even hope that by studying the dissolution of semiconductors with a finite length one will get a further clarification leading to an understanding of the dissolution kinetics of semiconductors. In fact, as we will see further on, the limit current depends upon the sizes of the semiconductor. The value of the limit current is related to the magnitude of r/ m [1], that is, to the ratio of the number of electrons and holes liberated or consumed when a germanium atom is transferred to the solution. By comparing theory with experiment one may be able to study the extent to which electrons and holes participate in the reaction as a function of the various physical characteristics, for instance, as a function of the magnitude of the electric fields in the contact, etc.

In the following we will discuss the one-dimensional problem. We take the x axis perpendicular to the germanium-electrolyte boundary. We will assume that the plane $x = 0$ corresponds to the said boundary. The region $x < 0$ comprises the electrolyte, and the region $x > 0$ represents n-type germanium. In the plane $x = w$ there is an ohmic contact.

In accordance with [4] and [5] we will characterize the ohmic contact by the magnitude of the surface recombination rate. In other words, we will assume that the hole current passing through the ohmic contact is given by the relation

$$j_p = e\,[p\,(w) - p_n]\,S, \tag{1}$$

where e is the absolute value of the electron charge; p_n is the hole concentration in the homogeneous semiconductor at equilibrium; p(w) is the hole concentration in the plane of the ohmic contact; S is the rate constant of surface recombination.

The region adjoining the ohmic contact is uncharged and in this region the minority carriers move by means of a diffusional mechanism. Therefore, we have the following equation, which relates the hole current to the gradient of the hole concentration in the diffusional region:

$$j_p = -eD_p \frac{dp}{dx}. \tag{2}$$

Here D_p represents the diffusion coefficient of the holes in the diffusional region. When the holes travel through the diffusional region there takes place recombination of holes. As usual, this process is described by the equation

$$\frac{\partial p}{\partial t} = -\frac{p - p_n}{\tau_p}, \tag{3}$$

where τ_p is the half-life of the holes, and dp/ dt is the number of holes recombined per unit time.

The continuity equation for holes has the form

$$\frac{dj_p}{dx} = e\frac{p_n - p}{\tau_p}.$$

By using (2) we get

$$\frac{p_n - p}{\tau_p} + D_p\frac{d^2p}{dx^2} = 0. \tag{5}$$

Equation (5), which is of the second order, determines the way in which the hole concentration changes along the semiconductor. Its solution contains two arbitrary constants, and in order to determine the latter constants we must specify the boundary conditions.

In the plane of the ohmic contact, evidently, the following relation must be fulfilled:

$$-eD_p\left.\frac{dp}{dx}\right|_{x=w} = e[p(w) - p_n]S. \tag{6}$$

Equation (6) is a boundary condition for our problem. In order to describe the hole distribution in the Debye layer adjoining the contact we must apply the equation

$$j_p = eu_p pE - eD_p\frac{dp}{dx}. \tag{7}$$

At the contact the germanium surface is highly enriched in holes. Since the change in hole concentration takes place over distances of the order of 10^{-4} cm, the gradient of the hole concentration is high and, therefore, the diffusional currents are always great in comparison with all j_p currents applied in electrochemistry, and these latter currents may be neglected. By substituting $j_p = 0$ into Eq. (7) we at once find that the holes are distributed according to Boltzmann's law. These considerations allow us to relate the hole concentration in the contact to the concentration at the boundary of the diffusional region.

In accordance with the considerations above, at equilibrium we have the relation

$$p_k(j=0) = p_n e^{-e\varphi/kT}, \tag{8}$$

where p_k (j = 0) represents the equilibrium hole concentration at the contact with the electrolyte, φ the equilibrium potential difference occurring in the semiconductor.

When an external potential u is applied, a current j begins to flow through the system. The concentration at the contact is related to the concentration $p(x_a)$ at the boundary of the quasi-neutral region by means of the equation

$$p_k(j) = p(x_a)e^{-e(\varphi+u)/kT}. \tag{9}$$

When eliminating $e^{e\varphi/kT}$ by means of the relations (8) and (9) we get

$$p(x_a) = \frac{p_k(j)}{p_k(j=0)}p_n e^{eu/kT}. \tag{10}$$

Relation (10) is that boundary condition of Eq. (5) which takes into account the germanium-electrolyte contact.

Just as we did in [1], we assume that in the Debye layer the recombination of electrons and holes is unimportant. Then, evidently, we have the equality

$$j_p(x=0) = j_p(x_a), \tag{11}$$

which means that the hole current does not change when it passes through the Debye layer.

The solution of Eq. (5) with the boundary conditions (6) and (10) is of the form

$$p(x) = p_n + p_n\left[\frac{p_k(j)}{p_k(j=0)}e^{eu/kT} - 1\right]\frac{D_p\,\mathrm{ch}\dfrac{x-w}{L_p} - SL_p\,\mathrm{sh}\dfrac{x-w}{L_p}}{D_p\,\mathrm{ch}\dfrac{w}{L_p} + SL_p\,\mathrm{sh}\dfrac{w}{L_p}}. \tag{12}$$

By means of the equations (2) and (12) one may find the hole current in the point $x = x_a$. We have

$$j_p(x_a) = j_p(x = 0) = \left[\frac{p_k(j)}{p_k(j=0)} e^{eu/kT} - 1\right] j_1, \tag{13}$$

where j_1 is determined by the formula

$$j_1 = \frac{eD_p p_n}{L_p} \cdot \frac{D_p \operatorname{sh} \frac{w}{L_p} + SL_p \operatorname{ch} \frac{w}{L_p}}{D_p \operatorname{ch} \frac{w}{L_p} + SL_p \operatorname{sh} \frac{w}{L_p}}. \tag{14}$$

When deriving the relations (13) and (14) we made use of the fact that $x_a \ll L_p$, $x_a \ll w$.

In order to get the polarization curve we must find out how the over-all current $\underline{j}$ depends upon the total applied voltage. In this it should be kept in mind that the total potential ψ is equal to $\psi = u + \Delta\psi_1$, where $\Delta\psi_1$ is the potential drop in the Helmholtz part of the double layer.

In accordance with [1] we will assume that the ratio of electron-to-hole current has a fixed value, that is, we will suppose that the following relation is satisfied:

$$\frac{j_p(0)}{j_e(0)} = \frac{r}{m}, \tag{15}$$

where j_e represents the electron current. Hence we get

$$j_p(0) = j\frac{r}{m+r}, \tag{16}$$

where $\underline{j}$ is the total current passing through the contact.

By means of the relations (13) and (15) we may find out how the over-all current $\underline{j}$ depends on the potential drop in the semiconductor. For the potential we have the relation

$$\frac{eu}{kT} = -\frac{\ln p_k(j)}{p_k(j=0)} + \ln\left(1 + \frac{j}{j_1}\frac{r}{m+r}\right). \tag{17}$$

In order to obtain the total potential drop we must still add the potential drop in the Helmholtz region. This potential drop $\Delta\psi_1$ is related to the over-all current by means of the following equation found by the theory of the retarded discharge [1]:

$$j = -j_0\left(\frac{p_k(j)}{p_k(j=0)}\right)^{\rho} e^{\beta(\Delta\psi_1 + \Delta\psi_0)/kT}.$$

By determining $\Delta\psi_1$ from this relation, and adding it to the left part of Eq. (17), we find the total potential drop:

$$\psi = \frac{1}{\beta}\ln\left(-\frac{j}{j_0}\right) + \left(1 - \frac{\rho}{\beta}\right)\ln\frac{p_k(j)}{p_k(j=0)} - \ln\left(1 + \frac{j}{j_1}\frac{r}{m+r}\right) \tag{18}$$

Strictly speaking, Eq. (18) is the polarization characteristic for anodic dissolution of germanium. In fact, it may be shown that, generally, the magnitude of $\ln\frac{p_k(j)}{p_k(j=0)}$ changes little in comparison with the first and the third terms. This may be done by investigating the behavior of holes in electric fields in the Debye layer.

We will now go over to discuss the polarization characteristic. At small currents where $|j/j_1| < 1$ one finds a logarithmic relation between the current and the voltage, that is, the usual law of Tafel is found.

Since the current $j < 0$, the presence of the third term points out that there exists a limit current, the value of which is equal to:

$$j_{\text{limit}} = \left(1 + \frac{m}{r}\right)\frac{eD_p p_n}{L_p} \cdot \frac{D_p \operatorname{sh} \frac{w}{L_p} + SL_p \operatorname{ch} \frac{w}{L_p}}{D_p \operatorname{ch} \frac{w}{L_p} + SL_p \operatorname{sh} \frac{w}{L_p}}. \tag{19}$$

It may be found how the current limit depends on the distance at $w \to \infty$. In this case, the formula for j_{limit} has the form

$$j_{\text{limit}} = \left(1 + \frac{m}{r}\right)\frac{eD_p p_n}{L_p} = e^2 n_i^2 D_p u \frac{\rho}{L_p}\left(1 + \frac{m}{r}\right).$$

This relation coincides with the result obtained in [1].

In the limit case $w \ll L_p$ the hyperbolic sines and cosines can be expanded into series, and for the limit current we get the equation

$$j_{\text{limit}} = \left(1 + \frac{m}{r}\right) \frac{eD_p p_n}{L_p} \frac{D_p \frac{w}{L_p} + SL_p}{D_p + Sw}. \tag{20}$$

At $S \to \infty$ the limit current converges to the value

$$j_{\text{limit}} = \left(1 + \frac{m}{r}\right) \frac{eD_p p_n}{L_p} \operatorname{cth} \frac{w}{L_n}. \tag{21}$$

At small values of S, Eq. (19) can be expanded into a series and we find:

$$j_{\text{limit}} = \left(1 + \frac{m}{r}\right) \frac{eD_p p_n}{L_p} \left(\operatorname{th} \frac{w}{L_p} + \frac{SL_p}{D_p \operatorname{ch}^2 \frac{w}{L_p}}\right).$$

The derived equations determine the limit current in the various cases.

In conclusion, the author expresses his gratitude to V. G. Levich, Corr. Member, AN SSSR, for valuable discussions.

LITERATURE CITED

1. Yu. A. Vdovin, V. G. Levich, and V. A. Myamlin, Doklady Akad. Nauk SSSR 126, No. 6 (1959).
2. E. A. Efimov and I. G. Ierusalimchik, Zhur. fiz. khim. 32, 1103 (1958).
3. Flyn, J. Electrochem. Soc. 105, 395 (1958).
4. N. A. Penin, Radiotekhnika i elektronika 2, 8, 1053 (1957).
5. A. V. Rzhanov, Doklady Akad. Nauk SSSR 98, No. 3 (1954).

All abbreviations of periodicals in the above bibliography are letter-by-letter transliterations of the abbreviations as given in the original Russian journal. *Some or all of this periodical literature may well be available in English translation.* A complete list of the cover-to-cover English translations appears at the back of this issue.

DEEMULSIFYING EFFECT OF SURFACE-ACTIVE SUBSTANCES AND THE STRUCTURAL MECHANICAL PROPERTIES OF THEIR ADSORPTION LAYERS

M. A. Filatova, S. A. Nikitina, A. B. Taubman,

and Academician P. A. Rebinder

Institute of Physical Chemistry, Academy of Sciences of the USSR
Translated from Doklady Akademii Nauk SSSR, Vol. 140, No. 4,
pp. 874-876, October, 1961
Original article submitted June 7, 1961

The exceptionally high stability of oil emulsions of the type "water in oil," as is well known, originates because they are highly stabilized by their structural surface layers of natural emulgators with a very complex composition, which embrace both surface-active and inactive components: naphthenates, resins, asphaltenes, and particles of highly disperse solid phases. For this reason the most general physicochemical method of breaking such emulsions consists of letting them be attacked by surface-active substances which, while being adsorbed on the surface of the boundary between a droplet and the surrounding medium, as a result of this adsorption or by making the surface more hydrophilic, expel the protective shell and thereby upset the stability of the emulsion [1-3].

Therefore, a deemulsifier will be effective only if, on the one hand, its surface activity is sufficiently high and, on the other hand, it has a considerable wetting ability in aqueous solutions, that is, it must have properties which in many cases are not combined in one and the same surface-active substance. This fact, obviously, also explains the difficulties arising when one tries to select effective deemulsifiers even among highly surface-active substances or to develop methods for the evaluation of the deemulsifying effect; because of this, the said methods bear an empirical character.

Therefore, as the most general method for such an evaluation it is appropriate to use measurements of the structural mechanical properties of adsorbed emulgator layers which stabilize inverse emulsions, and to study their changes effected by deemulsifiers [4]. The results of such measurements, evidently, should grossly characterize the changes in the properties of the emulsion systems, as arise when a deemulsifier interacts both with the surface-active and the inactive components of the protective films.

At the same time such measurements enable one to evaluate the structural mechanical properties of adsorbed layers of the deemulsifiers themselves, and this is essential because, if these properties are sufficiently sharply developed, not only the emulsion may be broken, but it may even be inverted under formation of an emulsion of the first type.

In the present study, by means of a standard SNS-2 equipment (designed for investigating the rheological properties of clay suspensions) which we have specially adapted for our measurements we have measured the stability [the two-dimensional shear stress limit (P_m)] for adsorbed layers formed from one sample of the "black" emulsifier of oil emulsions, which, by means of the procedure [6] was isolated from a mixture of oils originating from the northeastern deposits in the USSR and processed in the Gur'ev oil distillation plant. The oil phase of the emulsion consisted of a 0.1% solution of the emulgator in a 1:1 mixture of vaseline oil and xylene, the water phase contained 10% NaCl and various amounts of deemulsifier; as the latter we used the nonionic surface-active substance OP-10 and two brands of saponins (Kahlbaum and Baker), which form adsorbed layers of a high and a low stability, respectively [7]. The interphase surface tension, which was equal to 45.3 erg/ cm^2, decreased very little in the presence of the emulgator and amounted to 44.2 erg/ cm^2.

P_m was measured in the following way. The glass disc of the apparatus was suspended to the spring fiber in such a way that it intersected the boundary between the two liquids kept in the vessel which, together with the special little table, could be rotated at a constant velocity (0.2 rpm). In each experiment the rotation was continued as long as the increase in the torsion moment of the fiber did not result in breaking the interphase layer at the stress corresponding to the limit value P_m [5]. After the breaking, the structure of the adsorption layers of the systems

studied was thixotropically reestablished so rapidly (the stress relaxation time did not exceed 10-20 sec) that we were able to measure successively, at first during one minute and later during 30-60 min, beginning with very small values of the time ($\tau \sim 1$ min) during which the layers existed up to $\tau \sim 10$ hr and more, when a protective film had been formed (see figure, curve 1).

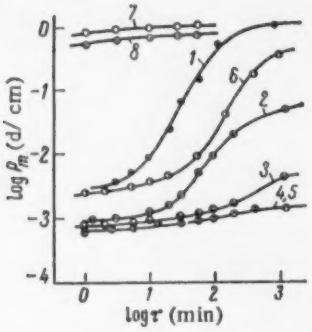

Curves of $P_m = f(\tau)$ for adsorbed layers of the "black" emulsifier in a 0.1% solution in a 1:1 mixture of vaseline oil and xylene on the boundary with a 10% solution of NaCl in water with or without a deemulsifier. 1)-5) OP-10 in the concentrations 0, 0.05%, 0.1%, 0.25%, and 0.5%, respectively; 6) "Baker" saponin 0.5%; 7) "Kahlbaum" saponin 0.5%; 8) "Kahlbaum" saponin 0.5%, solution without emulsifier.

In the figure curves of $P_m = f(\tau)$ are given for the adsorbed layer of the original black emulsifier on the boundary between its 0.1% solution in the hydrocarbon and a 10% solution of NaCl in water (curve 1), and for mixed adsorbed layers formed from this same emulsifier and a deemulsifier (OP-10 or saponin) added to the water phase in various concentrations (curves 2-7). The shape of curve 1 points out that the high stability of adsorbed layers of the "black" emulsifier (maximum value of $P_m \sim 1$ d per cm) results from their colloidal structure, which is formed after a long time and meanwhile has the tendency to a rapid thioxotropic recovery, as follows from the conditions which we used to measure P_m (at destruction of the adsorbed layers formed). This texture, obviously, has a complicated polymolecular structure analogous to that of protective monolayer films on the droplets of those emulsions which are stabilized by disperse (noncolloidal) solid emulsifiers [5]. Just such a structure is responsible for the exceptionally high stability of the emulsifier layers, which by at least three orders of magnitude exceeds the stability of adsorbed layers of the usual surface-active substances on a boundary between two liquid phases. As the concentration of the deemulsifier OP-10 in the water phase is raised from 0.05 to 0.5% (curves 2-5), there takes place not only a sharp (by 2-3 orders of magnitude) successive lowering of P_m, but also a regular change in the shape of the curves. Because the deemulsifier particles become ever more hydrophilic, the protective film formed from them is gradually destroyed and looses its ability to stabilize, so that the stability of the emulsion is lowered.

In good agreement with these data on the stability of interphase layers are the following results, obtained by measuring the stability of emulsions (at 70°) formed by shaking a solution of the "black" emulsifier in the oil phase with the water phase (volume oil:volume water = 3:100) containing 10% NaCl, together with the deemulsifier OP-10 (the stability was characterized by the time t required for the separation of half the amount of the emulsified water)

Concentration of the "black" emulsifier in the oil phase, %	0.1	0.1	0.1
Concentration of OP-10 in the water phase, %	0	0.25	0.5
Time required for the separation (t), min	$2 \cdot 10^3$	$2 \cdot 10^2$	$6 \cdot 10$

It is important to note that the destruction of the protective emulsifier film proceeds, as it interacts with the molecules of deemulsifier-wetting agent and, consequently, this destruction requires time. Therefore, under nonequilibrium conditions the water which gradually separates upon shaking the system, if there is enough of it, may form an external phase of an emulsion of the first type (oil in water) and then a multiple (mixed) emulsion originates [8], containing both types of emulsions in various volume ratios (dependent on the intensity and the duration of the stirring and on the water content). However, here the stabilization ability of the deemulsifier is of decisive importance.

If the structural-mechanical (stabilizing or structural-viscous) properties of its adsorbed layers are very weakly developed, as is the case for the highly surface-active deemulsifier OP-10 (the surface viscosity of the saturated layer in its 0.5% solution is of the order of magnitude of about 10^{-3} surf. poise, and the surface tension of its solution σ is about 30 erg/ cm^2), then the hydrophilization of the "black" emulsifier particles results in decreasing P_m to its lowest value and the destruction of the original emulsion takes place without formation of an oil-in-water emulsion (see curves 4 and 5).

When the saponins, which are much less surface-active substances (their 0.5% solutions have practically the same lowered limiting $\sigma \approx 40$ erg/ cm^2) are used, they are found to have a different effect dependent on the

structural-mechanical properties of their adsorbed layers. According to the data of [7], the surface viscosity of 0.5% solutions of saponins varies over seven orders of magnitude lying between 10^{-3} and 10^{4} surf. poise.

In agreement with this, as is evident from the figure, the first of the saponins has a relatively weak effect on the behavior of the original emulsion (curve 6), it somewhat lowers P_m but does not change the S-shape of the $P_m = f(\tau)$ curve, which shape is characteristic for the "black" emulsifier, and thus the latter, to a considerable extent, preserves its emulsifying properties. Because of this, in the said case the emulsion of the inverse type, as is obtained from various volumes of the water and the oil phase, is only partly broken and a multiple emulsion is formed.

In agreement with its high stabilizing properties, the "Kahlbaum" saponin behaves quite differently. As can be seen (curve 7), it completely changes the shape of the $P_m = f(\tau)$ curve: the linear relation, which is analogous to the curves 4 and 5 for OP-10, indicates that the colloidal structure of the "black" emulsifier is completely driven out from the boundary surface by a monomolecular saponin layer. At the same time, the values of P_m are practically identical to that characteristic for an adsorbed layer of the pure saponin ($P_m \sim 1$ d/cm), as is found when the "black" emulsifier is absent (see curves 7 and 8); this gives a reason to draw the conclusion that, in the present case, the saponin causes an inversion of the phases and the formation of a highly stable emulsion of the first type.

So, by measuring the structural-mechanical properties of interphase layers one is able, in fact, to characterize graphically the changes as occur in the stability of oil emulsions of the inverse type, when these emulsions interact with deemulsifiers.

LITERATURE CITED

1. B. P. Tonkoshurov, N. N. Serb-Serbina, Principles of the Chemical Deemulsification of Oils [in Russian] (1946); C. Dodd, J. Moore, and M. Denekas, Ind. Eng. Chem. 44, 2585 (1952); 45, 1759 (1953); N. Dunning, N. Gustafson, and A. Tohansen, Ind. Eng. Chem. 46, 591 (1954).
2. P. A. Rebinder, Kolloid. Zhur. 8, 157 (1946).
3. A. B. Taubman and A. F. Koretskii, Transactions of the All-Union Conference on the Application of Surface-Active Substances in Oil Industry [in Russian] (Ufa, 1961); A. F. Koretskii and A. B. Taubman, Doklady Akad. Nauk SSSR 124, 358 (1959).
4. A. A. Petrov, Cand. Dissertation [in Russian] (Oil Institute, AN SSSR, 1956).
5. A. F. Koretskii, Cand. Dissertation [in Russian] (Institute of Physical Chemistry, AN SSSR, 1960); A. B. Taubman and A. F. Koretskii, Doklady Akad. Nauk SSSR 140, No. 5 (1961).
6. V. G. Ben'kovskii and R. A. Pilyavskaya, Kolloid. Zhur. 13, 401 (1951); V. G. Ben'kovskii, Doklady Akad. Nauk SSSR 59, 1101 (1948).
7. K. V. Zotova and A. A. Trapeznikov, Doklady Akad. Nauk SSSR 117, No. 5, 833 (1957).
8. W. Clayton, Emulsions [Russian translation] (IL, 1950).

All abbreviations of periodicals in the above bibliography are letter-by-letter transliterations of the abbreviations as given in the original Russian journal. ***Some or all of this periodical literature may well be available in English translation.*** **A complete list of the cover-to-cover English translations appears at the back of this issue.**

THE DETECTION OF HO_2 RADICALS BY THE USE OF EPR SPECTROSCOPY

L. I. Avramenko and R. V. Kolesnikova

Institute of Chemical Physics, Academy of Sciences of the USSR
(Presented by Academician V. N. Kondrat'ev, May 20, 1961)
Translated from Doklady Akademii Nauk SSSR, Vol. 140, No. 5, pp. 1100-1101, October, 1961
Original article submitted May 17, 1961

The existence of a long-life HO_2 radical has been postulated in a great number of oxidation reactions. With the development of new experimental techniques it has been shown that the HO_2 radical indeed exists. Thus, Foner and Hudson showed [1], by means of mass spectroscopy, that HO_2 is formed in the reaction of H with molecular oxygen. The H atoms were generated by electric discharge in H_2. If the elementary reactions of the HO_2 radical are to be studied, there is a need to develop a method simpler than mass spectroscopy for the detection of this radical. The electron paramagnetic resonance (EPR) constitutes such a method. We could find no record in the literature that an EPR signal has been observed which could be positively attributed to the HO_2 radicals. In our experiments, the HO_2 radicals were generated by the reaction of H atoms with O_2 molecules at room temperature, under jet-stream conditions, and at a total pressure of 60 mm Hg. The linear jet velocity was 90 cm/sec. The H atoms were generated by silent discharge in an ozonizer tube filled with H_2. This tube was connected with the reaction vessel through a nozzle. Molecular oxygen was introduced into the vessel beyond the nozzle. The pressure dependence of the rate of formation of HO_2 radicals revealed that the reaction is trimolecular or, in other words, that it takes place in the gas phase. A detailed description of our apparatus and the results of our kinetic investigation of the reaction $H + O_2 + M$ will be published at a later date. The HO_2 radicals were frozen in a thin tube cooled with liquid nitrogen. The cold zone started about 4 cm beyond the point at which H and O_2 were mixed. After the reaction was over, the tube was sealed off and transferred, together with the cooling vessel, to the EPR machine.*

The EPR spectrum of HO_2 radicals frozen at 77°K.

The EPR spectrum was recorded on an IKhF-2 three-centimeter radiospectrometer with double modulation of the magnetic field [2]. In the figure we have reproduced the EPR spectrum of the HO_2 radicals generated in the gas phase and frozen at 77°K. One can readily see that the signal is unsymmetrical. The total signal width between points A and B is 23-26 oersted. The g factor of the HO_2 radical is practically the same as that of diphenylpicrylhydrazyl.

If the vessel was allowed to warm up and then cooled again at 77°K, the signal would disappear. In experiments where no oxygen was added (control experiments) no signal appeared. In addition to recording the EPR spectra, we also carried out a chemical analysis of the reaction products. In experiments where the EPR signal of HO_2 radicals was observed, H_2O_2 could be detected soon after the tube was opened. H_2O_2 was absent in control experiments where no signal was observed.

LITERATURE CITED

1. S. N. Foner and R. L. Hudson, J. Chem. Phys. 21, 1608 (1953).
2. A. G. Semenov and N. N. Bubnov, Instrumentation and Experimental Techniques [in Russian] (1959) Vol. 1, p. 92.

*We would like to thank G. A. Kapralov for recording the EPR spectra.

THE MECHANISM OF RECTIFICATION ON AN OXIDIZED ZIRCONIUM ELECTRODE

N. G. Bardina and P. D. Lukovtsev

Institute of Electrochemistry, Academy of Sciences of the USSR
(Presented by Academician A. N. Frumkin, May 19, 1961)
Translated from Doklady Akademii Nauk SSSR, Vol. 140, No. 5, pp. 1102-1105, October, 1961
Original article submitted May 16, 1961

The rectifying action of the oxide film on semiconductor metals is currently either attributed to a p-n transition in the film [1,2] or to a space charge in the oxide film and processes occurring at the oxide–electrolyte boundary [3-9].

The postulated p-n transitions in the oxide film have been confirmed experimentally by Smith [10], Vermilyea [11], and L. Young [6]. These workers, however, failed to consider the effect of electrolyte on these processes. Schmidt [12,13] explained the conductance in the oxide film observed after cathodic polarization of the electrode by postulating that protons from the electrolyte penetrate the film and give rise to a large number of carriers. The postulated space charge in the film and the barrier at the oxide–electrolyte boundary would indicate that by altering the potential at this boundary one should be able to change considerably the electrophysical properties of the entire film. Despite the great importance of data relating the resistance of films to the potential at the oxide–electrolyte boundary, all attempts to get this information in order to clarify the rectification mechanism have so far failed.

The method commonly used for investigating the effects of voltage on the properties of an electrode–solution boundary (in which a polarization current is applied to the electrode) cannot be used in this case, for should a current flow through the film it would be impossible to separate the potential drop at the phase boundary from the drop caused by the ohmic resistance. Moreover, one should remember that in the over-all potential difference at the electrode–solution boundary (which may attain several hundreds of volts during anodic polarization) the contribution from the voltage drop at the oxide–solution boundary is small and cannot be determined with sufficient accuracy.

To isolate from the total potential drop at the electrode–solution boundary only the component representing the oxide–solution boundary we investigated the resistance R and capacitance C of an oxidized zirconium electrode as a function of the potential of a redox medium. In this case we could assume that any change in the electrode–solution voltage will correspond to the change in the oxide–solution voltage, since the potential drop in the film resulting from resistance (iR) can be neglected when the voltage is measured in an apparatus with low current requirements.

The zirconium electrode (99.8% Zr; 0.02% Si, Al, and Fe; 0.01% Be) consisted of a 1 mm wire 2.5 mm in length which was anodized at 0° by a 260 μ amp/ cm^2 current in 0.2N H_2SO_4. The film width was calculated from the capacitance C (determined in 0.2N H_2SO_4 at 400 cps) by using the equation

$$\delta = \frac{\varepsilon}{4\pi C}.$$

For the dielectric constant ϵ we took the value of 20 [14,15]. Such a determination of film thickness was reproducible to 5-10%. The electrode–solution potentials were determined in the following systems: Fe^{2+}/Fe^{3+} at pH = 1.4, $Fe(CN)_6^{3-}/Fe(CN)_6^{4-}$ at pH = 8.4, and I^-/I_3^- at pH = 1.5. The particular choice of systems was motivated by the fact that they are all highly reversible [16-18], and that the transition from the oxidized to the reduced form is accompanied only by electron transfer. By varying the ratio of the oxidized to the reduced form from 1:0.001 to 0.001:1 while maintaining an over-all salt concentration of 0.5N, we were able to change the potential of the system by 0.3V.

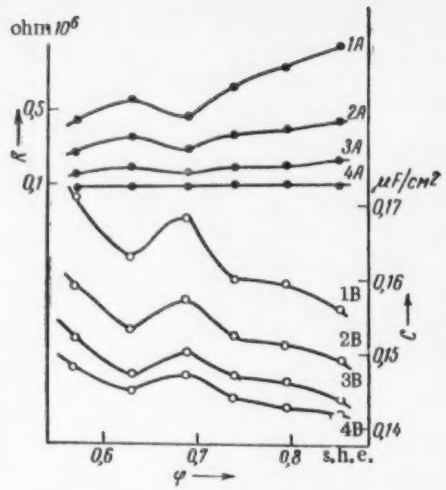

Fig. 1. The resistance (curves A) and capacitance (curves B) as a function of the redox potential of the medium containing the Fe^{++}/Fe^{+++} couple: 1) at 400 cps; 2) at 1000 cps; 3) at 2500 cps; 4) at 5000 cps.

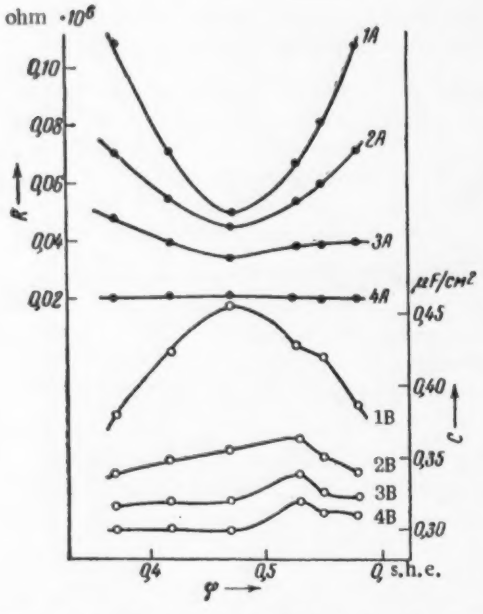

Fig. 2. The resistance (curves A) and capacitance (curves B) as a function of the redox potential of the $Fe(CN)_6^{3-}/Fe(CN)_6^{4-}$ couple: 1) at 400 cps; 2) 1000 cps; 3) 2500 cps; 4) 5000 cps.

The electrode resistance and capacitance was measured on an ac bridge at a 10-mv amplitude and frequencies between 400 and 5000 cps using films 500, 1000, and 1500 A thick. The results obtained in a circuit with R and C in series were recalculated to one in which the two components were in parallel, which more closely approximates the equivalent circuit of the oxidized zirconium electrode. Since it takes a while for the film to achieve equilibrium with the solution, we kept the system for 5 hr at a constant temperature of +30° before determining the capacitance and resistance. The oxidized zirconium electrode had the same potentials as would a platinum electrode submerged in identical solutions. We measured the potentials with reference to a Hg/Hg_2SO_4 electrode in 0.2N H_2SO_4 using a pH-E-M meter with a current consumption of $5 \cdot 10^{-15}$ amp per div.

In Fig. 1 we have shown how the resistance and capacitance of an electrode covered with a 1090 A thick oxide film varies with the voltage imposed on the Fe^{++}/Fe^{+++} system at the frequencies of 400, 1000, 2500, and 5000 cps. The figure shows that a potential drop from +0.85 to +0.57 (with reference to a s.h.e.) reduces the film resistance at 400 cps by one-half, while the capacitance increases by 10%. In addition to this, at 400 and 1000 cps the $C - \varphi$ curves exhibit a maximum, and the $R - \varphi$ curves a minimum at $\varphi = 0.69$ v, at which point the oxidized and reduced forms are in equal concentration (0.25N).

In Fig. 2 we have likewise reproduced the relationships between the resistance and capacitance of the same electrode (with an oxide film 1090 A thick) and the voltage imposed on a $Fe(CN)_6^{3-}/Fe(CN)_6^{4-}$ system at frequencies of 400, 1000, 2500, and 5000 cps. As the potential at 400 cps is increased above 0.4 v, the film capacitance at first increases by 10%, passes through a maximum, then drops to its original value; meanwhile, the resistance decreases by one-half and has a minimum at $\varphi = 0.47$ v, again at the point where the oxidized and reduced forms are in equal concentration.

With increasing frequency the extrema on the $C - \varphi$ and $R - \varphi$ curves become less pronounced, and at 5000 cps practically disappear in both the Fe^{++}/Fe^{+++} and the $Fe(CN)_6^{3-}/Fe(CN)_6^{4-}$ systems. Very similar curves were obtained on films 500 and 1500 A thick.

Two characteristic features of the $R - \varphi$ and $C - \varphi$ curves plotted in Figs. 1 and 2 are: the increasing capacitance and decreasing resistance as one proceeds toward more negative potentials, and the appearance of extrema at the point where the reduced and oxidized forms are in equal concentration. The extrema shown in Figs. 1 and 2 apparently result from the fact that the Fe^{++}/Fe^{+++} and $Fe(CN)_6^{3-}/Fe(CN)_6^{4-}$ systems, which are normally reversible on metals, lose their reversibility when the electrochemical reaction takes place on a semiconductor, since the transfer of electrons from the electrode to the ions might be hindered by the low concentration of electrons in the semiconductor.

As the concentration of either the oxidized or the reduced form increases, the resistance caused by the slowed electrochemical reaction decreases. This explains why the point at which the two forms are at the same concentration coincides with the minimum on the $R - \varphi$ curves. The maxima on the $C - \varphi$ curves apparently represent pseudocapacitance, which is connected with the nature of the electrochemical reaction. The disappearance of the extrema on both the $C - \varphi$ and $R - \varphi$ curves at high frequencies confirms our interpretation of their nature.

Although the general properties of an oxidized zirconium electrode are very similar in both the Fe^{++}/Fe^{+++} and the $Fe(CN)_6^{3-}/Fe(CN)_6^{4-}$ systems, there are certain small differences in its behavior. The extrema on the $C - \varphi$ and $R - \varphi$ curves have stronger maxima and disappear at lower frequencies in the $Fe(CN)_6^{3-}/Fe(CN)_6^{4-}$ system than they do in the Fe^{++}/Fe^{+++} system. This indicates that the former is more reversible. In addition to this, the electrode resistance and capacitance become practically independent of voltage in the $Fe(CN)_6^{3-}/Fe(CN)_6^{4-}$ system at higher frequencies in contrast with the Fe^{++}/Fe^{+++} system, where the resistance decreases and capacitance increases at lower positive voltages.

The fact that the film resistance in the Fe^{++}/Fe^{+++} system decreases by one-half, while the capacitance increases by 10% (which is equivalent to a 10% reduction in the film thickness) when the potential is decreased by 0.25 v, indicates that the film resistance is essentially concentrated in the layer adjacent to the electrolyte.

The theory that the film resistance depends very much on the potential finds even better confirmation if one compares the resistance of an oxidized zirconium electrode at different potentials maintained by various redox systems under conditions most favorable to the electrochemical reaction, i.e., in solutions where the oxidized and reduced forms are at the same concentration, 0.25N.

We found that the resistance of a 1000 A film in the Fe^{++}/Fe^{+++}, $Fe(CN)_6^{3-}/Fe(CN)_6^{4-}$, and I_3^-/I^- systems, which imposed upon the electrode the potentials of 0.72, 0.54, and 0.77 v, was $4.7 \cdot 10^5$, $0.5 \cdot 10^5$, and $0.2 \cdot 10^5$ ohms, respectively; consequently, a 0.25 v rise in voltage increases the resistance by a factor of 9.

The experimental data reproduced in this paper confirm the theory that the carriers are not distributed evenly throughout the film, and that the oxide–electrolyte boundary influences greatly the electrophysical properties of the entire film, and also indicate that the rectifying action of the oxide film observed when the voltage is shifted toward more negative values is connected with an increased concentration of charge carriers in the film layer adjacent to the electrolyte.

LITERATURE CITED

1. Y. Sasaki, J. Phys. Chem. Solids 13, Nos. 3-4, 177 (1960).
2. M. Kabayashi, Extended Abstract, Inst. Rad. Eng. Convention, Philadelphia, May, 1959.
3. H. E. Haring, J. Electrochem. Soc. No. 1, 30 (1952).
4. A. Decker, and H. Urquhart, J. Appl. Phys. 21, 708 (1950).
5. A. Smith, Canad. J. Phys. 35, 1154 (1957).
6. L. Young, Trans. Faraday Soc. 55, 842 (1959).
7. K. Boer, H. Hansch, and U. Kummel, Z. Phys. 155, 170 (1959); K. Boer, Z. Phys. 155, 184 (1959).
8. E. Adirovich, Z. Phys. 155, 195 (1959).
9. P. Winkel and B. Verkerk, Philips Res. Rept. 13, No. 6, 501 (1958).
10. A. W. Smith, Canad. J. Phys. No. 5, 591 (1959).
11. D. Vermilyea, J. Appl. Phys. 27, No. 8, 963 (1956).
12. P. F. Schmidt, J. Appl. Phys. 28, 278 (1957).
13. P. F. Schmidt, F. Huker, and R. F. Schwarz, J. Phys. Chem. Solids 15, Nos. 3-4, 270 (1960).
14. L. Young, Trans. Faraday Soc. 55, 632 (1959).
15. A. Charlesby, Acta Metal. 1, 340 (1953).
16. H. Gerischer, Z. Electrochem. 54, 366 (1950).
17. K. Vetter, Z. Electrochem. 55, 121 (1951).
18. J. Jordan and R. A. Javick, Paper presented at the Twelfth C.I.T.C.E. Conference, Brussels, April, 1961 [Russian translation].

THE BIRADICAL PARADOX

A. I. Burshtein and Yu. I. Naberukhin

Institute of Chemical Kinetics and Combustion,
Siberian Section of the Academy of Sciences of the USSR
(Presented by Academician V. N. Kondrat'ev, May 23, 1961)
Translated from Doklady Akademii Nauk SSSR, Vol. 140, No. 5,
pp. 1106-1109, October, 1961
Original article submitted May 18, 1961

1. In recent years several papers have appeared [1-3] dealing with the electron paramagnetic resonance of biradicals consisting of two triphenylmethyl radicals linked through an oxygen, methylene, or phenylene bridge. Such systems can be represented by a model in which we have two potential wells containing one electron each (Fig. 1).

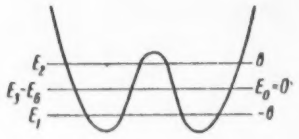

Fig. 1.

Analysis of the hyperfine structure of the spectrum indicates that each electron interacts only with the protons of its "own" well. This indicates that the frequency interaction $\delta/\hbar = 10^7\ \text{sec}^{-1}$ greatly exceeds the frequencies for the electronic transitions between the two wells, $\Delta\nu$ [4], resulting from the singlet-triplet splitting in the biradical $\Delta E = \hbar\Delta\nu$. On the other hand, the singlet-triplet splitting calculated theoretically by McConnell [5] is about $10^{11}\ \text{sec}^{-1}$, and obviously conflicts with the experimental data. This disagreement has therefore been referred to by McConnell as the biradical paradox [6].

As it is, McConnell based his calculations on the assumption that the ΔE for the singlet-triplet splitting depends only on the frequency of the electron transfer through the bridge, $b/\hbar$. Yet transitions of the frequency occur only in one-electron systems, and experiments have shown that if the bridge is short (one or two CH_2 groups), the frequency is indeed greater than $\delta/\hbar$ [7]. Where the biradicals differ greatly from these systems is in the fact that the true frequency of electronic transitions between the two wells $\Delta\nu$ (spin exchange) is quite distinct from the frequency for the electron transfer through a bridge $b/\hbar$, due to the electrostatic repulsion between the two electrons. If this electronic interaction is taken into consideration, as we have done in our present work, the spin exchange frequency $\Delta\nu$ turns out to be much smaller than $b/\hbar$ and even smaller than $\delta/\hbar$. This naturally also resolves the biradical paradox and renders the special hypotheses put forth to explain it superfluous [6,8].

2. The Hamiltonian for our system has the form $\hat{H}_A^{(1)} + \hat{H}_B^{(2)} + V_1 + V_2 + \frac{e^2}{r_{12}}$, where V_i is an operator giving the probability for the transfer of the ith electron from one well to another. If we neglect the last term, the orbital functions for an isolated electron $\psi_1 = \frac{1}{\sqrt{2}}(\varphi_A + \varphi_B)$, $\psi_2 = \frac{1}{\sqrt{2}}(\varphi_A - \varphi_B)$ can be expressed as a linear combination of the eigenfunctions φ_A and φ_B of the operators $\hat{H}_A$ and $\hat{H}_B$, which represent the ground state motion of the electrons in the left and right wells, respectively. Since the two wells are quite far apart, we can assume that the two functions do not overlap. The splitting of states ψ_1 and ψ_2 will be $b/2 = |\langle\varphi_A^1|V_1|\varphi_B^1\rangle| = |\langle\varphi_A^2|V_2|\varphi_B^2\rangle|$ (the superscript represents the electrons).

All the possible states of the investigated system can be represented by six two-electron wave functions,

$$\Phi_1 = \psi_2^1\psi_1^2\chi(0, 0),$$

$$\Phi_2 = \psi_2^1\psi_2^2\chi(0, 0),$$

$$\Phi_{\left\{\begin{smallmatrix}3\\4\\5\end{smallmatrix}\right\}} = \frac{1}{\sqrt{2}}(\psi_1^1\psi_2^2 - \psi_1^2\psi_2^1)\begin{Bmatrix}\chi(1, 1)\\ \chi(1, 0)\\ \chi(1, -1)\end{Bmatrix}, \qquad (1)$$

(more)

$$\Phi_6 = \frac{1}{\sqrt{2}}(\psi_1^1\psi_2^2 + \psi_1^2\psi_2^1)\,\chi\,(0,\,0),$$

which exhaust all the combinations of ψ_1 and ψ_2 and of spin functions $\chi(s, s_z)$ (where $\underline{s}$ is the total spin of the two electrons) allowed by the Pauli exclusion principle. If we ignore the electrostatic repulsion between the two electrons, functions (1) will give us the stationary solutions of the Schroedinger equation and the spectrum will consist of three equidistant terms with the middle one having fourfold degeneracy (Fig. 1). The splitting of the $\underline{b}$ terms would, in this case, depend entirely on the electron transfer through the bridge.

If a coulombic interaction is included in representation (1), the energy matrix assumes the form

$$H_{im} = \begin{pmatrix} \frac{Q+J}{2} - b & \frac{Q-J}{2} & 0 & 0 \\ \frac{Q-J}{2} & \frac{Q+J}{2} + b & 0 & 0 \\ 0 & 0 & \{J\} & 0 \\ 0 & 0 & 0 & Q \end{pmatrix}.$$

where Q and J are the coulomb integrals

$$Q = \int \frac{e^2}{r_{12}}(\varphi_A^1\varphi_A^2)^2\,d\tau, \quad J = \int \frac{e^2}{r_{12}}(\varphi_A^1\varphi_B^2)\,d\tau, \quad Q > J,$$

while the exchange integrals are assumed to be zero due to the absence of direct overlap between function φ_A and φ_B. After the elimination of the off-diagonal terms, the matrix yields the following energy levels:

$$E_{1,2} = \frac{Q+J}{2} \mp \frac{Q-J}{2}\sqrt{1 + \frac{4b^2}{(Q-J)^2}},$$
$$E_3 = E_4 = E_5 = J,$$
$$E_6 = Q.$$

For a rough approximation we can use the value of integral Q obtained for the 1s functions of hydrogen, Q = $= 2.7 \cdot 10^{16}$ sec^{-1}. If we combine this with the value of $\underline{b}$ calculated by McConnell (10^{10}-10^{12} sec^{-1}), we find that $\frac{b}{Q-J} \ll 1$. Hence,

$$E_1 \approx J - \frac{b^2}{Q-J}, \quad E_2 = Q + \frac{b^2}{Q-J},$$

the proper combination of functions for the individual wells will yield the correct stationary functions (see below), representing this limiting case,

$$\Psi_1 = \frac{1}{\sqrt{2}}(\varphi_A^1\varphi_B^2 + \varphi_B^1\varphi_A^2)\,\chi\,(0,\,0),$$
$$\Psi_2 = \frac{1}{\sqrt{2}}(\varphi_A^1\varphi_A^2 + \varphi_B^1\varphi_B^2)\,\chi\,(0,\,0).$$

$$\Psi_{\begin{Bmatrix}3\\4\\5\end{Bmatrix}} = \frac{1}{\sqrt{2}}(\varphi_B^1\varphi_A^2 - \varphi_A^1\varphi_B^2)\begin{Bmatrix}\chi\,(1,\,1)\\ \chi\,(s,\,0)\\ \chi\,(1,\,-1)\end{Bmatrix}, \qquad (2)$$

$$\Psi_6 = \frac{1}{\sqrt{2}}(\varphi_A^1\varphi_A^2 - \varphi_B^1\varphi_B^2)\,\chi\,(0,\,0).$$

Thus the electrostatic interaction between the electrons alters considerably the nature of the energy spectrum of the biradical (Fig. 2).

The great difference between the spectra shown in Figs. 1 and 2 and between the corresponding wave functions can be readily explained. Functions (1) and the corresponding energy spectrum were obtained within the framework of a one-electron approximation which, in considering the limitations imposed by the Pauli exclusion principle, neglects all the other interactions between the electrons of which the most important one is that represented by e^2/r_{12}. This approximation, on which the molecular orbital treatment in quantum chemistry and the one-electron model of a solid are based, is only valid when b >> Q, J. It is evident that as $\underline{b}$ decreases when the interacting centers become

more separated, the approximation will not be as good since J declines much more slowly than does b, while Q, which represents the repulsion between electrons in the same well, remains unchanged. When Q >> b we have a true two-electron problem, and the coulomb interaction has to be considered as a first-order effect. Figure 2 shows that it is responsible for the main splitting between polar and nonpolar states Q − J, whereas transitions between wells yield only a small splitting of the symmetric and antisymmetric states $[b^2/(Q-J)]$. Consequently, the singlet-triplet splitting in the examined biradicals $\Delta E = b^2/(Q-J) \approx 10^6$ sec^{-1} (if $b \approx 10^{11}$ sec^{-1}), which is not only much smaller than b, but also smaller than the hyperfine interaction constant δ.

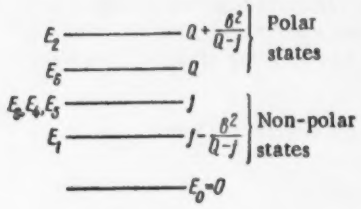

Fig. 2.

3. We will now introduce the hyperfine interaction between the electron spins and the spins of nuclei I_A and I_B. This will introduce additional terms

$$H_{14} = -\tfrac{1}{2}\delta\,(I_A - I_B), \quad H_{33} = -H_{55} = \tfrac{1}{2}\delta\,(I_A + I_B).$$

into the energy matrix constructed from functions in representation (2). Thus, if $I_A \neq I_B$, the hyperfine interaction will mix the ground state level Ψ_1 with the triplet level Ψ_4, which has a zero spin projection.

The transition probabilities can be evaluated in the same way as was done in [4]. Considering also the fact that in the presence of a magnetic field H levels with a nonzero projection of the total spin, E_3 and E_6, will be raised and lowered, respectively, by the amount $\hbar\gamma H = \hbar\omega_0$ (γ is the gyromagnetic ratio), it is easy to derive the EPR spectrum:

	Line frequency	Intensity
$I_A = I_B$,	$\omega_0 + \frac{1}{2}\delta\,(I_A + I_B)$	I_0
$I_A \neq I_B$	$\omega_0 \pm (\sqrt{B^2 + t^2} + B) + \frac{\delta}{2}(I_A + I_B)$	$\frac{I_0}{4}\left(1 - \frac{B}{\sqrt{B^2 + t^2}}\right)$
	$\omega_0 \pm (\sqrt{B^2 + t^2} - B) - \frac{\delta}{2}(I_A + I_B)$	$\frac{I_0}{4}\left(1 + \frac{B}{\sqrt{B^2 + t^2}}\right)$

$$t = \frac{\delta}{2}(I_A - I_B), \quad B = \frac{1}{2}\frac{b^2}{Q-J}.$$

Suppose each well contains one proton. Then, if $\frac{b^2}{Q-J} \ll \delta$, the spectrum will consist of two triplets with a splitting of $\frac{b^2}{Q-J}$ separated from each other by the amount δ. Since the triplet splitting is very small, it will not be experimentally detectable, and we will only observe the same doublet with a splitting δ as one gets from an isolated well containing one electron. As b increases, the splitting of each triplet also increases until at $\frac{b^2}{Q-J} \gg \delta$ the spectrum will consist of a single triplet with a total splitting of δ, as has been found in [3].

LITERATURE CITED

1. H. S. Jarrett, G. J. Sloan, and W. R. Vaughan, J. Chem. Phys. 25, 697 (1956).
2. D. C. Reitz and S. I. Weissman, J. Chem. Phys. 27, 968 (1957).
3. D. C. Reitz and S. I. Weissman, J. Chem. Phys. 33, 700 (1960).
4. A. I. Burshtein, Doklady Akad. Nauk SSSR 135, 886 (1960).
5. H. M. McConnell, J. Chem. Phys. 33, 115 (1960).
6. H. M. McConnell, J. Chem. Phys. 33, 1868 (1960).
7. V. V. Voevodskii, S. P. Solodovnikov, and V. M. Chibrikin, Doklady Akad. Nauk SSSR 129, 1082 (1959).
8. H. M. McConnell, Bull. Am. Phys. Soc. Ser. II, 4, 415 (1959).

SLOWING DOWN OF SURFACE REACTIONS ON CATALYSTS AND THE MOBILITY OF ADSORBED MOLECULES

V. É. Vasserberg, Academician A. A. Balandin,

and T. V. Georgievskaya

N. D. Zelinskii Institute of Organic Chemistry, Academy of Sciences of the USSR
Translated from Doklady Akademii Nauk SSSR, Vol. 140, No. 5,
pp. 1110-1113, October, 1961
Original article submitted May 19, 1961

From a study of the mechanism of the elementary stages of the dehydration reaction of the lower aliphatic alcohols on Al_2O_3 catalysts [1-3] we have shown that at the moment it is reacting with an active center of a catalyst, a molecule of a reacting substance is not an isolated structure which is incapable of reacting with neighboring molecules. Thus, [1] described a combined dehydration of isopropyl and ethyl alcohols in an adsorbed layer, and the proposal was made that radicallike intermediate forms are formed on the surface of the catalyst under conditions of catalytic dehydration. This proposal was then confirmed experimentally in [4] for the dehydration of iso-C_3H_7OH on magnesium sulfate. The dehydration of binary mixtures of different alcohols and esters in an adsorbed layer on the surface of a catalyst was considered in [3], and it was shown that in mixtures the decomposition rate of the individual components is, as a rule, less than for the individual substances at the same filling density.

In the present work a study was made of the dehydration genetics of iso-C_3H_7OH and trimethylcarbinol in the presence of various substances contained in an adsorbed layer on the catalyst surface, but not capable (in general or under the present conditions) of dehydration. The catalysts used were Al_2O_3, precipitated by bromine from aluminate solution, $Al_2O_3 + Fe_2O_3$, in Al_2O_3 precipitated by CO_2 from aluminate solution (catalysts Nos. 5, 6, 7 of [3]), as well as W_2O_5.*

For the properties of Al_2O_3 catalysts and the investigational technique see [3]. The W_2O_3 catalyst had a specific surface (from the nitrogen adsorption isotherm) of 14 M^2/g, the activation energy of dehydration in the adsorbed layer was 17.8 and 31.2 kilo-cal, and the value of t_{20}^0** = 76 and 187° for isopropyl and ethyl alcohols, respectively.

To study the effect of adsorbed extraneous substances on the reaction rate on oxidized aluminum catalysts, the standard reaction used was the dehydration of iso-C_3H_7OH, adsorbed on the catalyst in the amount 0.3 cm^3 (Stand. Temp. and Tres.)/ g which, for the various samples, corresponded with the density of filling of 2-4% of the monolayer. The effect of the following substances was studied (the figures in parentheses designate the catalyst numbers): acetone (5), dioxane (5,7), acetonitrile (5), acetoacetic ester (5), nitrous oxide (5,6,7). On W_2O_5 a study was made of the dehydration in adsorbed layers of C_2H_5OH, iso-C_3H_7OH, $(CH_3)_3COH$, and the system C_2H_5OH + iso-C_3H_7OH, $(CH_3)_3COH + CH_3OH$, $(CH_3)_3COH + C_2H_5OH$, $(CH_3)_3COH$ + iso-C_3H_7OH, $(CH_3)_3COH + H_2O$.

It turned out that acetone, itself completely undecomposable on the catalyst used and, as is well known, incapable of combining with iso-C_3H_7OH under ordinary conditions, shows a strong retarding effect on the dehydration of isopropyl alcohol in the adsorbed layer (Fig. 1, 3). As the quantity of adsorbed acetone is reduced, this retarding action is weakened, but it remains clearly evident even at a filling density of the order of 4-6% of the monolayer (Fig. 2, curves 1-4). Dioxane even at fillings of the order of 2-4% of the monolayer practically completely inhibits the dehydration of iso-C_3H_7OH both on catalyst No. 5 (see Fig. 1, curve 6) and on catalyst No. 7.

Acetonitrile shows a somewhat weaker retarding effect (see Fig. 1, curve 4), so that to get a comparable effect it is necessary to use a relatively larger filling density [4-5 cm^3 (S.T.P.)/ g].

---

*Obtained from A. A. Tolstopyatova, for which the authors express their gratitude to her.

**t_{20}^0 is the temperature at which the half period of decomposition $T_{0.5}$ is equal to 20 min.

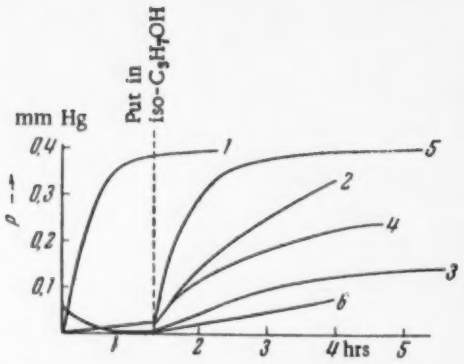

Fig. 1. Retardation of decomposition of iso-C_3H_7OH on catalyst No. 5 and adsorbed layer at 120°: 1) pure iso-C_3H_7OH; 2) iso-C_3H_7OH + acetoacedic ester [1.2 cm^3 (S.T.P.)/ g]; 3) iso-C_3H_7OH + CH_3COCH_3 [0.3 cm^3(S.T.P.)/ g]; 4) iso-C_3H_7OH + acetonitrile [5.3 cm^3(S.T.P.)/ g]; 5) iso-C_3H_7OH + nitrous oxide; 6) iso-C_3H_7OH + dioxane [0.3 cm^3(S.T.P.)/ g].

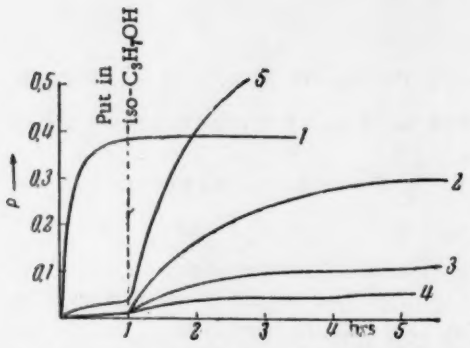

Fig. 2. Effect of amount of acetone on decomposition rate of iso-CH_3H_7OH on catalyst No. 5 in an adsorbed layer at 130°: 1) pure iso-C_3H_7OH; 2) the same + 3.0 cm^3(S.T.P.)/ g acetone; 3) the same + 0.6 cm^3(S.T.P.)/ g acetone; 4) the same + 5.3 cm^3 (S.T.P.)/ g acetone; 5) iso-C_3H_7OH + C_2H_5OH [5.3 cm^3 (S.T.P.)/ g] – combined dehydration.

Nitrous oxide showed no appreciable effect on the reaction, but this, possibly, is to be explained by the fact that the adsorption of this substance on the catalyst is relatively small, and with the same quantities put in as for the other substances investigated the filling density is small.

Experiments on the dehydration of ethyl and isopropyl alcohols in the adsorbed layer on W_2O_3 have shown that on this catalyst the reaction goes at considerably lower temperatures than on Al_2O_3. Thus, at a filling density of the order of 20-30% of the monolayer, the half-decomposition period $T_{0.5}$ of iso-C_3H_7OH at 120° is less than one minute, and at 100° it is 6-7 min. For C_2H_5OH at 150° practically no reaction was observed, and at 170° and 190°, $\tau_{0.5}$ is equal, respectively, to 70 and 18 min. For the system iso-C_3H_7OH + C_2H_5OH, the filling density for iso-C_3H_7OH was the same, and the quantity of C_2H_5OH put in was equal to 5.3 cm^3(S.T.P.)/ g, which, for such a small volume of specific surface, should cause a degree of covering which is close to a monolayer. Under these conditions it was noted above all that even at 100-120° pure C_2H_5OH shows an unexpectedly large absolute decomposition rate,which shows up from the increase in ethylene pressure in the gaseous phase, although the extent of decomposition (because of the large quantities of alcohol originally present) remains insignificant.

Trimethylcarbinol on W_2O_5 at 30-80° (and higher) forms no gaseous products. The isobutylene formed is obviously completely polymerized on the catalyst. The fact that, in this case, none of the original alcohol remained unchanged on the catalyst was proved by heating the catalyst to 300° after the adsorption. Here the alcohol should be completely dehydrated with evolution of butylene, which was not observed (Fig. 3).

However, if there are considerable quantities of previously adsorbed C_2H_5OH, iso-C_3H_7OH, or H_2O (but not N-pentane) in the adsorbed layer on the catalyst, even at temperatures of 20-40° trimethylcarbinol undergoes the normal dehydration reaction with formation of isobutylene, desorbed from the surface of the catalyst into the gas phase (Fig. 2). Thus, the presence of hydroxyl-containing substances in the adsorbed layer practically completely inhibits the polymerization reaction. A similar effect of C_2H_5OH on the decomposition of iso-C_3H_7OH on Al_2O_3 + Fe_2O_3 catalyst was noted in [3].

The results of the present work, as well as [2] and [3], show that dehydration of alcohols on oxide catalysts in an adsorbed layer at low temperatures is no simple monomolecular reaction with one-stage evolution of water, but has a more complicated mechanism. The facts which we have found relative to the mutual influence of the molecules in the adsorbed layer may be explained on the basis of two different assumptions: 1) change in the electronic properties of the catalyst as a result of adsorption of the second component of the mixture, and 2) direct interaction of the adsorbed molecules or active components on the catalyst surface. The first of these two possibilities is considerably less probable, since a change in electronic properties of this sort is important only in semiconductors, while

at the temperatures used in our experiments Al_2O_3 as a dielectric. In addition, this assumption fails to explain the causes of the different, and sometimes even opposite, effect of additives of the same type, such as alcohols, esters, etc.

On the other hand, from many formal signs, from the accelerating or retarding effect of extraneous substances, from the dependence of this effect on the reaction temperature and the concentration of additives, from the fact of a critical concentration of initial substances required to reach a definite reaction rate (as, for example, in the case of the dehydration of C_2H_5OH on W_2O_5 at 100-120°), etc., these processes suggest chain reactions involving free radicals in the gaseous phase. If the presence of flat chains cannot yet be considered established, the presence of radicallike surface forms under our experimental conditions has been proved experimentally from the presence of the para-orthotransformation of hydrogen at the instant the dehydration reaction takes place [4]. On the other hand, this agrees with the fact of hydrocarbon radical exchange under dehydration conditions, established by us using radiochemical means [5]. The ideas presented make the second explanation considerably more probable, i.e., the reaction proceeds by direct interaction of the adsorbed molecules to form intermediate transitional complexes.

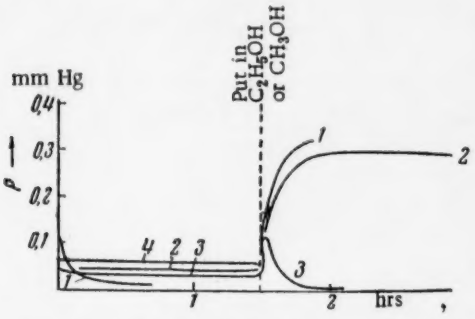

Fig. 3. Decomposition of trimethylcarbinol on W_2O_5 at 40°: 1) pure trimethylcarbinol; 2) trimethylcarbinol + C_2H_5OH (large filling density); 3) the same + C_2H_5OH (small filling density); 4) the same + CH_3OH (large filling density).

The question of the nature of these complexes has so far been unexplained, but attention is called to the fact that all the additives used (except N-pentane, which shows no retarding effect) contain atoms which have unshared electron pairs which appear, in particular, in the considerable degree of polarity shown by the molecules in question. The absence of dipole moment in dioxane is only an apparent exception, since it is explained by internal compensation of the charges of two oxygen atoms with unshared electron pairs. It is a well-known fact that compounds of this sort have a considerable affinity for addition reactions and can, as in the case of NO_2, serve as free radical traps. Actually they all retard the dehydration in the adsorbed layer. The absence of any effect from nitrous oxide is due apparently to the fact that it is very weakly adsorbed on Al_2O_3.

This kind of retarding action from neighboring adsorbed molecules can, apparently, along with simple adsorptive replacement, caused by difference in relative adsorption coefficients, be the cause of the effect observed by many authors (see for example [6, 7]) of the nature of the solvent on the reaction rate of catalytic hydration.

Along with the collective dehydration mechanism considered to take place in the adsorbed layer, it must not be assumed that there is no possibility of a simple one-stage mechanism involving rather fast desorption of the reaction products. At the low temperatures and rather long lifetime of the intermediate surface forms which occurred in our experiments, a greater role ought to be played by the collective mechanism. At the high temperatures characteristic of dehydration in the usual spray catchers and atmospheric pressure conditions may be created which are more favorable to the one-step mechanism. This difference in reaction mechanism may be the explanation of what was observed in [1], namely, the difference between the activation energy of the dehydration reaction in a monolayer and under ordinary conditions.

Finally, the facts which we have observed, in our opinion, allow us to draw one more conclusion. Both in the interaction between the molecules of two different substances in the adsorbed layer and in the polymerization of an olefin, formed from alcohol, it is necessary for the molecules, which are originally located far from one another because of the small degree of filling at the start (up to 6-8% of the monolayer), to get close enough together to allow chemical forces to act. The question of whether it is possible to have diffusion on the surface of the catalyst, which is of fundamental importance for understanding of the mechanism of catalytic processes, has often been discussed in the literature (see, for example, the review [8]), but it has been solved differently by different authors. The judgments expressed on this question by different authors are based either on indirect experiments or on general thermodynamic concepts relating to the possible nature of the adsorbed layer. Our experimental data show conclusively that it is possible to have surface diffusion on Al_2O_3 and W_2O_5 catalysts even with relatively tightly bound chemisorbed molecules at temperatures of 60-150°.

LITERATURE CITED

1. V. É. Vasserberg and A. A. Balandin, Collection: Problems of Kinetics and Catalysis [in Russian] (AN SSSR Press, 1960) Vol. 10, p. 356.
2. V. É. Vasserberg, A. A. Balandin, and T. V. Georgievskaya, Doklady Akad. Nauk SSSR 134, 371 (1960).
3. V. É. Vasserberg, A. A. Balandin, and T. V. Georgievskaya, Doklady Akad. Nauk SSSR 110, No. 4 (1961).
4. V. É. Vasserberg, A. A. Balandin, and I. R. Davydova, Doklady Akad. Nauk SSSR 136, 377 (1961).
5. V. É. Vasserberg, A. A. Balandin, and G. I. Levi, Kinetika i Kataliz 2, No. 2 (1961).
6. D. V. Sokol'skii (Editor), Papers on Catalysis [in Russian], Collection of Transactions of the Institute of Chemistry of the Academy of Sciences, KazakSSR 2 (1959).
7. B. D. Polkovnikov, Candidates Dissertation [in Russian] (Institute of Organic Chemistry, AN SSSR, 1957); L. Kh. Freidlin, E. F. Litvin, and Yu. Yu. Kaup, Doklady Akad. Nauk SSSR 139, No. 6 (1961).
8. D. P. Timofeev, Usp. khimii 29, 404 (1960).

All abbreviations of periodicals in the above bibliography are letter-by-letter transliterations of the abbreviations as given in the original Russian journal. *Some or all of this periodical literature may well be available in English translation.* A complete list of the cover-to-cover English translations appears at the back of this issue.

THEORY OF THE AUTOOSCILLATIONS OF THE ELECTROCHEMICAL SYSTEMS FREE OF PASSIVATION AND WITH A FALLING CHARACTERISTIC

A. Ya. Gokhshtein

Institute of Electrochemistry, Academy of Sciences of the USSR
(Presented by Academician A. N. Frumkin, April 5, 1961)
Translated from Doklady Akademii Nauk SSSR, Vol. 140, No. 5,
pp. 1114-1117, October, 1961
Original article submitted April 4, 1961

As has been reported in [1], A. N. Frumkin and the author observed experimentally, and investigated the periodic undamped autooscillations which occur during the reduction of $S_2O_8^{2-}$ on dropping and resting mercury electrodes. Subsequently, these oscillations have been observed by A. N. Frumkin, O. A. Petrii, and N. V. Nikolaeva-Fedorovich [2] with the anions $PtCl_4^{2-}$, $S_2O_8^{2-}$, and $Fe(CN)_6^{3-}$, and by the author with $PtCl_6^{2-}$. However, no theory of these oscillations has been given. The majority of the periodic phenomenon of electrochemistry have to do with the appearance of a passivating film on the electrode, or the formation of a new phase. A substantial contribution to the theory of these phenomenon was made by the papers of U. F. Frank [3,4] and Yu. A. Chizmadzhev [5]. In the case under consideration there are no surface formations of this sort. A theory of the phenomenon observed is given below. It proceeds on two assumptions: a) the characteristic $p(\varphi)$ of the system has a falling portion; b) transfer of matter from the solution to the electrode surface is a slow process. With diffusional transfer, the dropping concentration from its value $\overline{C}$ in the mass of the solution to value of C on the surface occurs in a layer of finite thickness l. The conditions of formation of the layer are determined by the geometry of the epi-electrode space or by different means of stirring (in the case of a drop electrode, tangential oscillations of its surface are important). The current density i and the electrode potential φ during irreversible electroreduction of the anions are connected to the relationship [6], $i = Cp(\varphi)$. Here, $p(\varphi)$ is a single-valued, positive, differentiable function. Excess electrolyte is present in the solution in such an amount that a falling portion is maintained on the polarization characteristic.

For the circuit consisting of the electrolytic cell with polarizing electrode surface S and series resistance R, at the end of which is applied the voltage v:

$$a)\ ir + \varphi = v; \quad b)\ i = Cp(\varphi); \quad c)\ Cp(\varphi)r + \varphi = v, \tag{1}$$

where r = RS. The roots of Eq. (1c) determine the possible states of the system. Several roots of Eq. (1c) can, in general, correspond with an instantaneously fixed value of the epi-electrode concentration $C = C_k$ = const and, consequently, there are several possible states of the system. Nonstationary states may occur among the possible states of the system, i.e., the states which satisfy Eq. (1c) only at a given moment of time, along with stationary states, which satisfy Eq. (1c) for all values of time. We shall determine the number of the latter for $C = C_k$. In the stationary state, the concentration of the material required in the electrode reaction is distributed linearly in the diffusional layer. Here the current satisfies the condition

$$i = G(\overline{C} - C), \quad G = nFD/l, \tag{2}$$

where D is the diffusion coefficient, nF is the quantity of electricity per mol. of substance. Thus, of the number of possible states of the system corresponding with $C = C_k$ there cannot be more than one stationary state. Further, it follows from a comparison of Eqs. (1) and (2) that for fixed values of r and v stationary states may be realized only for some values of C. We shall find these states. The functional relationship between i_0 (the index 0 indicates a stationary state) and φ is found by eliminating C from Eqs. (1b) and (2):

$$i_0(\varphi) = G\overline{C}/[1 + G/p(\varphi)]. \tag{3}$$

Since i_0 must simultaneously satisfy Eq. (1a), the possible stationary states (i_0, φ_0) are given by the roots of

$$i_0(\varphi)r + \varphi = v, \tag{4}$$

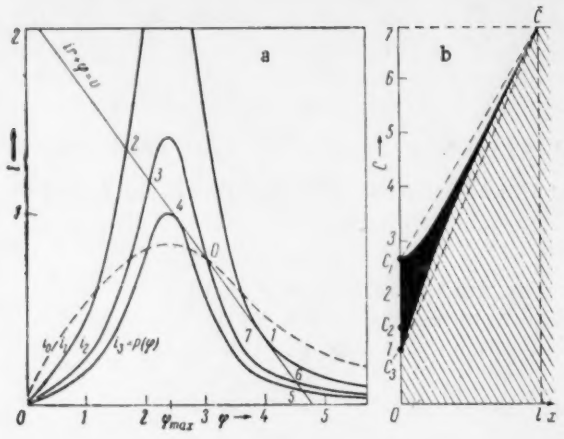

which is one of the forms of combining Eqs. (1a), (1b), and (2). If Eq. (4) has one root, the stationary state of the system is unique. The curve of $i_0(\varphi)$ is usually taken experimentally (polarization curve with a hump), and serves here as a starting point for a discussion of the concrete system. This is a practical method of determining the possible stationary states. From Eq. (4) there may be found as the points of intersection of the polarization curve with the straight line $i = (v - \varphi)/r$. If (i_0, φ_0) lies on the following branch of $i_0(\varphi)$, it also lies on a following branch $p(\varphi)$ [the hump on $i_0(\varphi)$ has a weakly pronounced maximum at the same value of φ_{max} as $p(\varphi)$]. It follows from Eq. (3) that $|i_0'(\varphi)| < |C_0(\varphi)p'(\varphi)|$. Since $p(\varphi) > 0$, it also follows from Eq. (3) that $i_0(\varphi)$ is bounded. We shall now consider the case of a unique stationary state. Omitting, for brevity of presentation, the rigid solution of the problem, which was obtained from a study of the integral diffusion equations for an arbitrary function $p(\varphi)$, we adduce the following conditions: the unique stationary state is unstable if the inequality $C_0p'(\varphi_0) < -(1/r)$ is fulfilled.

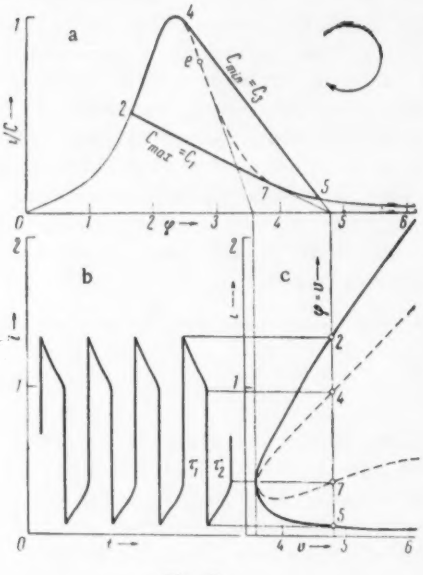

The meaning of this condition, as well as the nature of the oscillational process, may be seen from Fig. 1, which gives a concrete numerical example. The meaning of the arbitrary units of C, $\underline{i}$, and φ is curved from the figure. The value of $p(\varphi)$ was fixed, with $G = 0.137$ and $\overline{C} = 7$. Then $i_0(\varphi)$ was determined from Eq.(3). The straight line (1a) for fixed $\underline{r}$ and $\underline{v}$ is tangent above and below to curves i_1 and i_3. They correspond with the critical concentration $C_1 = C_{max} = 2.67$, $C_3 = C_{min} = 1.00$. The point of intersection of the straight line (1a) with the curve $i_0(\varphi)$ (dotted) gives the stationary state ($C_2 = C_0 = 1.41$). There are no other points of intersection; therefore, the stationary state 0 is unique. The inequality given above means: 1) at the point 0 is located on the falling part of the curve $i_2(\varphi) = C_0p(\varphi)$; 2) that at the point 0, the curve $i_2(\varphi)$ is steeper than the straight line (1a). This location of the curves $i = Cp(\varphi)$ relative to the straight line $ir + \varphi = v$ is responsible for the fact that if C is increased, φ increases and $\underline{i}$ decreases. The range of potentials φ, in which this relative distribution of curves is maintained, is bounded by the potentials of the points 4 and 7, where the points of intersection become points of tangency. This region represents only a part of the potentials on the falling branch of the function $p(\varphi)$ and, as is shown below, marks out the part of this function which is not working during the time of oscillation. For oscillations to occur in the system, the point, which gives the state of the system, must get out of the "nonworking" region. It may be shown that fulfilling the instability condition given above ensures getting the system outside the limits of the "nonworking" region at the right time. The oscillations occur in the following way. Since the stationary state 0 is unstable, and the system cannot exist for a long

time in a "nonworking" part, it passes over during some period of time into state 1 on i_1 (or 4 on i_3). The consumption of matter (ordinate of point 1) is less than the supply from the solution (the stationary current of matter corresponding with concentration C_1, as given by the point of intersection of $i_1(\varphi)$ with $i_0(\varphi)$, which is located above point 1: for state 1 on curve i_1, $(i_1)_1 < G\overline{C} - C_1]$. The current through the boundary $x = l$, corresponding with concentration C_1, is higher than the stationary current, and thus all the more exceeds the consumption of matter at the boundary $x = 0$. Therefore, C, and together with it the characteristic $i = Cp(\varphi)$, increases up to the point where it ceases to be tangent at point 1, after which the system goes over into state 2 on the same characteristic. Here, on the other hand, the consumption of matter in the reaction exceeds the supply, and C gradually decreases from C to C_3, and the state of the system is gradually displaced along the straight line from point 2 to point 4. Here the consumption of matter is still large $[(i_3)_4 > G(\overline{C} - C_3)$, $i_3(\varphi)$ and $i_0(\varphi)$ intersect below the point 4], the characteristic $i = Cp(\varphi)$ continues to drop, and the system jumps over into point 5. The consumption drops sharply, C increases, and the system gradually shifts from 5 to 7, after which the cycle (1, 2 – 3 – 4, 5 – 6 – 7) repeats itself. Figure (1b) gives a schematic representation of the concentration distribution in the diffusional layer as the function of distance x from the electrode surface. The dotted lines indicate the stationary distributions, which would correspond with the critical epi-electrode concentration C_1 and C_3. The blacked-in area is equal to the maximum change Q in the quantity of matter in the diffusional layer during the oscillation, $Q < \frac{1}{2}l\,(C_1 - C_3)$. The concentration distributions oscillate, and in the process of change may depart somewhat from the limits of this figure.

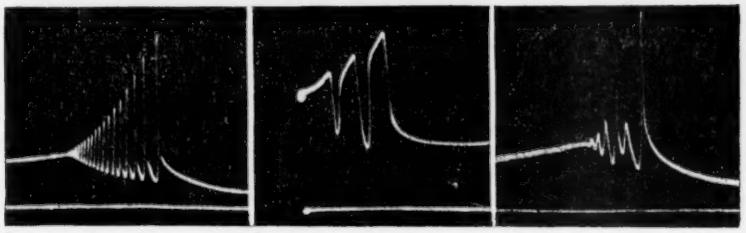

a b c

Fig. 3. Curves of $i - (v,t)$ for a voltage decreasing (from right to left) with time: a) $5 \cdot 10^{-3}$M $K_2S_2O_8$ + 0.05% gelatin, mercury drop electrode, S = = 0.18 mm², second electrode normal calomel, added resistance RM = 0, 1.3 v/sec; b) 10^{-2}M $K_2S_2O_8$ + 10^{-3}M $CdSO_4$ + 0.05% gelatin, S = 0.65 mm², RM = 10,000 ohms, remaining conditions the same as in a; c) 10^{-2}M $(NH_4)S_2O_8$, interference of oscillations occurring differently on different parts of the drop, periodic extinction of oscillations.

In Fig. 2 the cycle (1, 2 – 3 – 4, 5 – 6 – 7) is shown in the different set of coordinates. In Fig. 2a the state of the system is described by the point of intersection of the fixed curve $i/C = p(\varphi)$ with the straight line $i/C = = (v - \varphi)/rC$, the slope of which changes in the process of oscillation with the preelectrode concentration C. Here, the state of the system is moved around the closed circuit in the direction shown by the arrow. The "nonworking" part of the curve $p(\varphi)$ is shown dotted. As v is reduced, the cycle pulls itself up into the point e, and the oscillations stop. The cycle has no breaks at the points 4 and 7, and they accordingly correspond with smooth curves in the $i - t$ plot. The dependence of the break-point currents (points 4, 7) and the amplitude of the oscillations on v is shown in Fig. 2c. The mean currents in the upper part (I_1) and the lower part (I_2) of the oscillation are given by the function $p(\varphi)$. Therefore, for small values of l it is correct to write $\tau_2/\tau_1 = (I_1 - I_0)/(I_0 - I_2)$, where I_0 is the mean oscillatory current. Increasing l and reducing $\overline{C}$ causes a reduction in I_0 and, consequently, an increase in the relative length of that phase of the oscillation in which the current is small (τ_2), as well as an increase in the period $\tau_1 + \tau_2$. If, however, Eq. (4) has several roots in some region Δv (or Δr), this region plotted to $i - v$ (or $i - r$) coordinates may, under proper conditions, correspond with a band in which there are no oscillations. This conclusion requires experimental proof.

The conditions under which the oscillation occurs are: 1)(i_0,φ_0) lies on the falling branch of the $i_0(\varphi)$ curve, i.e., $|\varphi_0| > |\varphi_{max}|$, where, for example, for $S_2O_8^{2-}$, $\varphi_{max} \approx -0.35$ volt (Normal Calomel Electrode) [7]; 2) (i_0,φ_0) is unique; this will always occur if $\max|i_0'(\varphi)| < 1/r$, which may be achieved by increasing $\overline{C}$ and l simultaneously;

3) $|C_0p'(\varphi_0)| > 1/r$. Since $|i_0'(\varphi)| < |C_0p'(\varphi)|$, then (2) and (3) may be satisfied immediately by taking v and r such that $|i_0'(\varphi_0)| < 1/r < |C_0p'(\varphi_0)|$.

The varieties of autooscillation which could be observed experimentally (Figs. 3a and 3b) are in agreement with the facts established theoretically. Their properties become intelligible [1], in particular the sometimes-occurring breakpoint of the peak of the oscillation at the polarographic maximum, since the potential of the peak lies right in the region of the polarographic maximum. The distortions on converting from $i - v$ to $i - \varphi$ [1] are caused, as a calculation of the potential distribution showed, by failure to take account, the high resistance of the solution in the shielded part of the electrode. Connecting a high resistance in series with the cell reduces the effect of the resistance of the solution. As may be seen from what has been said, the form of the electrode, and at low frequencies (less than 10 cycles per second), even the capacitance, is of no fundamental importance in producing the oscillations in question. If there is no excess electrolyte present the scheme of oscillation remains the same. According to the calculations the instability of the stationary state is not effected by adding capacitance to the system. The period of the oscillation at low frequencies exceeds the "time constant" of the system by more than ten times.

The author expresses his gratitude to Academician A. N. Frumkin, whose advice and comments formed the basis for many of the conclusions in the present paper, and expresses his obligation to Corresponding Member, AN SSSR V. G. Levich for valuable discussion.

LITERATURE CITED

1. A. Ya. Gokhshtein and A. N. Frumkin, Doklady Akad. Nauk SSSR 132, 388 (1960).
2. A. N. Frumkin, O. A. Petrii, and N. V. Nikolaeva-Fedorovich, Doklady Akad. Nauk SSSR 136, 1158 (1961).
3. U. F. Frank, Zs. phys. Chem. 3, 183 (1955).
4. U. F. Frank, Werkstoff u. Korr, H. 7, 401 (1960).
5. Yu. M. Chizmadzhev, Doklady Akad. Nauk SSSR 133, 1136 (1960).
6. A. N. Frumkin, V. S. Bagotskii, Z. A. Iofa, and B. N. Kabanov, Kinetics of the Electrode Processes [in Russian] Moscow, 1952.
7. G. M. Florianovich and A. N. Frumkin, Zhur. Fiz. Khim. 29, 1827 (1955).

All abbreviations of periodicals in the above bibliography are letter-by-letter transliterations of the abbreviations as given in the original Russian journal. *Some or all of this periodical literature may well be available in English translation.* A complete list of the cover-to-cover English translations appears at the back of this issue.

EFFECT OF THE PHYSICOCHEMICAL NATURE OF A LUBRICANT ON ITS EFFECTIVENESS IN THE PRESSURE TREATMENT OF METALS

V. M. Korbut, S. Ya. Veiler, and N. V. Petrova

Institute of Physical Chemistry, Academy of Sciences of the USSR

(Presented by Academician P. A. Rebinder, May 18, 1961)
Translated from Doklady Akademii Nauk SSSR, Vol. 140, No. 5,
pp. 1118-1120, October, 1961
Original article submitted May 13, 1961

In pressure treatment of metals without lubricants adhesion of the metal to the instrument causes, principally, deformation of the surface layers and, consequently, the deformation is nonuniform over the cross section of the metal. If a liquid surface-active lubricant is put on the metal, or a solid lubricating layer is formed with considerably less shearing stress τ than the metal being treated, the distribution of deformation over the cross section will be more uniform and all the additional deformation of the surface layer of the metal being treated, caused by friction, will be concentrated in the lubricating layer [1].

Thus, in studying the mechanism of the effective lubricants when the metal is being pressure treated, the immediate object for investigation becomes the lubricating layer at the contact zone between the metal and the instrument, how it is formed, and how it behaves during the treatment. As a measure of the lubricating action we have taken the shearing stress τ [1,2] of the lubricating layer formed on the surface of the metal (the plasticized layer in the case of liquid lubricants, or the solid coating in the case of solid lubricants). Sample lubricants were hydrocarbons, alcohols, and acids. The method of deformation was drawing of bars.

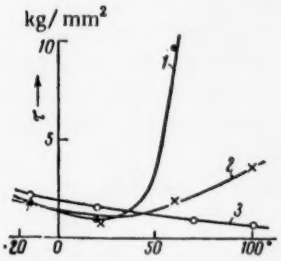

Resistance to displacement in the lubricating layer τ as a function of temperature in drawing aluminum (ϵ = 7%) with paraffin (1), cetyl alcohol (2), and stearic acid (3).

The influence on the lubricating effect of physicochemical interaction of the lubricating substance with the metallic surface may be traced, if we compare the results obtained from drawing aluminum with hydrocarbons, organic alcohols, and acids above their melting points. The alcohols, as a result of their tendency to be adsorbed on the metallic surface, are incomparably more effective lubricants, than the adsorptionally inactive hydrocarbons. While with liquid alcohols it is possible to deform the metal to a higher degree (up to 36%), with liquid hydrocarbons we are limited to 7% compression at a value of τ = 8-10 kg/mm^2. This large value of τ shows directly that the liquid hydrocarbons are squeezed out of the zone of contact between the metal and the instrument, and any subsequent shift in the deformation occurs in the surface layer of the metal itself (τ_{Al} = 9 kg/mm^2). The relatively low values of τ when liquid alcohols are used as lubricants are due to the relatively high ductility of the lubricating layer formed from adsorptional plastification of the metal surface.

Raising the temperature when using liquid alcohol as a lubricant causes some increase in the value of τ. The same temperature increase when using stearic acid causes a decrease in the value of τ, from the formation of a film of solid soap on the metal which, apparently, has a lower value of τ than the layer of metal plasticized by the adsorptively active liquid lubricant. It is well known that the alcohols do not form chemical compounds with the metal and are adsorbed reversibly. Therefore, raising the temperature hinders the effect by shifting the equilibrium to the desorption side as the temperature is increased.

A liquid flow lubricant is effective only if it can interact with the metal to form a plastic layer on the surface, which acts as a lubricant during the treatment. If the lubricant is in the solid plastic state and, consequently, has sufficiently high mechanical and structural properties, its adsorptional activity in the formation of the lubricating layer becomes a matter of secondary interest, and the principal role begins to be played by the structural and mechanical properties of the lubricant itself [1,3].

Lowering the temperature causes an increase in the shearing stress τ in the solid lubricating layer (hindering the lubricating effect) when drawing with solid lubricants with various physicochemical properties (paraffin, cetyl alcohol, and stearic acid). Corresponding changes in the mechanical properties with a change in temperature are also observed in the volume of these lubricants [4].

TABLE 1. Effect of Temperature on the Drawing Force of Aluminum with Transformer Oil. ϵ = 7%

t, °C	150	100	50	20	0	−15	−60
F, kg	293	296	273	286	190	94	60

On the other hand, lowering the temperature may be favorable, and even the decisive factor with liquid adsorptionally inactive lubricants. Thus, the lubricative efficiency of hydrocarbons increases quite considerably with freezing (the maximum possible degree of compression increases from 7 to 32%, with a sharp drop in the values of τ, as a matter of transferring the additional deformation surface out of the surface layer of the metal into the layer of solid lubricant). Lowering the temperature shows the same effect on the lubricating properties of a commercial product, transformer oil (Table 1).

The figure shows the over-all picture of the effect of temperatures from −15 to +100° on the properties of the lubricating layer during aluminum drawing with three sample lubricants: paraffin, cetyl alcohol, and stearic acid. Up to the softening temperature the nature of the curves for the three lubricants is the same, since, in the solvent state, these substances have approximately equal shearing resistance, while the difference in their adsorptional activity cannot show up as a result of hardening. Raising the temperature to the melting point causes a sharp increase in the resistance to displacement (drop in lubricating effect) in the case of surface-inactive paraffin. Liquid alcohol and acid continue to be effective, but on account of another mechanism than in the case of solid lubricants, in particular on account of adsorptive modification of the metal surface, i.e., the creation of a plastic lubricating layer in the metal itself. The divergence between the curves for cetyl alcohol and stearic acid with further increase in temperature has to do with chemical fixation of the acid molecules, while the alcohol molecules are partially desorbed.

TABLE 2. Resistance to displacement in the Lubricating Layer (τ, kg/mm^2) as a Function of the Degree of Deformation (ϵ, %) in Drawing Aluminum, Covered with Stearic Acid and a Phase Film of Polyisobutylene

ϵ, %	7.0	11.4	15.2	24.4	31.0	36.0
Stearic acid	2.0	1.5	1.1	0.78	0.60	0.51
Polyisobutylene film	1.6	1.0	0.94	0.62	0.53	0.31

Under pressure treatment, the structure of the lubricating layer is destroyed by the tangential component of the compressive force. This is observed as a reduction in the resistance to displacement in the lubricating layer (under the conditions of the treatment) with increasing deformation.

A study of the rheological properties of metals [5] makes it possible to observe that increasing the displacement stress lowers the effective viscosity (i.e., it increases the flow). The same thing happens on the surface of the metal in the lubricating layer during pressure treatment, and this result is independent of how the lubricating layer is formed. A regular reduction in the resistance to displacement in the lubricating layer, as the degree of deformation is increased (increasing the compressive forces), is observed in the solid lubricating layer and in the layer which represents the product of physicochemical interaction between the lubricant and the metal surface, i.e., in the plastificated layer. An exception is provided by liquid flowing, adsorptionally inactive, lubricating media, which are, in general, not capable of forming a stable lubricating layer.

We express deep gratitude to Professor V. I. Likhtman for his valuable advice and discussion of the results of the study.

LITERATURE CITED

1. S. Ya. Veiler and V. I. Likhtman, Zhur. Tekh. Fiz. 28, No. 9, 2025 (1958).
2. S. Ya. Veiler, V. I. Likhtman, and P. A. Rebinder, Doklady Akad. Nauk SSSR 110, No. 6, 985 (1956).
3. V. M. Korbut, S. Ya. Veiler, and V. I. Likhtman, Doklady Akad. Nauk SSSR 130, No. 2, 307 (1960).
4. V. M. Korbut, Doklady Akad. Nauk SSSR 124, No. 1, 72 (1959).
5. V. I. Likhtman and V. S. Ostrovskii, Doklady Akad. Nauk SSSR 119, No. 3, 484 (1958).

THE KINETICS OF THE GROWTH OF A CARBON SURFACE DURING THE THERMAL DECOMPOSITION OF METHANE OVER THE RANGE OF TEMPERATURE 1400-1700°C

I. L. Mar'yasin and P. A. Tesner

All-Union Scientific Investigation Institute of Natural Gas
(Presented by Academician M. M. Dubinin, May 11, 1961)
Translated from Doklady Akademii Nauk SSSR, Vol. 140, No. 5, pp. 1121-1124, October, 1961
Original article submitted May 9, 1961

At the present time, carbon formation by the thermal decomposition of hydrocarbons is extremely important in industry. A number of authors [1-5] have studied the kinetics of the process at temperatures up to 1000-1200°. The main features observed in the study of the kinetics of this process were: (i) the first-order relation between the reaction rate and hydrocarbon concentration; (ii) the rapid retardation of the reaction rate by hydrogen; and (iii) the high temperature rate coefficient. One of the authors of this paper [6] showed earlier that the energy of activation of this process decreases with increased temperature. The kinetics of the growth of the carbon surface at temperatures of 1600-2100° were studied by Brown and Watt [7]. But the values of the reaction rates and activation energies obtained by these authors were misleading because of the effect of diffusion. The present work is devoted to the measurement of the rate of growth of a carbon surface brought about by the thermal decomposition of methane at 1400-1700°C.

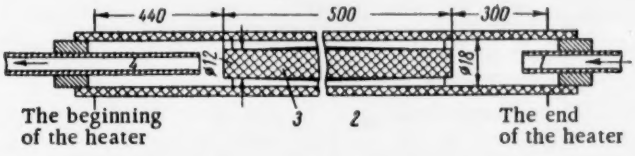

Fig. 1. The sketch of the position of a graphite rod inside the reaction space of a high-temperature furnace: 1) inlet tube for gas; 2) graphite reaction tube; 3) graphite rod; 4) outlet tube for gas.

The experimental method used was to determine the rate of growth of the carbon film forming on the graphite rod. This rod (diameter 12 mm, length 500 mm) was placed in the reaction space of a high-temperature furnace provided with a shaped graphite heater. Figure 1 shows the position of the rod. A mixture of methane and hydrogen is passed through the annular space between the rod and walls of the reaction tube. The experiments were carried out with methane concentrations of 2-10% and gas flows from 4-10 liter/min. With high concentrations of methane, carbon black was deposited, and with lower concentrations gasification of the graphite was observed.

In the experiments using nitrogen or helium diluents instead of hydrogen, very different results were obtained. Even at a temperature of 1500° with a methane concentration of more than 1%, carbon black formation was observed and it was not possible to investigate the thickness of the carbon film formed.

The thickness of the carbon film was obtained by measuring the diameters of the rod over its whole length by means of a hand micrometer with an accuracy of ±0.01 mm. The measurement of temperature in the center of the graphite heater was carried out with the help of high-temperature tungsten–rhenium thermocouples [8]. The earlier experiments showed that the difference between the temperature of the rod and the center of the heater did not exceed 20-30°. As a result, in each experiment, the curve for the relation between the rate of increase of the carbon

layer and temperature (determined by the temperature field of the furnace) was obtained. Figure 2 reproduces typical curves of this relation for different initial concentrations of methane and gas-flow velocities at 1600° in the center of the furnace. The reaction rate constants α are found from the first-order equation

$$\alpha = \frac{\gamma dr / dt}{C_x}, \qquad (1)$$

where dr/dt is the rate of growth of the film, cm/sec; γ is the density of the film, g/cm²; C_X is the methane concentration in the given section of the reaction space, g/cm³.

All the values of α found from formula (1) for different gas flows and concentrations of methane at each temperature were treated by a correlation method. Figure 4 reproduces the relation between the reaction rate constant and temperature in Arrhenius coordinates, where the correlation points are plotted on the graph.

The activation energy of the decomposition reaction of methane, corresponding to the straight line on Fig. 4, is 36 kcal/mole. The relation between the reaction rate and the temperature may be expressed by the formula

$$K_s^1 = 2042Ce^{-18200/T}. \qquad (2)$$

Here, the methane concentration C is expressed in g/cm³, and the reaction rate K_s in g/cm² · sec. The values of the rate constant obtained permitted us to determine the activation energy at different temperatures from the equation

$$N_a = N_0 e^{-E/RT}, \qquad (3)$$

where N_a is the number of reacted moles, N_0 the number of total collisions of the molecules at the surface; E is the activation energy. The respective values of E are given in the table.

The extent to which the results are in error due to diffusion was calculated by both theoretical and experimental methods. Under stationary conditions

$$K_s = \beta (C_x - C_s), \qquad (4)$$

where β is the diffusion velocity coefficient of methane in hydrogen, cm/sec; C_X is the concentration of methane along the flow axis, g/cm³.

The diffusion velocity coefficient was found from the formula β = Nu D/d [9], where Nu is the Nusselt number, D is the diffusion coefficient of methane in hydrogen, and d is the equivalent diameter. The diffusion coefficient at 1900° equals $3.8 \cdot 10^{-3}$ m²/sec. In the calculation of this coefficient, the temperature coefficient is assumed to be 1.75 [10]. The equivalent diameter equals $6 \cdot 10^{-3}$ m. The Nusselt number under our experimental conditions equals 3.66 [11].

From these original data obtained from the literature, the value of β from formula (5) equals 230 cm/sec. The difference between the concentration of methane along the flow axis and the concentration at the surface for the section of the reacting space where the reaction rate at 1900° equals $2.8 \cdot 10^{-5}$ g/cm² · sec, is $1.2 \cdot 10^{-7}$ g/cm³.

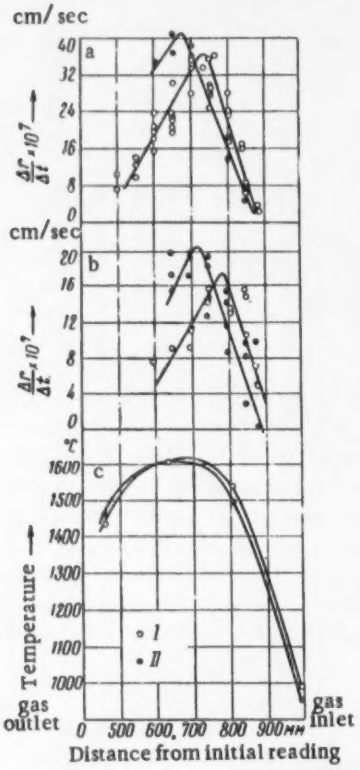

Fig. 2. Variation in the rate of growth of a carbon film along the length of the rod at 1600° in the center of the furnace. A is a 10% concentration of methane at the inlet; B is a 5.3% concentration of methane at the inlet; C is the temperature field of the furnace at 1600°. I) Gas flow velocity 3.6 liter/min; II) gas flow velocity 10 liter/min.

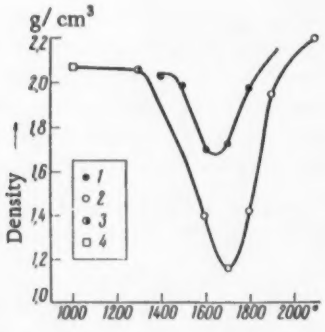

Fig. 3. Relation between density of carbon films and their temperatures of formation: 1) our results; 2) results of [7]; 3) results of [4]; 4) results of [5].

Comparison of this value with the methane concentration along the flow axis, equal to $5 \cdot 10^{-5}$ g/cm^3 for the same section, shows that the decrease in concentration is about 0.4%. Hence, it is possible to conclude that diffusion does not limit the reaction rate and the reaction rate, in practice, is determined only by chemical kinetics.

Activation Energy of the Decomposition Reaction of Methane on the Surface at Different Temperatures

Temp., °C	Reaction rate constant, cm/sec · 10^2	Proportion of reacted molecules, $e^{-E/RT} \cdot 10^5$	Activation energy from Eq. (3), kcal/mole
1400	3.9	0.56	40.0
1500	7.2	1.40	39.2
1600	12.0	2.29	39.7
1700	20.0	4.09	39.6

The effect of diffusion on the reaction rate was confirmed experimentally by comparing the kinetic constants with the constants obtained by decomposing methane on the surface of powdered corundum particles, size 0-2μ. The powder, together with the gas flow, was passed through the reaction space under the same conditions as in the experiments with the rods.

The increase in the radius of the particles and the rate of increase of the carbon film was determined on the basis of determining the content of carbon in the powder and its specific surface. The results from these tests were compared with those with rods, and it was found that, in both cases, the rate of growth of the films was similar. This indicates that complications due to pronounced diffusion are absent since the decomposition of methane on the surface of particles which are commensurate with the length of the free molecular path, may be considered as independent of the diffusion velocity.

The main importance of the results is that the reaction rate constants which are found are not misleading, because of diffusion, and we are able to calculate the absolute rate of growth of the carbon layer over the range 1400 to 1700° with concentrations of methane and hydrogen up to 10%.

Qualitative experiments with methane diluted with nitrogen and helium showed a significantly greater rate of growth of the films in comparison with experiments in which the methane was diluted with hydrogen. In the experiments which were carried out under vacuum by Brown and Watt [7], with undiluted methane, the rate of growth of the films under similar partial pressures of methane and similar temperatures, despite the effect of diffusion, proved to be 3 to 4 times more than in our tests. This indicates that in the temperature range investigated, and similarly with significantly lower temperatures [2], the rate of decomposition of the carbon molecules on the surface is considerably retarded by hydrogen. The retardation which is found is obviously explained by the activated adsorption of hydrogen by the carbon surface.

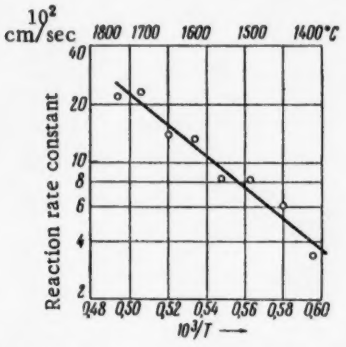

Fig. 4. Relation between the reaction rate constant α for the decomposition of methane at the surface and the temperature.

It is of interest to consider the similarity between the activation energy values calculated from the slope of the straight line in Arrhenius coordinates and calculated from Eq. (3). This result shows that the value of the steric factor in this equation in fact equals unity [6,12], and that the formation of the carbon surface is limited by the molecular collisions on the surface and, in the same way as at a lower temperature [2], no doubt represents a purely molecular process. It is also of interest to observe that the activation energy of the process in the range of temperatures 1400-1700° remains constant, whereas, in the range 800-1300° [6] it decreases approximately by 20 kcal/mole.

Comparison of our data for the density of the carbon films with those from the literature (Fig. 3) shows a sharply defined minimum at a temperature about 1700°, which may be explained in the following manner.

At temperatures up to 1300°, the high carbon density is explained by the small rate of growth of the film. Hence, the molecules react with the most active atoms of the carbon surface and a very dense structure is developed. With an increase of temperature, the rate of growth of the film increases and its degree of order falls. By increasing the temperature above 1700°, despite the continuing rise in the rate of increase of the film, the rate at which the structure becomes ordered increases rapidly, as a result of which it reaches the value of 2.2 g/cm^3 at 2100°, i.e., it

approaches the density of graphite. In our tests, the substantially greater absolute values of the densities of the films is probably explained by the retarding action of hydrogen because the published data refers to methane, undiluted with hydrogen.

LITERATURE CITED

1. P. A. Tesner and A. I. Echeistova, Doklady Akad. Nauk SSSR 87, No. 6, 1029 (1952).
2. P. A. Tesner and I. S. Rafal'kes, Treatment and Transport of Natural Gas [in Russian] (1953) p. 3.
3. P. A. Tesner, Seventh Symposium on Combustion, 1958, p. 546.
4. D. B. Murphy, H. B. Palmer, and C. R. Kinney, Industrial Carbon and Graphite (1958) p. 77.
5. R. O. Grisdale, A. C. Pfister, and W. Roosbroeck, Bell Syst. Techn. J. 30, 271 (1951).
6. P. A. Tesner, Gazovaya promyshlennost' No. 2, 45 (1960).
7. A. R. Brown and W. Watt, Industrial Carbon and Graphite (1958) p. 86.
8. S. K Danishevskii, Zav. laboratoriya No. 12, 1470 (1958).
9. D. A. Frank-Kamenetskii, Diffusion and Heat Transfer in Chemical Kinetics [in Russian] (AN SSSR Press, 1947) p. 26.
10. L. Andrussow, Zs. Electrochem. 54, 566 (1950).
11. S. S. Kutateladze and V. M. Borishanskii, Manual on Heat Transfer [in Russian] (959) p. 97.
12. P. A. Tesner, Gazovaya promyshlennost' No. 2, 48 (1961).

All abbreviations of periodicals in the above bibliography are letter-by-letter transliterations of the abbreviations as given in the original Russian journal. *Some or all of this periodical literature may well be available in English translation.* A complete list of the cover-to-cover English translations appears at the back of this issue.

CHEMICAL REACTIONS UNDER CHROMATOGRAPHIC CONDITIONS

Corr. Member, AN SSSR, S. Z. Roginskii,

M. I. Yanovskii, and G. A. Gaziev

Institute of Chemical Physics, Academy of Sciences of the USSR
Translated from Doklady Akademii Nauk SSSR, Vol. 140, No. 5,
pp. 1125-1127, October, 1961
Original article submitted June 7, 1961

When chemical reactions are carried out in a flow in contact with the surface of a condensed phase, at first they are always accompanied by a, albeit partial, separation of the components in the reacting mixture. This separation may occur in the chemical reactions: 1) of gases and liquids catalyzed by solids; 2) of gases and liquids reacting homogeneously in the presence of solids which are able to sorb the components of the reacting mixture to various extents; 3) of gases and vapors reacting homogeneously over the surfaces of liquids in which the separate components are soluble; 4) in topochemical reactions of solids in a flow, etc.

Under the conditions of a usually protracted dynamical experiment the chromatographic effects are deviations, which occur at the start but fade away after some time. After this, in each cross section perpendicular to the direction of the flow, there is established a constant ratio between the concentrations of the substances fed and those of the products, and this ratio corresponds to the stationary course of the process under dynamical conditions.

By using the special methods of analytical chromatography one may create conditions under which separation takes place in the greatest part of the time during which the substances pass through the reactor. Then, as will be evident further on, the separation may have an essential effect on the character of the chemical processes and, therefore, one may speak about the fundamental chromatographic conditions for carrying out chemical reactions.

In analyzing chemical processes under chromatographic conditions, we confine ourselves to the case where the rate of the chemical process is markedly lower than that of mass transfer between the phases. As starting point we will take the most simple and demonstrative case of a substance portion injected as a pulse into the flow of carrier gas passed through the reactor. Such a method of carrying out a reaction began recently to become of importance for studying catalytic processes [1,2].

Let us consider the reaction

$$\nu_A A \rightarrow \nu_B B + \nu_C C.$$

Into the flow we inject the mixture A + B + C. We will assume that the distributions coefficients b_i of the substances between the two phases have different values.

When $b_A < b_B < b_C$, at some distance from the reactor inlet three bands will have been formed (Fig. 1a). If no reaction occurs, these bands will travel along the reactor while drawing apart gradually. If reaction does occur, in the band of A the substances B and C are generated continuously and they will form unusual tails at the rear of the band for the reactant A (Fig. 1b). When $b_A > b_B > b_C$ the band of the reactant A will be preceded by ghost bands of B and C (Fig. 1c). The case $b_B < b_A < b_C$ is shown in Fig. 1d.

So, although all components are present in the mixture fed and the products are generated in the course of the reaction, under chromatographic conditions one will find a more or less complete separation of the products from the original reacting substance. We note that the described picture must be qualitatively the same both for homogeneous and heterogeneous reactions. The formation of zones for the individual components of the reaction and for any foreign substances present in the system leads to several special particularities of the chromatographic regime. Let us discuss some of them:

1. Reversible reactions of the type

$$A \rightleftarrows B + C + \ldots + N$$

When $b_i \neq b_N$, if only for one pair of products, the reaction only proceeds from the left to the right. It is interesting to note that only at $b_B = b_C = \ldots b_N$ the reaction under chromatographic conditions can proceed in both directions and preserve its reversible character. The particularities of this case are already evident from the most simple example of the isomerization reaction

$$A \rightleftarrows B.$$

When the substance A is fed to the reactor, (when $b_A < b_B$), the A band will be accompanied by a tail of B from which, in its turn, A will be formed. So, from the amount of nonreacted A one may determine the rate of the forward reaction.

When A and B are fed simultaneously, the picture does not change essentially, and simultaneously in the band of A the practically irreversible forward reaction will proceed and in that of B the reverse reaction.

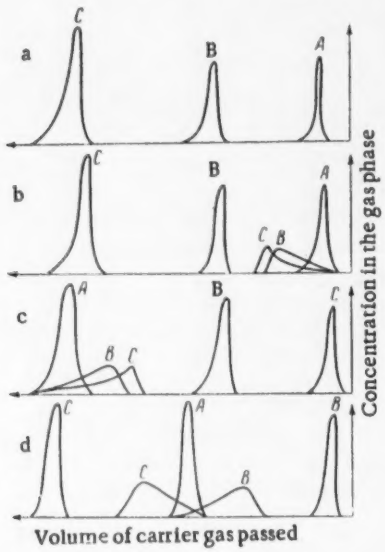

Fig. 1. Concentration curves to be found when a chemical reaction is carried out under pulse chromatography conditions: a) $b_A < b_B < b_C$ (no reaction occurs); b) $b_A < b_B < b_C$; c) $b_A > b_B > b_C$; d) $b_B < b_A < b_C$.

2. A reaction in which two or more original substances participate

$$\nu_A A + \nu_B B + \ldots \rightarrow \nu_K K + \nu_M M + \ldots$$

If only for one pair of the original substances the distribution coefficients are unequal, $b_i \neq b_j$, after some time, as is required for separating the corresponding bands, the reaction comes to a standstill. On the contrary, a reaction which requires the participation of two or more molecules of one original substance ($nA \rightarrow B + C + \ldots$) is possible,* since here no separation of the bands for the original substances takes place. Until now we discussed general cases of chemical reactions proceeding under chromatographic conditions. We will dwell in more detail on some particular cases:

a) A homogeneous reaction in which active admixtures (inhibitors, indicators, and poisons) participate:

$$nA\,(+ X + Y) \rightarrow B + C,$$

where X and Y are active admixtures.

When X and Y are sorbed reversibly, and $b_A \neq b_X$, $b_A \neq b_Y$, inhibition and initiation must disappear, because X and Y are absent in the band of A. This is also valid in that case where the acceleration or the retardation of the reaction (the mechanism does not matter) is provoked by reaction products. Positive and negative autocatalysis are equally impossible under chromatographic conditions. The effect of a chromatographic regime on the particularities of chain reactions (termination, kinetics, etc.) deserves a separate discussion.

b) Heterogeneous catalysis when volatile contact poisons are present

$$A\,(+ X + Y) \rightarrow B + C + \ldots$$

In this case, reversible and irreversible adsorption of X,Y should be discussed separately. When the adsorption is reversible, neither X nor Y will have any effect, since in the reaction zone they are absent.

When the adsorption is irreversible, the effect of the poison is confined to the zone, the width of which is determined by the amount of poison in the portion injected and the adsorptive capacity of the catalyst with respect to

*A typical example of a bimolecular reaction which may proceed under chromatographic conditions is $HI + HI \rightarrow I_2 + H_2$.

the poison. After the band of A has passed the poisoned zone, the effect of the poison stops. Repeated admission of samples leads to a gradual broadening of the poisoned zone. This type of experiment enables one to make clear how the poison acts. Because in the reaction zone the products are absent, the kinetic laws of heterogeneous catalysis are simplified considerably. Therefore, in the kinetics of reactions on homogeneous and heterogeneous surfaces those terms which take into account adsorption of products and reversible poisons (promotors) are absent in the equation for the reaction rates. Owing to this, from the temperature dependency of the rate constant one obtains an activation energy, which is closer to the actual value. In particular, in the case of Langmuir kinetics, all terms corresponding to the adsorption heat of strongly adsorbed reaction products and reversible contact poisons disappear from E_{obs}. Dependent on the degree of coverage θ_A, two cases are possible:

$$E_{chr} = E_{act} - \nu_A Q_A \text{ (at } \theta_A << 1);$$

$$E_{chr} = E_{act} \text{ (at } \theta_A = 1),$$

where Q_A is the adsorption heat of the reacting component A.

Therefore, by carrying out a reaction in the usual stationary dynamical way, and in the pulse modification of the chromatographical regime, one may show whether it is retarded by its products.

Above we discussed the chromatographical regime for the case where the rate of the catalytic reaction is considerably smaller than that of the adsorption. In several cases the rate of a heterogeneous catalytic process is determined by the adsorption rate. Such reactions may be conveniently studied by carrying them out in a bed under chromatographic conditions. To do this, a portion of one component of the reactant mixture is injected into the column. The course of the reaction will be determined by the sequence in which the reacting components are admitted, and by the nature of their bonds with the surface. By varying this sequence one may establish the actual reaction mechanism. It is particularly promising to combine the method of tagged atoms with the chromatographical procedure.

In the near future we intend to publish experimental data on the study of the regularities of catalytic reactions carried out under chromatographic conditions.

LITERATURE CITED

1. D. W. Bassett and H. W. Habgood, J. Phys. Chem. 64, No. 6, 769 (1960).
2. W. Hall, D. MacIver, and H. Weber, Ind. and Eng. Chem. 52, No. 5, 421 (1960).

DEGREE OF DISPERSION AND STABILITY OF EMULSIONS STABILIZED BY SOLID EMULSIFIERS

A. B. Taubman and A. F. Koretskii

Institute of Physical Chemistry, Academy of Sciences of the USSR
(Presented by Academician P. A. Rebinder, May 12, 1961)
Translated from Doklady Akademii Nauk SSSR, Vol. 140, No. 5, pp. 1128-1131, October, 1961
Original article submitted May 5, 1961

The stability of type M/W emulsions, stabilized with highly dispersed solid particles, is, in many cases, much greater than when they are stabilized with adsorbing layers of surface-active agents [1]. This is because of the large mechanical strength of the interphase protective layers of particles which are formed as an independent surface phase on the water – oil interface. Here, as we have shown, there is a direct relation between the strength of these layers and the stability of the emulsions [1,2].

Along with this, the point of view is generally recognized that a high degree of dispersion of the emulsifiers is one of the necessary conditions for effective action at an optimum particle dimension of the order of 1-10μ [3,4]. However, the data which we have obtained shows that this relation does not always hold, and that the degree of dispersion is not the decisive factor in the stabilizing effect of solid emulsifiers, but rather the structural and mechanical properties of the interphase protective layers which they form.

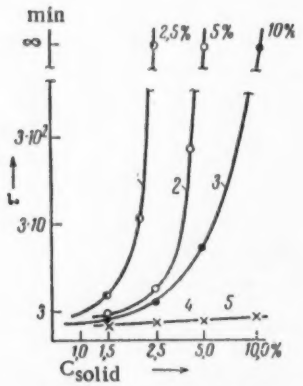

Fig. 1. Emulsifying powers of solid emulsifiers as a function of their degree of dispersion: 1) precipitated calcium carbonate (D < 3μ); 2) Oglanly bentonite (D << 1μ); 3) aluminum oxide (D ≈ 6-40μ); 4) ground glass (D < 3μ); 5) the same (D ≈ 100μ).

To measure the structural strength of these layers (the limiting two-dimensional displacement stress P_m), we used a standard SNS-2 apparatus, intended for the study of clay solutions (suspensions), which, after some modifications and improvements which we made, could be used as a simple universal apparatus suitable for measuring the mechanical properties of both surface layers and emulsant systems in volume [1]. In the first case, the coaxial metallic cylinders of the apparatus are replaced by a glass disc (30 mm in diameter and 4 mm thick), suspended on an elastic tungsten filament in such a position that its perimeter traverses the interface between the liquid phases, formed by the emulsion and located in a glass crystallizing vessel. At a constant small rate of deformation produced by rotating this vessel (at a rate of 0.2 rpm), the change in the turning moment (M dyne · cm), and, consequently, in the two-dimensional displacement stress (P dyne · cm^{-1}) of the intact structure was measured as a function of time (τ_k) right up to failure at $P = P_m$, which corresponds to a pronounced maximum in the curve of P against τ_k [5-7]. The measurement of the disc displacement (angle of twist of the filament) was made optically.

The value of P_m was calculated from the formula

$$P_m = \frac{M}{2\pi R^2} = \frac{C_0\theta_m^0}{360R^2} = \frac{C_0 S_m}{360R^2 n} \text{ (dyne · cm}^{-1}\text{)}$$

where R is the radius of the disc, C_0 is the torsion constant of the filament, θ_m^0 and S_m are the angle of twist of the filament expressed, respectively, in degrees and centimeters of the reading scale, and n is the factor for converting θ_m^0 into S_m. For the filaments which we used, of length 25-30 cm and diameter 0.05-0.2 mm, the value of C_0 varied over the range 5-1000 dyne · cm · radian^{-1}.

If the metallic cylinders are replaced with glass ones having a rifled surface,* the apparatus could be used to measure the displacement stress in the volume of concentrated high-stability emulsions, stabilized by solid emulsifiers.

The protective layers of solid particles were formed at a water – carbon tetrachloride interface by precipitating them out of the upper phase (water suspension), in an amount which calculations showed corresponded with the thickness of the emulsifier layer on the emulsion drops. The emulsions were prepared by shaking up cylinders containing both phases in one to one volume ratio, a water suspension of emulsifier and vaseline oil (or CCl_4) carefully purified from polar contaminates. The stability of the emulsions was evaluated from the free settling time (τ) required for half of the volume of oil to separate out in the free state [for values of $\tau >$ 50 hr the emulsions were arbitrarily considered to be infinitely stable ($\tau = \tau_\infty$)].

The degree of dispersion of the emulsifier particles (D = 2R) showed a concentration of the basic fraction (in percent of the total number of particles), corresponding with the maximum in the dimension distribution curve. The emulsifiers used were the following mineral powders: 1) precipitated calcium carbonate [D (70%) < 3μ]; 2) Oglanly bentonite [D (80%) << 1μ]; 3) aluminum oxide [D (85%) ≈ 6-40μ]; 4) two samples of ground glass with different degrees of dispersion having particles D (80%) < 3μ and D (75%) ≈ 100μ.

The conclusion which we arrived at above, that there is no conclusive relation between the stability of the emulsion and the degree of dispersion of the solid emulsifier particles, is confirmed by the data given in Fig. 1.

As may be seen, in calcium carbonate suspensions (D < 3μ, specific surface S_0 equal to 5.1 m^2/g), stable oil emulsions are forced at a concentration of solid phase as small as 2.5% (curve 1), while a bentonite suspension (D << << 1μ, $S_0 \sim 300$ m^2/g) stabilizes it fully only at an emulsifier concentration greater than 4-5% (curve 2). The same result is given by aluminum oxide (D ≈ 6-40μ), and not less than a 10% suspension (curve 3). It is, in general, impossible to get emulsions with glass powder (or with any of the varieties of quartz) independently of the degree of dispersion (curves 4 and 5).

We have shown previously [8] that if the oil phase contains even traces of surface-active agents, which are capable of chemo-adsorptive interaction with the emulsifier particles, the stability of the emulsions formed is increased sharply, especially in those cases where ions of an electrolyte are present in the water phase at the same time, which give insoluble soaps with the surface-active agent [2]. Obviously, the protective surface structures arising here, even though they come from one and the same emulsifier, should form emulsions of a different degree of dispersion, depending on how strong they are.

Figure 2 shows a microphotograph of a vaseline oil emulsion stabilized by one and the same emulsifier – aluminum oxide (D≈ 6-40μ) – in a 10% water suspension: a) in the absence of additives; b) with the oil containing 0.001% oleic acid; and c) containing the same quantity of acid in the oil and a concentration of 0.01N aluminum chloride in the water phase.

Actually, it may be seen that the mean dimensions of the emulsion drop drop off sharply and in order from 1.5-2.0 mm to 0.5-1.0 mm, and then to 0.05-0.1 mm. Strength measurements of the interphase layers have shown that, corresponding to these three cases of stabilization, the values of P_m are 0.008, 0.015, and 9.8 dynes/cm and, in the last case, a very large margin of excess strength makes the emulsions practically infinitely stable. In a number of cases they have been kept without appreciable change over a two-year period of observation.

Here the thickness of the protective coverings drop from 6-8 layers of loosely packed particles (a) to one strongly structurized layer (c), as a result of which the limiting emulsion stability could be achieved by using not a 10% suspension, but only a 1% suspension of Al_2O_3. It follows from this that not only the stability of the emulsions, but their degree of dispersion, is directly determined by the mechanical properties of the protective coatings, which arise in the form of coagulational structures at the interphase [9], and depends only a slight degree on the degree of dispersion of the emulsifier particles.

The essence of this effect is that coalescence of the oil phase drops, occurring after dispersion (which would cause an increase in dimensions), and is hindered to various degrees, depending on how pronounced the "armoring"

*The selective wetting of the walls of the glass cylinders (as distinct from metallic) by the external water phase of type M/W emulsions, and their special rifling, with projections of very small coverage, prevents partial destruction of the emulsions and separation in the free state of a lubricating oil film, which usually causes slip of the liquid near the wall [1].

action of the emulsifier is, which is, in turn, determined by the structural strength of the stabilizing film. System 2c obviously shows the original high limiting degree of dispersion of the drops, which is produced during dispersion. It is quite obvious that highly dispersed emulsions with drop dimensions of another order of magnitude (1μ or less), can be prepared only by using surface-active agents as emulsifiers, which considerably lowers the surface tension (work of formation) of the interface between the phases forming the emulsion.

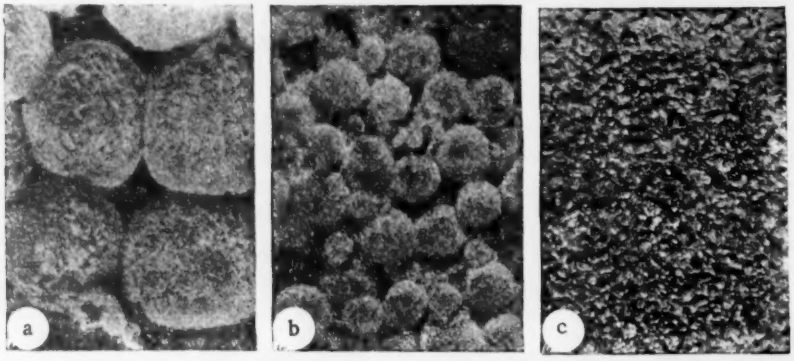

Fig. 2. Structure of the protective coatings and degree of dispersions of vaseline oil emulsions in water stabilized with Al_2O_3 (10×): a) pure oil – water; b) oil plus 0.001% $C_{17}H_{33}COOH$ – water; c) oil plus 0.001% $C_{17}H_{33}COOH$ – 0.01N aqueous solution of $AlCl_3$.

The results given make it possible to explain a number of peculiarities of the emulsification of viscous petroleum residues as seen in the technology of mechanically washing the surface of walls of petroleum tanks and petroleum handling vessels, which we have dealt with previously. A solid emulsifier has been used for this purpose, namely, bentonite clay [10], and later water-soluble surface-active agents (PAV) with electrolytes added [11], for example, sodium dodecylbenzolsulfonate plus Na_2CO_3 plus Na_2SiO_3, etc. It was shown that the emulsifying power of PAV during washing was so weak that the necessary effect could be achieved only in high concentration solutions (4-5%). However, if polyvalent ions are added to these solutions from salts of the strength, for example, of the Mg^{2+} ion, or if sea water is used, the required concentration can be reduced to 0.5% and lower.

The cause of this marked enhancement of the emulsifying power of PAV appeared to be that they form a highly dispersed (colloid) solid phase, consisting of precipitates of $MgCO_3$ and $MgSiO_3$, which mainly take on themselves the function of stabilizing the emulsions. The presence of a solid phase is observed nephelometrically, and is confirmed by the fact that, after passing the solution through a filter, it is completely deprived of emulsifying power.

Here the carbonate particles whose surface is easily modified (they become hydrophobic), react chemisorptively with the acid components of the petroleum compound (naphthenic acids, etc.), and thus gain the ability to form structurated, mechanically stable surface protective coatings which, depending on the degree of modification, can permanently stabilize an emulsion of either the direct or the reverse type [8]. Chemically, however, the inert magnesium silicate particles maintaining their original hydrophilic nature, are only able to form unstable emulsions of the first kind and, thus, are antagonistic both to the natural "black" emulsifiers, contained in the petroleum compounds, and to the magnesium carbonate in case it becomes more hydrophobic than is necessary.

Using these peculiarities in the properties of solid emulsifiers and in the structuration process of protective emulsion coatings, we can, over a wide range and in a delicate way, regulate both the stability and type of the emulsion and the degree of dispersion, which is what we did to obtain optimum engineering effectiveness.

In conclusion, we express deep thanks to P. A. Rebinder for his interest in the work and his valuable advice.

LITERATURE CITED

1. A. F. Koretskii, Candidates Dissertation [in Russian] (Institute of Physical Chemistry, AN SSSR, Moscow, 1960).
2. A. B. Taubman and A. F. Koretskii, Kolloid. Zhurn. 20, 5, 676 (1958).

3. J. Schulman and J. Lej, Trans. Faraday Soc. 50, 598 (1954).
4. V. Kleipton, Emulsions [Russian translation] (IL, 1950) p. 256.
5. P. A. Rebinder, Collection: New Methods of Physicochemical Investigation of Surface Properties [in Russian] (Transactions of the Institute of Physical Chemistry, AN SSSR) 1, 5 (1950).
6. A. A. Trapeznikov and V. A. Fedotova, Transactions of the Third All-Union Conference on Colloid Chemistry [in Russian] (AN SSSR Press, 1956) p. 65.
7. A. A. Petrov, Candidates Dissertation [in Russian] (Petroleum Institute, AN SSSR, Moscow, 1956).
8. A. B. Taubman and A. F. Koretskii, Doklady Akad. Nauk SSSR 124, No. 2, 358 (1959).
9. P. A. Rebinder, Kolloid. Zhurn. 20, 5, 527 (1958).
10. A. B. Taubman and A. F. Koretskii, Vestn. AN SSSR No. 9, 62 (1954).
11. A. F. Koretskii and A. B. Taubman, Collection: Mechanization of Cleaning the Petroleum Fleet [in Russian] (Astrakhan, 1959) p. 87

All abbreviations of periodicals in the above bibliography are letter-by-letter transliterations of the abbreviations as given in the original Russian journal. *Some or all of this periodical literature may well be available in English translation.* A complete list of the cover-to-cover English translations appears at the back of this issue.

THERMOMECHANICAL CURVE STUDY OF THE THERMAL TRANSFORMATIONS OF SOME RUBBERS

B. Ya. Teitel'baum, T. A. Yagfarova, M. P. Dianov, and É. F. Gubanov

A. E. Arbuzov Chemical Institute, Institute of Organic Chemistry of the Kazan Branch of the Academy of Sciences of the USSR
(Presented by Academician B. A. Arbuzov, May 19, 1961)
Translated from Doklady Akademii Nauk SSSR, Vol. 140, No. 5, pp. 1132-1135, October, 1961
Original article submitted April 13, 1961

The method of recording thermomechanical curves [1] gives a wide range of possibilities for studying the different processes which occur during the heating of polymeric materials. It has proved especially convenient when using automatic recording of the deformation of samples under applied stress at continuous and uniform increase in temperature. In this case it can be put in a class with such widespread methods of investigation as thermography, which, to tell the truth, has very limited applicability to polymers.

It does not seem to us that the thermomechanical curve method has been used to a sufficient degree in the study of rubbers. A. A. Tager and his co-workers [2] have shown how effective this method is in studying the processes going on during the heating of synthetic sodium butadiene rubber. The curves obtained by Kargine's balance method [3], using periodic loading, go through a maximum which corresponds with the maximum flow of the polymer. The reduction in flow at higher temperatures is described by the authors to the formation of bridging bonds and space networks.

We have set ourselves the task of studying the processes which occur during the heating of rubbers, by conducting thermomechanical curves using the technique of applying the constant load with uniform increase of the temperature of the sample [4].

Refinement of the technique has made it possible to achieve automatic recording of the curves directly in temperature-deformation coordinates* [5].

The record is taken on an ÉPP-09 electronic recording voltmeter. As one coordinate the pin records the e.m.f. of a thermocouple giving the temperature of the test sample. The second coordinate is provided by the chart which is not moved continuously, but according to the deformation of the material. The plunger placed on the sample is connected to an electronic relay which starts the drive motor of the recorder. (Here, depending on the direction of the deformation, the motor runs in a forward or backward direction.) This same mechanism moves a micrometer screw which "shadows" the contact as it is displaced with penetration of the plunger into the sample. The rubber samples were cut out in the form of tablets 4 mm in diameter and 2 mm high. The end of the plunger, which applies pressure to the sample, had a flat point 2.0 mm in diameter. The samples were heated at a linear rate from −120 to +450°. A kind of dry nitrogen at the temperature of the cell was constantly blown through the cell, which gave better heat conduction to the sample and reduced the possibility of its being destroyed by oxidation.

The rate of heating of all the experiments was 2°/min, and the load was 3.2 kg/cm^2. In a number of cases other weights were used. All the thermomechanical rubber curves which we took were reduced to a single scale on the deformation axis (for which purpose a simple special device was used, based on optical projection). The deformation is shown in relative percent.

* What is being investigated, in the strict sense of the word, is not the deformation of the sample, but the penetration, and the method should be called thermopenetrographic.

It is a well-known fact that amorphous polymers of sufficiently high molecular weight give characteristic thermomechanical curves showing regions of glass-like, high elasticity, and viscous flow states, as well as transitional regions between them. The regions of high elasticity deformation of the curve correspond with the horizontal segment which, however, frequently rises somewhat because of the accompanying plastic deformation of the polymer.

The thermomechanical curves of natural rubber (Fig. 1, 1) show an additional "stepping" in the region of the high-elasticity state. This element of the curve is completely reproducible. We observed it in the curves of samples, taken from different sources, stored for a different length of time under various conditions. It should be noticed that in previous work on thermomechanical properties where the curves were constructed from points [6], this property of natural rubber was not observed.

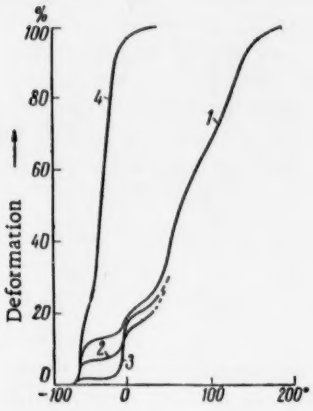

Fig. 1. Natural rubber melting curve: 1) unchanged sample; 2) sample held in thermostat at −25° for 1.5 hr; 3) the same, for 3 hr; 4) sample previously heated to 250°.

We have been able to show that the phenomenon of "stepping" has to do with melting of the crystalline phase of the rubber, which occurs near 0°C. Since, from the data in the literature [7], the optimum temperature for the crystallization of rubber is −25°C, we kept samples of rubber at a fixed temperature in a thermostat for 1.5 or 3 hr, then they were cooled down below the glassing point, after which the mechanical curve was recorded in the usual way. It turned out that the form of the curve depends upon how long the sample has been kept in the thermostat at the optimum crystallization temperature. The ratio of the heights of the first and second flats drops off with increasing time in the thermostat (Figs. 1, 2, and 3). This leads to the conclusion that the second flat owes its origin to melting of the crystalline phase. It is characteristic that not one of the synthetic rubbers investigated, including SKI isoprene, showed this phenomenon.

Every one of the synthetic rubbers investigated showed a completely different glassing point T_g (this temperature is the same at different applied loads within the limits of the experimental accuracy). The curves of a number of synthetic rubbers (Fig. 2) are of the same form, and the differences are caused, apparently, mostly by differences in the molecular weight.

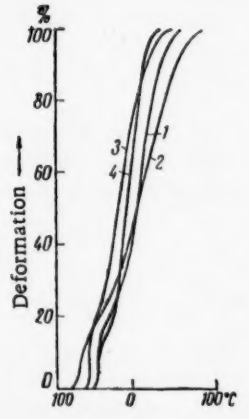

Fig. 2. Synthetic rubbers, prepared with alkaline catalysts: butadiene SKB (1), SKB (2), SKBM (3), and Tiperylene SKP (4).

In all the curves there is a sharp rise at the point T_g; however, there is no clearly marked horizontal step, which shows that starting at the transition temperature, elastic deformation of the rubber is accompanied by plastic deformation.

A substantial difference from the other curves is shown by the curve for one of the samples of butadiene rubber, prepared with the lithium catalyst SKLD, which has very small plasticity. Right after the increase in deformation at about 200°C, there is a horizontal step, which continues up to a very high temperature. Only above 400° does the sample melt (Fig. 3a). The other SKLD sample having higher plasticity gave a thermomechanical curve which is not different in form from the curves of the other synthetic rubbers (B on the same figure).

It would be natural to assume that the peculiar form of the curves of the first SKLD sample is to be explained by the fact that, as a result of the small plasticity, the penetration is not completed at temperatures where the polymer is stable. In view of this, the experiment is being continued in the temperature region where destruction occurs, and directly afterward reconstruction of the polymer into a rigid structure, which melts at a very high temperature (thermovulcanization). To check the correctness of the ideas expressed, the SKLD sample was subjected to a previous heating at 250° under the usual experimental conditions (but without applying load), after which it was cooled. Then a thermomechanical curve was taken on this previously heated sample. It turned out that, although the glassing temperature T_g was maintained, the sample took on completely different elastic–plastic properties (curve A-1). The heated sample shows no plastic deformation up to temperatures around 400°. (The reverse deformation curve in the temperature region 100-300° is caused, ap-

parently, by a change in the volume and elastic properties of the materials, possibly connected with its cooling schedule after heating.) This experiment shows clearly that if the SKLD sample is heated to 250°, it is converted into a rigid high-melting material.

It would be natural to assume that such properties should be shown by a SKLD sample which has high plasticity. We heated the sample B to a temperature of 250° (lying beyond the limits of its penetration by the 3.2 kg/cm² weight, i.e., in the region of the flow state), and, after cooling, the thermomechanical curve was taken. Here we got the curve B-1, which is almost the same as the one which was given under the same conditions by the sample having lower plasticity (A-1). It is worth considering that nothing of this sort was shown by rubber heated to 150° (B-2). The curve, in this case, goes somewhat more to the left than for the original polymer. This shows that some reduction in molecular weight has occurred, i.e., some destruction, but no structuration whatever. Further to the left on the graph is the curve of a sample of the same material, subjected to previous thermoplastification on rolls, using the minimum amount of chemical plasticizor (B-3).

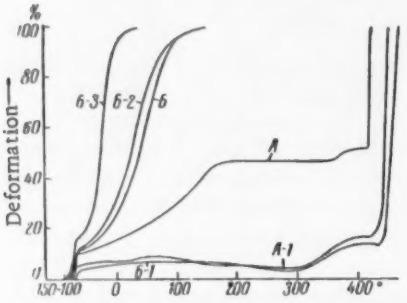

Fig. 3. Synthetic SKLD rubber (butadiene, polymerized in the gaseous phase with a lithium catalyst): A) small plasticity; B) high plasticity; 1) sample heated to 250°; 2) sample heated to 150°; 3) plasticized on rolls.

The result obtained made it possible to assume that the structuration at high temperatures may be observed, even in the thermopenetration curve of other synthetic rubbers, if they are heated to 250° in the flow state.

In the experiment made on the sample of ordinary SKB, these assumptions have been confirmed. The corresponding curves are similar to those found for SKLD, and are not given here. It is interesting that the sample of sterically regular SKD butadiene rubber prepared by synthesis with a complex catalyst, showed the same general picture (Fig. 4). Heating, even in this case, produced a rigid high-melting product. It was a matter of interest to study the behavior of natural rubber under similar conditions. The natural rubber sample was heated, just as it was done in the previous samples, to 250°. The thermal penetration curve taken after cooling is shown in Fig. 1, curve 4, which also gives the curves for unchanged natural rubber. As may be seen from comparison, heating the rubber produces a more plastic product with more pull at room temperature. This testifies to the previous destruction, when accompanied by the formation of rigid structures. Synthetic SKI isoprene rubber behaves in a way which is completely similar to natural rubber in this respect. The curves which we obtained (as shown in Fig. 4), show that there is destruction even in this rubber, but there is no observable formation of rigid high-melting structures.

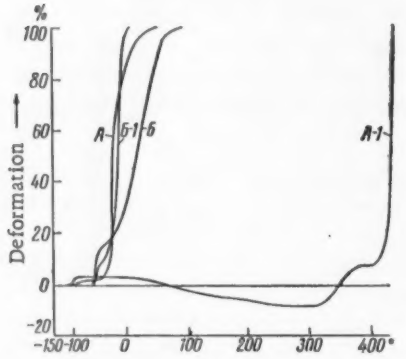

Fig. 4. Synthetic rubbers prepared with a complex catalyst: A) butadiene SKD; B) isoprene SKI; 1) samples previously heated to 250°.

It is worth considering that even synthetic piperylene SKP rubber behaves in a way that is similar to isoprene rubber but not to butadiene rubber. We do not give the curves here. Because of this, it becomes easily possible to distinguish butadiene rubbers (independent of the method of synthesis), and methyl butadiene rubbers (natural or synthetic) by heating them to 250° and then taking the thermomechanical curves.

Thus, in some ways, the work given has shown that the study of thermomechanical properties with an automatic recording device is an effective method of investigating rubbers. Thermomechanical curves have been obtained for natural and a number of synthetic rubbers, and their thermal transformation processes have been studied. It has been shown that butadiene rubbers heated to 250° form rigid "knit" structures, at the same time that pentadiene rubbers undergo destruction under the same circumstances. The crystallization of natural rubber has been investigated, and the temperature region in which the crystalline phase melts has been made clear.

The authors are grateful to M. G. Beregovskii for furnishing the rubber samples and for discussion of the experimental results.

LITERATURE CITED

1. V. A. Kargin and M. N. Shteding, Khim. Prom. No. 2, 74 (1955).
2. A. A. Tager, T. B. Gordeeva, D. Yu. Karlinskaya, and L. M. Kurochkin, Khim. Prom. No. 4, 209 (1955).
3. V. A. Kargin and T. I. Sogolova, Zhur. Fiz. Khim. 23, 530 (1949).
4. B. L. Tsetlin, V. M. Gavrilov, N. A. Velikovskaya, and V. V. Kochkin, Zavod. Lab. 22, 352 (1956).
5. B. Ya. Teitel'baum, Advanced Scientific, Engineering, and Industrial Experimentation [Russian translation] (Center for Foreign Technical and Experimental Information, 1961) Series 32, No. 4/2.
6. A. Tager, M. Iovleva, T. Kantor, and L. Muzheva, Zhur. Fiz. Khim. 27, 1227 (1954).
7. B. A. Dogadkin, Chemistry and Physics of Rubbers [in Russian] (Moscow-Leningrad, 1947).

All abbreviations of periodicals in the above bibliography are letter-by-letter transliterations of the abbreviations as given in the original Russian journal. *Some or all of this periodical literature may well be available in English translation.* A complete list of the cover-to-cover English translations appears at the back of this issue.

THE EFFECT OF PARAMAGNETIC CONTAMINATES ON THE NUCLEAR MAGNETIC RESONANCE SPECTRA OF SOME ORGANIC SUBSTANCES

Yu. Ya. Shamonin and K. A. Gol'dgammer

Physicotechnical Institute of the Kazan Branch of the Academy of Sciences of the USSR
(Presented by Academician A. E. Arbuzov, May 18, 1961)
Translated from Doklady Akademii Nauk SSSR, Vol. 140, No. 5,
pp. 1136-1137, October, 1961
Original article submitted May 16, 1961

Up to the present time, the effect of paramagnetic contaminates on proton resonates in liquids has been studied by nuclear relaxation methods [1-4].

It was a matter of interest to find out what effect paramagnetic substances would have on the individual lines of the proton resonance fine structure, observed in organic liquids using a highly homogeneous field H_0. The materials chosen for study were several alcohols and glacial acetic acids. The paramagnetic contaminates were: $MnCl_2$, $Mn(CH_3CO_2)_2 \cdot 2H_2O$ and $CuCl_2$. The proton resonates measurements were made at a frequency of 30 mc, and the homogeneity of the field H_0 in the volume of the sample, was of the order of 10^{-6}. At this degree of homogeneity, the standard alcohol CH_2CH_2OH gives three lines corresponding with the CH_3, CH_2, and OH groups having the relative intensities 3:2:1 (Fig. 1a). All the lines in the pure standard alcohol have the same width and half-height, corresponding to about 9 millioersteds. This width is due to the nonhomogeneity and instability of the constant magnetic field. The true width of the line $1/T_2$, in the pure alcohol, is known to be incomparably less.

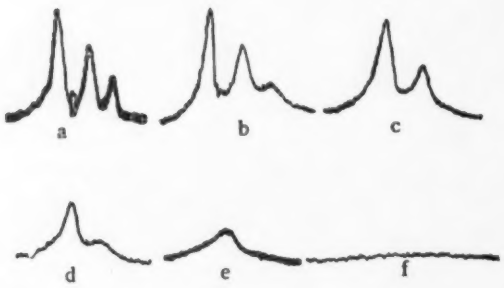

Fig. 1. Nuclear magnetic resonance spectrum of C_2H_5OH as a function of Mn^{2+} concentration.

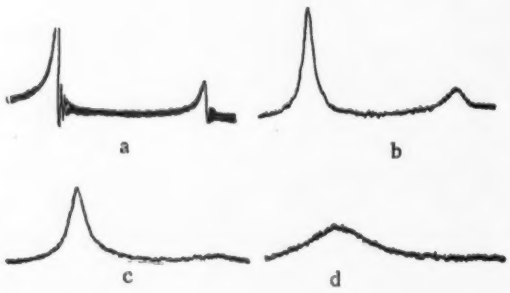

Fig. 2. Nuclear magnetic resonance spectrum of CH_3COOH as a function of Mn^{2+} concentration.

If anhydrous magnesium chloride is added to the alcohol in concentrations and, from 0.00065 mol/liter $MnCl_2$ to 0.4 mol/liter $MnCl_2$, a gradual change in spectrum occurs. First only broadening of the lines is observed, in which the OH line changes most of all (Fig. 1b). At the concentration end equal to 0.004 mol per liter, the OH line practically disappears (Fig. 1c). Further increase in the $MnCl_2$ concentration causes intense broadening of the CH_2 line (Fig. 1d), which disappears at N = 0.08 mol/liter (Fig. 1e), and, finally, at concentration N = 0.4 mol/liter the CH_3 line practically disappears (Fig. 1f).

The effect of anhydrous cupric chloride on the C_2H_5OH spectrum is entirely similar to the effect of magnesium chloride, but the concentrations of $CuCl_2$ requires are approximately 15 times higher.

In addition to ethyl alcohol, the spectra of ethylene glycol $HOCH_2CH_2OH$ and ethylene chlorhydrin $ClCH_2CH_2OH$, also consists of two lines we are studying. In the presence of $MnCl_2$, the line corresponding to the OH group first broadens and disappears, and after that the one belonging to the CH_2 group.

Finally, measurements were made on glacial acetic acid containing manganese acetate $Mn(CO_2CH_3)_2 \cdot 2H_2O$. Pure CH_3COOH gives two lines with the intensity ratio 3:1 (Fig. 2a). Dissolving the paramagnetic substance causes broadening of both lines (Fig. 2b), but the line corresponding to the OH group broadens faster and disappears at $N \approx$ $\approx$ 0.015 mol/liter (Fig. 2c). With further increase in concentration, the CH_3 line continues to broaden (Fig. 2d), but it was not possible to get complete disappearance because the manganese acetate was not sufficiently soluble in CH_3COOH.

The results presented are interesting both from the point of view of the theory of proton relaxation in liquids, and from the point of view of the study of the structure of the solutions. Since, in the presence of paramagnetic substances the observed width of the fine structure lines exceeds the width caused by the nonhomogeneity of the field H_0, we are dealing with a true time T_2. With paramagnetic particles in the solution this time is, generally speaking, different for each line of the fine structure. The data which we have obtained on ethyl alcohol shows that the value of $1/T_2$ for each individual fine-structure line is approximately proportional to the square of the magnetic moment of the ion, and, likewise, apparently (if we consider the relative intensity of the fine-structure lines), inversely proportional to the cube of the distance between the paramagnetic ions and the protons of the group in question. This last relationship is in agreement with measurements on proton resonance in different complexes of Fe^{3+} [3]. It is also interesting to note the following. It is known from [4] that the spin-lattice proton relaxation time T_1 for C_2H_5OH containing 0.02 mol/liter Mn^{2+} is equal to 0.003 seconds. However, our measurements show that the relaxation time T_2 for the CH_3 group at the indicated concentration of Mn^{2+} is approximately 0.015 seconds, and for the remaining groups it is incomparably shorter. Hence, it follows that the widths of the fine-structure line in ethyl alcohol, containing Mn^{2+}, are determined mainly not by spin-lattice, but by spin-spin interaction ($T_1 \gg T_2$).

One can expect great things from the observed phenomenon, especially in the study of the structure of solvates in solutions. First of all, one can find out in a concrete case by what group the molecule being solvated attaches itself to the paramagnetic particle. In particular, it follows from our measurements that the alcohol molecules attaches itself to the paramagnetic particle through the OH group, while the acetic acid molecule is attached to the $= C = O$ group. By making more accurate quantitative measurements, there is no doubt but that it will be possible to measure the distance between the paramagnetic particle and the nearest group of the solvating molecule.

It is to be assumed that other methods, such as spin-echo, will make it possible to observe the existence of some of the proton relaxation times in solution similar to the ones we measured. However, our method has obvious advantages not only as regards simplicity and clarity, but also in view of the fact that, in principle, it allows one to determine any desired number of times T_2 corresponding to different proton groups.

The authors express profound gratitude to B. M. Kozyrev and A. I. Rivkind for their aid in discussing the experimental results.

LITERATURE CITED

1. N. Blombergen, E. M. Purcell, and R. V. Pound, Phys. Rev. 73, 678 (1948).
2. B. M. Kozyrev and A. N. Rivkind, Zhur. Expt. i Theoret. Fiz. 27, 1 (7), 69 (1954).
3. A. N. Rivkind, Doklady Akad. Nauk SSSR 102, No. 6, 1107 (1955); Zhur. neorg. khim. 2, No. 6, 1263 (1957).
4. A. I. Rivkind, Doklady Akad. Nauk SSSR 117, No. 3, 450 (1957).

All abbreviations of periodicals in the above bibliography are letter-by-letter transliterations of the abbreviations as given in the original Russian journal. *Some or all of this periodical literature may well be available in English translation.* A complete list of the cover-to-cover English translations appears at the back of this issue.

THE EXPLOSION PRESSURE LIMIT FOR GASEOUS HYDRAZOIC ACID AS A FUNCTION OF THE SPARK PULSE POWER

T. A. Aizatullin, V. G. Voronkov and V. P. Zubov

M. V. Lomonosov Moscow State University

(Presented by Academician N. N. Semenov, May 24, 1961)
Translated from Doklady Akademii Nauk SSSR, Vol. 140, No. 6,
pp. 1356-1357, October, 1961
Original article submitted April 18, 1961

According to existing notions, the limit pressure of explosion (inflammation) is lowered to a certain threshold value when the energy of the spark impulse is increased and further raising of the spark intensity no longer has any effect. Some authors [1] explain this phenomenon by assuming the existence of two different inflammation mechanisms.

An examination of the explosive properties of gaseous hydrazoic acid does not confirm these conclusions. The experimental results indicate that the limit pressure decreases continuously as the intensity of the spark pulse is raised.

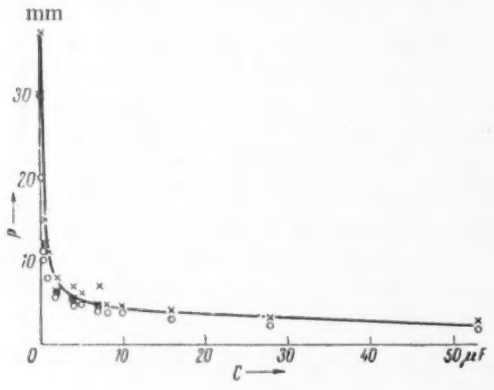

Fig. 1.

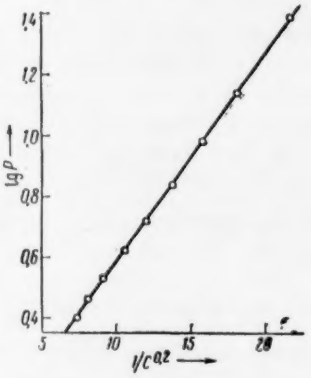

Fig. 2.

The experiments were carried out in a spherical glass vessel with a diameter of 11 cm and sealed electrodes which formed a 3-mm spark gap in the center of the sphere. The electrodes were connected to the two ends of the secondary winding of a car bobbin; through the primary winding the charge of a capacitor of fixed capacity loaded to a constant voltage was discharged. The explosion pressure limit of hydrazoic acid was determined at room temperature; the original pressure in the explosion vessel was successively lowered from experiment to experiment until explosion at the given intensity of the spark pulse was suppressed. The hydrazoic acid was obtained by the reaction between pure stearic acid and sodium azide.

The results obtained when we studied how the limit pressure of explosion depends on the capacity of the capacitors discharged over the spark gap are shown in Fig. 1. When plotting the logarithms of the limit pressures along the axis of ordinates and the reciprocal capacity of the discharged capacitors along the axis of abscissas we obtain a linear relation (see Fig. 2), which smoothly expresses the monotonous decrease of the limit pressure occurring as the capacity of the discharged capacitors is raised.

Further experiments have shown that the character of the relation between the limit pressure and the capacity of the discharged capacitors remains the same, even if one goes over to explosive mixtures of gaseous hydrazoic

acid with various gases, although the magnitude of the limit pressure, in this case, as a rule, becomes greater. As an illustration, in Fig. 3 the pressure limit for a mixture of hydrazoic acid (25%) and air (75%) dried over calcium chloride which had been heated, is plotted versus the capacity of the discharged capacitors. Such a relation becomes still more smooth if one takes into account how the coefficient of spark efficiency depends on the capacity of the capacitor and on the pressure of the explosive mixture.

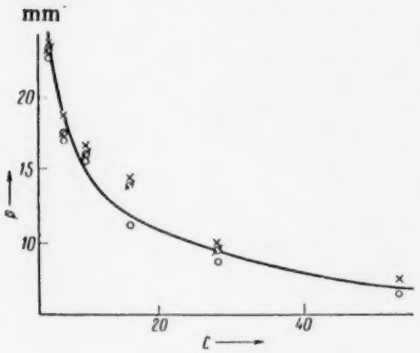

Fig. 3.

The obtained experimental results are well described by an empirical formula of the following form: $\lg P = A/C^n + B$, where P is the limit vapor pressure of hydrazoic acid at which inflammation is possible under the given conditions of the experiment and the capacity of the capacitors discharged over the spark gap; C is the said capacity; A, B, and n are constants for a given mixture, but they depend on its composition.

From a comparison with the experimental results of other authors [3], it became clear that this formula quite satisfactorily describes these processes. This must mean that the hypothesis postulated by previous authors, namely, the existence of a certain threshold for the limit pressure below which inflammation is impossible at any intensity of the spark pulse, does not follow directly from their experimental data and, consequently, it has no quite sufficient experimental foundation.

On the contrary, the above-expressed conclusion, that the limit pressure of explosion is lowered continuously, as the intensity of the spark is raised, follows clearly from our experiments and is in complete agreement with previously published experimental results.

Obviously, N. N. Semenov's known formula [4]: $\lg(P/T^{1+2/n}) = \frac{A}{T} + B$, which was derived for thermal self-ignition of fuel mixtures, expresses a more general law embracing not only oxidations, but also decompositions, and not only thermal self-ignition, but also spark ignition of the most different gaseous explosive systems.

LITERATURE CITED

1. L.N. Khitrin, Physics of Combustion and Explosion [in Russian] (Moscow, 1957).
2. Ya. B. Zel'dovich and N. N Simonov, Zhur. fiz. khimii 23, 1361 (1949).
3. A. Kowalsky, Z. phys. Chem. (B), 11, 56 (1931); T. A. Kontorova, Zhur. fiz. khimii 4, 64 (1933); Ya. B. Zel'dovich and N. N. Simonov, Zhur. fiz. khimii 23, 1361 (1949); S. A. Kamenetskaya and S. Ya. Pshezhetskii, Zhur. fiz. khimii 32, 1122 (1958); M. B. Blance, P. G. Guest, G. Elbe, and B. Lewis, J. Chem. Phys. 15, 11, 798 (1947).
4. N. N. Semenov, Chain Reactions [in Russian] (Moscow, 1934).

All abbreviations of periodicals in the above bibliography are letter-by-letter transliterations of the abbreviations as given in the original Russian journal. *Some or all of this periodical literature may well be available in English translation.* A complete list of the cover-to-cover English translations appears at the back of this issue.

EXPLOSION METHOD AND HEAT OF FORMATION OF CF_4, CF_3Cl, $CFCl_3$, AND CCl_4

V. F. Baibuz

Institute of Mineral Fuels, Academy of Sciences of the USSR
(Presented by Academician V. N. Kondrat'ev, May 27, 1961)
Translated from Doklady Akademii Nauk SSSR, Vol. 140, No. 6,
pp. 1358-1360, October, 1961
Original article submitted May 24, 1961

The explosion method is one of the experimental methods of determining the thermodynamic properties of gases at high temperatures. The basis of the method lies in the measurement of the pressure when the gas mixture is exploded, and the subsequent calculation of the specific heat or thermochemical values of the gases. The description of the explosion method, and the method of calculating the explosion temperatures, were given in [1,3-5]. Although the explosion method has been known for more than fifty years, the absence of a reliable method of calculation or a method of determining the values of the losses in energy, prevented this method from being applied in experimental thermochemistry. In the present work an experimentally based method is suggested for calculating the temperature of explosion taking into account possible energy losses. A complete, detailed experimental description of the apparatus used in the present investigation was described earlier [4,6].

The results of the earlier work [3, 9-19], and the results obtained by exploding mixtures of H_2, CO, and O_2 in spherical bombs with polished and blackened surfaces, makes it possible to put forward the following theory for the mechanism of the loss of energy occurring with explosions in a spherical bomb. Due to thermal conduction of the gaseous mixture, the major part of the heat loss occurs over a very short period of time immediately after the maximum explosion pressure is attained. Because of the cooling of the walls of the bomb, the layer of gas directly contiguous to the walls cannot burn at the instant of time when the maximum explosion pressure is reached. This results in a certain quantity of heat not being evolved. Consequently, it follows that the total energy losses when an explosion occurs in the spherical bomb must be made up of two parts: (1) heat, lost as a result of its removal at the wall of the bomb; (2) heat, which is not evolved because a certain layer of gas directly contiguous to the walls of the bomb does not burn.

Since it is therefore no longer possible, in this theory, to consider the explosion process as adiabatic, then, as a consequence, the method for calculating the explosion temperature must also be changed. To derive a new method for calculating the explosion temperature, the theory of normal flame propagation velocity has many advantages. It follows from this theory that as the flame is propagated in the gaseous medium, a preheated zone [7] or a thermal zone of the flame, is formed before the flame front. The gas mixture is preheated in this zone by means of molecular thermal conduction up to a certain temperature T_p, at which the reaction proceeds fairly rapidly. Thus, during flame propagation in the spherical bomb the following equation applies:

$$\lambda\left(\frac{\partial T}{\partial x}\right)=\frac{up(H_{T_p}-H_{T_0})}{RT_0\left(\frac{p}{p_0}\right)^{\frac{\gamma-1}{\gamma}}}.$$

Here λ is the thermal conductivity of the gas mixture; $(\partial T/\partial x)$ is the maximum value of the temperature gradient in the flame zone; u is the normal flame propagation velocity; p is the pressure; T_0 and p_0 are the initial temperature and pressure of the mixture; $H_{T_p}-H_{T_0}$ is the heat content of the mixture by heating it from temperature T_0 to T_p; R is the gas constant; γ is the adiabatic constant.

Since the flame is comparatively far from the walls of the bomb, the value $(\partial T/\partial x)_{wall}$, which determines the heat transfer at the wall, is small and, consequently, the quantity of heat emitted by the gas to the wall is also small. As the flame approaches the wall, the value of $(\partial T/\partial x)_{wall}$ suddenly increases and, consequently, the

quantity of heat emitted by the gas to the wall must also rapidly increase. Because of the rise in the heat emitted at the wall in the course of a certain period of time, the flame will not be in a condition to heat a certain layer of gas mixture close to the walls of the bomb up to the temperature T_p and as a result this layer cannot burn before the maximum explosion pressure is attained.

Assuming that, at the wall,

$$\left(\frac{\partial T}{\partial x}\right)_{\text{wall}} = c_1 \frac{T_p - T_0}{\Delta x},$$

where Δx is the width of the layer of unburned gas, and c_1 is a certain constant for the layer of gas adjacent to the walls of the bomb, then the heat balance equation may be written in the following form:

$$\frac{u_к p_e (H_{T_p} - H_{T_0})}{RT_0 (p_e / p_0)^{\frac{\gamma-1}{\gamma}}} = \frac{u_к p_e (H_{T_к} - H_{T_0})}{RT_0 (p_e / p_0)^{\frac{\gamma-1}{\gamma}}} + c_1 \lambda \frac{T_p - T_0}{\Delta x}. \quad (1)$$

Here T_k is the temperature of the unburned gas mixture at the instant when the maximum explosion pressure P_e is reached; U_k is the value of the normal burning velocity at the walls of the bomb.

On the basis of the calculation of the burning velocity in a spherical bomb [3], the value of the normal burning velocity at the walls of the bomb equals

$$u_к = \frac{c_2}{p_e - p_0} \left(\frac{p_0}{p_e}\right)^{1/\gamma} \frac{dp}{dt}, \quad (2)$$

where c_2 is a constant, and the value of dp/dt is assumed as close to p_e.

Assuming that $T_к = \frac{T_p + T_0}{2}$, and using (1) and (2), we obtain

$$\Delta x = \frac{c_0 \lambda T_0 (p_e / p_0 - 1)}{\frac{H_{T_p} - H_{T_0}}{T_p - T_0} \frac{dp}{dt}}. \quad (3)$$

In expression (3) the value c_0 depends mainly on the parameters of the experimental apparatus, and is determined by an experimental method.

From this theory of an unburned layer of gas at the walls of the bomb, and from the equation of state of an ideal gas, it is easy to obtain an expression for the temperature of the explosion

$$T_e = T_0 \frac{p_e}{\alpha p_0} \left[1 + \frac{3\Delta x}{r_0} (2\alpha - 1)\right],$$

where r_0 is the radius of the spherical bomb; $\alpha = \Sigma m_e / \Sigma m_i$; Σm_i is the number of moles participating in the reaction, and Σm_e is the number of moles of the combustion products.

To obtain the heat balance equation it is assumed in the theory that, in the absence of heat losses, the quantity of heat received by the gas layer at the wall of the bomb is sufficient to heat this layer up to the temperature T_p. Hence,

$$\sum m_e \Delta E^0_{f_T} = \sum m_e (E_{T_e} - E_{T_0}) + \sum m_i \Delta E^0_{f_{T_0}} + \sum \Delta m (E_{T_p} - E_{T_0}).$$

Here $\Delta E^0_{f T_0}$ is the heat of formation of the components of the mixture at the temperature T_0; $E_{T_e} - E_{T_0}$ is the change in the internal energy by heating from T_0 to T_e and $\Sigma \Delta m$ is the number of moles of unburned mixture.

To confirm the theory proposed above, to explain the mechanism of the energy loss, and to confirm the method used to calculate the temperature of explosion, we carried out a series of experiments on mixtures of H_2, O_2, CO, and H_2O. The results of the experiments confirmed that the method proposed to calculate the explosion temperature was correct and demonstrated that the maximum deviation of the values of the heat balance in all experiments did not exceed 170 cal/mole of the original mixture. The average value was 59 cal/mole or 0.5% of the total heat evolved by the explosion.

Our results, obtained by exploding mixtures of hydrogen and oxygen and mixtures of these gases with water vapor, contradict the results of Wohl and Elbe [20] and Wohl and Magat [21], who state that the addition of small amounts of water vapor considerably reduces the energy losses in the explosion of H_2 and O_2 mixtures. A critical examination of the method of experimental investigation [20, 21], and a comparison of this method with that used in the present investigation, permits us to state that the reason for the incorrect results of these authors was that they neglected the absorption of water vapor by the walls of the explosion vessel.

The results of the earlier theoretical and experimental work permitted us to use the explosion method to determine the heat of formation of CF_4, CF_3Cl, $CFCl_3$, and CCl_4. By exploding mixtures of H_2, O_2, and CO with the respective halogen substituted methane, we obtained the following values for the heats of formation for these compounds:

$$\Delta H^0_{f\,298}\ (CF_4,\ \text{gas}) = -220.1 \pm 1.4\ \text{kcal/mole},$$
$$\Delta H^0_{f\,298}\ (CF_3Cl,\ \text{gas}) = -166.2 \pm 2.2\ \text{kcal/mole},$$
$$\Delta H^0_{f\,298}\ (CFCl_3,\ \text{gas}) = -\ 66.4 \pm 2.1\ \text{kcal/mole},$$
$$\Delta H^0_{f\,298}\ (CCl_4,\ \text{gas}) = -\ 24.6 \pm 1.9\ \text{kcal/mole}.$$

Within the limits of experimental error our values for the heats of formation agree with the most reliable values of $\Delta H^0_{f\,298}$ obtained by other authors (cf. the review by Yudin and Khachkuruzov [8]).

LITERATURE CITED

1. A. M. Gurvich and Yu. Kh. Shaulov, Thermodynamic Investigations by the Explosion Method and the Calculation of Combustion Processes [in Russian] (Moscow, 1955).
2. Ya. B. Zel'dovich and D. A. Frank-Kamenetskii, Doklady Akad. Nauk SSSR 19, 693 (1938).
3. B. Lewis and G. Elbe, Combustion, Flames and Explosion of Gases (Academic Press, Inc., New York, 1951).
4. V. A. Medvedev, Dissertation [in Russian] (Inst. goryuch. iskopaemykh, AN SSSR, 1955).
5. V. A. Medvedev, Zhur. Fiz. Khim. 32, 1851 (1958).
6. V. A. Medvedev, V. V. Korobov, and V. F. Baibuz, Zhur. Fiz. Khim. 33, 58 (1959).
7. L. N. Khitrin, The Physics of Combustion and Explosion [in Russian] (Moscow, 1957).
8. B. F. Yudin and G. A. Khachkuruzov, Tr. Gos. inst. prikl. khim. 42, 132 (1959).
9. P. J. Daniell, Proc. Roy. Soc. A126, 393 (1930).
10. W. T. David, Phil. Trans. Roy. Soc. A211, 375 (1912).
11. W. T. David, Proc. Roy. Soc. A98, 183 (1920).
12. W. T. David, Proc. Roy. Soc. A98, 303 (1920).
13. W. T. David, J. R. Brown, and A. H. El Din, Phil. Mag. 14, 764 (1932).
14. W. T. David and R. M. Parkinson, Phil. Mag. 15, 96 (1933).
15. R. W. Fenning and A. C. Wiffin, Phil. Trans. Roy. Soc. A238, 142 (1939).
16. W. E. Garner and D. A. Hall, J. Chem. Soc. 1930, 2038.
17. W. E. Garner, D. A. Hall, and F. E. Harvey, J. Chem. Soc. 1931, 641.
18. W. E. Garner and C. H. Johnson, J. Chem. Soc. 1928, 281.
19. B. Lewis and G. Elbe, Phil. Mag. 20, 44 (1935).
20. K. Wohl and G. Elbe, Z. phys. Chem. 5b, 241 (1929).
21. K. Wohl and M. Magat, Z. phys. Chem. 19B, 117 (1932).

All abbreviations of periodicals in the above bibliography are letter-by-letter transliterations of the abbreviations as given in the original Russian journal. *Some or all of this periodical literature may well be available in English translation.* A complete list of the cover-to-cover English translations appears at the back of this issue.

EQUILIBRIUM DISTRIBUTION OF TRITIUM IN HYDROGEN ISOTOPE EXCHANGE

Ya. M. Varshavskii and S. É. Vaisberg

Institute of Radiation and Physicochemical Biology,
Academy of Sciences of the USSR
(Presented by Academician A. N. Frumkin, May 23, 1961)
Translated from Doklady Akademii Nauk SSSR, Vol. 140, No. 6,
pp. 1361-1363, October, 1961
Original article submitted May 23, 1961

In recent years tritium has found wide application as a tracer atom, since it is the only radioactive isotope of hydrogen. As we know, the use of tracer atoms presupposes that the isotopes used have identical properties. At the same time, the considerable difference in mass between tritium and protium may lead to a marked difference in the chemical properties of these two hydrogen isotopes and, in particular, to a severely nonuniform distribution of tritium between hydrogen-containing substances during tritium–protium exchange. Thus, in tritium–protium exchange, it is always necessary to know and take account of the equilibrium (thermodynamic) isotope effect, characteristic of the system under study. A quantitative measure of this effect is known to be the value of the distribution coefficient $\alpha = ([T]/[H])_1 : ([T]/[H])_2$, where the indices 1 and 2 designate the reacting components, for which the ratios of the equilibrium concentrations of tritium and protium are being found.

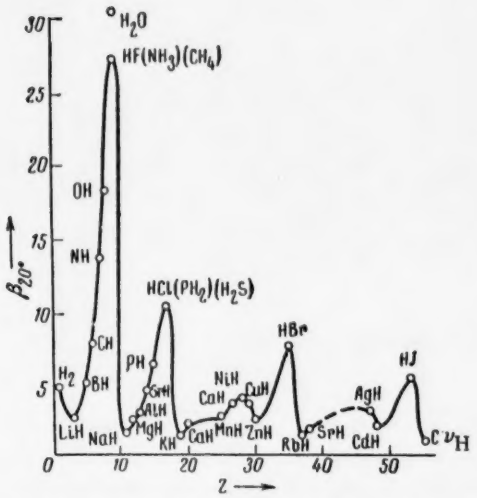

The β-factor as a function of the atomic number of the element, bound with hydrogen.

Information on the tritium distribution coefficients in systems of hydrogen-containing substances is extremely scarce. Unfortunately, at the present time, the lack of experimental data cannot be met by calculating the tritium–protium exchange constants according to the methods given by Urey [1], Bigeleisen and Mayer [2], and Tatevskii [3], and then finding the distribution coefficient [4-7], since we are hampered by lack of the data required for the calculations on the fundamental frequencies of the vibration-rotation spectra of tritium-containing substances, with the exception of tritium-containing hydrogen and water [1,8]. However, there is the possibility of finding approximate values of the tritium distribution coefficients for any system of hydrogen-containing substances, by using the law which we have found for the distribution of the isotopes of any monovalent element [5,6]. According to this law, the distribution coefficient of an isotope between a pair of substances is equal to the ratio of the β-factors* of these substances.

The value of the β-factor is, to a first approximation, determined exclusively by the number of outer electrons, and the number of completed electron shells in the atom of the element, which is bound in the molecule of the substance in question with the isotope under study (including the outer electrons, associated with any other atoms in the molecule). Starting from this law, the β-factor of any hydrogen-containing substance in the tritium–protium

*The β-factors [5-7] serve as a quantitative measure of the difference in thermodynamic equivalents between two isotopes of some element in a given substance. They are calculated from the fundamental vibrational frequencies of the two isotopic forms of the substance and, in contrast with the ratio of sums over the state, they do not contain the symmetry numbers of these forms.

TABLE 1

Atomic number	Element	Vibrational frequency, cm^{-1} hydrate	Vibrational frequency, cm^{-1} tritide	$\beta_{20°}$	Atomic number	Element	Vibrational frequency, cm^{-1} hydrate	Vibrational frequency, cm^{-1} tritide	$\beta_{20°}$
1	H	4154,65	878,0	4,8	20	Ca	1260	745,0	2,1
3	Li	1359,2	878,0	2,7	25	Mn	1580	928,7	2,9
5	B	2268	1417	5,0	27	Co	1890	1109	4,0
6	C	2732	1694	7,8	28	Ni	1926,6	1130,9	4,1
7	N	3300	2029	13,7	29	Cu	1866,0	1094,2	3,9
8	O	3571,6	2180	18,3	30	Zn	1497,3	877,5	2,7
9	F	3958,4	2397	27,4	35	Br	2559,3	1495,9	7,9
11	Na	1132,9	680,6	1,9	37	Rb	908,5	530,6	1,6
12	Mg	1432,9	859,6	2,5	38	Sr	1172,2	684,4	2,0
13	Al	1624,3	970,7	3,0	47	Ag	1691,9	985,8	3,3
14	Si	2080	1242	4,6	48	Cd	1338,1	779,4	2,3
15	P	2380	1417	6,3	53	I	2230,1	1297,6	5,7
17	Cl	2885,7	1711	10,5	55	Cs	875,5	509,3	1,5
19	K	964,5	570,7	1,7					

TABLE 2.

Substance	$\beta_{20°}$*	Tritium distribution coefficient, $\alpha_{20°}$														
		H_2	CH_4	NH_3	H_2O	HF	PH_3	H_2S	HCl	HBr	HJ	LiH	NaH	KH	RbH	CsH
H_2	4,8	1	0,17	0,17	0,15	0,18	0,46	0,46	0,46	0,61	0,84	1,8	2,5	2,8	3,0	3,2
CH_4	(27,6)	5,7	1	1	0,87	1,0	2,64	2,64	2,64	3,50	4,85	10,2	14,6	16,15	17,15	18,4
NH_3	(27,6)	5,7	1	1	0,87	1,0	2,64	2,64	2,64	3,50	4,85	10,2	14,6	16,15	17,15	18,4
H_2O	31,6	6,6	1,14	1,14	1	1,2	3,0	3,0	3,0	4,0	5,6	11,8	16,7	18,6	19,7	21,0
HF	27,4	5,7	1	1	0,87	1	2,6	2,6	2,6	3,46	4,8	10,2	14,4	16,0	17,1	18,3
PH_3	(10,5)	2,2	0,38	0,38	0,33	0,39	1	1	1	1,33	1,84	3,9	5,5	6,2	6,6	7,0
H_2S	(10,5)	2,2	0,38	0,38	0,33	0,39	1	1	1	1,33	1,84	3,9	5,5	6,2	6,6	7,0
HCl	10,5	2,2	0,38	0,38	0,33	0,39	1	1	1	1,33	1,84	3,9	5,5	6,2	6,6	7,0
HBr	7,9	1,7	0,28	0,28	0,25	0,29	0,75	0,75	0,75	1	1,39	2,90	4,20	4,70	5,0	5,3
HI	5,7	1,2	0,21	0,21	0,2	0,21	0,54	0,54	0,54	0,72	1	2,10	3,0	3,35	3,56	3,8
LiH	2,7	0,6	0,10	0,10	0,09	0,10	0,26	0,26	0,26	0,34	0,48	1	1,42	1,60	1,70	1,80
NaH	1,9	0,4	0,07	0,07	0,06	0,07	0,18	0,18	0,18	0,24	0,33	0,70	1	1,1	1,2	1,3
KH	1,7	0,36	0,06	0,06	0,05	0,06	0,15	0,15	0,15	0,22	0,30	0,63	0,90	1	1,1	1,1
RbH	1,6	0,33	0,06	0,06	0,05	0,06	0,15	0,15	0,15	0,21	0,28	0,60	0,85	0,94	1	1,1
CsH	1,5	0,30	0,05	0,05	0,05	0,05	0,14	0,14	0,14	0,20	0,26	0,56	0,80	0,88	0,94	1

*In parentheses are given the values of the β-factors, provisionally taken equal to the β-factors of the corresponding hydrogent halides.

exchange ratio may be equated to the corresponding β-factor of a diatomic hydride of an element, the atom of which in the hydride molecule is isoelectronic with the atom of the element bound to the hydrogen atom being exchanged in the molecule of the substance. For example, the β-factors of CH_4, NH_3, and H_2O, as well as other compounds with C − H, N − H, and O − H bonds (but not free radicals or separate ions) may be equated to the β-factor of HF, since, in the molecules of all these compounds, the number of outer electrons (including the associated ones) in the C, N, O, and F atoms is the same and equal to 8, and the number of completed electron shells is also the same. For BH_3 and other boron hydrides, the β-factor may be equated to the β-factor of the NH radical (6 outer electrons). For SiH_4, PH_3, and H_2S, the β-factors are close to the β-factor of HCl, etc. Here, the β-factors for tritium–protium exchange of diatomic hydrides (including free radicals), are easily calculated, starting with the known observable vibrational frequencies of these hydrides, ν_H [9], and the vibrational frequencies of the corresponding tritides (ν_T), found from the ratio of the reduced masses of the tritide (μ_T) and the hydride (μ_H):

$$\nu_T = \nu_H \sqrt{\mu_T/\mu_H}, \quad \beta = \frac{\nu_T}{\nu_H} \frac{1 - e^{hc\nu_H/kT}}{1 - e^{-hc\nu_T/kT}} e^{-\frac{hc}{2kT}(\nu_H - \nu_T)}$$

Table 1 gives values for the β-factors at 20°. The curve of the β-factor as a function of the atomic number of the element, bound with hydrogen, is similar to the corresponding curve for deuteron exchange [5-7], and is shown in the figure. Table 2 gives values of the tritium distribution coefficient ($\alpha = \beta_1/\beta_2$) in various pairs of systems of hydrogen-containing substances at 20°. As we have shown [5-7], the law which makes it possible to find the approximate value of the hydrogen isotope distribution coefficient in any given system of hydrogen-containing substances

is in complete agreement with the numerous data to be found on deuteron exchange [7]. The validity of this law in the case of tritium is supported by the fact that the β-factors of water, calculated from the known observable* vibrational frequencies in the H_2O and T_2O molecules, and equal to 31.6 (for 20°), is close to the β-factor of hydrogen fluoride (27.4). These numerical values are also characteristic of the degree of approximation to which the law gives the values of the β-factors and the distribution coefficients.

LITERATURE CITED

1. H. C. Urey, J. Chem. Soc. 1947, 562.
2. J. Bigeleisen, and M. Mayer, J. Chem. Phys. 15, 261 (1947).
3. V. M. Tatevskii, Zhur. Fiz. Khim. 25, 261 (1951).
4. A. I. Brodskii, Zhur. Fiz. Khim. 9, 755 (1937).
5. Ya. M. Varshavskii and S. É. Vaisberg, Doklady Akad. Nauk SSSR 100, 97 (1955).
6. Ya. M. Varshavskii and S. É. Vaisberg, Zhur. Fiz. Khim. 29, 523 (1955).
7. Ya. M. Varshavskii and S. É. Vaisberg, Uspl. khim. 29, 1434 (1957).
8. P. Stats, H. Morgan, and J. Goldstein, J. Chem. Phys. 24, 916 (1956).
9. G. Hertzberg, Spectra and Structure of Diatomic Molecules [Russian translation] (IL, 1949).

All abbreviations of periodicals in the above bibliography are letter-by-letter transliterations of the abbreviations as given in the original Russian journal. *Some or all of this periodical literature may well be available in English translation.* A complete list of the cover-to-cover English translations appears at the back of this issue.

---

*Although for the H_2O and T_2O molecules the corrected frequency values and all the corrections for anharmonic vibrations are known, we used the observable (i.e., uncorrected) values, in order not to introduce any more errors into the comparison with the results of the calculations for the other hydrides, where the corrections are unknown.

PHOTOIONIZATION OF ESTERS AND METAL CARBONYLS IN THE GASEOUS PHASE

F. I. Vilesov and B. L. Kurbatov

Kazhdanov Leningrad Government University

(Presented by Academician A. N. Terenin, May 30, 1961)
Translated from Doklady Akademii Nauk, SSSR, Vol. 140, No. 6,
pp. 1364-1367, October, 1961
Original article submitted May 18, 1961

In a paper by one of the authors [1], the photoionization method was used to find values of the first adiabatic ionization potentials of a number of compounds, the molecules of which contain the carbonyl group. It was shown, for the case of ketones, that the induction interaction between the carbonyl and the methyl groups obeys the law of additivity and falls off inversely proportional to the square of the distance between these groups. To check the validity of these laws for other classes of compounds, the photoionization method [2] is used in the present paper to measure the first adiabatic ionization potentials of esters and some of their halogen derivatives, as well as a number of ethers, and some volatile metal carbonyls. As in the case of ketones, in these classes of compounds the first ionization potentials are caused by splitting off one of the valence electrons of the oxygen, which do not take part in the chemical bond. The values found for the ionization potentials are given in Tables 1, 2, and 3, where they are arranged according to classes of compounds in the order of decreasing ionization potential.

TABLE 1.

Compound	Ionization potential, ev	Ketone ionization potential, ev	Difference, ev
Ethyl acetate 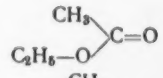	10,08±0,02	9,54	0,54
n-Propyl acetate 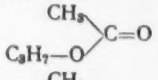	10,02±0,02	9,47	0,55
n-Butyl acetate 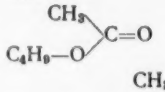	10,00±0,03	9,44	0,56
Iso-butyl acetate 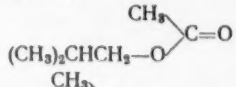	9,94±0,03	9,36	0,58
n-Pentyl acetate 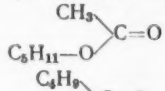	9,92±0,02	9,40	0,52
Methyl valerate 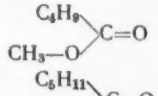	9,87±0,02	9,44	0,43
Ethyl caproate 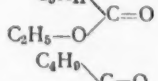	9,67±0,03	9,19	0,48
Butyl valerate 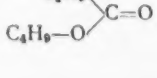	9,57±0,03	9,10	0,47

The first ionization potentials of esters are 0.45-0.55 ev higher than the ionization potentials of the corresponding ketones, which shows that there is a reduction in the electron density in the vicinity of the oxygen atom of the carbonyl group. The unengaged electron pairs of the oxygen in the ester group are conjugated with the π-electrons

TABLE 2.

Compound	Ionization potential, ev	Ester ionization potential, ev	Ketone ionization potential, ev
Methyl ester of monochloracetic acid	$ClCH_2$, CH_3-O	10,35±0,03	10,25	9,71
Methyl ester of dichloracetic acid	Cl_2CH, CH_3-O	10,44±0,03	10,25	9,71
Ethyl ester of monochloracetic acid	$ClCH_2$, C_2H_5-O	10,20±0,03	10,08	9,54
Ethyl ester of trichloracetic acid	Cl_3C, C_2H_5-O	10,44±0,03	10,08	9,54
Ethyl ester of monobromacetic acid	$BrCH_2$, C_2H_5-O	10,13±0,03	10,08	9,54
Ethyl ester of monobrombutyric acid	$BrCH_2CH_2CH_2$, C_2H_5-O	9,85±0,02	—	9,26

of the carbonyl group. This produces a reduction in positive charge in the vicinity of the carbon atom, which manifests itself in a reduction of reactivity of the carbonyl group toward nucleophilic reagents [3]

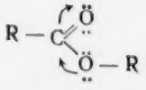

This should apparently favor a certain amount of increase in the electron density in the vicinity of the oxygen atom of the carbonyl group, and a reduction in the ionization potentials of esters as compared with the corresponding ketones. The opposite result, which is found experimentally, indicates that in the present case the transfer of electronic charge from conjugation effect to the oxygen atom of the carbonyl group either does not occur, or occurs to an insignificant extent in comparison with the negative induction effect, which is caused by the oxygen atom of the ester group. Consequently, the changes in ionization potential in esters occur as the result of superposition of the positive inductive effect of the alkyl groups, and the negative inductive effect of the oxygen atom in the ester group

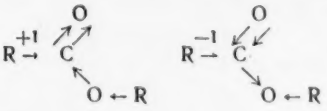

The last column of Table 1 gives the differences in ionization potential between the esters and the corresponding ketones. As the alkyl chain in the ester group is lengthened, this difference remains constant and equal to 0.55 ev with an accuracy up to the experimental error of ± 0.02-0.03 ev, which, beyond question, testifies to the high degree of additivity of the induction effects oriented in opposite directions. The differences between the ionization potentials of neighboring members of the series of esters given fall off as the length of the alkyl chain is increased and, as in the case of ketones, they may be represented with a high degree of accuracy in the form of an inverse square function of the distance between the hydrogen atom being replaced by methyl group and the oxygen of the ester

$$\Delta I_p \simeq \frac{K}{[l\,(n+1)]^2},$$

where ΔI_p is the difference in ionization potentials between two neighboring members of the series, l (n + 1) is the relative distance between the oxygen of the ester and the hydrogen atom which is being replaced with a methyl group to form the (n + 1)-th member of the series, k is a constant having, as in the case of ketones, a numerical value equal to about 0.7 ev. The high degree of additivity of the induction effects, observed in lengthening the esteric group, is somewhat disturbed in lengthening the alkyl group, which is directly united to the carbonyl carbon. Thus, the difference between the ionization potentials of the methyl ester of valeric acid and methyl butyl ketone is only

TABLE 3.

Compound		Ionization potential, ev
Ethyl ether	$C_2H_5\diagdown O\diagup C_2H_5$	9,55±0,03
n-Propyl ether	$C_3H_7\diagdown O\diagup C_3H_7$	9,28±0,05
n-Butyl ether	$C_4H_9\diagdown O\diagup C_4H_9$	9,18±0,05
β-Chloroethyl ether	$ClCH_2CH_2\diagdown O\diagup ClCH_2CH_2$	9,85±0,03
Tetrahydrofuran	$CH_2—CH_2\diagdown O\diagup CH_2—CH_2$	9,49±0,02
Dimethyl sulfoxide	$CH_3\diagdown S=O\diagup CH_3$	8,85±0,05
Chromium carbonyl	$CCr(CO)_6$	8,03±0,03
Molybdenum carbonyl	$Mo(CO)_6$	8,12±0,03
Tungsten carbonyl	$W(CO)_6$	8,18±0,03
Iron carbonyl	$Fe(CO)_5$	7,95±0,03
Nickel carbonyl	$Ni(CO)_4$	8,28±0,03
Diethyl ketone	$C_2H_5COC_2H_5$	9,34±0,02
Ethyl-tert.-butyl ketone	$C_2H_5CO(CH_3)_3C$	8,98±0,02
Iso-propyl-tert.-butyl ketone	$(CH_3)_2CHCOC(CH_3)_3$	8,82±0,02

0,43 ev. However, for the butyl ester of valeric acid it is increased to 0,47 ev. This nonequivalence of the alkyl groups may be caused by weakening of the induction effect of the chain of conjugated bonds O − C = O, or by a space factor.

The laws just given may be used successfully to find the first adiabatic ionization potentials of esters with an accuracy which is not worse than 0,05-0,1 ev.

The additivity of the various induction effects, which change the ionization potential of esters, is maintained with an accuracy of 0,02-0,03 ev for the halogen derivatives, where the negative induction effect of the esteric oxygen is increased by the halogen atom. As an illustration of this, Table 2 gives the ionization potentials of several chlorine and bromine derivatives of esters of acetic acid. For comparison, the ionization potentials of the unsubstituted esters are also given along with the corresponding ketones. It is clear from Table 2 that replacing a hydrogen atom with chlorine in the methyl group united directly with the carbonyl carbon causes an increase of 0,10 ± ± 0,02 ev in the ionization potential. If two or three hydrogen atoms are replaced, an increase in the ionization potential occurs amounting, respectively, to 0,18 and 0,36 ev, which is in good agreement with the additivity rule. Replacing a hydrogen atom with bromine leads to a similar, but approximately two times smaller, effect, which is easily understood, since bromine is less electronegative than chlorine.

Table 3 gives values of the ionization potentials of the number of ethers, ketones, and some volatile metal carbonyls. The ionization energies of these compounds are unknown, or have been measured with low accuracy [4].

With ethers, no sharp breaks in the photoionization curves were observed, which may result from the considerable difference between the interatomic distances in the molecule and in the corresponding positive ion, and the ionization potentials are determined with a large amount of error (0,05 ev). Such large errors do not permit setting up a reliable quantitative relationship between the structure of the molecules and the ionization potentials, although the qualitative nature of the reduction in ionization potentials is similar to that of esters. It seems to us that this indicates that in ionization what is torn off is one of the p-electrons of the oxygen atom, which does not participate in the formation of the chemical bond. From the example of diethyl ether and tetrahydrofuran, the ionization

potentials of which are, respectively, 9.53 and 9.49 ev, it is clear that cyclization, as in the case of ketones, causes a reduction in ionization potential. The ionization potentials of the several ketones, given in Table 3, all fit into the quantitative relations which are discussed previously in [1].

The first ionization potentials of metal carbonyls, given in Table 3, are probably due to tearing off one of the valence electrons which participate in the formation of the metal – carbon bond, or to one of the p-electrons of the oxygen atom in the carbonyl group. The small difference (0.2-0.3 ev) between the ionization potentials of the carbonyls of different metals (at the same time that the ionization potentials of the metallic atoms differ by 1.0-1.2 ev), as well as ionization potential values close to 8 ev, indicate that the metal – carbon bond is, to a considerable degree, double, while the carbonyl bond is to some degree triple. The small increase in ionization potentials in the carbonyl series consisting of chromium, molybdenum, and tungsten is obviously a matter of the increase in ionization potentials of the atoms of the metals in question. These conclusions, which follow from the measured ionization potentials, are in agreement with the data on the lengths of the intramolecular bonds.

The authors sincerely thank Academician A. N. Terenin for direction of the work and valuable discussion in evaluating the results obtained.

LITERATURE CITED

1. F. I. Vilesov, Doklady Akad. Nauk SSSR 132, 1332 (1960).
2. F. I. Vilesov and A. N. Terenin, Doklady Akad. Nauk SSSR 115, 744 (1957); F. I. Vilesov, Pribory i Tekhn. Éksp. No. 4, 89 (1958).
3. O. A. Reutov, Theoretical Problems of Organic Chemistry [in Russian] (Moscow, 1956); A. Remik, Electronic Concepts in Organic Chemistry [Russian translation] (IL, 1950).
4. K. Watanabe, J. Chem. Phys. 26, 542 (1957); T. M. Sugden and A. D. Walsh, Nature 148, 373 (1941); J. D. Morrison and J. C. Nicholson, J. Chem. Phys. 20, 1021 (1952).

All abbreviations of periodicals in the above bibliography are letter-by-letter transliterations of the abbreviations as given in the original Russian journal. *Some or all of this periodical literature may well be available in English translation.* A complete list of the cover-to-cover English translations appears at the back of this issue.

FORMATION OF AMALGAMS OF METALS OF THE IRON GROUP ON A MERCURY DROP ELECTRODE

V. F. Ivanov and Z. A. Iofa

M. V. Lomonosov Moscow State University
(Presented by Academician A. N. Frumkin, May 19, 1961)
Translated from Doklady Akademii Nauk SSSR, Vol. 140, No. 6,
pp. 1368-1371, October, 1961
Original article submitted May 8, 1961

The possibility of forming amalgams of metals difficultly soluble in mercury when they are being reduced on a mercury drop electrode (m.d.e.) is something that is being discussed in the literature right up to the present time. The authors of [1-3] propose that metals of the iron group (Cr, Mn) do not form amalgams, but cover the mercury with a layer of precipitated metal. On the other hand, in [4], the cause of the high overvoltage shown by metals of the iron group at an m.d.e. is explained in terms of hindrance in the formation of amalgams. It is well known from data taken on the mercury standard electrode (m.s.e.) that electrolysis of salts of Fe, Ni, and Co can produce the corresponding amalgams in concentrations up to 1% [5]. The resulting systems, however, do not consist of a single phase, but are colloidal solutions of the metals in mercury.

From the data of [6], using the hanging mercury-drop method combined with continuous recording of the inverse course of the polarographic curve makes it possible to arrive at the anode solubility of Ni and Co. But in [7] an oscillographic method with inverse scanning shows that, in the reduction of iron-group metals, no anode solution peaks are formed; thus, the data from the published papers do not agree with one another.

In the present paper an attempt has been made to discover the nature of the metal reduced on mercury as a function of the conditions under which the cathode process is carried out.

Orientational observations, made on the m.s.e. with a current density of 0.1 amp/ cm^2, have shown that electrodeposition of iron from 0.05N $FeSO_4$ on a background of saturated Na_2SO_4 solution is not, in the first 10-15 minutes after turning on the current, accompanied by any visible liberation of hydrogen. The current, consequently, is consumed in the formation of an amalgam which, apparently, is in the colloidal state. At the end of this period of time, liberation of hydrogen begins. At the same time, the mercury surface begins to swell and becomes rough. After the experiment the mercury at the cathode has the consistency of a paste, but retains the characteristic mercury luster. If the sulfate solutions are replaced with chlorides (10N $CaCl_2$ or 10N LiCl), at the same acidity, Fe^{2+} concentration, and current density, visible liberation of hydrogen begins almost immediately after turning on the current. After the experiment the cathode mercury is comparatively easily removed from the dark gray, powdery mass of reduced iron. Experiments with acidified solutions of 10N $Ca(ClO_4)_2$ gave a result which is no different from the results obtained with sulphate solutions.

Thus, the nature of the reduced metal depends on the nature and concentration of the background anion, which affects the structure of the double layer and the composition of the ion being discharged [8]. One is led to the same conclusion by measuring the reduction potential of a metal as a function of the nature of the background and the time of electrolysis on the m.s.e. In the case of discharge on a background of concentrated chlorides (Fig. 1, curves 1 and 2), what is found is lower polarization and a shorter delay in liberating hydrogen, rather than on a background of concentrated sulphates (curve 3) at the same current density. The arrows on the figure show the time at which visible hydrogen liberation began.*

To solve the problem of the nature of the reduction products of metals of the iron group on the m.d.e., we used the method of monocyclic inverse scanning on an oscillographic polarograph, Tsfasman type TsLA-01. To the

*In the polarization of a fixed mercury drop under a microscope, it is possible to observe the formation of microcrystals and liberation of H_2 from them.

growing mercury drop (dropping period 5-6 sec), a potential of −1.8 v (delay potential φ_3) was applied for 2-3 sec (delay period t). The scanning rate V was varied from 1 to 8 v/sec.

Figure 2, curve 1 shows the oscillogram of Ni in 1N KCL with inverse scanning from −1.8 to 0 v, connected in after the delay indicated. The oscillogram shows the cathode reduction wave ($\varphi_{\frac{1}{2}}$ = −1.2), and the nickel solution anode peak (φ = −0.3 against n.c.e.). In 10N $CaCl_2$ (curve 2), the cathode wave goes over smoothly into the anode peak in the potential range −0.6 to −0.4. Consequently, the reduction of nickel becomes practically reversible, which agrees with the data of [9]. For iron and cobalt at φ_3 = −1.8 v, it was not possible to find an anode wave of the solution of the metals deposited on the mercury.

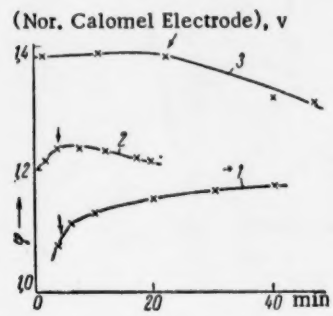

Fig. 1. Reduction potential of Fe^{2+}, and time at which visible hydrogen liberation starts as a function of background and length of electrolysis on the m.s.e. [Fe^{2+}] = = 0.05N, pH ~ 1, i = $4 \cdot 10^{-4}$ amp/cm^2: 1) 10N $CaCl_2$; 2) 5N $CaCl_2$; 3) saturated Na_2SO_4 solution.

The above-described oscillographic method was used to make experiments on Kemul's mercury hanging drop (m.h.d.) electrode. The concentration of the solutions investigated was of the order $1 \cdot 10^{-3}$ to $5 \cdot 10^{-3}$N. The background consisted of 0.01 and 0.1N solutions of KCl, oscillograms of which had been taken previously. The value of t varied from 2 sec to 2 min, with V = 0.125 v/sec.

As on the m.d.e., at φ_3 = −1.6 to −1.8 v, and t from 14 sec to 1 min, the inverse scanning oscillograms for Fe on the m.h.d. showed no metal solution anode peak, except a cusp on the negative branch of the mercury solution peak (φ = +0.06 v), which possibly belongs to iron (Fig. 3, curve 1). It was noted that the height and area of the mercury solution peak depend on [Fe^{2+}] and t. This may be explained by combined solution of Fe and Hg (curve 2). The data obtained are in agreement with the data of [6].

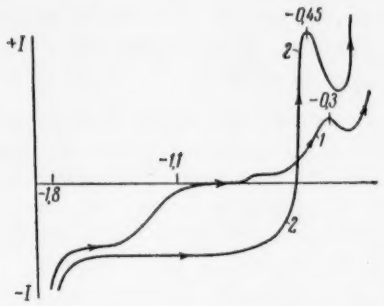

Fig. 2. Inverse scanning oscillograms for reduction of Ni^{2+} on m.d.e. pH ~ 4.7, t = 2 sec, V = 1.0 v/sec: 1) background 1.0N KCl; 2) background 10N $CaCl_2$.

However, if φ_3 was set equal to (−1.1) to (−1.2) v, the oscillogram (Fig. 3, curve 4) shows an iron solution anode peak at φ = −0.47 v. This peak is not found if φ_3 is more negative than −1.4 v. The magnitude of the peak depends on [Fe^{2+}]t (curves 3 and 4). A peak can also be observed at t = 2-3 sec. A check showed that these peaks could be reproduced on the m.d.e. It must be noted that in acidified solutions this peak is not observed. If the solution is neutralized, the peak may again be observed. The peak disappears if, after delay at φ_3 = −1.2 v, we set φ_3 = −1.8 v. If the cell is disconnected from the apparatus, the peak drops off according to the length of time disconnected (compare curves 4 and 5).

The peak of cobalt anode solution appears at a more positive potential (φ = −0.15 v). The conditions for its formation are the same as for iron (Fig. 4, curves 1 and 2).

At very negative delay potentials (φ_3 = −1.5 v), the peak in question does not appear, but the height and area of the peak corresponding to the solution of mercury is increased, and its potential is displaced toward the positive side. As for iron, the last-mentioned fact apparently has to do with simultaneous solution of Co and Hg. If at the start we set φ_3 = −1.1 v, look for a peak at φ = −0.15 v, and then set φ = −1.6 v, we can see that it gradually disappears after several successive scans. Deposition of nickel on the m.h.d. has several peculiar properties. On a fresh drop, the anode peak (φ = −0.3 v) appears even at rather negative values of φ_3 (Fig. 2, curve 1). On the m.h.d., after several successive scans lasting 10-14 sec, the peak disappears. It can be seen again on the same drop, only at lower values of φ_3, and a value of t not less than 1 min.

Thus, the data obtained show that metals, deposited at low cathode polarizations, are dissolved anodically at potentials which are more negative than the solution potential of mercury, namely: −0.47, −0.3, and −0.15 for Fe, Ni, and Co, respectively. It may be considered that the peaks indicated are anode solution peaks of the solid phase of the metal in question. An indication of the existence of a solid phase under these conditions is furnished by the absence of similar peaks, but sufficiently negative values of φ_3. In the latter case, the metal apparently goes over

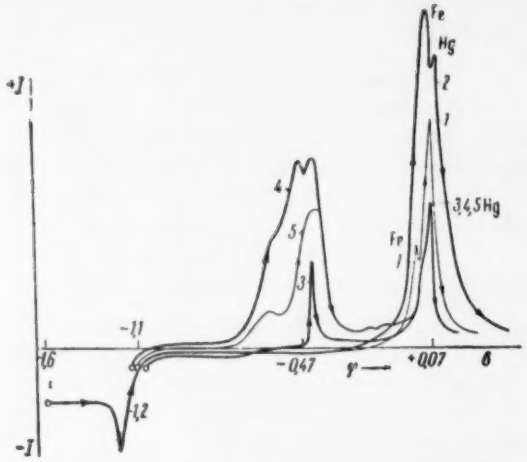

Fig. 3. Inverse scanning oscillograms for reduction of Fe^{2+} on Kemul's electrode. Background 0.1N KCl, V= = 0.125 v/ sec, t = 14 sec: 1) $\varphi_3 = -1.6$ v, $[Fe^{2+}] = 1 \cdot 10^{-3}$N; 2) $\varphi_3 = -1.6$ v, $[Fe^{2+}] = 5 \cdot 10^{-3}$N; 3) $\varphi_3 = -1.1$ v, $[Fe^{2+}] = 1 \cdot 10^{-3}$N; 4) $\varphi_3 = -1.1$ v, $[Fe^{2+}] = 5 \cdot 10^{-3}$N; 5) same as 4, but after disconnecting cell for 10 sec.

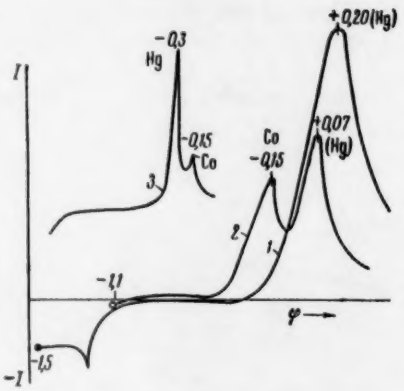

Fig. 4. Inverse scanning oscillograms for reduction of Co^{2+} on Kemul's electrode. Background 0.1N KCl, V = 0.125 v/ sec, t = 14 sec, $[Co^{2+}] = 5 \cdot 10^{-3}$N: 1) $\varphi_3 = 1.5$ v; 2) $\varphi_3 = 1.1$ v; 3) same as 2, but background 5N $CaCl_2$.

into the mercury, forming colloidal solutions or suspensions, and anode solution occurs at potentials close to the mercury solution potentials. Hence, it follows that the conditions determining the magnitude of the cathode polarization in the reduction of iron-group metals at the m.d.e. (nature and concentration of background, possibility of complex formation, shift of the ψ_1-potential, the presence of surface-active substances, etc.), can, in considerable degree, determine the character of the end products resulting from the deposition of these metals.

The experimental results may be explained if we assume that, first of all, in the electrode deposition of iron-group metals on the surface of the m.d.e., in addition to the dependence on the magnitude of the polarization, what occurs is formation of a solid phase consisting of microcrystals of Fe, Ni, or Co. The further process of transferring the metals into the mercury depends on the extent to which the microcrystals are wettable by mercury and, consequently, on the increase in the difference of surface tensions at the microcrystal – solution and mercury – solution boundaries, which may be a matter of some difference in the potentials on the mercury and on the microcrystal, since the reduction of metal ions and hydrogen go more easily on the latter than on mercury, as well as a matter of difference in position of the zero points of Fe and Hg. A considerable role in the wetting process is probably played by the degree of oxidation of the microcrystals, which increases with reduction in the cathode polarization and acidity of the solution. With increasing acidity or polarization of the cathode process, the surface of the crystals is cleaned of oxide film, and they become more easily wetted by mercury, which causes the anode peaks to disappear on the inverse scanning oscillograms. In using the data of polarization measurements we must keep in mind the possibility of differences in state of the metal deposited on the m.d.e. at different values of potential.

The authors express deep thanks to Academician A. N. Frumkin for his constant interest in the work and many valuable pieces of advice.

LITERATURE CITED

1. I. Kol'tgof and D. Lingein, Polarography [in Russian] (1948).
2. A. G. Stromberg and K. R. Voronova, Zhur. Fiz. Khim. 33, 318 (1959).
3. A. Trofimov and S. Kobarelova, Izv. Khim. Inst. B'lg. An 7, 133 (1960).
4. Ya. Geirovskii, The Polarographic Method [in Russian] (Moscow, 1937); J. Heyrovsky and R. Kalvoda, Oszillographische Polarographie mit Wechselstrom (Berlin, 1960).

5. M. T. Kozlovskii, Mercury and Amalgams in Electrochemical Methods of Analysis [in Russian] (Alma-Ata, 1956).
6. W. Kemula, Proceedings of the Second International Congress of Polarography (Cambridge, 1959).
7. H. Davis and H. Shalgosky, J. Polarographic Soc. No. 1, 12 (1960).
8. V. F. Ivanov and Z. A. Iofa, Doklady Akad. Nauk SSSR 137, 1149 (1961).
9. N. Tanaka, R. Tamamushi, and M. Kodama, Bull. Chem. Soc. Japan 33, No. 1 (1959).

All abbreviations of periodicals in the above bibliography are letter-by-letter transliterations of the abbreviations as given in the original Russian journal. *Some or all of this periodical literature may well be available in English translation.* A complete list of the cover-to-cover English translations appears at the back of this issue.

SOME GENERAL INEQUALITIES OF CHEMICAL THERMODYNAMICS

A. S. Pleshanov

G. M. Krzhizhanovskii Energetics Institute, Academy of Sciences of the USSR
(Presented by Academician V. N. Kondrat'ev, June 3, 1961)
Translated from Doklady Akademii Nauk SSSR, Vol. 140, No. 6,
pp. 1371-1375, October, 1961
Original article submitted June 2, 1961

It is known that thermodynamic equilibrium of any system occurs at the minimum in the thermodynamic potential of the system Φ (with variable p and T), or at the minimum in the free energy F (with variable v and T). A condition for a clearly defined minimum, in addition to $\delta\Phi = 0$ ($\delta F = 0$), is the requirement $\delta^2\Phi > 0$ ($\delta^2 F > 0$). A positive value of the second variation of the characteristic functions means thermodynamic stability of the system. For arbitrary reacting systems, the thermodynamic equilibrium condition $\delta\Phi = 0$ ($\delta F = 0$) is a condition for chemical equilibrium, and for ideal gases it represents, in the last analysis, the mass action law. As to the thermodynamic stability of such systems, a direct demonstration may be made in the case of ideal gases (a demonstration for a single reaction is given, for example, in [1]). Here we shall derive the conditions for thermodynamic stability of arbitrary reacting ideal gas systems, with the intention of using the results to derive a number of general inequalities of chemical thermodynamics.

The chemical equilibrium conditions have the form (i = 1, 2, . . . , k):

$$\begin{aligned} \delta\Phi &= \sum_i \left(\frac{\partial\Phi}{\partial N_i}\right)_{p,T} \delta N_i = \sum_i \mu_i(p, T)\,\delta N_i = 0, \\ \delta F &= \sum_i \left(\frac{\partial F}{\partial N_i}\right) \quad \delta N_i = \sum_i \mu_i(v, T)\,\delta N_i = 0, \end{aligned} \tag{1}$$

where

$$\begin{aligned} \mu_i(p, T) &= \mu_i^0(p, T) + RT \ln (N_i/N), \\ \mu_i(v, T) &= \mu_i^0(v, T) + RT \ln N_i \end{aligned} \tag{2}$$

are the chemical potentials of an ideal gas in the variables p, T and v, T, respectively [the first terms in (2) are independent of the number of moles N_i and N].

Using the representations (s, t = 1, 2, . . . , r),

$$\delta N_i(p, T) = \sum_s \nu_{is}\delta\alpha_s, \quad \delta N_i(v, T) = \sum_s \nu_{is}\,\delta\beta_s, \tag{3}$$

which are forms of the steady-flow relationship, Eq. (1) may be otherwise written:

$$\delta\Phi = \sum_{s,i} \nu_{is}\mu_i\delta\alpha_s = \sum_s \varphi_s\delta\alpha_s = 0,$$

$$\delta F = \sum_{s,i} \nu_{is}\mu_i\delta\beta_s = \sum_s f_s\delta\beta_s = 0.$$

Since the variable $\delta\alpha_s$ and $\delta\beta_s$ are independent, $\varphi_s = f_s = 0$. Using (2) and (3), the desired second variations of the characteristic functions may be represented in the form

$$\frac{\delta^2\Phi}{NRT} = \sum_{s,t} \Phi_{s,t}\frac{\delta\alpha_s}{N}\frac{\delta\alpha_t}{N}, \quad \frac{\delta^2 F}{NRT} = \sum_{s,t} F_{st}\frac{\delta\beta_s}{N}\frac{\delta\beta_t}{N}, \tag{4}$$

where

$$\Phi_{st} = \sum_i \frac{\nu_{is}\nu_{it}}{x_i} - \nu_s\nu_t = F_{st} - \nu_s\nu_t = \Phi_{ts}, \qquad F_{st} = \sum_i \frac{\nu_{is}\nu_{it}}{x_i} = F_{ts}. \tag{5}$$

where $\nu_s = \sum_i \nu_{is}$ is the total stoichiometric coefficient of the reaction s.

The condition for positive values of the bilinear forms (4) consists in having positive values for all the principal diagonal elements and principal minors of the corresponding matrices $\|\Phi_{st}\|$ and $\|F_{st}\|$. In view of the arbitrariness of the number of reactions, it is obviously sufficient to show that the principal diagonal elements and the complete determinants of the matrices $\|\Phi_{st}\|$ and $\|F_{st}\|$ are positive.

We shall introduce the characteristic matrix of our system, which obviously completely determines the properties of the system:

$$\|M\| = \begin{Vmatrix} \nu_{11}\nu_{12}\cdots\nu_{1r}\ x_1 \\ \nu_{21}\nu_{22}\cdots\nu_{2r}\ x_2 \\ \vdots\ \vdots\ \ \vdots\ \ \vdots \\ \nu_{k1}\nu_{k2}\cdots\nu_{k\,r}x_k \end{Vmatrix}. \tag{6}$$

By means of a direct calculation using the normalizing condition $\sum_i x_i = 1$, it is not difficult to show that the principal diagonal elements of the matrix $\|\Phi_{st}\|$ have the form

$$\Phi_{ss} = \frac{1}{2}\sum_{i_1,i_2} \frac{m^2_{i_1,i_2;s}}{x_{i_1}x_{i_2}} > 0,$$

where $m_{i_1,i_2,s}$ are the square minors of $\|M\|$, the elements of which are found at the intersections of the rows having indices $i_1 \neq i_2$ with the columns having indices s and r + 1. The positive value of F_{ss} is obvious. The conditions $\Phi_{ss} > 0$ and $F_{ss} > 0$ are sufficient for thermodynamic stability of one reaction in the system, and have already been found in [1].

Let $\Delta_{i_1, i_2,\ldots,i_{r+1}}$ be the minors of $\|M\|$ of order r + 1, consisting of the rows with indices $i_1 \neq i_2 \ldots \neq i_{r+1}$, and let $\delta_{i_1, i_2,\ldots,i_r}$ be the minors of order r of the first r columns and rows of $\|M\|$ with the same indices. For the complete determinants Δ and δ of the matrices $\|\Phi_{st}\|$ and $\|F_{st}\|$, there are the following representations, obtained inductively:

$$\Delta = \frac{1}{(r+1)!}\sum_{i_1,i_2,\ldots,i_{r+1}} \frac{\Delta^2_{i_1,i_2,\ldots,i_{r+1}}}{x_{i_1}x_{i_2}\cdots x_{i_{r+1}}} > 0,$$

$$\delta = \frac{1}{r!}\sum_{i_1,i_2,\ldots,i_r} \frac{\delta^2_{i_1,i_2,\ldots,i_r}}{x_{i_1}x_{i_2}\cdots x_{i_r}} > 0.$$

It is obvious that at least one of the $m_{i_1,i_2,s}$ and $\Delta_{i_1,i_2,\ldots,i_{r+1}}$ is different from zero, because otherwise, in view of the fact that some of the ν_{is} are necessarily negative, a meaningless conclusion would be reached, namely, that some of the x_i are negative. The fact that at least one of the $\delta_{i_1,i_2,\ldots,i_r}$ is different from zero follows from the condition that the reactions are independent. Thus, the conditions for positive values of the forms (4) are fulfilled, and this means that the system under consideration is thermodynamically stable, if at least one reaction is actually taking place.

The molar heat capacities have the form

$$c_p/R = \sum_j \frac{c_{p_i}}{R}x_i + \sum_i \frac{H_i}{RT}u_i, \quad c_v/R = \sum_i \frac{c_{v_i}}{R}x_i + \sum_i \frac{U_i}{RT}v_i, \tag{7}$$

where $u_i = \frac{1}{N}\left(\frac{\partial N_i}{\partial \ln T}\right)_p$, $v_i = \frac{1}{N}\left(\frac{\partial N_i}{\partial \ln T}\right)_v$.

Making the substitutions $u_i = \sum_s \nu_{is}\gamma_s$, $v_i = \sum_s \nu_{is}\delta_s$, we obtain, for the chemical parts of the heat capacities, the expressions

$$c_{p_{ch}}/R = \sum_s \left(\frac{Q_{p_s}}{RT}\right)\gamma_s, \quad c_{v_{ch}}/R = \sum_s \left(\frac{Q_{v_s}}{RT}\right)\delta_s, \tag{8}$$

where $Q_{p_s} = \sum_i \nu_{is} H_i$ —the heat effect of the reaction p = const, Q_{vs} is equal to $\sum_i \nu_{is} U_i = Q_{p_s} - \nu_s RT$ at v = = const.

Taking logarithms of the equations of the mass action law in the form (9), and then differentiating with respect to T at p = const and v = const,

$$\prod_i N_i^{\nu_{is}} = \left(\frac{N}{p}\right)^{\nu_s} K_{p_s} = \left(\frac{V}{RT}\right)^{\nu_s} K_{p_s}, \tag{9}$$

where K_{ps} is the equilibrium constant, we obtain the systems for determining γ_s and δ_s:

$$\sum_t \Phi_{st}\gamma_t = \frac{Q_{p_s}}{RT}, \quad \sum_t F_{st}\delta_t = \frac{Q_{v_s}}{RT}. \tag{10}$$

Here, use is made of the relation $\partial \ln K_{ps}/\partial \ln T = d \ln K_{ps}/d \ln T = Q_{ps}/RT$.

From (8) and (10), in view of the demonstrated thermodynamic stability of the system, we obtain the results which interest us:

$$c_{p_{ch}}/R = \sum_{s,t} \Phi_{st}\gamma_s\gamma_t > 0, \quad c_{v_{ch}}/R = \sum_{s,t} F_{st}\delta_s\delta_t > 0. \tag{11}$$

This is the first pair of general inequalities of chemical thermodynamics.*

We shall consider the quantities

$$\left(\frac{\partial \ln \mu}{\partial \ln p}\right)_T = -\left(\frac{\partial \ln N}{\partial \ln p}\right)_T = -\sum_i p_i, \quad \left(\frac{\partial \ln \mu}{\partial \ln \rho}\right)_T = \left(\frac{\partial \ln N}{\partial \ln v}\right)_T = \sum_i q_i, \tag{12}$$

where μ is the molecular weight of the system, p_i is equal to $\frac{1}{N}\left(\frac{\partial N_i}{\partial \ln p}\right)_T$ and q_i is equal to $\frac{1}{N}\left(\frac{\partial N_i}{\partial \ln v}\right)_T$.

Making the substitutions $\sum_s \nu_{is}\xi_s$, q_i and $\sum_s \nu_{is}\eta_s$, we obtain

$$\left(\frac{\partial \ln \mu}{\partial \ln p}\right)_T = -\sum_s \nu_i \xi_s, \quad \left(\frac{\partial \ln \mu}{\partial \ln \rho}\right)_T = \sum_s \nu_s \eta_s. \tag{13}$$

Taking logarithms of Eq. (9), and then differentiating with respect to pv at T = const, we obtained the systems for determining ξ_s and η_s:

$$\sum_t \Phi_{st}\xi_t = -\nu_s, \quad \sum_t F_{st}\eta_t = \nu_s. \tag{14}$$

From (13) and (14), in view of the demonstrated thermodynamic stability of the system, we obtain the results which interest us:

$$\left(\frac{\partial \ln \mu}{\partial \ln p}\right)_T = \sum_{s,t} = \Phi_{st}\xi_s\xi_t > 0, \quad \left(\frac{\partial \ln \mu}{\partial \ln \rho}\right)_T = \sum_{s,t} F_{st}\eta_s\eta_t > 0. \tag{15}$$

This is the second pair of general inequalities of chemical thermodynamics.

*Reference [2] gives a demonstration of the positive value of only the over-all c_p and c_v.

To satisfy the inequality (11), it is sufficient for at least one Q_{p_s}, Q_{v_s} pair to be different from zero; to satisfy the inequality (15) it is sufficient for at least one ν_s to be different from zero.

Using further the relation between Φ_{st} and F_{st}, it is not difficult to obtain the inequality

$$\left(\frac{\partial \ln \mu}{\partial \ln p}\right)_T \left[\left(\frac{\partial \ln \mu}{\partial \ln p}\right)_T - \left(\frac{\partial \ln \mu}{\partial \ln \rho}\right)_T\right] = \sum_{s,t} F_{st} (\xi_s + \eta_s)(\xi_t + \eta_t) > 0. \tag{16}$$

Thus, in view of (15),•

$$0 < \left(\frac{\partial \ln \mu}{\partial \ln \rho}\right)_T < \left(\frac{\partial \ln \mu}{\partial \ln p}\right)_T; \tag{17}$$

$$0 < \left(\frac{\partial \ln p}{\partial \ln \rho}\right)_T = \left(\frac{\partial \ln \mu}{\partial \ln \rho}\right)_T \Big/ \left(\frac{\partial \ln \mu}{\partial \ln p}\right)_T < 1. \tag{18}$$

In addition, from the equation of state we have

$$0 < \left(\frac{\partial \ln \mu}{\partial \ln \rho}\right)_T = 1 - \left(\frac{\partial \ln p}{\partial \ln \rho}\right)_T < 1. \tag{19}$$

The dimensionless isothermal velocity of sound $(\partial \ln p/\partial \ln \rho)_T$ may also be represented as:

$$0 < \left(\frac{\partial \ln p}{\partial \ln \rho}\right)_T = \left(\frac{\partial \ln p}{\partial \ln \rho}\right)_v \Big/ \left(\frac{\partial \ln v}{\partial \ln T}\right)_p = \frac{1 - (\partial \ln \mu / \partial \ln T)_v}{1 - (\partial \ln \mu / \partial \ln T)_p} < 1. \tag{20}$$

It follows from (20), in particular, that at $(\partial \ln \mu/\partial \ln T)_v > 1$ we have $1 < (\partial \ln \mu / \partial \ln T)_v < (\partial \ln \mu/\partial \ln T)_p$, and at $(\partial \ln \mu / \partial \ln T)_v < 1$ we have $(\partial \ln \mu / \partial \ln T)_p < (\partial \ln \mu / \partial \ln T)_v < 1$.

Since $(c_p - c_v)/R = (\partial \ln p/\partial \ln T)_v (\partial \ln v/\partial \ln T)_p$, (20) gives the evaluation

$$\left[1 - \left(\frac{\partial \ln \mu}{\partial \ln T}\right)_v\right]^2 - 1 < \frac{c_{p_{ch}} - c_{v_{ch}}}{R} < \left[1 - \left(\frac{\partial \ln \mu}{\partial \ln T}\right)_p\right]^2 - 1. \tag{21}$$

At $(\partial \ln \mu / \partial \ln T)_v < 0$, from (21) we have $c_{p_{ch}} - c_{v_{ch}} > 0$, and, in addition,

$$\left(\frac{\partial T}{\partial v}\right)_u = \frac{p}{c_v}\left(\frac{\partial \mu}{\partial \ln T}\right)_v < 0, \quad \left(\frac{\partial T}{\partial p}\right)_h = -\frac{v}{c_p}\left(\frac{\partial \mu}{\partial \ln T}\right)_p > 0.$$

LITERATURE CITED

1. Ya. B. Zel'dovich, Zhur. Fiz. Khim. 11, 685 (1938).
2. L. Landau and E. Lifshitz, Statistical Physics [in Russian] (Moscow-Leningrad, 1951).

All abbreviations of periodicals in the above bibliography are letter-by-letter transliterations of the abbreviations as given in the original Russian journal. *Some or all of this periodical literature may well be available in English translation.* A complete list of the cover-to-cover English translations appears at the back of this issue.

•Reference [2] demonstrates only that $(\partial \ln p/\partial \ln \rho)_T$ is positive.

FORMATION OF ACETYLENE ON ADIABATIC COMPRESSION OF METHANE

D. S. Tsiklis and M. D. Borodina

State Scientific Research and Planning Institute of the Nitrogen Industry and of Products of Organic Synthesis

(Presented by Academician S. I. Vol'fkovich, May 4, 1961)
Translated from Doklady Akademii Nauk SSSR, Vol. 140, No. 6, pp. 1376-1379, October, 1961
Original article submitted April 28, 1961

The reaction of formation of acetylene from methane

$$2CH_4 = C_2H_2 + 3H_2 \quad (1)$$

takes place within very short intervals of time, i.e., of the order of 0.001 sec. At temperatures up to 3000°K, acetylene is thermodynamically unstable, so that it is necessary to subject the reaction products to cooling which is as rapid as possible. These characteristics of the process involved lead to the assumption that the method of adiabatic compression of gases is suitable for carrying out the reaction under consideration.*

The work described in this instance was carried out with the purpose of verifying the correctness of that assumption. The experiments were conducted in equipment which is described in detail in [4] and [5]. The content of acetylene in the gas after the experiments was determined by a colorimetric method [6]. In cases when the content of acetylene was greater than 0.1%, the determination was made by an argentometric method [7].

The equilibrium constant of reaction (1) can be calculated from the equation (2)**

$$\lg K = -\frac{18077}{T} + 13{,}09 \lg T - 0{,}0_2347T + 0{,}0_6335T^2 - \frac{107520}{T^2} - 23{,}9. \quad (2)$$

Knowing the equilibrium constant, and assuming that at high temperatures (temperatures amounting to thousands of degrees) the volatilities of methane, hydrogen, and acetylene do not differ significantly from the pressure even at high degrees of compression, we calculated the equilibrium concentrations of acetylene at the pressures of 1, 1000, and 10,000 atm.

A calculation showed that at atmospheric pressure and a temperature which amounts, for instance, to 1500°K, the reaction goes almost to completion, and that at a pressure of 10,000 atm up to 2% of acetylene may form at this temperature. It follows from the equation of the methane adiabate that a temperature of 1500°K can be obtained by compressing methane to 1300 atm. However, we did not find any acetylene in the gas even after compressing pure methane to 10,000 atm.

After assuming that a higher temperature is required for the formation of acetylene at high pressures, we investigated the compression of mixtures of methane with nitrogen, helium, argon, xenon, krypton, and hydrogen, gases, the heat capacity of which is lower than that of methane and the compression temperature of which is higher. We investigated mixtures of methane with nitrogen containing 2, 4, 14, and 38% by volume of methane; with argon containing 2, 4, 6, 7, and 14% of methane; with helium containing 3, 6, and 14% of methane; with xenon containing quantities of methane beginning with 7%; with krypton containing 3% of methane; and with hydrogen containing

*Lately one encounters in the literature, with increasing frequency, publications which deal with the investigation of gas reactions in equipment in which adiabatic compression is applied, either by compressing the gas mixture with a piston [4] or by using a shock wave [2,3].

**According to Ya. S. Kazarnovskii.

Yield of Acetylene in Relation to the Pressure after Compression of Mixtures of Methane with Nitrogen, Argon, Helium, and Xenon.

Pressure in kg/cm² after compression	Mixture of CH_4 with N_2								Mixture of CH_4 with Ar								Mixture of CH_4 with He								CH_4+Xe		CH_4+Kr	
	2% CH_4		4%		14%		38%		2%		4%		6%		7%		14%		3%		6%		14%		7%		3%	
	a	η	a	η	a	η	a	η	a	η	a	η	a	η	a	η	a	η	a	η	a	η	a	η	a	η	a	η
300	0,002	0,95	—	—	—	—	—	0,006	0,13	13,7	0,05	2,7	0,04	1,5	0,02	0,7	0,006	0,10	0,05	5,1	—	—	0,04	0,5	—	—	0,14	10,1
500	0,006	1,62	0,002	0,11	—	—	—	0,007	0,18	19,4	0,14	7,6	0,08	3,1	0,05	1,7	0,218	3,8	0,06	6,7	0,005	—	0,30	0,06	2,00	0,01	0,30	15 11,0
1000	0,025	3,85	0,018	2,40	—	—	—	0,008	0,02	2,2	0,29	16,3	0,19	7,6	0,11	3,8	0,116	2,1	0,09	9,2	0,03	1,8	0,10	3,0	0,07	2,3	0,18	13,6
1500	0,053	6,90	0,041	2,65	0,004	0,12	0,0007	0,008	0,01	1,2	0,38	21,8	0,29	11,9	0,17	6,0	0,056	1,0	0,11	10,9	0,08	3,6	0,07	1,6	0,13	4,1	0,21	16,4
2000	0,080	9,50	0,032	1,78	0,011	0,35	0,0008	0,009	0,009	1,1	0,44	26,0	0,39	16,5	0,23	8,2	0,026	0,5	0,12	12,1	0,16	6,3	0,03	0,8	0,18	5,9	0,24	19,2
2500	0,076	8,64	0,027	1,33	0,029	0,56	0,0009	0,010	0,008	1,0	0,48	29,1	0,43	18,7	0,29	10,6	0,017	0,3	0,14	13,2	0,25	16,7	0,02	0,6	0,22	7,5	0,26	21,3
3000	0,063	6,92	0,022	1,03	0,025	0,46	0,0010	0,0105	0,007	0,9	0,49	30,4	0,45	20,0	0,35	13,1	0,015	0,3	0,14	14,3	0,35	19,4	0,01	0,4	0,27	9,0	0,29	24,4
4000	0,041	4,41	0,016	0,80	0,019	0,33	0,0014	0,012	0,006	0,8	0,50	32,5	0,45	20,7	0,44	17,1	0,013	0,3	0,16	15,3	0,32	17,6	0,007	0,3	0,33	11,6	0,35	30,7
5000	0,027	2,87	0,012	0,69	0,014	0,26	0,0020	0,018	0,005	0,6	0,49	33,1	0,44	21,1	0,48	19,3	0,011	0,2	0,16	16,3	0,29	15,8	0,007	0,2	0,38	13,8	0,37	32,7
6000	0,019	2,00	0,009	0,57	0,012	0,22	0,0034	0,027	0,004	0,5	0,47	33,1	0,44	21,3	0,49	20,4	0,009	0,2	0,17	17,1	0,26	14,2	0,006	0,2	0,41	15,7	0,34	31,8
7000	0,014	1,47	0,007	0,48	0,011	0,20	0,0060	0,045	0,002	0,3	0,45	32,6	0,43	21,7	0,47	20,2	0,007	0,2	0,17	17,7	0,24	12,7	0,006	0,1	0,42	17,4	0,32	30,5
8000	0,0105	1,10	0,006	0,40	0,011	0,20	0,0040	0,036	0,001	0,1	0,43	32,1	0,43	22,0	0,45	19,8	0,005	0,1	0,17	18,1	0,21	11,3	0,005	0,1	0,43	18,8	0,30	29,1
9000	0,010	1,06	0,005	0,30	0,011	0,20	0,0028	0,025	0,001	0,1	0,40	30,5	0,42	22,3	0,41	18,4	0,003	0,1	0,17	18,4	0,18	9,9	0,005	0,1	0,44	20,0	0,28	27,7

Note: a = content of acetylene in the gas mixture in volume percent; η = yield of acetylene in percent.

4 and 14% of methane. We employed in the investigation methane having a purity of 99.5%, helium and argon of a purity of 99.9%, and xenon and krypton which were 100% pure. The electrolytic hydrogen and nitrogen which were used had been preliminarily freed of oxygen.

The results of the investigation are listed in the table, which contains graphically adjusted data on the content of acetylene in the gas given in volume percent, and on the yield of acetylene (η).

To calculate the yield of acetylene, the composition of the mixture after the experiment had to be determined. In cases when we worked with mixtures of methane and nitrogen, the composition of the mixture after compression, as could be established by mass-spectrographic analysis, differed little from the initial composition. For instance, a mixture which contained 5.5% of methane and 94.5% of nitrogen before being compressed, contained, after compression, in addition to acetylene, 94.9% of N_2, 0.6% of O_2, 0.036% of CO_2, 3.5% of CH_4, 0.13% of C_2H_4, and a small quantity of higher hydrocarbons.

In the cases when mixtures of methane with argon, hydrogen, helium, xenon, and krypton were compressed (i.e., mixtures with gases the molecular weight of which differs significantly from that of nitrogen), it was necessary to take into consideration changes in the composition of the mixture resulting from leakage and outflow of the gas. When the piston moved through the shaft of the adiabatic compression apparatus at the start of the process of compression, i.e., at the time when the piston began to move, the pressure of the propellant gas (nitrogen) was higher than the pressure within the shaft, so that a part of the nitrogen leaked into the gas being investigated through the clearance between the piston and the wall of the shaft. As the piston approached the closed end of the shaft, the pressure within the shaft increased, while that of the nitrogen used as a propellant decreased. As a result, there was outflow of the gas being compressed through the clearance between the piston and the wall of the shaft.

The leakage and outflow could not have a significant effect on the composition of the mixture when mixtures with nitrogen were investigated. On the other hand, when mixtures of methane with hydrogen or with other gases were investigated, the addition of nitrogen had a significant effect in changing the composition of the mixture. To take account of these changes, we determined the molecular weight of mixtures obtained after compression of argon and other gases with nitrogen at different pressures of the nitrogen used as a propellant, and obtained curves on the basis of which the molecular weight of the mixtures with methane, which were being

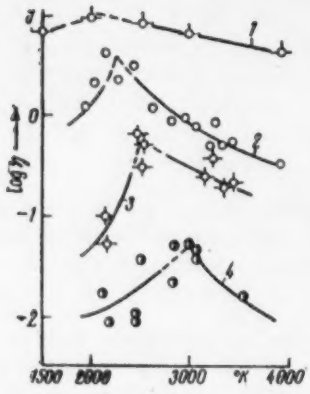

Fig. 1. Curves showing the relation between the yield of acetylene η and the pressure (temperature): 1) mixture of 2% CH_4 and 98% N_2; 2) mixture of 4% CH_4 and 96% N_2; 3) 14% CH_4 + 86% N_2; 4) 38% CH_4 + + 62% N_2.

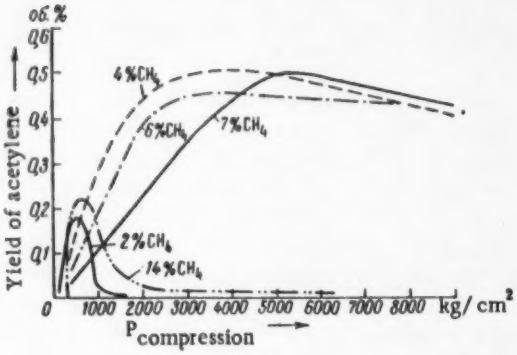

Fig. 2.

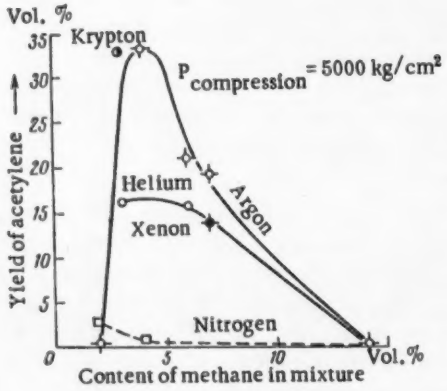

Fig. 3.

investigated, was determined. Knowing the molecular weight of the mixture before and after compression, and assuming that a mixture of constant composition leaks during the motion of the piston along the channel, one can calculate the composition of the mixture after compression. The calculation of the yield η was carried out by relating the volume percentage of acetylene in the mixture to an equilibrium concentration of acetylene that would have formed from a mixture, the composition of which was determined under consideration of leakage and outflow.

The data obtained by us indicated that at higher contents of nitrogen in the mixture the yield of acetylene was also higher (approximately 9% in the cases of a mixture containing 98% of nitrogen – c.f. Fig. 1). The curves expressing the dependence of the acetylene yield η on the pressure (the temperature) exhibited a pronounced maximum which moved to lower temperatures (pressures) as the content of the methane in the mixture decreased. At high temperatures formation of carbon black was observed. After compression of mixtures of methane with helium, argon, xenon, and krypton, there was formation of large quantities of acetylene. The nature of the curves expressing the dependence of the yield of acetylene on the pressure upon compression of mixtures of methane with argon differed from the corresponding curves for nitrogen (Fig. 2).

As distinguished from mixtures with nitrogen, the mixtures with argon and helium have a composition at which the yield reaches a maximum (Fig. 3). It can be seen from Fig. 3 that the yield of acetylene was higher in mixtures with argon than those with helium, xenon, and krypton. This indicates that, although the heat capacity of monoatomic gases is the same and, consequently, the temperature of compression is also the same, the nature of the gas apparently has an effect on the process. This assumption is confirmed by the fact that no acetylene is formed in mixtures with hydrogen.

Let us consider the process of transmission of energy following a collision of molecules [8]. At high densities of the gas, when collisions of molecules with the wall can be regarded as negligible in quantity in comparison with collisions in the mass of the gas, changes in the properties of the gas take place as a result of molecular collisions.

The molecules may enter into a chemical reaction when they have a sufficient amount of energy. They acquire this energy as a result of favorable collisions with molecules having an average energy. The processes of energy exchange have been considered using rigid spheres as models. It is known that a decomposition of a methane

molecule may take place when this molecule has a sufficient amount of vibrational energy. Consideration of the case of exchange of vibrational energy [8] indicates that the transfer of energy is more effective when the masses which collide are comparable in magnitude.

If we consider the experiments with monoatomic gases from this point of view, we can make the following approximate calculation. If we assume the mass of methane to be equal to unity, we find that the masses of the other gases are as follows: $M_{He} = 0.25$, $M_{Ar} = 2.5$, $M_{Kr} = 5.3$, $M_{Xe} = 8.1$. On the basis of this calculation, the most efficient transfer of energy must take place between methane and argon. Actually, the highest yield of acetylene resulted when mixtures of methane with argon were compressed.

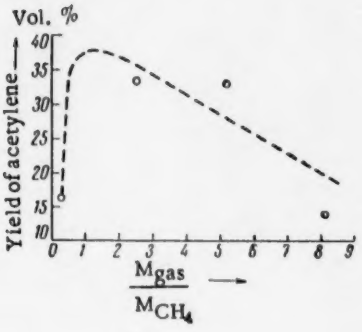

Fig. 4.

The course of the curve on Fig. 4, where the yield of acetylene has been plotted in relation to the relative mass of the diluent gas, indicates that the maximum yield must result when M is approximately equal to unity.*

The absence of acetylene upon compression of a mixture of methane with hydrogen confirms the concept [9] that the first stage of the decomposition of methane must involve splitting off of hydrogen:

$$CH_4 \rightarrow CH_2 + H_2$$

Addition of hydrogen to the mixture must inhibit the reaction formulated above and prevent formation of acetylene, notwithstanding the fact that the temperature of compression is approximately the same as in the case of a mixture with nitrogen.

LITERATURE CITED

1. P. A. Longwell and B. H. Sage, J. Chem. and Eng. Data 5, 322 (1960).
2. G. B. Skinner and W. E. Ball, J. Phys. Chem. 64, 1025 (1960).
3. G. B. Skinner and E. M Sokoloski, J. Phys. Chem. 64, 1028 (1960).
4. Yu. N. Ryabinin, Zhur. Exptl. i Theor. Fiz. 23, 461 (1953).
5. D. S. Tsiklis, Technique of Physicochemical Investigations at High Pressures [in Russian] (1958).
6. Analytical Control of Production in the Nitrogen Industry [in Russian] (1957) Vol. 3, p. 47.
7. L. Barnes and L. J. Modilini, Anal. Chem. 27, 1025 (1955).
8. S. W. Benson, The Forendations of Chemical Kinetics (1960).
9. L. Belchets and E. K. Riedel, J. Am. Chem. Soc. 57, 1168 (1935).

All abbreviations of periodicals in the above bibliography are letter-by-letter transliterations of the abbreviations as given in the original Russian journal. *Some or all of this periodical literature may well be available in English translation.* A complete list of the cover-to-cover English translations appears at the back of this issue.

---

*The point for xenon refers to a mixture of xenon with 7% of methane. By analogy with the other mixtures, one may assume that for a mixture of 3% of methane with xenon the yield will increase to approximately 20%, and that the point for xenon will then be located on the curve.

RADIATION-CHEMICAL TRANSFORMATIONS OF IRON IONS IN $HClO_4$ SOLUTIONS SATURATED WITH HYDROGEN AND OXYGEN UNDER PRESSURE

V. N. Shubin and P. I. Dolin

Institute of Electrochemistry, Academy of Sciences of the USSR
(Presented by Academician A. N. Frumkin, April 18, 1961)
Translated from Doklady Akademii Nauk SSSR, Vol. 140, No. 6, pp. 1380-1383, October, 1961

It was found in preceeding work [1,2] that reliable conclusions on the mechanism of the radiolysis in the absence of oxygen of aqueous solutions of compounds containing iron ions can be made on the basis of results obtained under conditions when the products of the radiolysis of water are completely used up in competing reactions, the velocities of which can be controlled by changing the concentrations of the dissolved substances. Most suitable for this purpose proved to be a system containing Fe^{2+}, Fe^{3+}, H_2, and H^+, in which the direction of the radiolysis process and its velocity are determined by the competition of Fe^{2+} and H_2 for OH radicals and the competition of Fe^{3+} and H^+ for H atoms.

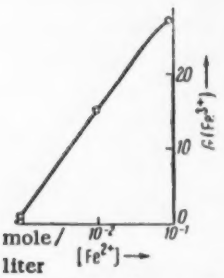

Fig. 1. Dependence of the oxidation yield on the concentration of Fe^{2+}. $[Fe^{3+}] \simeq 10^{-3}$M; $[HClO_4] \simeq 10^{-2}$M; P_{O_2} = 10.2 atm; $[Fe^{2+}]/[H_2] \simeq$ const.

In the radiolysis of Fe^{2+} and Fe^{3+} solutions containing oxygen, one may expect that the process will be determined by the competition of Fe^{3+} and O_2 for H atoms, and the competition of Fe^{2+} and Fe^{3+} for HO_2 radicals. The ratio of the velocities of the two last-mentioned competing reactions must be affected by the dissociation of HO_2, which depends on the pH of the solution. In the presence of H_2, competition of H_2 and Fe^{2+} for OH radicals must arise.

The following mechanism has been postulated for the radiation-chemical oxidation of Fe^{2+} solution in the presence of O_2 [3]:

$$H + O_2 \rightarrow HO_2; \quad (1)$$

$$HO_2 + Fe^{2+} \rightarrow Fe^{3+} + HO_2^-; \quad (2)$$

$$HO_2^- + H^+ \rightarrow H_2O_2; \quad (3)$$

$$H_2O_2 + Fe^{2+} \rightarrow + Fe^{3+}OH^- + OH; \quad (4)$$

$$OH + Fe^{2+} \rightarrow Fe^{3+} + OH^-. \quad (5)$$

In the presence of Fe^{3+}, the following reactions are also supposed to take place [4]:

$$H + Fe^{3+} \rightarrow Fe^{2+} + H^+; \quad (6)$$

$$HO_2 \rightleftarrows H^+ + O_2^-; \quad (7)$$

$$O_2^- + Fe^{3+} \rightarrow Fe^{2+} + O_2. \quad (8)$$

Systems of this type were investigated by Allen and Rotschild [5,6]. It was established that under the conditions in question there is competition of Fe^{2+} and O_2 for H atoms (or H_2^+), in such a manner that the ratio of the velocity constants of these reactions does not depend on the pH. By employing the mechanism formulated above, these authors determined from experimental data the values for the ratios k_6/k_1 and $k_2/k_{Fe^{3+},HO_2}$.

However, in order to obtain a confirmation for the mechanism postulated, one must carry out the most complete experimental check of the relation between the velocity of the total process and the ratio between the velocities of the competing reactions, which can be set by changing the concentrations of the reacting substances. The relation in question follows from the reaction mechanism. Data on the subject are not available in the literature.

On the other hand, the assumption has been made [7], that the reactions (2) and (3) should be replaced by the reaction

$$2HO_2 \rightarrow H_2O_2 + O_2. \tag{9}$$

In this case, the relation between the velocity of the total process and the concentrations of the dissolved substances will obviously be different.

If H_2 is present in the system indicated, the possibility exists that a chain reaction may take place [8]. The chain will include reactions (1)-(4) or (1), (9), and (4), and also the reaction

$$OH + H_2 \rightarrow H_2O + H. \tag{10}$$

The chain will be terminated by reactions (5)-(8).

In the present work, results are reported of an investigation of the action of γ-rays emitted from a Co^{60} source on solutions of Fe^{2+} and Fe^{3+} ions after these solutions had been saturated with H_2 and O_2 under pressure. The effects of changes in the concentration of the dissolved substances, and also of the concentration of H^+ ions were studied.

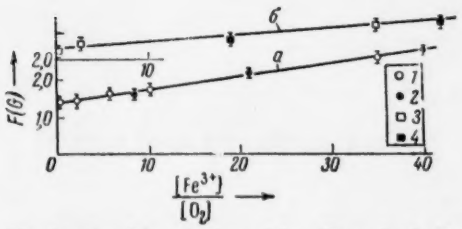

Fig. 2. Graphic solution of Eq. (I) on the basis of data in Table 1: a) concentration of $HClO_4$ ~ ~ 0.12M; 1) dependence on $[O_2]$; 2) dependence on $[Fe^{3+}]$; b) concentration of $HClO_4$ ~ ~ $5 \cdot 10^{-3}$M; 3) dependence on $[O_2]$; 4) dependence on $[Fe^{3+}]$.

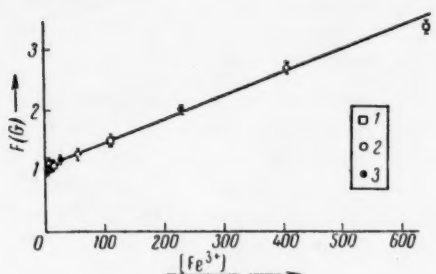

Fig. 3. Graphic solution of Eq. (I) on the basis of data in Table 3: 1) dependence on $[Fe^{3+}]$; 2) dependence on $[Fe^{3+}]$; 3) dependence on $[H^+]$.

EXPERIMENTAL

The cell and equipment for work under pressure were described earlier [8]. The solution, which had been saturated with air, was placed into a steel bomb into which H_2 and O_2 were fed separately one after the other until the required pressure was reached. The oxygen supplied from a cylinder was purified by passing it through a trap immersed in liquid nitrogen.

The experiments were carried out with $Fe(ClO_4)_2$ and $Fe(ClO_4)_3$ solutions which had been prepared by dissolving spectroscopically pure iron in twice-distilled $HClO_4$. All solutions employed in the work in question were made by using twice-distilled water. The magnitude of the radiation dose comprised approximately $1.75 \cdot 10^{15}$ ev/ $cm^3 \cdot$ sec. The concentration of Fe^{2+} was determined by means of o-phenanthroline.

DISCUSSION OF RESULTS

It can be easily seen that if the radiolysis process includes reaction (9), then the oxidation yield will not depend on $[Fe^{2+}]$ when the concentration of all other substances and the value of $[Fe^{2+}]/[H_2]$ remain constant. It follows from Fig. 1, where results of experiments of this type are presented, that the oxidation yield must show a strong dependence on $[Fe^{2+}]$. This proves that the radiolysis takes place with participation of reactions (2) and (3) rather than of the reaction (9).

Then, if we assume that the radiolysis yield is determined by reactions (1)-(8) and (10), we will obtain the following expression* which relates the radiation-chemical yields to the velocities of the competing reactions:

$$\left(1+\frac{k_6[Fe^{3+}]}{k_1[O_2]}\right)\left(1+\frac{k_8}{k_2}K_{HO_2}\frac{[Fe^{3+}]}{[Fe^{2+}][H^+]}\right)= \frac{[G(Fe^{3+})-G_H-G_{OH}-2G_{H_2O_2}]/(1+k_5[Fe^{2+}]/k_{10}[H_2])}{G(Fe^{3+})-G_H-G_{HO}-2G_{H_2O_2}+2[G_H+(G_{OH}+G_{H_2O_2})/(1+k_5[Fe^{2+}]/k_{10}[H_2])]}+ + \frac{4[G_H+(G_{OH}+G_{H_2O_2})/(1+k_5[Fe^{2+}]/k_{10}[H_2])}{G(Fe^{3+})-G_H-G_{OH}-2G_{H_2O_2}+2[G_H+(G_{OH}+G_{H_2O_2})/(1+k_5[Fe^{2+}]/k_{10}[H_2])]}\equiv F(G). \tag{I}$$

*In deriving Eq. (I), a method was used of which a detailed description had been given before [8].

Consideration of Eq. (I) indicates that if, in one of the expressions in parentheses on the left side, the ratio of concentrations remains constant, while in the other expression in parentheses the ratio of concentrations changes, then the expression on the right side must be a linear function of the second ratio.

TABLE 1. Dependence of $G(Fe^{3+})$ on the Concentrations of O_2 and Fe^{3+}. P_{H_2} = 50 atm: $[Fe^{3+}]/[Fe^{2+}] \simeq 13$

Acceptor:	O_2					Fe^{3+}					
Concentration, mM	0.28	0.98	1.68	4.48	14.3	190	100	39	20	11	9.2
$G(Fe^{3+})$, moles/100 ev	3.4	11.9	13.5	18.5	21.5	5	6.7	12.2	–	18.5	–
$[H^+] \sim 0.12M$											
$[H^+] \sim 5 \cdot 10^{-3}M$[6]			–	–	6.6	7	–	–	–	6.7	–	6.6

The dependence of the yield on the concentration of O_2 is given in Table 1. A graphic solution of Eq. (I) on the basis of data in Table 1 is shown in Fig. 2. From the inclination of the straight line we calculate the value of k_6/k_1 to be $2.45 \cdot 10^{-2}$. The length of the section cut off by the straight lines on the axis of ordinates is equal to:

$$1 + \frac{k_6}{k_2} K_{HO_2} \frac{[Fe^{3+}]}{[Fe^{2+}][H^+]},$$

from which we find that

$$\frac{k_6}{k_2} K_{H_2O} \simeq 3{,}1 \cdot 10^{-3} \text{ м/л}.$$

It is obvious that if the Fe^{2+} ion can compete with O_2 for H atoms by reacting with these atoms as follows,

$$Fe^{2+} + H \rightleftarrows FeH^{2+} \xrightarrow{+H^+} Fe^{3+} + H_2, \qquad (11)$$

then the first expression in parentheses in Eq. (I) will assume the following form:

$$1 + (k_6[Fe^{3+}] + k_{11}[Fe^{2+}])/k_1[O_2].$$

In this case, the yield must depend on $[Fe^{2+}]$ under the conditions that $[Fe^{3+}]/[O_2]$, $[Fe^{2+}]/[H_2]$, and $[Fe^{3+}]/[Fe^{2+}] \cdot [H^+]$ are constant. Table 2 gives the results of experiments in which the ratio $[Fe^{2+}]/[O_2]$ was changed while the conditions mentioned above were observed. It can be seen that the oxidation yield for all practical purposes did not change when the value of $[Fe^{2+}]/[O_2]$ was changed by two orders of magnitude. This demonstrates, in a convincing manner, that a reaction of the type (11) does not have to be taken into consideration under the conditions in question.*

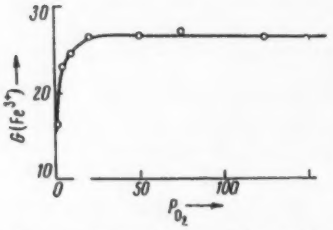

Fig. 4. Dependence of the oxidation yield on the pressure of O_2 above the solution. $[HClO_4] \simeq 0.1M$; $[Fe^{3+}] \simeq 8 \cdot 10^{-3}M$; $[Fe^{2+}] \simeq 1.2 \cdot 10^{-3}M$; P_{H_2} = 50 atm.

It follows from Eq. (I) that a graphic solution of it on the basis of data pertaining to the dependence of the yield on $[O_2]$ and on $[Fe^{3+}]$ must be capable of being represented by a single straight line. The dependence of the yield on the concentration of Fe^{3+} is given in Table 1. A graphic solution of Eq. (I) on the basis of these data is represented in Fig. 2. The results obtained show good agreement with data pertaining to the dependence of $G(Fe^{3+})$ on $[O_2]$.

Allen and Rotschild obtained the value of 0.007 ± 50% for k_6/k_1 in 0.8N H_2SO_4 solutions. If we take into consideration [2] that $[Fe^{3+}]_{eff} \simeq 0.27\,[Fe^{3+}]_{total}$ in sulfuric acid, we find that k_6/k_1 will be equal to $2.6 \cdot 10^{-2}$ ± 50%, which is in good agreement with the value obtained by us.

In order to demonstrate that the mechanism of the radiolysis includes reactions (2), (7), and (8), the relations between the yield of Fe^{3+} and the concentrations of H^+, Fe^{2+}, and Fe^{3+} at $[Fe^{3+}]/[O_2]$ = const were studied.

The results of the experiments in question are given in Table 3. A graphic solution of Eq. (I) on the basis of the results in Table 3 is shown in Fig. 3. From the inclination of the straight line, we find that $k_8K_{HO_2}/k_2 = 3.6 \cdot 10^{-3}$ m/liter.

*It follows from this that the competition of Fe^{2+} and O_2 for a radical particle, which was observed by Allen and Rotschild, took place for the ion-radical H_2^{2+}.

TABLE 2. Effect of the concentration of Fe^{2+} on $G(Fe^{3+})$ $[Fe^{3+}] \sim 9 \cdot 10^{-3}$M; $P_{O_2} = 3.2$ atm: $[Fe^{2+}]/[H_2] \sim 0.8$; $[Fe^{2+}] \cdot [H^+] \sim 4.5 \cdot 10^{-4}$

Concentration of Fe^{2+}, moles/liter	$9 \cdot 10^{-4}$	$9.7 \cdot 10^{-3}$	$9.2 \cdot 10^{-2}$
$G(Fe^{3+})$, moles/100 ev	14.2*	15.5	14.5

*A correction has been made for the effect resulting from the direct action of radiation on $HClO_4$.

TABLE 3. Dependence of the Yield on the Concentration of Fe^{3+}, Fe^{2+}, and H^+. $[Fe^{3+}]/[O_2] \simeq$ const

Acceptor:	Fe^{3+}			Fe^{2+}			H^+		
Concentration, mM	63	8.4	0.15	0.14	0.81	8.3	5.1	45	450
$G(Fe^{3+})$, moles/100 ev	3.7	25	43.5	−1	17.5	19.5	7.5	17	22

For $k_{Fe^{3+}, HO_2}/k_2$, Allen and Rotschild found 0.11 ± 15% and 0.3 ± 50% at pH = 2.1 and pH = 2.7, respectively. If we take into consideration that the reduction of Fe^{3+} by HO_2 radicals takes place according to reactions (7) and (8), and that $[Fe^{3+}]_{eff} \simeq 0.27[Fe^{3+}]_{total}$, we find for $k_8K_{HO_2}/k_2$, $3.75 \cdot 10^{-3}$ m/liter ± 15% and $2.4 \cdot 10^{-3}$ m/liter ± 50%, respectively, which is in good agreement with the value obtained in our experiments.

These results indicate that oxygen is a very active acceptor of H atoms. Under the circumstances, it appeared of advantage to apply oxygen for the clarification of the role which excited water molecules play in the radiolysis of Fe^{2+} and Fe^{3+} solutions, using the method of conjugated acceptors [7]. One can easily see that if excited molecules of water will participate in the reaction under the conditions in question, the expression (I) will be transformed into the inequality

$$\left(1+\frac{k_6[Fe^{3+}]}{k_1[O_2]}\right)\left(1+\frac{k_8}{k_2}K_{H_2O}\frac{[Fe^{3+}]}{[Fe^{3+}][H^+]}\right) > F(G). \qquad \text{(II)}$$

To check this conclusion, we determined the yield in relation to the pressure of oxygen above the solution. The results obtained are represented in Fig. 4. In the region of low concentrations the yield increased with the increase of oxygen pressure, because reaction (6) was suppressed by reaction (1). On further increase of the pressure, the yield reached a constant value which remained unchanged up to oxygen concentrations of approximately 0.1M (150 atm). A calculation carried out on the basis of data in Fig. 4 indicated that for the horizontal part of the curve the condition described by (I) rather than (II) was satisfied. It follows from this that at $[O_2] \leq 0.1$M excited water molecules do not participate in the reactions of the oxidation of Fe^{2+}. All of the results obtained in the work described indicate that the mechanism of radiolysis of Fe^{2+} and Fe^{3+} solutions in the presence of O_2 and H_2, which includes reactions (1)-(8) and (10), describes quantitatively the experimentally established relations between the total process and the concentrations of the substances which participate in the competing reactions that take place.

LITERATURE CITED

1. V. N. Shubin and P. I. Dolin, Doklady Akad. Nauk SSSR 138, No. 1 (1961).
2. V. N. Shubin and P. I. Dolin, Doklady Akad. Nauk SSSR 139, No. 1 (1961).
3. F. H. Kreuz and H. A. Dewhurst, J. Chem. Phys. 17, 1337 (1949).
4. W. G. Barb, J. H. Bakeudale, P. George, and K. R. Hargrave, Trans. Faraday Soc. 47, 591 (1951).
5. A. O. Allen and W. G. Rotschild, Radiation Res. 7, 591 (1957).
6. A. O. Allen, V. D. Hogau, and W. G. Rotschild, Radiation Res. 7, 603 (1957).
7. V. D. Orekhov, A. I. Chernova, and M. A. Proskurnin, Collection of Investigations in Radiation Chemistry [in Russian] (AN SSSR Press, 1955) p. 85.
8. V. N. Shubin and P. I. Dolin, Zhur. Fiz. Khim. 43, 2480 (1960).

Soviet Journals Available in Cover-to-Cover Translation

ABBREVIATION	RUSSIAN TITLE	TITLE OF TRANSLATION	PUBLISHER	TRANSLATION BEGAN Vol.	Issue	Year
AÉ	Atomnaya énergiya	Soviet Journal of Atomic Energy	Consultants Bureau	1	1	1956
Akust. zh.	Akusticheskii zhurnal	Soviet Physics – Acoustics	American Institute of Physics	1	1	1955
	Antibiotiki	Antibiotics	Consultants Bureau	4	1	1959
Astr(on). zh(urn).	Astronomicheskii zhurnal	Soviet Astronomy–AJ	American Institute of Physics	34	1	1957
Avto(mat). svarka	Avtomaticheskaya svarka	Automatic Welding	British Welding Research Association (London)		1	1959
	Avtomatika i Telemekhanika	Automation and Remote Control	Instrument Society of America	27	1	1956
	Biofizika	Biophysics	National Institutes of Health*		1	1957
	Biokhimiya	Biochemistry	Consultants Bureau	21	1	1956
Byull. éksp(erim). biol. i med.	Byulleten' éksperimental'noi biologii i meditsiny	Bulletin of Experimental Biology and Medicine	Consultants Bureau	41	1	1959
DAN (SSSR) / Dokl(ady) AN SSSR	Doklady Akademii Nauk SSSR	The translation of this journal is published in sections, as follows:				
		Life Sciences: Doklady Biochemistry Section	American Institute of Biological Sciences	106	1	1956
		Life Sciences: Doklady Biological Sciences Sections (Includes: Anatomy, biophysics, cytology, ecology, embryology, endocrinology, evolutionary morphology, genetics, histology, hydrobiology microbiology, morphology, parasitology, physiology, zoology sections)	American Institute of Biological Sciences	112	1	1957
		Life Sciences: Doklady Botanical Sciences Sections (Includes: Botany, phytopathology, plant anatomy, plant ecology, plant embryology, plant physiology, plant morphology sections)	American Institute of Biological Sciences	112	1	1957
		Chemical Sciences: Proceedings of the Academy of Sciences of the USSR, Section: Chemical Technology	Consultants Bureau	106	1	1956
		Chemical Sciences: Proceedings of the Academy of Sciences of the USSR, Section: Chemistry	Consultants Bureau	106	1	1956
		Chemical Sciences: Proceedings of the Academy of Sciences of the USSR, Section: Physical Chemistry	Consultants Bureau	112	1	1957
		Earth Sciences: Doklady Earth Sciences Sections (Includes: Geochemistry, geology, geophysics, hydrogeology, mineralogy, paleontology, petrography, permafrost sections)	American Geological Institute	124	1	1959
		Earth Sciences: Proceedings of the Academy of Sciences of the USSR, Section: Geochemistry	Consultants Bureau	106-123	1-6	1957-1958
		Earth Sciences: Proceedings of the Academy of Sciences of the USSR, Sections: Geology	Consultants Bureau	106-123	1-6	1957-1958
		Mathematics: Doklady Soviet Mathematics	The American Mathematics Society	131	1	1961
		Physics: Soviet Physics–Doklady (Includes: Aerodynamics, astronomy, crystallography, cybernetics and control theory, electrical engineering, energetics, fluid mechanics, heat engineering, hydraulics, mathematical physics, mechanics, physics, technical physics, theory of elasticity sections)	American Institute of Physics	106	1	1956
		Physics: Proceedings of the Academy of Sciences of the USSR, Applied Physics Sections (does not include mathematical physics or physics sections)	Consultants Bureau	106-117	1	1956-1957
Derevoobrabat. prom-st'.	Derevoobrabatyvayushchaya promyshlennost'	Wood Processing Industry	Timber Development Association (London)		9	1959
	Élecktrosvyaz	Telecommunications	Massachusetts Institute of Technology*		1	1957
Éntom(ol). oboz(renie)	Éntomologicheskoe obozrenie	Entomological Review	American Institute of Biological Sciences	38	1	1959
Farmakol. (i) toksikol(ogiya)	Farmakologiya i toksikologiya	Pharmacology and Toxicology	Consultants Bureau	20	1	1957
FMM	Fizika metallov i metallovedenie	Physics of Metals and Metallography	Acta Metallurgica*	5	1	1957
Fiziol. zhurn. SSSR (im. Sechenova)	Fiziologicheskii zhurnal im. I. M. Sechenova	Sechenov Physiological Journal USSR	National Institutes of Health*		1	1957
Fiziol(ogiya) rast.	Fiziologiya rastenii	Plant Physiology	American Institute of Biological Sciences	4	1	1957
	Geokhimiya	Geochemistry	The Geochemical Society		1	1958
FTT	Fizika tverdogo tela	Soviet Physics–Solid State	American Institute of Physics	1	1	1959
Izmerit. tekh(nika)	Izmeritel'naya tekhnika	Measurement Techniques	Instrument Society of America		1	1959
Izv. AN SSSR, O(td). Kh(im). N(auk)	Izvestiya Akademii Nauk SSSR: Otdelenie khimicheskikh nauk	Bulletin of the Academy of Sciences of the USSR: Division of Chemical Sciences	Consultants Bureau		1	1952

continued

Izv. AN SSSR, O(td). T(ekhn). N(auk): Met(all). i top.	(see Met. i top.)					
Izv. AN SSSR Ser. fiz(ich).	Izvestiya Akademii Nauk SSSR: Seriya fizicheskaya	Bulletin of the Academy of Sciences of the USSR: Physical Series	Columbia Technical Translations		1	1954
Izv. AN SSSR Ser. geofiz.	Izvestiya Akademii Nauk SSSR: Seriya geofizicheskaya	Bulletin (Izvestiya) of the Academy of Sciences USSR: Geophysics Series	American Geophysical Union		1	1954
Izv. AN SSSR Ser. geol.	Izvestiya Akademii Nauk SSSR: Seriya geologicheskaya	Izvestiya of the Academy of Sciences of the USSR: Geologic Series	American Geological Institute		1	1958
Kauch. i rez.	Kauchuk i rezina	Soviet Rubber Technology	Research Association of British Rubber Manufacturers	18	1	1959
	Kinetika i kataliz	Kinetics and Catalysis	Consultants Bureau	1	3	1960
	Koks i khimiya	Coke and Chemistry USSR	Coal Tar Research Association (Leeds, England)		1	1958
Kolloidn. zh(urn).	Kolloidnyi zhurnal	Colloid Journal	Consultants Bureau	14	1	1952
	Kristallografiya	Soviet Physics – Crystallography	American Institute of Physics	2	1	1957
Metalov. i term. obrabot. metal.	Metallovedenie i termicheskaya obrabotka metallov	Metal Science and Heat Treatment of Metals	Acta Metallurgica	6	1	1958
	Metallurg	Metallurgist	Acta Metallurgica		1	1957
Met. i top.	Metallurgiya i topliva	Russian Metallurgy and Fuels	Eagle Technical Publications		1	1960
Mikrobiol.	Mikrobiologiya	Microbiology	American Institute of Biological Sciences	26	1	1957
OS	Optika i spektroskopiya	Optics and Spectroscopy	American Institute of Physics		6	1959
	Pochvovedenie	Soviet Soil Science	American Institute of Biological Sciences		1	1958
	Priborostroenie	Instrument Construction	British Scientific Instrument Research Association		1	1959
Pribory i tekhn. éks(perimenta)	Pribory i tekhnika éksperimenta	Instruments and Experimental Techniques	Instrument Society of America		1	1957
Prikl. matem. i mekh.	Prikladnaya matematika i mekhanika	Applied Mathematics and Mechanics	American Society of Mechanical Engineers		1	1958
PTÉ	(see Pribory i tekhn. éks.)					
	Problemy Severa	Problems of the North	National Research Council of Canada			
Radiotekh.	Radiotekhnika	Radio Engineering	Massachusetts Institute of Technology*	12	1	1957
Radiotekh. i élektronika	Radiotekhnika i élektronika	Radio Engineering and Electronics	Massachusetts Institute of Technology*	2	1	1957
	Stanki i instrument	Machines and Tooling	Production Engineering Research Assoc.		1	1959
	Stal'	Stal (In English)	Iron and Steel Institute		1	1959
Stek. i keram.	Steklo i keramika	Glass and Ceramics	Consultants Bureau	13	1	1956
Svaroch. proiz-vo	Svarochnoe proizvodstvo	Welding Production	British Welding Research Association		4	1959
Teor. veroyat. i prim.	Teoriya veroyatnostei i ee primenenie	Theory of Probability and Its Applications	Society for Industrial and Applied Mathematics		1	1956
Tsvet. Metally	Tsvetnye metally	Nonferrous Metals	Primary Sources		1	1960
UFN	Uspekhi fizicheskikh Nauk	Soviet Physics – Uspekhi (partial translation)	American Institute of Physics	66	1	1958
UKh	Uspekhi khimii	Russian Chemical Reviews	The Chemical Society (London)		1	1960
UMN	Uspekhi matematicheskikh nauk	Russian Mathematical Surveys	London Mathematical Society	15	1	1960
Usp. fiz. nauk	(see UFN)					
Usp. khim(ii)	(see UKh)					
Usp. matem. nauk	(see UMN)					
Usp. sovr. biol.	Uspekhi sovremennoi biologii	Russian Review of Biology	Oliver and Boyd		48	1959
Vest. mashinostroeniya	Vestnik mashinostroeniya	Russian Engineering Journal	Production Engineering Research Assoc.		4	1959
Vop. gem. i per. krovi	Voprosy gematologii i perelivaniya krovi	Problems of Hematology and Blood Transfusion	National Institutes of Health*		1	1957
Vop. onk.	Voprosy onkologii	Problems of Oncology	National Institutes of Health*		1	1957
Vop. virusol.	Voprosy virusologii	Problems of Virology	National Institutes of Health*		1	1957
Zav(odsk). lab(oratoriya)	Zavodskaya laboratoriya	Industrial Laboratory	Instrument Society of America	25	1	1959
ZhAKh Zh. anal(it). khimii	Zhurnal analiticheskoi khimii	Journal of Analytical Chemistry USSR	Consultants Bureau	7	1	1952
ZhETF Zh. éksperim. i teor. fiz.	Zhurnal éksperimental'noi i theoreticheskoi fiziki	Soviet Physics–JETP	American Institute of Physics	28	1	1955
ZhFKh Zh. fiz. khimii	Zhurnal fizicheskoi khimii	Russian Journal of Physical Chemistry	The Chemical Society (London)		7	1959
ZhMÉI Zh(urn). mikrobiol. épidemiol. i immunobiol.	Zhurnal mikrobiologii, épidemiologii i immunobiologii	Journal of Microbiology, Epidemiology and Immunobiology	National Institutes of Health*		1	1957
ZhNKh Zh(urn). neorgan(ich). khim(ii)	Zhurnal neorganicheskoi khimii	The Russian Journal of Inorganic Chemistry	The Chemical Society (London)		1	1959
ZhOKh Zh(urn). obshch(ei) khimii	Zhurnal obshchei khimii	Journal of General Chemistry USSR	Consultants Bureau	19	1	1949
ZhPKh Zh(urn). prikl. khimii	Zhurnal prikladnoi khimli	Journal of Applied Chemistry USSR	Consultants Bureau	23	1	1950
ZhSKh Zh(urn). strukt. khimii	Zhurnal strukturnoi khimii	Journal of Structural Chemistry	Consultants Bureau	1	1	1960
ZhTF Zh(urn). tekhn. fiz.	Zhurnal teknicheskoi fiziki	Soviet Physics–Technical Physics	American Institute of Physics	26	1	1956
Zh(urn). vyssh. nervn. deyat. (im. Pavlova)	Zhurnal vysshei nervnoi deyatel'nosti (im. I. P. Pavlova)	Pavlov Journal of Higher Nervous Activity	National Institutes of Health*		1	1958

*Sponsoring organization. Translation through 1960 issues is a publication of Pergamon Press.

ABBREVIATIONS MOST FREQUENTLY ENCOUNTERED IN RUSSIAN GEOLOGICAL SCIENCES LITERATURE

Abbreviation (Transliterated)	Significance
ANII	Arctic Scientific Research Institute
FIAN	Physics Institute, Academy of Sciences, USSR
Geologizdat	Geological Press
GGGT	Geological-Hydrological-Geodetic Trust
GGI	State Hydrological Institute
GGK	Main Geodetic Committee
GGO	Main Geological Observatory
GGU	Main Hydrographic Administration
GITI	State Scientific-Technical Press
GITTL	State Technical and Theoretical Literature Press
GOI	State Oceanography Institute
GONTI	State United Scientific-Technical Press
Goskhimizdat	State Chemical Press
GOST	All-Union State Standard
GTTI	State Technical-Theoretical Press
IGD	Institute of Mining
IGN	Institute of Geological Sciences
IL	Foreign Literature Press
ISN (Izd. Sov. Nauk)	Soviet Science Press
Izd. AN SSR	Academy of Sciences USSR Press
Izd. MGU	Moscow State University Press
MGI	Moscow Geodetic Institute
MOIP	Moscow Society of Naturalists
NGRI	Petroleum Geological Prospecting Institute
NIIG	Scientific Research Institute of Hydro-Engineering
NIIGGR	Scientific Research Institute of Geophysical and Geochemical Methods of Prospecting
ONTI	United Scientific-Technical Press
OTI	Division of Technical Information
OTN	Division of Technical Science
PIN	Paleontological Institute (of Acad. Sci. USSR)
TsNIGRI	Central Scientific Research Institute of Geological Surveying
TsVTI	Central Office of Economic Information
UF	Ural Branch
VGO	All-Union Geographical Society
VGRO	All-Union Geological Prospecting Association
VNIGRI	All-Union Petroleum Scientific Research Geological Prospecting Institute
VNII	All-Union Scientific Research Institute of Instruments
VNIIGAZ	All-Union Scientific Research Institute of the Gas Industry
VSEGEI	All-Union Geological Scientific Research Institute

Note: Abbreviations not on this list and not explained in the translation have been transliterated, no further information about their significance being available to us. - Publisher.